Springer Protocols

Methods in Molecular Biology 491

Potassium Channels

Methods and Protocols

Edited by

Jonathan D. Lippiat

Humana Press

Potassium Channels

METHODS IN MOLECULAR BIOLOGY™

John M. Walker, SERIES EDITOR

476. Redox-Mediated Signal Transduction: *Methods and Protocols* edited by *John T. Hancock, 2008*
475. Cell Fusion: *Overviews and Methods,* edited by *Elizabeth H. Chen, 2008*
474. Nanostructure Design: *Methods and Protocols,* edited by *Ehud Gazit and Ruth Nussinov, 2008*
473. Clinical Epidemiology: *Practice and Methods,* edited by *Patrick Parfrey and Brendon Barrett, 2008*
472. Cancer Epidemiology, Volume 2: *Modifiable Factors,* edited by *Mukesh Verma, 2008*
471. Cancer Epidemiology, Volume 1: *Host Susceptibility Factors,* edited by *Mukesh Verma, 2008*
470. Host-Pathogen Interactions: *Methods and Protocols,* edited by *Steffen Rupp and Kai Sohn, 2008*
469. Wnt Signaling, Volume 2: *Pathway Models,* edited by *Elizabeth Vincan, 2008*
468. Wnt Signaling, Volume 1: *Pathway Methods and Mammalian Models,* edited by *Elizabeth Vincan, 2008*
467. Angiogenesis Protocols: *Second Edition,* edited by *Stewart Martin and Cliff Murray, 2008*
466. Kidney Research: *Experimental Protocols,* edited by *Tim D. Hewitson and Gavin J. Becker, 2008*
465. Mycobacteria, Second Edition, edited by *Tanya Parish and Amanda Claire Brown, 2008*
464. The Nucleus, Volume 2: *Physical Properties and Imaging Methods,* edited by *Ronald Hancock, 2008*
463. The Nucleus, Volume 1: *Nuclei and Subnuclear Components,* edited by *Ronald Hancock, 2008*
462. Lipid Signaling Protocols, edited by *Banafshe Larijani, Rudiger Woscholski, and Colin A. Rosser, 2008*
461. Molecular Embryology: *Methods and Protocols, Second Edition,* edited by *Paul Sharpe and Ivor Mason, 2008*
460. Essential Concepts in Toxicogenomics, edited by *Donna L. Mendrick and William B. Mattes, 2008*
459. Prion Protein Protocols, edited by *Andrew F. Hill, 2008*
458. Artificial Neural Networks: Methods and Applications, edited by *David S. Livingstone, 2008*
457. Membrane Trafficking, edited by *Ales Vancura, 2008*
456. Adipose Tissue Protocols, Second Edition, edited by *Kaiping Yang, 2008*
455. Osteoporosis, edited by *Jennifer J. Westendorf, 2008*
454. SARS- and Other Coronaviruses: *Laboratory Protocols*, edited by *Dave Cavanagh, 2008*
453. Bioinformatics, Volume II: *Structure, Function and Applications*, edited by *Jonathan M. Keith, 2008*
452. Bioinformatics, Volume I: *Data, Sequence Analysis and Evolution*, edited by *Jonathan M. Keith, 2008*
451. Plant Virology Protocols: *From Viral Sequence to Protein Function*, edited by *Gary Foster, Elisabeth Johansen, Yiguo Hong, and Peter Nagy, 2008*
450. Germline Stem Cells, edited by *Steven X. Hou and Shree Ram Singh, 2008*
449. Mesenchymal Stem Cells: *Methods and Protocols*, edited by *Darwin J. Prockop, Douglas G. Phinney, and Bruce A. Brunnell, 2008*
448. Pharmacogenomics in Drug Discovery and Development, edited by *Qing Yan, 2008*
447. Alcohol: *Methods and Protocols*, edited by *Laura E. Nagy, 2008*
446. Post-translational Modification of Proteins: *Tools for Functional Proteomics*, Second Edition, edited by *Christoph Kannicht, 2008*
445. Autophagosome and Phagosome, edited by *Vojo Deretic, 2008*
444. Prenatal Diagnosis, edited by *Sinhue Hahn and Laird G. Jackson, 2008*
443. Molecular Modeling of Proteins, edited by *Andreas Kukol, 2008.*
442. RNAi: Design and Application, edited by *Sailen Barik, 2008*
441. Tissue Proteomics: *Pathways, Biomarkers, and Drug Discovery*, edited by *Brian Liu, 2008*
440. Exocytosis and Endocytosis, edited by *Andrei I. Ivanov, 2008*
439. Genomics Protocols, Second Edition, edited by *Mike Starkey and Ramnanth Elaswarapu, 2008*
438. Neural Stem Cells: *Methods and Protocols*, Second Edition, edited by *Leslie P. Weiner, 2008*
437. Drug Delivery Systems, edited by *Kewal K. Jain, 2008*
436. Avian Influenza Virus, edited by *Erica Spackman, 2008*
435. Chromosomal Mutagenesis, edited by *Greg Davis and Kevin J. Kayser, 2008*
434. Gene Therapy Protocols: Volume II: *Design and Characterization of Gene Transfer Vectors*, edited by *Joseph M. LeDoux, 2008*
433. Gene Therapy Protocols: Volume I: *Production and In Vivo Applications of Gene Transfer Vectors*, edited by *Joseph M. LeDoux, 2008*
432. Organelle Proteomics, edited by *Delphine Pflieger and Jean Rossier, 2008*
431. Bacterial Pathogenesis: *Methods and Protocols*, edited by *Frank DeLeo and Michael Otto, 2008*
430. Hematopoietic *Stem Cell Protocols*, edited by *Kevin D. Bunting, 2008*
429. Molecular Beacons: *Signalling Nucleic Acid Probes, Methods and Protocols*, edited by *Andreas Marx and Oliver Seitz, 2008*
428. Clinical Proteomics: *Methods and Protocols*, edited by *Antonia Vlahou, 2008*
427. Plant Embryogenesis, edited by *Maria Fernanda Suarez and Peter Bozhkov, 2008*
426. Structural Proteomics: *High-Throughput Methods*, edited by *Bostjan Kobe, Mitchell Guss, and Huber Thomas, 2008*
425. 2D PAGE: *Sample Preparation and Fractionation*, Volume II, edited by *Anton Posch, 2008*
424. 2D PAGE: *Sample Preparation and Fractionation*, Volume I, edited by *Anton Posch, 2008*
423. Electroporation Protocols: *Preclinical and Clinical Gene Medicine*, edited by *Shulin Li, 2008*
422. Phylogenomics, edited by *William J. Murphy, 2008*

METHODS IN MOLECULAR BIOLOGY™

Potassium Channels

Methods and Protocols

Edited by

Jonathan D. Lippiat

Institute of Membrane and Systems Biology, Faculty of Biological Sciences
University of Leeds, Leeds, LS2 9JT, UK

Humana Press

Editor
Jonathan D. Lippiat
Institute of Membrane and Systems Biology
Faculty of Biological Sciences
University of Leeds
Leeds, LS2 9JT, UK

Series Editor
John M. Walker
School of life Sciences
University of Hertfordshire
Hatfield, Hertfordshire
AL10 9AB, UK

ISSN: 1064-3745 e-ISSN: 1940-6029
ISBN: 978-1-934115-65-7 e-ISBN: 978-1-59745-526-8
DOI: 10.1007/978-1-59745-526-8

Library of Congress Control Number: 2008931178

Cover illustration: Chapter 5, Figure 1

Printed on acid-free paper

springer.com

Preface

Potassium channels are important regulators of membrane excitability, which in turn determines cellular function. They form a super-family of ion channels that are regulated by a diverse range of chemical and physical stimuli. In excess of 80 genes in the human genome encode pore-forming potassium channel subunits. Diversity is further enhanced by alternative splicing of subunit mRNA, heteromeric assembly between pore-forming subunits, or by association with accessory proteins. The basis of several inherited diseases lies in potassium channel gene mutations, and the pharmacological manipulation of potassium channel function is increasingly important as a strategy in the treatment of disease. This provides researchers with the challenge of developing tools and experimental procedures to probe potassium channel function and identify chemicals that modulate their behaviour.

We have progressed since the initial mid-twentieth century studies of delayed rectifier, anomalous rectifier, and leak potassium currents, and now ask questions such as "What does a potassium channel look like?", "How do changes in membrane potential gate a potassium channel?", or "Which proteins assemble to form a potassium channel complex in this particular cell?". Many of these questions cannot be answered by electrophysiological techniques alone, thus scientists have adopted techniques from other disciplines to assist their studies.

This volume describes a range of experimental approaches that have been developed to investigate potassium channel structure, function, pharmacology, cell biology, gene expression, and their role in disease. Many of these techniques study potassium channels as cellular proteins as well as the resultant membrane biophysics. They are proteins that are synthesised according to mRNA sequence, trafficked to the correct location in the cell at the appropriate time, interact with other protein components, change conformation following stimulation, all in addition to providing a conduit for potassium ions to cross membranes. Naturally, content covering the topic of ion channels would not be without electrophysiological techniques, but here they are focused on those that enable the study of intracellular modulation, which is of particular importance to many potassium channels.

All investigators, including new researchers and discipline-hopping scientists, will benefit from this volume. Within the various chapters you will also find protocols for several standard laboratory techniques, such as cell culture, transfection, *Xenopus* oocyte preparation, Western blotting, and whole-cell patch clamp recording. Indeed, the techniques found in this book can be applied to the study of many other types of ion channel. There is an increasing trend to answer scientific questions using a wide range of approaches and it is hoped that the techniques outlined in this volume will help provide finishing touches to research projects or provide new avenues of investigation.

Leeds, UK — Jonathan D. Lippiat

Contents

Contributors

Eric A. Accili • *Department of Cellular and Physiological Sciences, University of British Columbia, Vancouver, British Columbia, BC, Canada*

David J. Beech • *Institute of Membrane and Systems Biology, Faculty of Biological Sciences, University of Leeds, Leeds, UK*

Andrea Brüggemann • *Nanion Technologies GmbH, Munich, Germany*

Lie Chen • *Centre for Integrative Physiology, College of Medicine and Veterinary Medicine, University of Edinburgh, Edinburgh, UK*

Alex Cheong • *Institute of Membrane and Systems Biology, Faculty of Biological Sciences, University of Leeds, Leeds, UK*

Mark L. Dallas • *School of Medicine, University of Leeds, Leeds, UK*

Caroline Dart • *School of Biological Sciences, University of Liverpool, Liverpool, UK*

Jim Deuchars • *Institute of Membrane and Systems Biology, Faculty of Biological Sciences, University of Leeds, Leeds, UK*

Susan A. Deuchars • *Institute of Membrane and Systems Biology, Faculty of Biological Sciences, University of Leeds, Leeds, UK*

Tino Dyhring • *NeuroSearch A/S, Ballerup, Denmark*

Sian Ellard • *Institute of Biomedical and Clinical Science, Peninsula Medical School, Exeter, UK*

Cecilia Farre • *Nanion Technologies GmbH, Munich, Germany*

Niels Fertig • *Nanion Technologies GmbH, Munich, Germany*

Sarah E. Flanagan • *Institute of Biomedical and Clinical Science, Peninsula Medical School, Exeter, UK*

Samuel J. Fountain • *Institute of Membrane and Systems Biology, Faculty of Biological Sciences, University of Leeds, Leeds, UK*

Chris S. Gandhi • *Division of Chemistry and Chemical Engineering, Howard Hughes Medical Institute, California Institute of Technology, Pasadena, CA, USA*

Michael George • *Nanion Technologies GmbH, Munich, Germany*

Claudia Haarmann • *Nanion Technologies GmbH, Munich, Germany*

Ali Haythornthwaite • *Nanion Technologies GmbH, Munich, Germany*

Ray M. Helliwell • *Millipore UK, Cambridge, UK*

Tina H. Johansen • *NeuroSearch A/S, DK-2750 Ballerup, Denmark*

Susanne Jørgensen • *NeuroSearch A/S, DK-2750 Ballerup, Denmark*

Robert W. Kirby • *Biomedical Research Centre, Faculty of Health and Wellbeing, Sheffield Hallam University, Sheffield, UK*

Mohamed Kreir • *Nanion Technologies GmbH, Munich, Germany*

Kim Lawson • *Biomedical Research Centre, Faculty of Health and Wellbeing, Sheffield Hallam University, Sheffield, UK*

Florian Lesage • *Institut de Pharmacologie Moléculaire et Cellulaire, CNRS, 06560 Valbonne Sophia-Antipolis, France*

Jonathan D. Lippiat • *Institute of Membrane and Systems Biology, Faculty of Biological Sciences, University of Leeds, Leeds, UK*

Neil G. McKay • *Biomedical Research Centre, Faculty of Health and Wellbeing, Sheffield Hallam University, Sheffield, UK*

Peter Proks • *Department of Physiology, Anatomy and Genetics, University of Oxford, Oxford, UK*

Riccardo Olcese • *Division of Molecular Medicine, Department of Anesthesiology, David Geffen School of Medicine at University of California, Los Angeles, CA, USA*

Lezanne Ooi • *Institute of Membrane and Systems Biology, Faculty of Biological Sciences, University of Leeds, Leeds, UK*

Adi Raveh • *Department of Biological Chemistry, Weizmann Institute of Science, Rehovot, Israel*

Eitan Reuveny • *Department of Biological Chemistry, Weizmann Institute of Science, Rehovot, Israel*

Inbal Riven • *Department of Physiology and Pharmacology, Sackler School of Medicine, Tel Aviv University, Tel Aviv, Israel*

Laura J. Sampson • *Department of Cell Physiology and Pharmacology, University of Leicester, UK*

Guillaume Sandoz • *Institut de Pharmacologie Moléculaire et Cellulaire, CNRS, 06560 Valbonne Sophia-Antipolis, France*

Kenju Shimomura • *Department of Physiology, Anatomy and Genetics, University of Oxford, Oxford, UK*

Michael J. Shipston • *Centre for Integrative Physiology, College of Medicine and Veterinary Medicine, University of Edinburgh, Edinburgh, UK*

Asipu Sivaprasadarao • *Institute of Membrane and Systems Biology, Faculty of Biological Sciences, University of Leeds, Leeds, UK*

Andrew J. Smith • *Institute of Membrane and Systems Biology, Faculty of Biological Sciences, University of Leeds, Leeds, UK*

Sonja Stoelzle • *Nanion Technologies GmbH, Munich, Germany*

Paolo Tammaro • *Department of Physiology, Anatomy and Genetics, University of Oxford, Oxford, UK*

Andrei I. Tarasov • *Section of Cell Biology, Division of Medicine, Faculty of Medicine, Imperial College London, London, UK*

Alison M. Thomas • *Department of Medicine, University College London, London, UK*

Andrew Tinker • *Department of Medicine, University College London, London, UK*

Gina M. Whitaker • *Department of Cellular and Physiological Sciences, University of British Columbia, Vancouver, British Columbia, BC, Canada*

Ian C. Wood • *Institute of Membrane and Systems Biology, Faculty of Biological Sciences, University of Leeds, Leeds, UK*

Chapter 1

Identifying Transcriptional Regulatory Regions Using Reporter Genes and DNA–Protein Interactions by Chromatin Immunoprecipitation

Lezanne Ooi and Ian C. Wood

Summary

A comprehensive understanding of regulatory protein interactions with their target genes is fundamental to determining transcriptional networks and identifying important events in the regulation of gene expression. Here we describe how transcriptional regulatory regions are to be identified using luciferase assays (including the transfection of cells by Amaxa and lipid-based reagents) and how protein–DNA interactions are to be characterised by chromatin immunoprecipitation (ChIP) coupled with quantitative PCR. Together these techniques provide a powerful combination for investigating potassium channel gene regulation.

Key words: Electroporation, Transient transfection, Luciferase assays, Chromatin immunoprecipitation, Quantitative PCR.

1.1. Introduction

The transcription of potassium channel genes is highly regulated during development, resulting in unique expression profiles in different cell types. Dynamic changes in the transcription of some potassium channel genes are important in normal physiology *(1)* and also contribute to disease states *(2, 3)*. Understanding how the expression of these genes is controlled will enhance our understanding of physiology, in addition to providing potential targets for novel therapeutics.

Jonathan D. Lippiat (ed.), *Methods in Molecular Biology, Potassium Channels, vol. 491*

Book doi: 10.1007/978-1-59745-526-8

Proteins that bind DNA are major determinants of expression patterns and may have either a positive or negative effect on transcription. The transcription rate of a particular gene in a specific cell is therefore dependent on the balance between activating and inhibiting transcription factors. Identifying the regulatory regions of genes and the proteins that are recruited to these sequences is thus crucial to our understanding of gene regulation. Reporter assays can provide a wealth of information on DNA sequences that are important for potassium channel gene regulation *(4–7)* but these assays have been limited by an inability to transfect some cell types, particularly primary cells. The development of transfection methods such as the Amaxa system has allowed efficient transfection of reporter genes to analyse promoter activity in cells, such as primary vascular smooth muscle cells, that were previously difficult to transfect. A huge improvement in our understanding of gene regulation has been mediated by reporter gene assays coupled with the direct measurement of the transcription factor occupancy of promoters. In the cell, the DNA is wrapped around histone proteins in a complex called chromatin and the study of the interactions of transcription factors with their target genes has been made possible by a technique termed chromatin immunoprecipitation (ChIP) *(8)* (**Fig. 1.1**).

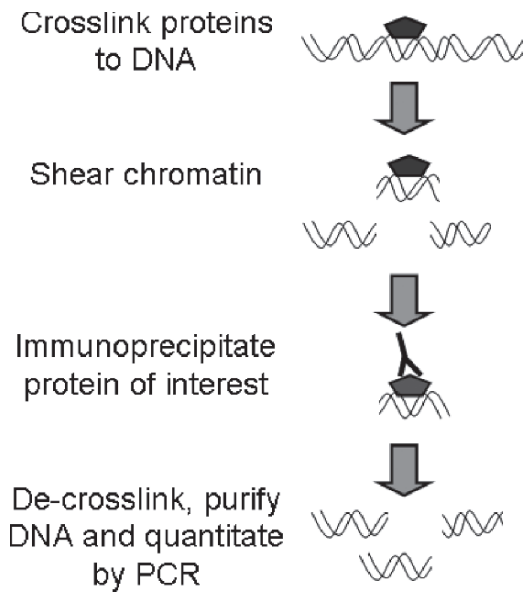

Fig. 1.1. Chromatin immunoprecipitation. Proteins are crosslinked to their chromatin binding sites in living cells, the chromatin is then sheared and divided. In one portion, a protein of interest is immunoprecipitated, along with its bound target DNA sequences. Other pools of chromatin are either subjected to a background immunoprecipitation or negative control (e.g. IgG), a positive control for immunoprecipitation (e.g. an antibody to the histone protein H3, that should be present at all sites) or do not undergo immunoprecipitation (representing input DNA). On reversal of the crosslinks and purification of the DNA, sequences of DNA that were bound by the protein of interest are more enriched than the same sequences in the negative control, as determined by quantitative PCR.

Here we describe how to perform luciferase and ChIP assays that can be used to examine protein–DNA interactions in many cell types. We also show results for these experiments from our study of the regulation of the potassium channel gene KCNN4 which encodes the KCa3.1 potassium channel, by the transcription factor Repressor Element 1-Silencing Transcription factor (REST) in vascular smooth muscle cells.

1.2. Materials

1.2.1. Electroporation Using Amaxa

1. Cell culture medium: DMEM, 10% foetal calf serum, 2 mM glutamine, streptomycin (10 g/L) and penicillin (10 g/L); pre-warmed to 37°C
2. Trypsin/EDTA
3. Phosphate buffered saline (PBS)
4. 6-well cell culture plates
5. Haemocytometer
6. Polypropylene centrifuge tubes, 50 ml
7. Nucleofector kit (Amaxa)
8. Electroporator (Amaxa)
9. Plasmid DNA

1.2.2. Transfection with Lipid-Based Reagents

1. Cell culture medium: DMEM, 10% foetal calf serum, 2 mM glutamine, streptomycin (10 g/L) and penicillin (10 g/L); pre-warmed to 37°C
2. Serum free media (e.g. Opti-MEM (Invitrogen))
3. Lipid transfection reagent (e.g. Lipofectamine with Plus reagent (Invitrogen))
4. 24-well cell culture plates
5. PBS
6. Sterile, round bottomed 14 ml centrifuge tubes
7. Plasmid DNA

1.2.3. Luciferase Assays

1. PBS
2. Microtitre, 96-well plates or single luminometer tubes
3. Dual luciferase assay kit (Promega)
4. Luminometer

1.2.4. Chromatin Immunoprecipitation and Quantitative PCR

1. Cell lysis buffer (CLB): 10 mM Tris–HCl pH 8.0, 10 mM NaCl, 0.2% NP-40, 10 mM sodium butyrate, 1× "Mini Complete" protease inhibitors tablet (Roche). Add a fresh protease inhibitor tablet and then keep the buffer on ice.

2. Formaldehyde solution (37%; toxic – use in fume cupboard).
3. 2 M Glycine.
4. Phosphate buffered saline (PBS).
5. Nuclear lysis buffer: 50 mM Tris–HCl pH 8.1, 10 mM EDTA, 1% SDS, 10 mM sodium butyrate, 1× "Mini Complete" protease inhibitor tablet (Roche). Add a fresh protease inhibitor tablet and then keep the buffer on ice.
6. IP dilution buffer (IPDB): 20 mM Tris–HCl pH 8.1, 150 mM NaCl, 2 mM EDTA, 1% Triton X-100, 0.01% SDS, 10 mM sodium butyrate, 1× "Mini Complete" protease inhibitor tablet (Roche). Add a fresh protease inhibitor tablet and then keep the buffer on ice.
7. Glass test tube (for sonication). We use a tube with the following dimensions: 7.5-cm length, 1-cm diameter.
8. Normal rabbit IgG.
9. Antibody to your query DNA binding protein (e.g. anti-REST).
10. Anti-H3 antibody.
11. Protein G-Sepharose.
12. IP wash buffer 1: 20 mM Tris–HCl pH 8.1, 50 mM NaCl, 2 mM EDTA, 1% Triton X-100, 0.1% SDS. Cool on ice before use.
13. IP wash buffer 2: 10 mM Tris–HCl pH 8.1, 250 mM LiCl, 1 mM EDTA, 1% NP-40, 1% deoxycholic acid. Cool on ice before use.
14. TE pH 8.0: 10 mM Tris–HCl pH 8.0, 1 mM EDTA. Cool on ice before use.
15. IP elution buffer: 100 mM $NaHCO_3$, 1% SDS.
16. RNase A: 10 mg/ml.
17. 5 M NaCl.
18. Proteinase K: 10 mg/ml stock.
19. tRNA: 5 mg/ml stock.
20. 1:1 Phenol/chloroform.
21. Chloroform.
22. Glycogen: 1 mg/ml.
23. 3 M Sodium acetate, pH 5.2.
24. Ethanol.
25. HPLC grade water.
26. Biorad iQ supermix.

1.2.5. Equipment

1. Bandelin Sonoplus sonicator
2. iCycler iQ PCR system

1.3. Methods

1.3.1. Electroporation Using Amaxa

The Amaxa technology has greatly enhanced the number of cell types that are amenable to transfection and increased the efficiency with which cells can be transfected. This is particularly true of primary cells, such as vascular smooth muscle cells, which are refractory to transfection by other means. (Before designing a transfection experiment, *see* **Note 1**.)

1. Prepare 6-well plates by adding 1 ml of cell culture medium to each well and place in a 37°C incubator.
2. Pre-warm Nucleofector solution to room temperature.
3. Remove the flasks of cells from the incubator and aspirate the media.
4. Wash the cells with 10 ml of PBS.
5. Add 1 ml of trypsin/EDTA to the cells and return to the incubator until the cells detach from the plate (approximately 2–5 min, depending on the cell type).
6. Add 10 ml of the media containing serum to each flask to inactivate the trypsin and transfer the cells to a 50 ml centrifuge tube.
7. Make a note of the final volume and remove a drop of the cell suspension to count the cell number in the haemocytometer.
8. Maintain centrifuge tubes at 100×*g* for 5 min to pellet cells.
9. Whilst the cells are centrifuging, count the cells using the aliquot removed in **step 6** and determine the total cell number in the centrifuge tube.
10. Also prepare a tube containing DNA (*see* **Note 2**) for each transfection to be carried out. Aliquot 3 µg of the promoter-firefly luciferase plasmid and 12 ng of the pRL-CMV control plasmid. The total volume of DNA should not exceed 5 µl.
11. After centrifugation, aspirate the supernatant and re-suspend the cells in the Nucleofector solution to a final concentration of 5×10^6 cells/ml.
12. Concentrating on one tube at a time, add 100 µl of cell suspension to the DNA.
13. Pipette the cell suspension/DNA mixture into an Amaxa certified cuvette.
14. Select the appropriate Nucleofector programme, insert the cuvette into the electroporator and begin the electroporation by pressing the X button.
15. Immediately remove the cuvette and add 500 µl of the pre-warmed cell culture media.

16. Add 200 µl of cell suspension to each of the 3 wells in a 6-well plate containing 1 ml of the pre-warmed culture media from **step 1**.
17. Repeat **steps 11–15** for each DNA transfection.
18. Incubate the cells at 37°C in a humidified incubator in 5% CO_2 for 24–48 h.
19. Harvest the cells and perform luciferase assays as described in **Subheading 1.3.3**.

1.3.2 Transfection Using Lipid-Based Methods

Lipid-based transfection methods have several advantages over the Amaxa system in that first, they do not require any specialist equipment; they can be carried out in most laboratories equipped for cell culture and second, they are generally less toxic to the cells than electroporation. Many currently used cell lines are amenable to transfection with lipid-based reagents, often allowing high transfection efficiencies to be achieved. There are many different lipid-based transfection reagents currently available and some of these require specific conditions, such as the absence of serum or antibiotics, whilst others boast extremely low cellular toxicity. Initial optimisation experiments should be performed to identify the optimal concentration of plasmid DNA and the DNA/lipid ratio that provides the highest transfection efficiency. Depending on the cell type, transfection efficiencies of 50–80% should be routinely achievable. (Before designing a transfection experiment, *see* **Note 1**.)

1. One day prior to transfection, trypsinise the cells and aliquot them into 24-well plates so that they are approximately 80% confluent at the time of transfection. Provide sufficient numbers of wells so that each firefly luciferase plasmid can be transfected into three individual wells.
2. On the day of transfection, warm all the reagents and the cell culture media to room temperature.
3. Prepare one 14 ml centrifuge tube for each sample to be transfected by adding 150 µl of serum free medium, 750 ng of firefly luciferase plasmid and 3 ng of CMV-*Renilla* luciferase plasmid (*see* **Note 2**).
4. Add 7.5 µl of Plus reagent (*see* **Note 3**) and incubate at room temperature for 20 min.
5. Aliquot sufficient Opti-MEM into a separate 14 ml tube so that 150 µl can be added to each sample (e.g. ten transfections would require 1.5 ml Opti-MEM) and add the appropriate amount of Lipofectamine (a ratio of 4 µl Lipofectamine/1 µg works well in our experience, so for ten transfections add 30-µl Lipofectamine), mix and incubate at room temp for 20 min.
6. Add 150 µl of Lipofectamine/Opti-MEM mixture to each tube containing DNA, mix and incubate at room temperature for 20 min.

7. During this incubation remove the cells from the incubator, aspirate the media and wash each well once with 2 ml of PBS, add 2 ml of Opti-MEM and return to the incubator.
8. After the DNA/Lipofectamine incubation is complete add 1.2 ml of Opti-MEM to each tube and mix. Remove the cells from the incubator, aspirate the medium and add 500 µl of transfection mixture to each well.
9. Return the cells to the incubator and leave for a minimum of 4 h (*see* **Note 4**).
10. After incubation with the transfection mixture, remove the cells from the incubator, aspirate the media and replace them with 2 ml normal growth media. Return the cells to the incubator and leave them for at least 24 h.

1.3.3. Luciferase Assays

1. Remove the transfected cell cultures from the incubator and aspirate the media.
2. Add PBS (0.5 ml per well for a 24-well plate or 1 ml per well for a 6-well plate) to wash the cells.
3. Aspirate the PBS.
4. Add 100 µl of passive lysis buffer to each well.
5. Place the plate onto an orbital shaker and shake for 15 min. Ensure that the shaking has sufficient vigour for the passive lysis buffer to cover the entire surface of the well.
6. Whilst the cells are lysing, remove the firefly luciferase substrate and the 'Stop and Glow' (for *Renilla* luciferase) reagents from the freezer and warm to room temperature.
7. Scrape and pipette the passive lysis buffer into a 1.5 ml microcentrifuge tube.
8. Transfer 50 µl of each cell lysate into a well of a 96-well plate or into a luminometer tube.
9. Set the programme on the luminometer to wait for 2 s and then measure for 10 s.
10. If using a 96-well luminometer, set the software to indicate which of the wells contain cell lysate and prime the injectors using the firefly luciferase and *Renilla* luciferase substrates. Priming is accomplished by inserting the tubing into the buffer and then instructing the instrument to take the buffer into the tubing. Some luminometers allow the complete recirculation of the buffer so that the excess buffer can be recovered at the end of the experiment. With respect to other luminometers any buffer left in the tubing at the end of the experiment cannot be recovered and is wasted (*see* **Note 5**).
11. Place the 96-well plate into the instrument and begin the measurement.

12. If using a single tube luminometer, measure the luciferase and then the *Renilla* luciferase activity for each sample before progressing to the next one. To do this, add 100 µl of luciferase substrate into the first tube, vortex briefly, insert into the luminometer and read. Remove the tube, add 100 µl of the Stop and Glow buffer, vortex briefly, insert into the luminometer and read.
13. Repeat the process in **step 12** for each tube.
14. Express data as relative light units (RLUs) from luciferase per RLU and from *Renilla* luciferase (*see* **Note 6**). We perform each transfection in triplicate and calculate the average and the SEM of firefly luciferase/*Renilla* luciferase for each promoter-luciferase plasmid (**Fig. 1.2**).

1.3.4. Identifying DNA–Protein Interactions by Chromatin Immunoprecipitation

One advantage of ChIP is that interactions of endogenous proteins with their target DNA sequences in the cell can be measured and is therefore considered biologically, to be a more relevant assay than *in vitro* experiments, such as reporter assays. We have used this protocol to identify interactions of the transcription factor REST with its DNA binding sites in ion channel genes, amongst many others and have carried out this protocol using cell lines ***(9–12)*** and primary cells, including vascular smooth muscle cells *(3)*, cardiac myocytes ***(13)*** and brain tissue ***(14)*** (*see* **Note 7**).

1. Harvest 1×10^7 cells (approximately 1 × 10 cm dish, 80–90% confluent) per immunoprecipitation (i.e. use 3×10^7 cells if you are going to include a negative and positive control immunoprecipitation, *see* **step 12**). Wash cells twice in 10 ml ice-cold PBS.
2. Add 270 µl of formaldehyde solution (37%; final concentration 1%) to 10 ml PBS per plate to crosslink the DNA–protein

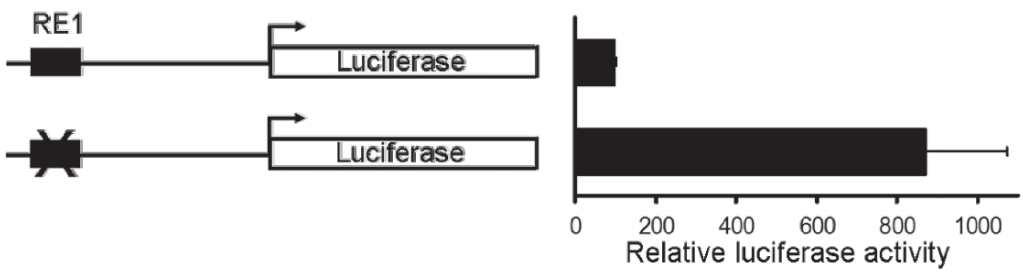

Fig. 1.2. Luciferase activity of the *KCNN4* promoter in A7r5 smooth muscle cells. The figure shows mean firefly luciferase activity normalised to *Renilla* luciferase activity driven from the co-transfected pRL-CMV plasmid of the wild type *KCNN4* promoter containing a binding site for the transcription factor REST (RE1, *top*) and a *KCNN4* promoter containing a mutated site that does not bind REST (*bottom*). Data shown are mean ± SEM, $n = 3$. REST is a repressor ***(15)***; therefore the presence of a functional binding site in the promoter leads to down-regulation of *KCNN4* promoter activity driving luciferase expression, while mutation of this site alleviates repression.

interactions. Incubate at room temperature with gentle agitation for 10 min.

3. Add 630 µl of 2 M glycine (final concentration of 125 mM) and incubate for 5 min at room temperature with gentle shaking to stop the crosslinking reaction.
4. Scrape the cells into a 50 ml polypropylene centrifuge tube on ice and centrifuge the cells at 300×*g* for 6 min at 4°C.
5. Re-suspend the pellet with 1.5-ml ice-cold PBS. Centrifuge the cells at 400×*g* for 5 min at 4°C.
6. Gently re-suspend the cell pellet in 1.5× cell pellet volume of CLB. Re-suspend the cells by pipetting them up and down and incubate them for 10 min on ice. Centrifuge at 1,200×*g* for 5 min at 4°C to collect the nuclei.
7. Remove the supernatant and re-suspend the nuclei in 1.2 ml of nuclei lysis buffer (NLB) and incubate them on ice for 10 min. Add 0.8 ml of IPDB and transfer them to a glass test tube.
8. Sonicate the sample using the microtip (small probe). Keep the tip of the probe just below the surface and keep the sample on ice at all times. Use the Bandelin Sonoplus sonicator at 40% power; the settings are the following (these settings may vary from instrument to instrument):
   (a) No. of bursts: 8
   (b) Length of bursts: 30 s
   (c) Duty cycle: 7 (intermittent bursts 70% burst)

Allow the samples to cool for 1 min on ice between each pulse. Using these conditions, the DNA is sheared to approximately 300–700 bp fragments. Transfer the sheared chromatin to 2 ml microcentrifuge tubes and centrifuge at 16,000×*g* for 5 min at 4°C.

9. Transfer the supernatant to a 15 ml polypropylene tube and add IPDB to bring the volume up to that required for **step 12** (i.e. 4.32 ml for three immunoprecipitations and an input control).
10. Prepare Protein G-Sepharose (PGS) beads: Make up 1 ml 5% BSA in IPDB. Wash 1 ml of PGS beads three times in 1 ml IPDB (beads should make up 50% of the volume). Re-suspend the beads in 5% BSA. Rotate at room temperature for 1 h. Wash the beads two times in 1 ml IPDB and re-suspend them in 1 ml IPDB (beads should make up 50% of the volume). Store rotating at 4°C.
11. Pre-clear chromatin by adding 100 µg of normal IgG and incubate for 1 h at 4°C on a rotating wheel. Add 200 µl of the homogeneous protein G-Sepharose suspension and incubate for 3 h at 4°C on a rotating wheel.
12. Centrifuge the beads at 1,200×*g* for 2 min at 4°C. Use the supernatant to set up the following conditions.

Negative control: 1.35 ml chromatin + 5 µg rabbit IgG

Query antibody: 1.35 ml chromatin + 5 µg anti-REST antibody

Positive control: 1.35 ml chromatin + 5 µg histone H3 antibody
Use 270 µl of the chromatin to set up an input control and store samples at –20°C.

13. Incubate overnight at 4°C with rotation.
14. Centrifuge the samples at 16,000×*g* for 5 min at 4°C. Transfer the samples to new 1.5 ml microcentrifuge tubes and add 100 µl of the homogenous PGS suspension. Incubate for at least 3 h at 4°C with rotation.
15. Centrifuge the PGS beads at 16,000×*g* for 20 s at 4°C. Remove the supernatant and wash the pellet twice with 750 µl of IP wash buffer 1. For each wash, vortex briefly and centrifuge at 5,000×*g* for 2 min at 4°C. Leave the tubes undisturbed for a minute before removing the supernatant.
16. Wash the pellet similarly, once with 750 µl of IP wash buffer 2 and twice with 750 µl of TE pH 8.0.
17. Elute the immune complexes (DNA–protein–antibody) from the beads by adding 225 µl of IP elution buffer. Vortex briefly and centrifuge at 5,000×*g* for 2 min. Repeat this step and combine both the eluates in the same tube.
18. Add 0.5 µl of RNase A (10 mg/ml stock) and 27 µl of 5 M NaCl to each sample. Also add 0.5 µl of RNase A (10-mg/ml stock) and 16 µl of 5 M NaCl to the input sample. Incubate the samples at 65°C for 6 h to de-crosslink.
19. Add 9 µl of proteinase K (10-mg/ml stock) and incubate overnight at 45°C.
20. Add 2 µl tRNA (5 mg/ml stock) immediately before adding 500 µl of phenol/chloroform. Vortex well, centrifuge at 16,000×*g* for 5 min at room temperature. Transfer the aqueous layer to new 2 ml microcentrifuge tubes and repeat this step once with 500 µl of chloroform.
21. Add 5 µg of glycogen, 1 µl of tRNA (5-mg/ml stock) and 50 µl of 3-M sodium acetate pH 5.2 to each sample. Vortex well and add 1.25 ml of 100% ethanol. Precipitate at –70°C for 30 min.
22. Centrifuge at 16,000×*g* for 20 min at 4°C. Wash the pellet with 500 µl of ice-cold 70% ethanol.
23. Remove the supernatant and air dry the pellets for 10 min. Re-suspend the pellets in 100 µl of HPLC grade water for the input and 50 µl of HPLC grade water for the other samples.
24. Electrophorese 5 µl of each input sample on a 1% agarose, 1× TAE gel to check DNA fragment sizes and quantitate the enrichment of your immunoprecipitated protein in a region of interest by quantitative PCR. Store samples at –20°C.

1.3.5. Quantitative PCR

1. Perform quantitative PCR in a 96-well plate using the iCycler iQ system (BioRad, *see* **Note 9**). SYBR green I is used to measure amplification as it occurs in real time as the fluorescence of the reporter increases when it intercalates into double stranded DNA. The cycle at which fluorescence increases above the background is termed the threshold cycle (Ct), which is measured during the exponential phase of the PCR. Primers should be designed to amplify sequences of DNA between 50 and 150 bp, with a melting temperature of above 60°C. All reactions should be carried out at least in duplicate.
2. Generate standard curves using the Cts from known starting amounts of the DNA, which can then be used to determine the starting quantities of test samples.
3. Each reaction has a final volume of 20 µl and consists of
   - 2 µl of DNA template
   - 1 µl of sense primer (500 nM final concentration)
   - 1 µl of antisense primer (500 nM final concentration)
   - 10 µl of 2× iQ supermix (100 mM KCl, 40 mM Tris–HCl pH 8.4, 0.4 mM dNTP, 50 U/ml iTaq, 50 mM $MgCl_2$, SYBR green I, 20 nM fluorescein) (BioRad)
   - 6 µl of HPLC grade water
4. Perform PCR reactions using an initial incubation at 95°C for 3 min, to activate the Taq, followed by 45 cycles of
   - 95°C for 30 s
   - 60°C for 30 s
   - 72°C for 30 s
5. Perform a melt curve of the products in the reaction by denaturation at 95°C for 30 s, annealing at 58°C for 10 s, followed by 45 cycles consisting of
   - Measurement of fluorescence for 10 s
   - Increment of incubation temperature by 1°C

This records the total fluorescence generated by SYBR green I binding to double stranded DNA as the temperature changes, with the peak of the trace corresponding to the melting temperature of the product.

6. Calculate the fold enrichment of the immunoprecipitation by dividing the starting quantities of DNA in the immunoprecipitated samples by that of the control antibody (IgG). Use a combination of melt curves and electrophoresis of the products through an agarose gel to check the PCR product sizes, in order to verify the amplification of specific products. If possible, a negative control region should be included in the PCR (a DNA sequence that is >1 kb from any of the binding sites for your query protein). We use a sequence

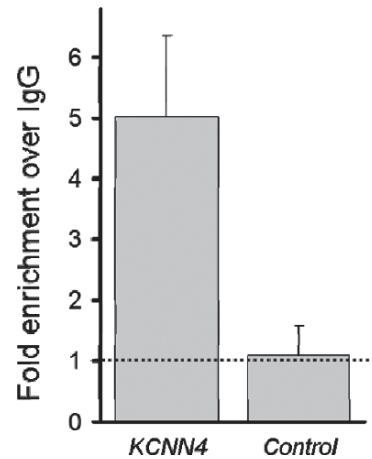

Fig. 1.3. Chromatin immunoprecipitation of the REST binding site in the *KCNN4* promoter from primary human saphenous vein smooth muscle cells. Chromatin was precipitated with anti-REST antibody (P18, Santa Cruz) or with IgG (to identify background precipitation levels). The presence of the *KCNN4* promoter in the anti-REST sample, relative to levels of DNA precipitated by IgG was assessed using quantitative PCR. The *dashed line* represents the level of background precipitation. A control DNA sequence >5 kb from any of the REST binding sites is used as a negative control region. Data shown are mean ± SEM, $n = 3$ and indicate that REST binds to the *KCNN4* promoter in smooth muscle cells *in vivo*.

of DNA that is >5 kb from any of the REST binding sites (**Fig. 1.3**).

1.4. Notes

1. In order to compare expression levels of transfected reporter genes two controls are important. First, co-transfection of a reference plasmid is imperative to allow normalisation for transfection efficiency. A reference plasmid would consist of a second reporter gene (such as *Renilla* luciferase, chloramphenicol acetyltransferase or β-galactosidase) whose expression is driven by a strong, constitutively active promoter (such as Cytomegalovirus (CMV), Simian virus 40 (SV40) or Elongation factor-1 alpha (EF-1 alpha)). The reference plasmid should drive equal expression of its reporter gene in each of the transfected samples and any variation in reporter activity will be the result of differences in the transfection efficiency. By normalising the luciferase expression to the activity of the second reporter gene any variation arising due to differences in transfection efficiency would be accounted for. It is also important to use a baseline or reference promoter driving luciferase with which to relate the promoter activity of your test gene.

2. For efficient DNA transfection into cells, preparation of high quality plasmid DNA is essential. It is best to prepare DNA using a commercial kit based on ion exchange chromatography. Removal of endotoxins during the plasmid isolation procedure also enhances transfection efficiency and many companies supply plasmid isolation kits that will remove endotoxin contamination. For simple measurement of luciferase activity resulting from the transfection of a single plasmid, a 24 h incubation, post-transfection is a sufficient length of time.
3. This step is optional; we find that the use of the Plus reagent in association with Lipofectamine increases transfection efficiency.
4. Cells can remain in the transfection mixture for up to 24 h. We have found that the efficiency of transfection is greater in the case of a 4 h incubation as compared to a 2 h one but efficiency is not different for longer incubation periods up to 24 h. Depending on the cell type, extended periods of incubation in the absence of serum may be deleterious leading to cell death.
5. Luminometers can be obtained that read from single tubes or read 96-well plates and contain automatic injectors. The latter are more expensive but allow the rapid throughput of large numbers of luciferase assays without requiring the constant presence of the user. However, the requirement for injection lines to be primed with luciferase and *Renilla* luciferase substrates means that high throughput luminometers can be wasteful of reagents if only a small number of samples are to be assayed at any one time. It is also important not to prime the tubes for a 96-well plate luminometer until just before the samples are ready to be assayed so that the reagent is not left sitting in the tubes for an extended period as this often results in abnormally low readings for the first samples.
6. Often, data is presented as firefly luciferase activity relative to activity obtained by transfection of either a plasmid lacking any eukaryotic promoter sequence or a plasmid containing a known promoter sequence (for example, a constitutively active viral derived promoter, such as CMV or the full length promoter for the gene of interest). One problem with using a known promoter sequence such as CMV is that it does not have the same activity in all cell types and hence a comparison between cells can be problematic. Conversely, using the background level of activity obtained from a firefly luciferase plasmid lacking any eukaryotic promoter sequences results in all data being normalised to a low signal with a greater tendency to show variability.
7. ChIP on tissue is carried out essentially as described here but using 450–600 mg frozen tissue. Freeze the tissue in liquid nitrogen, dice it into small pieces in 5 ml PBS, 1% formaldehyde and agitate at 4°C for 10 min. Add 125 mM glycine (final

concentration) to quench fixation and transfer the tissue to a polypropylene tube and centrifuge the sample at 400×*g* for 5 min at 4°C. Wash the pellet three times in PBS and centrifuge again at 400×*g* for 5 min at 4°C. Homogenise the sample in 3 ml PBS in a Dounce homogeniser by plunging it 25 times and keeping it on ice at all times. Centrifuge the homogenised tissue at 400×*g* for 5 min at 4°C and re-suspend it in the CLB containing 1% SDS. Transfer to a glass test tube and continue the ChIP protocol from **step 8 Subheading 1.3.4.**

8. Try to design primers for quantitative PCR as close to the putative binding site as possible.
9. Many other quantitative PCR systems and reagents are available, for example, Applied Biosystems, Invitrogen and Stratagene, which have their own systems, although we have not tested these.

Acknowledgement

This work was supported by the British Heart Foundation and the Wellcome Trust.

References

1. Ghanshani, S., Wulff, H., Miller, M. J., Rohm, H., Neben, A., Gutman, G. A., Cahalan, M. D., and Chandy, K. G. (2000) Up-regulation of the IKCa1 potassium channel during T-cell activation. *J Biol Chem* **275**, 37137–37149.
2. Kohler, R., Wulff, H., Eichler, I., Kneifel, M., Neumann, D., Knorr, A., Grgic, I., Kampfe, D., Si, H., Wibawa, J., Real, R., Borner, K., Brakemeier, S., Orzechowski, H.-D., Reusch, H.-P., Paul, M., Chandy, K. G., and Hoyer, J. (2003) Blockade of the intermediate-conductance calcium-activated potassium channel as a new therapeutic strategy for restenosis. *Circulation* **108**, 1119–1125.
3. Cheong, A., Bingham, A. J., Li, J., Kumar, B., Sukumar, P., Munsch, C., Buckley, N. J., Neylon, C. B., Porter, K. E., Beech, D. J., and Wood, I. C. (2005) Downregulated REST transcription factor is a switch enabling critical potassium channel expression and cell proliferation. *Mol Cell* **20**, 45–52.
4. Fountain, S. J., Cheong, A., Li, J., Dondas, N. Y., Zeng, F., Wood, I. C., and Beech, D. J. (2007) Kv1.5 potassium channel gene regulation by Sp1 transcription factor and oxidative stress. *Am J Physiol Heart Circ Physiol* **293**, H2719–H2725.
5. Gan, L., Hahn, S. J., and Kaczmarek, L. K. (1999) Cell type-specific expression of the Kv3.1 gene is mediated by a negative element in the 5′ untranslated region of the Kv3.1 promoter. *J Neurochem* **73**, 1350–1362.
6. Costantini, D. L., Arruda, E. P., Agarwal, P., Kim, K.-H., Zhu, Y., Zhu, W., Lebel, M., Cheng, C. W., Park, C. Y., Pierce, S. A., Guerchicoff, A., Pollevick, G. D., Chan, T. Y., Kabir, M. G., Cheng, S. H., Husain, M., Antzelevitch, C., Srivastava, D., Gross, G. J., Hui, C.-c., Backx, P. H., and Bruneau, B. G. (2005) The homeodomain transcription factor Irx5 establishes the mouse cardiac ventricular repolarization gradient. *Cell* **123**, 347.
7. Gong, N., Bodi, I., Zobel, C., Schwartz, A., Molkentin, J. D., and Backx, P. H. (2006) Calcineurin increases cardiac transient outward K+ currents via transcriptional up-regulation of Kv4.2 channel subunits. *J Biol Chem* **281**, 38498–38506.

8. Kuo, M.-H., and Allis, C. D. (1999) In vivo cross-linking and immunoprecipitation for studying dynamic protein:DNA associations in a chromatin environment. *Methods* **19**, 425–433.
9. Ooi, L., Belyaev, N. D., Miyake, K., Wood, I. C., and Buckley, N. J. (2006) BRG1 chromatin remodeling activity is required for efficient chromatin binding by the transcriptional repressor rest and facilitates rest-mediated repression. *J Biol Chem* **281**, 38974–38980.
10. Wood, I. C., Belyaev, N. D., Bruce, A. W., Jones, C., Mistry, M., Roopra, A., and Buckley, N. J. (2003) Interaction of the repressor element 1-silencing transcription factor (REST) with target genes. *J Mol Biol* **334**, 863–874.
11. Belyaev, N. D., Wood, I. C., Bruce, A. W., Street, M., Trinh, J.-B., and Buckley, N. J. (2004) Distinct RE-1 silencing transcription factor-containing complexes interact with different target genes. *J Biol Chem* **279**, 556–561.
12. Bruce, A. W., Donaldson, I. J., Wood, I. C., Yerbury, S. A., Sadowski, M. I., Chapman, M., Gottgens, B., and Buckley, N. J. (2004) Genome-wide analysis of repressor element 1 silencing transcription factor/neuron-restrictive silencing factor (REST/NRSF) target genes. *Proc Natl Acad Sci USA* **101**, 10458–10463.
13. Bingham, A. J., Ooi, L., Kozera, L., White, E., and Wood, I. C. (2007) The repressor element 1-silencing transcription factor regulates heart-specific gene expression using multiple chromatin-modifying complexes. *Mol Cell Biol* **27**, 4082–4092.
14. Zuccato, C., Belyaev, N., Conforti, P., Ooi, L., Tartari, M., Papadimou, E., MacDonald, M., Fossale, E., Zeitlin, S., Buckley, N., and Cattaneo, E. (2007) Widespread disruption of repressor element-1 silencing transcription factor/neuron-restrictive silencer factor occupancy at its target genes in Huntington's disease. *J Neurosci* **27**, 6972–6983.
15. Ooi, L. and Wood, I. C. (2007) Chromatin crosstalk in development and disease: lessons from REST. *Nat Rev Genet* **8**, 544–554.

Chapter 2

Quantitative RT-PCR Methods for Investigation of Low Copy Potassium Channel Gene Expression in Native Murine Arteries

Alex Cheong, Samuel J. Fountain, and David J. Beech

Summary

Voltage-gated K^+ channels (K_V channels) are encoded by the *KCNx* gene family and have such a wide range of properties that it is necessary to identify the precise expression profile that is instrumental in governing the electrical phenotype of a cell and its response to extrinsic factors. Real-time quantitative RT-PCR methodology has been developed and validated for specific RNA species in vascular smooth muscle cells. We have shown that most of the *KCNA* gene family, encoding the major $K_V\alpha1$ subunits, was markedly up-regulated in the resistance artery compared to the thoracic aorta, in line with reported patch-clamp recordings. Thus quantitative real-time RT-PCR data can be translated into physiological response.

Keywords: Potassium channel, Real-time RT-PCR, Smooth muscle.

2.1. Introduction

KCNA genes are mammalian homologues of the *Drosophila* melanogaster *Shaker* K^+ channel gene. Each of the *KCNA* gene products are K^+ pore-forming subunits that can be functional homotetramers, or heterotetramers consisting of any $K_V\alpha1$ but not α- or β-subunits of other K_V channels *(1)*. $K_V\alpha1$ subunits are known to be expressed throughout the vasculature including the cerebral arteries *(2–4)*, the mesenteric artery *(5, 6)* the pulmonary arteries *(7, 8)*, the coronary arteries *(9)*, the renal artery *(10)*, the portal vein *(11)* and the aorta *(5, 6, 12)*. Such differential phenotypes may be a mechanism for physiological control of a blood vessel and local tissue perfusion.

Jonathan D. Lippiat (ed.), *Methods in Molecular Biology, Potassium Channels, vol. 491*

Book doi: 10.1007/978-1-59745-526-8

Several challenges present themselves when using small tissues such as murine mesenteric arteries: the isolation of RNA from a specific type of cell – in our case the smooth muscle layer, the small amount of RNA which can be isolated, and the low copy number of genes encoding the potassium channels. Nonetheless, the advent of real-time quantitative RT-PCR has provided a reliable and straightforward methodology which we have used to describe the distinctive cell-specific expression patterns of *KCNA* genes between a conduit artery and a resistance artery *(6)*.

Coupled with other techniques such as immunocytochemistry, western blot and electrophysiology, quantitative real-time RT-PCR can provide solutions to translate the expression profile of potassium channel genes and proteins into functional signals.

2.2. Materials

2.2.1. Tissue Dissection

1. Hank's solution for dissection: 137-mM NaCl, 5.4-mM KCl, 0.34-mM NaH_2PO_4, 0.44-mM K_2HPO_4, 8-mM glucose, 5-mM HEPES, 0.01-mM $CaCl_2$, pH 7.4 with NaOH. Filtered through 0.2-μm membrane filter (NUNC), and kept on ice.
2. Dumonstar 55 dissection forceps.
3. Scalpel, size 10.
4. Sylgard 184 silicone elastomer (Dow Corning).
5. Entomological pins (local Hobby shop).
6. Endothelial removal solution: 0.1% (v/v) Triton X-100 in water.
7. Perfusion syringe for endothelial removal (1-ml Terumo syringe with Microlance 3, BD).

2.2.2. RNA Isolation and Quantification

1. Liquid nitrogen for snap-freezing tissue immediately after dissection.
2. Tissue homogeniser (Kinematica).
3. Tri-Reagent (Sigma; *see* **Note 1**).
4. Bromophenol chloroform.
5. Glycogen to act as charge carrier for RNA (Sigma).
6. Isopropanol.
7. 75% ethanol in water.
8. DNAse I (Ambion) for removal of DNA contamination.

9. DNAse inactivating reagent (Ambion).
10. RiboGreen and ribosomal RNA standards (Molecular Probes) for quantification of RNA (*see* **Note 2**).
11. PCR grade water.
12. Tris–EDTA (TE).
13. Bench-top centrifuge for quick-spin.
14. Cooled centrifuge for 13,000 rpm at 4°C.
15. LightCycler instrument (v1.5, Roche).

2.2.3. cDNA Preparation

1. Transcriptor reverse transcriptase (Roche).
2. dNTPs (Roche).
3. Oligo-dT and random primers (Roche) or gene-specific primers (Sigma).
4. DNase inhibitor (Roche).
5. PCR grade water (Roche).
6. Water bath (thermal cycler preferable).

2.2.4. RT-PCR

1. LightCycler FastStart DNA Master SYBR Green I kit (*see* **Note 3**).
2. LightCycler glass capillaries (20 µl).
3. LightCycler capillary cooling box.
4. LightCycler instrument (v1.5).

2.2.5. Gel Electrophoresis

1. Agarose.
2. Tris–borate–EDTA electrophoresis buffer (*see* **Note 4**).
3. Ethidium bromide (*see* **Note 5**).
4. 100-bp DNA ladder (New England Biolabs).
5. Electrophoresis chamber and power supply.
6. Transilluminator.

2.3. Methods

2.3.1. Dissection of Tissues

1. Sacrifice 8- week-old male C57/BL5 mice by CO_2 asphyxiation and cervical dislocation, in accordance with the local legislature and code of practice.
2. Surgically remove the thoracic aorta (approximately 0.75 mm in diameter) and place on ice-cold Hank's solution.

3. Pin out the blood vessel using entomological pins on a Sylgard-coated dissection plate (*see* **Note 6**) and submerge it in ice-cold Hank's solution.
4. Remove the fat completely by dissection.
5. Flush out the blood cells from the lumen with Hank's solution.
6. Perfuse the lumen briefly with the endothelial removal solution (*see* **Note 7**).
7. Using fine forceps, completely remove the adventitial layer (*see* **Note 8**).

2.3.2. RNA Isolation

1. The medial layer of the individual aorta is placed in a sterile 1.5 ml Eppendorf tube and snap-frozen in liquid nitrogen immediately after dissection. This sample can be stored at –80°C until required.
2. Pipet 0.5 ml of Tri-Reagent into the tube and homogenise the tissue at maximum speed for 2 min.
3. Make sure there is no carryover for the next sample by thoroughly cleaning the aggregate in molecular biology grade water.
4. Add an extra 0.5 ml of Tri-Reagent to the tube, giving a final volume of 1 ml.
5. Add 100 µl of bromophenol chloroform, mix and quick-spin.
6. Leave for 15 min at room temperature to allow separation.
7. You should be able to see separation of the protein, DNA, and RNA phases.
8. Centrifuge at 16,000×*g* for 15 min at 4°C.
9. The protein, DNA and RNA phases should be clearly defined now.
10. Carefully pipet the clear RNA solution above the white DNA ring into a sterile 1.5 ml Eppendorf tube. You should get approximately 600 µl (*see* **Note 9**).
11. Add 12.5 µl of glycogen, mix and quick-spin.
12. Add 600 µl of ice-cold isopropanol to the clear solution.
13. Mix thoroughly and leave on ice for 30 min.
14. Centrifuge at 16,000×*g* for 15 min at 4°C.
15. There should be a white pellet at the bottom of the Eppendorf tube.
16. Carefully pipet out the solution and pipet in 1 ml of ice-cold 75% ethanol.

17. Vortex the Eppendorf tube to wash the pellet and quick-spin.
18. Carefully pipet out the 75% ethanol and repeat the wash step.
19. Remove as much ethanol as possible and leave the pellet to air-dry.
20. Reconstitute the pellet in 10 µl of TE buffer.
21. Add 1.3 µl of 10× DNase buffer and mix.
22. Add 3 µl of DNase I and mix.
23. Incubate at 37°C for 45 min for DNA digestion.
24. Add 5 µl of DNase inactivation reagent. Leave for 5 min and quick-spin. The smooth muscle RNA is ready for quantification.

2.3.3. RNA Quantification Using Ribogreen

1. Prepare sufficient volume (10 µl per sample) of a working concentration of RiboGreen reagent at 1:200 dilution in TE buffer.
2. Protect the working solutions from light by covering them with foil or placing them in the dark, as RiboGreen is susceptible to photo-degradation.
3. Prepare a 10 µg/ml solution of ribosomal RNA standards in TE. This is provided in the RiboGreen Quantification kit.
4. Dilute the 10 µg/ml RNA solution to give final RNA concentrations in the TE buffer in the range of 0.1, 0.2, 0.4, 0.6, 0.8 and 1 µg/ml.
5. Transfer 10 µl of the RNA standards into individual LightCycler glass capillaries.
6. Dilute the unknown RNA 100-fold in the TE buffer and transfer 10 µl into a LightCycler glass capillary.
7. Add 10 µl of RiboGreen reagent per capillary.
8. Quick-spin in the LightCycler centrifuge.
9. Load into the LightCycler and leave for 5 min to allow the reaction to occur.
10. Start the LightCycler software and select the real-time Fluorimeter.
11. Record the Fluorescence F1 values for each sample.
12. Subtract the background F1 value of the reagent blank from that of each of the samples.
13. Use the subtracted data to construct a standard curve of fluorescence vs. RNA concentration.
14. The unknown RNA concentration can be determined from the equation of the standard curve (**Fig. 2.1**, *see* **Note 10**).

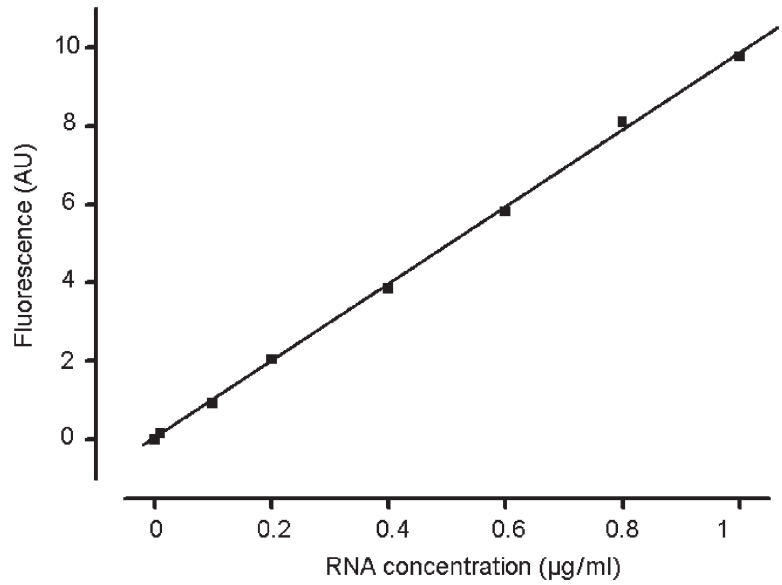

Fig. 2.1. RNA quantification curve.

2.3.4. cDNA Preparation

1. Calculate the volume of RNA required for cDNA synthesis. We usually use 0.5–1 µg.
2. Total reaction volume is 20 µl.
3. Add either gene-specific primers (final concentration 1 µM) or random hexamers (final concentration 60 µM) and oligo-dT primers (final concentration 2.5 µM) (*see* **Note 11**).
4. Add PCR grade water up to 13 µl of the reaction volume.
5. Incubate at 65°C for 10 min, then place immediately on ice for 1 min.
6. Add 4 µl of Transcriptor RT Reaction Buffer 5×.
7. Add 0.5 µl of 40 U/µl Protector RNase Inhibitor.
8. Add dNTP mix (final concentration of 1-mM each).
9. Add 0.5 µl of 20 U/µl Transcriptor Reverse Transcriptase (final concentration 10 U).
10. Vortex and quick-spin.
11. If using random hexamers and oligo-dT, incubate at 25°C for 10 min.
12. Incubate at 55°C for 30 min.
13. Incubate at 85°C for 5 min to heat-inactivate the reverse transcriptase.
14. Place on ice and store at 4°C.

2.3.5. VRT-PCR Primer Design

Primers should be designed with the aid of appropriate software, e.g. Roche provides the LightCycler Primer Design software. Attention should be paid to the optimal size of the amplicon produced during the reverse transcription (*see* **Note 12**). Real-time products are usually less than 200 bp.

The following guidelines should be observed for optimal and accurate primer design:

1. The primer's 3 ends should be free from secondary structures, repetitive sequences, palindromes and highly degenerate sequences.
2. Forward and reverse primers should not have significant complementary sequences.
3. Forward and reverse primers should have equal GC contents, ideally between 40 and 70%, with equal melting temperatures (60°C). Moreover, if there is a constant melting temperature for all primers, RT-PCR runs can be performed together in the LightCycler.

2.3.6 . RT-PCR

This protocol uses the Roche LightCycler FastStart DNA Master SYBR Green I kit.

2.3.6.1. Reaction Mix

1. Prepare the LightCycler Reaction mix by pipetting 10 µl from vial 1a, containing FastStart Taq DNA polymerase, into vial 1b, containing reaction buffer, dNTP mix, SYBR Green I and 10-mM $MgCl_2$.
2. For a 20-µl reaction, mix 2 µl of LightCycler Reaction mix, 2 µl of cDNA, forward and reverse primers (at optimised concentration), optional additional $MgCl_2$ (vial 2; *see* **Note 13**) and PCR grade water (vial 3).
3. Negative controls (such as RNA reverse-transcribed in the *absence* of the reverse transcriptase, i.e. no-RT) should always be included in real-time runs and, wherever possible, appropriate positive controls should also be included.
4. Transfer the reaction into 20-µl LightCycler glass capillaries and load it into the LightCycler carousel.
5. Quick-spin in the LightCycler centrifuge and load into the LightCycler instrument.

2.3.6.2. RT-PCR Protocol

The following procedure is optimised for use with the LightCycler 1.5 instrument. The primers used for performing the RT-PCR experiments are given in **Table 2.1**.

The RT-PCR protocol is divided into four steps:

(a) Pre-incubation to activate the FastStart Taq DNA polymerase.

(b) Amplification of the target DNA (denaturation, annealing and extension).

(c) Melting curve for PCR product identification.

(d) Cooling for complete hybridisation.

1. Pre-incubate at 95°C for 10 min to activate the FastStart Taq DNA polymerase.
2. Incubate at 95°C for 10 s to denature the cDNA.
3. Incubate at 55°C for 6 s to start the annealing process with the primers.
4. Incubate at 72°C for 16 s to start extension of the amplicon, and acquire fluorescent reading.

Table 2.1
PCR primers for potassium channel mRNA detection (reproduced from ref. *6*)

Gene	Accession no.	Primer 5′–3′	Amplicon size (bp)	Amplicon T_m (°C)	Efficiency[a]
β-*actin*	NM_007393	F_1 CACTATTGGCAACGAGC R_1 CGGATGTCAACGTCAC	126	83.1	1.82 ± 0.05
KCNA1 (K_Vα1.1)	NM_010595	F_1 TCTAGCGCAGTGTACTT R_1 GGCTATGCTATTGTTCATA	378	88.3	1.76 ± 0.05
KCNA2 (K_Vα1.2)	NM_008417	F_1 TCGATCCCCTCCGAAA R_1 CTAAGGGCACGTTCACA	114	86.5	1.81 ± 0.03
		F_2 CACCCACAAGACACCT R_2 GGCGGTTGCGATCAAA	192	85.1	1.96 ± 0.02
KCNA3 (K_Vα1.3)	NM_008418	F_1 GCTTCCCGAGTTTCGC R_1 CCCATTACCTTGTCGTTC	298	88.9	1.89 ± 0.06
		F_2 AGGACAGACGCTGAAG R_2 AGTTGGAAACAA TCACAGG	287	87.6	1.86 ± 0.03
KCNA4 (K_Vα1.4)	NM_021275	F_1 CCCTAAGAGCCAGCAT R_1 GGTTAAGACACCCGCA	245	ND	ND
KCNA5 (K_Vα1.5)	NM_008419	F_1 GAGCCGTTGAAGTGGT R_1 AAATGCACTCGTCAGC	215	81.5	2.10 ± 0.05
KCNA6 (K_Vα1.6)	NM_013568	F_1 CGCTGTCTACTTCGCAG R_1 CTCGATGTGGAGTCGG	380	ND	ND
KCNA7 (K_Vα1.7)	NM_010596	F_1 CCTAAGGGTCATCCGA R_1 CCCATAGCCAACCGTG	259	ND	ND
KCNAB1 (K_Vβ1)	NM_010597	F_1 AAATGACGGTGTGAGT R_1 CAGTATGTTATCAATCTCG	127	84.8	2.17 ± 0.01
KCNB1 (K_Vα2.1)	NM_008420	F_1 AGCAATAGCGTTCAACTT	239	87.0	1.78 ± 0.06

ND not determined, *F* forward, *R* reverse

[a]Mean ± SEM efficiency determined for ≥4 independent cDNA templates

5. Repeat **steps 2–4** for 40 cycles.
6. Incubate at 65°C for 15 s.
7. Ramp up the temperature to 95°C at a rate of 0.1°C/s while continuously acquiring fluorescent readings (*see* **Note 14**).
8. Cool the reaction to 40°C and hold for 30 s for complete hybridisation.

2.3.7. RT-PCR Quantification

2.3.7.1. Identification of the Desired Amplicon

Real-time PCR reactions can be analysed by melting curve analysis to differentiate primer dimers from specific PCR products. A typical plot of the dissociation curve is shown in **Fig. 2.2**. However, if the raw data from a melting profile are presented as a first derivative plot of fluorescence units against temperature, this provides a clearer view of the rate of SYBR Green I loss and the temperature range over which it occurs (**Fig. 2.2**). Primer dimers usually melt at lower temperatures than specific PCR products and thus the small peaks are most likely primer dimers of non-specific product formation. It is also useful to analyse the results by agarose gel electrophoresis to correlate product length with melting peaks, to identify PCR artefacts (**Fig. 2.3**) and to sequence the PCR product to validate the result.

1. To pour an agarose gel, agarose powder is mixed with the electrophoresis buffer to the desired concentration (2%). Prevent it from boiling over.
2. Heat in a microwave oven until completely melted.
3. Cool the solution to about 60°C before adding ethidium bromide to the gel (final concentration 0.5 µg/ml).
4. Pour the solution into a casting tray containing a sample comb and allow to solidify at room temperature.
5. After the gel has solidified, remove the comb, taking care not to rip the bottom of the wells. If there are excess lanes

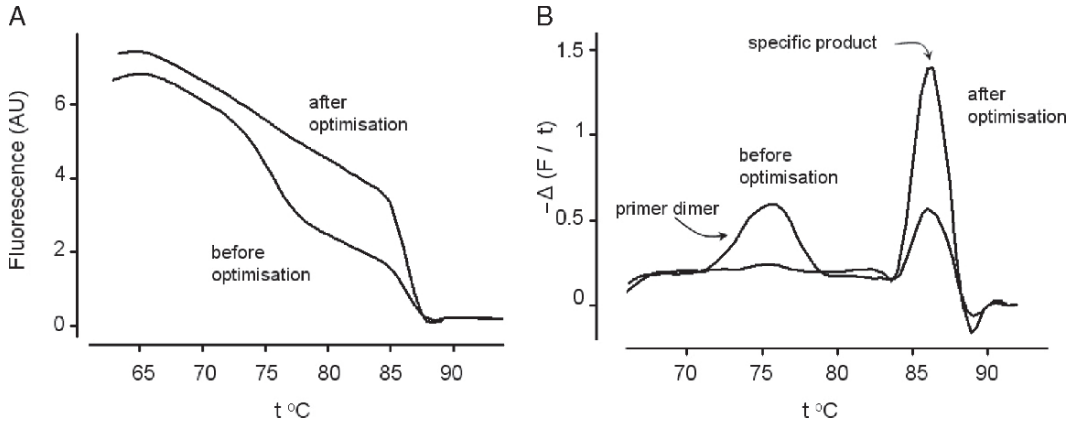

Fig. 2.2. Melting curve for aorta samples investigated by RT-PCR for $K_V\alpha 1.3$. (A) Dissociation curves before and after optimisation of the PCR reaction. (B) First derivative plot of fluorescence against temperature reveals the initial presence of a primer dimer prior to optimisation. This subsequently disappears after improving reaction conditions, leaving a single specific melting curve.

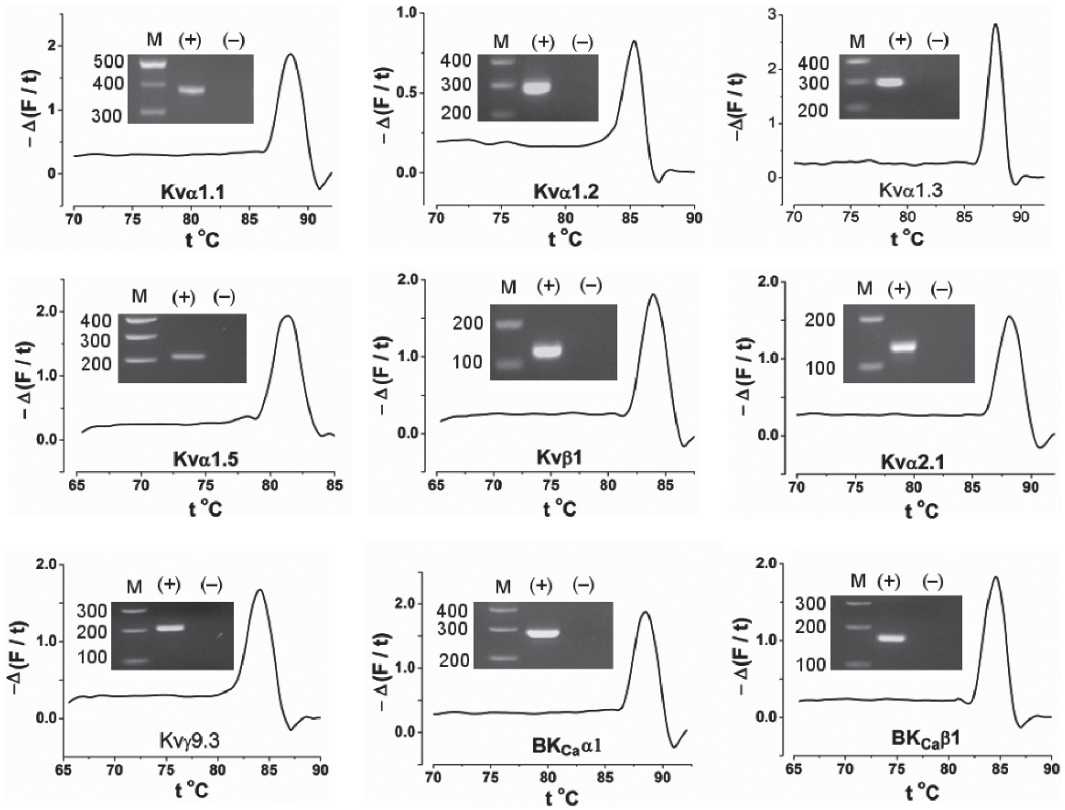

Fig. 2.3. Specificity of detection in aorta samples using F_1/R_1 primer sets (**Table 2.1**). Derivative melting curve analyses are shown with inset agarose gels (reproduced from **ref. 6**).

available, that section of the gel can be cut out with a scalpel blade and stored at 4°C for future use.

6. The gel, still in its plastic tray, is inserted horizontally into the electrophoresis chamber and just covered with electrophoresis buffer.
7. Samples mixed with the loading buffer are then pipetted into the sample wells.
8. Close the lid and run the gel at 50–70 V. DNA will migrate towards the positive electrode (usually coloured red).
9. When adequate migration has occurred, DNA fragments are visualised by the ethidium bromide bound between the bases of the DNA.
10. Place the gel on an ultraviolet transilluminator to visualise vthe DNA and take a photograph of the gel.

2.3.7.2. Quantification Analysis

Real-time PCR results can be analysed in a variety of ways depending on the application. Analyses of quantitative standards can be used to generate PCR curves and from these the

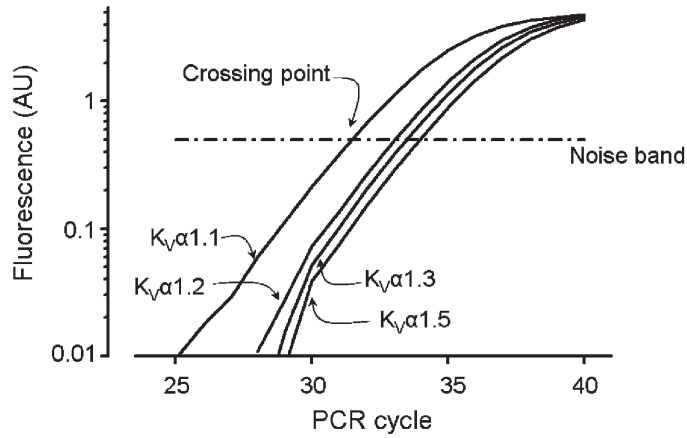

Fig. 2.4. SYBR Green fluorescence-cycle plots for *KCNx* genes in aorta. Crossing point (C_p) is the intersection with the horizontal dotted line (set at 0.5).

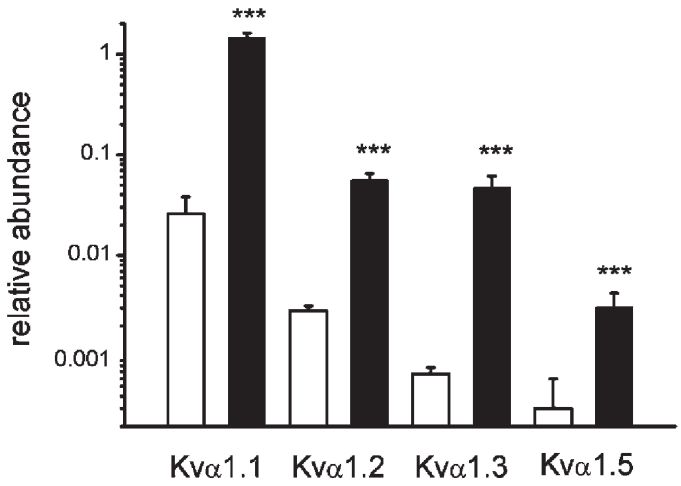

Fig. 2.5. Conduit vs. resistance artery for RNA encoding $K_V\alpha1$ (reproduced from **ref. 6**).

cycle number at which the fluorescent signal increases above a predetermined background value (C_p, crossing point) can be determined (**Fig. 2.4**). This crossing point can be used for the comparison of results from sample to sample and can be used to generate quantitative results.

2.3.7.3. Relative Quantification

1. Record the crossing point of the gene of interest (e.g. *KCNA1*) and an appropriate housekeeper gene (e.g. *β-actin*).
2. Use the equation $2^{C_p(\beta\text{-actin})} / 2^{CP(KCNA1)}$ to calculate the relative abundance of *KCNA1* to *β-actin* (*see* **Note 15**).

Fig. 2.5 shows the SYBR Green-cycle plots for *KCNx* genes in the samples from the two different vascular beds: the aorta and the mesenteric. Analysis of the relative abundance of the RNA shows that there is significantly more $K_V\alpha1.1$, 1.2, 1.3 and 1.5 in the mesenteric artery than in the aorta.

2.4. Notes

1. Tri-Reagent is toxic and prolonged exposure to phenol fumes or contact with skin can be hazardous. If possible, please use a fume hood.
2. RiboGreen is an ultrasensitive fluorescent nucleic acid stain for measuring RNA concentration in solution.
3. SYBR Green I is a minor groove-binding dye which typically exhibits 20–100-fold fluorescence enhancement on binding to double-stranded DNA.
4. Tris–borate–EDTA (TBE) is used for small (<1 kb) DNA and shows increased resolution of small DNA whereas Tris–acetate–EDTA (TAE) is used for DNA recovery and electrophoresis of large (>12 kb) DNA.
5. Ethidium bromide is an intercalating agent commonly used as a nucleic acid stain in molecular biology laboratories for techniques such as agarose gel electrophoresis. When exposed to ultraviolet light, it will fluoresce with a red-orange colour, intensifying almost 20-fold after binding to DNA. Ethidium bromide may be a very strong mutagen, and may possibly be a carcinogen or teratogen, although this has never been definitively proved. High concentration of ethidium bromide (e.g. when the colour of the gel is dark pink or red) should be placed in the biohazard box for incineration.
6. Sylgard is a silicone elastomer. Mix the base part to the curing part at a ratio of 10:1, pour sufficient volume into a 10-cm culture dish with a sufficient depth of 5 mm and leave for 4 h at 65°C before use. The use of the Sylgard-coated surface will prolong the life of the dissection forceps and provide a base for pinning the entomological pins.
7. The act of removing the endothelial layer can damage the tissue. A wire myography experiment can be done to validate the vessel health and complete the endothelial removal. Phenylephrine (10 μM) and acetylcholine (1 μM) will induce contraction in the intact aorta but not in the endothelial-denuded vessel.
8. Co-staining of aorta sections with an antibody against smooth muscle α-actin and a nuclear stain such as DAPI will validate the removal of the endothelial and adventitial layers.
9. DNA and protein can be recovered from the remaining solution by further precipitation.
10. The Microsoft EXCEL macrofunction is a very handy tool to work out the solutions to the RNA concentration equation.

11. Priming of the cDNA reaction from the RNA template can be done using random primers, oligo-dT, or gene-specific primers. The melting temperature T_m of random primers and oligo-dT is low, and hence neither of these can be used with thermostable RT enzymes without a low temperature pre-incubation step. Random primers are by definition non-specific, but yield the most cDNA and are the most useful for transcripts with significant secondary structure. cDNA synthesis with oligo-dT is more specific than random priming, although it will not prime RNAs that lack a poly-A tail such as ribosomal 16S. Gene-specific primers synthesise the most specific cDNA and provide the most sensitive method for quantification, but the RT-PCR reactions are restricted to the genes primed for. In the case of *KCNx* genes in smooth muscle cells, we synthesised cDNA using gene-specific primers to improve detection.
12. Optimal primer concentration should be determined, with a final concentration ranging from 0.1 to 0.5 µM for both primers. For some assays, the optimal concentration for the two primers will not be the same, and it will be necessary to use asymmetric priming, where a lower concentration of one primer is used, to achieve good melting curves. If the problem persists, it is advisable to design new primers.
13. A key variable is the magnesium chloride ($MgCl_2$) concentration since Mg^{2+} affects the specificity and the yield of PCR *(13)*. Concentrations that are too high may lead to incomplete denaturation and low yields, and can also lead to increased production of non-specific products and primer artefacts including primer dimers. Levels that are too low reduce the ability of polymerase to extend the primers. Optimum $MgCl_2$ concentration in the LightCycler instrument ranges from 1 to 5 mM. It is recommended that a $MgCl_2$ titration be performed for each primer set.
14. This will dissociate the SYBR Green from any double-stranded DNA, including any primer dimers, contaminating DNA, and PCR products from mis-annealed primers.
15. Quantitative RT-PCR can be expressed relative to an internal standard. Relative quantification determines the changes in steady-state mRNA levels of a gene relative to the levels of an internal control, usually a housekeeping gene such as *β-actin*, GAPDH or ribosomal 16S. Therefore, relative quantification does not require standards with known concentrations and all samples are expressed as an *n*-fold difference relative to the housekeeper gene, and the number of target gene copies are normalised to the housekeeper gene. If the aim is to compare the relative abundance of *1* gene in *different* tissues, knowing the PCR efficiency is not important,

as it will cancel out. Hence, remembering that DNA amplification is exponential and assuming a 100% PCR efficiency (i.e. each cycle brings a doubling of the product and hence an efficiency value of 2), the equation for the relative abundance of *KCNx* to a housekeeper gene is as described under **Subheading 2.3.7.3**.

However, if the aim is to compare the relative abundance of *2* genes in the *same* tissue, it is necessary to determine the PCR efficiency when using each primer set. The PCR efficiency for a given primer set can be easily obtained by performing RT-PCR using the primer set on serial DNA dilutions. The PCR efficiency is then calculated from the slope value for the derived standard curve:
Efficiency E_{geneX} using X primer set = $10^{-1/\text{slope}}$.
Thus,

$$\text{Relative abundance of } X = \frac{E_{housekeeper}^{C_p(housekeeper)}}{E_{genex}^{C_p(KCNx)}}.$$

Acknowledgements

This work was supported by the British Hearth Foundation and the Wellcome Trust.

References

1. Coetzee, W.A., Amarillo, Y., Chiu, J., Chow, A., Lau, D., McCormack, T., Moreno, H., Nadal, M.S., Ozaita, A., Pountney, D., Saganich, M., Vega-Saenz de Miera, E., and Rudy, B. (1999) Molecular diversity of K^+ channels. *Ann. NY Acad. Sci.* **868**, 233–285.
2. Cheong, A., Dedman, A.M., and Beech, D.J. (2001) Expression and function of native potassium channel K(V)alpha1 subunits in terminal arterioles of rabbit. *J. Physiol.* **534**, 691–700.
3. Albarwani, S., Nemetz, L.T., Madden, J.A., Tobin, A.A., England, S.K., Pratt, P.F., and Rusch, N.J. (2003) Voltage-gated K+ channels in rat small cerebral arteries: molecular identity of the functional channels. *J. Physiol.* **551**, 751–763.
4. Chen, T.T., Luykenaar, K.D., Walsh, E.J., Walsh, M.P., and Cole, W.C. (2006) Key role of Kv1 channels in vasoregulation. *Circ. Res.* **99**, 53–60.
5. Cox, R.H., Fromme, S.J., Folander, K.L., and Swanson, R.J. (2008) Voltage gated K(+) channel expression in arteries of Wistar–Kyoto and spontaneously hypertensive rats. *Am. J. Hypertens.* **21**, 213–218.
6. Fountain, S.J., Cheong, A., Flemming, R., Mair, L., Sivaprasadarao, A., and Beech, D.J. (2004) Functional up-regulation of KCNA gene family expression in murine mesenteric resistance artery smooth muscle. *J. Physiol.* **556**, 29–42.
7. Yuan, X.J., Wang, J., Juhaszova, M., Golovina, V.A., and Rubin, L.J. (1998) Molecular basis and function of voltage-gated K^+ channels in pulmonary arterial smooth muscle cells. *Am. J. Physiol.* **274**, L621–L635.
8. Moudgil, R., Michelakis, E.D., and Archer, S.L. (2006) The role of k+ channels in determining pulmonary vascular tone, oxygen sensing, cell proliferation, and apoptosis:

implications in hypoxic pulmonary vasoconstriction and pulmonary arterial hypertension. *Microcirculation* **13**, 615–632.

9. Chai, Q., Xu, X., Jia, Q., Dong, Q., Liu, Z., Zhang, W., and Chen, L. (2007) Molecular basis of dysfunctional Kv channels in small coronary artery smooth muscle cells of streptozotocin-induced diabetic rats. *Chin. J. Physiol.* **50**, 171–177.
10. Fergus, D.J., Martens, J.R., and England, S.K. (2003) Kv channel subunits that contribute to voltage-gated K+ current in renal vascular smooth muscle. *Pflugers Arch.* **445**, 697–704.
11. Thorneloe, K.S., Chen, T.T., Kerr, P.M., Grier, E.F., Horowitz, B., Cole, W.C., and Walsh, M.P. (2001) Molecular composition of 4-aminopyridine-sensitive voltage-gated K(+) channels of vascular smooth muscle. *Circ. Res.* **89**, 1030–1037.
12. Fountain, S.J., Cheong, A., Li, J., Dondas, N.Y., Zeng, F., Wood, I.C., and Beech, D.J. (2007) K(v)1.5 potassium channel gene regulation by Sp1 transcription factor and oxidative stress. *Am. J. Physiol.* **293**, H2719–H2725.
13. Oste, C. (1988) Polymerase chain reaction. *Biotechniques* **6**, 162–167.

Chapter 3

Cloning of Potassium Channel Splice Variants from Tissues and Cells

Lie Chen and Michael J. Shipston

Summary

Potassium channels display considerable functional diversity. Alternative pre-mRNA splicing represents one of the most powerful post-transcriptional mechanisms to create physiological diversity by generating multiple protein products from a single gene. Due to the modular nature of proteins, alternative splicing can profoundly modify potassium channel structure, function and regulation. Alternative pre-mRNA splicing is exploited by most genes but is particularly prevalent in single gene families as exemplified by the gene (*KCNMA1*), which encodes large conductance calcium- and voltage-gated potassium (BK) channel α-subunits. Importantly, alternative pre-mRNA splicing is kept under spatiotemporal control by circulating hormones and cellular activity, as well as being differentially modified during development and in different tissues. While the sequencing of numerous genomes has further demonstrated the importance of splicing in generating diversity from a limited genome size, a major challenge is to define splice variants that are expressed in tissues and their functional role. Here we describe strategies and protocols to experimentally define and isolate splice variant mRNA transcripts in multiple tissues and provide a platform to characterise the effect of splice variants on channel function and physiology.

Key words: Alternative splicing, *KCNMA1,* BK channel, Calcium-activated potassium channel, RT-PCR, mRNA.

3.1. Introduction

Potassium channels play a central role in diverse physiological processes, from the setting of cell resting potentials to the control of blood pressure, neuronal excitability, endocrine hormone secretion and electrolyte balance. The eclectic role of potassium channels in physiology requires mechanisms to generate considerable diversity in channel properties and function. The pore-forming α-subunits of potassium channels are encoded by multiple gene families and may assemble as heteromeric complexes to form the

Jonathan D. Lippiat (ed.), *Methods in Molecular Biology, Potassium Channels, vol. 491*

Book doi: 10.1007/978-1-59745-526-8

functional pore. In addition, potassium channels can assemble with, and be regulated by, an array of accessory subunits and distinct intracellular signalling complexes.

An important additional post-transcriptional mechanism for generating physiological diversity in potassium channels is through alternative pre-messenger RNA splicing. Alternative pre-mRNA splicing represents one of the most powerful post-transcriptional mechanisms to generate physiological diversity from a limited genome by generating multiple protein isoforms from a single gene *(1–5)*. More than 70% of human genes display alternative pre-mRNA splicing *(1–5)* and mis-splicing events are major determinants of human disease *(6–8)*. Alternative pre-mRNA splicing is utilised extensively by single gene families ***(4)***, as exemplified by the gene (*KCNMA1*), which encodes large conductance calcium- and voltage-activated (BK) potassium channels ***(9–11)***. Alternative pre-mRNA splicing of the BK channel α-subunit plays a major role in determining the functional properties of BK channels and multiple sites of splicing have been identified in the α-subunit ***(10***, ***11)***. Alternatively spliced variants can display different calcium- and voltage-sensitivities ***(12–15)***, regulation by protein phosphorylation ***(15–18)*** and other intracellular signalling cascades ***(19***, ***20)*** as well as cell-surface expression ***(14***, ***21***, ***22)***.

Importantly, BK channel alternative pre-mRNA splicing is spatiotemporally regulated in a dynamic manner via cellular excitability, circulating hormones and during development ***(23–25)***. The ability to rapidly identify splice variants that are expressed in tissues is thus of paramount importance to further our understanding of alternative splicing in the regulation and function of potassium channels in health and disease.

Here we present strategies and protocols that we have successfully employed ***(15)*** to isolate and characterise existing and novel sites of splicing C2 BK channel mRNA splice variants in mammalian tissues (**Fig. 3.1**).

We discuss strategies to generate high quality total RNA from cells and tissues, convert this to cDNA and PCR to amplify splice variants for the gene of interest, and exploit a rapid subcloning procedure to allow rapid identification and sequencing of novel splice variants.

3.2. Materials

3.2.1. Isolation of Total RNA from Tissues and Cells

All procedures in this section require the use of RNase-free reagents and consumables (*see* **Subheading 3.3.1.2**). All solutions should be treated with 0.1% diethylpyrocarbonate (DEPC) to inactivate RNases and autoclaved as for **step 1** below, except for Tris–HCl buffers, which should be made with RNase-free water.

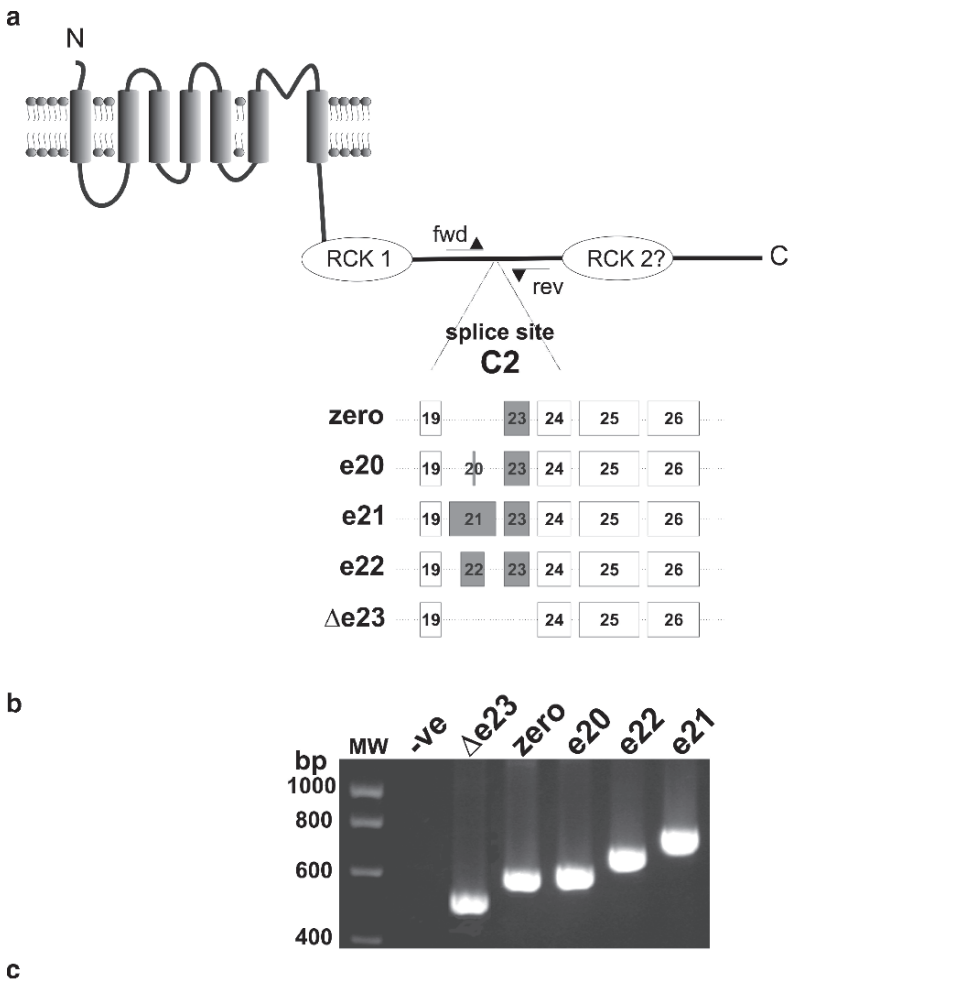

Fig. 3.1. Analysis of splice variant mRNA transcripts at the intracellular C-terminal C2 site of splicing in the murine BK channel. (**a**) Pore-forming α-subunit of large conductance calcium- and voltage-activated potassium (BK) channels encoded by the *KCNMA1* gene. The C2 site of splicing is located in the intracellular C-terminus of the channel. Alternative pre-mRNA splicing in the mouse at site C2 results in five different splice variants at this site as illustrated schematically. In the ZERO variant exon 19 is spliced to exon 23, in variants e20, e21 (also known as STREX) and e22 the respective exon is included between exons 19 and 23. *Open boxes* indicate constitutive exons whereas *shaded boxes* indicate alternatively spliced exons identified in mouse. *The number* in each box refers to the respective murine exon. Note that exon 23 was previously considered as a constitutive exon; however, analysis revealed a novel variant in which exon 23 is skipped (Δe23). This results in a frame shift and a premature truncation of the protein (*see* **ref. *15***). The PCR screening strategy employed a forward (fwd) PCR primer located in exon 15 and a reverse (rev) primer in exon 25 to span several putative exons and introns. (**b**) Representative SYBR® Safe stained DNA agarose gel (as in **Subheading 3.3.3.3**) illustrating size fractionation of different sized PCR amplicons. This corresponds to the different site C2 splice variants, resulting from the PCR screen identified using the strategy outlined. (**c**) Translation of the DNA sequence of identified PCR amplicons reveals the different amino acid sequences (single amino acid code) resulting from the alternative splicing decisions for each variant. Amino acids in bold indicate the respective splice variant specific insert sequences.

1. RNase-free water: add 0.1% DEPC to 18-MΩ quality distilled water in an RNase-free bottle, shake vigorously and leave to stand overnight with loose fitting cap. Autoclave for at least 15 min on a standard wet-cycle. Aliquot small working stocks (~10 ml) for day to day use in RNA extraction procedures. Discard working stock regularly.
2. Qiagen RNeasy mini spin column kit (includes spin columns, buffers RLT, RW1 and RPE, Cat. no. 74104).
3. Ethanol: use 96–100% ethanol stored in small aliquots at room temperature.
4. Ultrapure agarose: have separate stocks for RNA and DNA gels.
5. 10-mM Tris–HCl, pH 7.0 made up in RNase-free water: store in small aliquots at room temperature.
6. RNA gel buffer (RGB): prepare 10× stock in RNase-free water with 200-mM 3-[*N*-morpholino]propanesulfonic acid (MOPS), 50-mM sodium acetate and 10-mM EDTA, pH to 7.0 with NaOH. Autoclave and store at room temperature.
7. RNA gel running buffer (RGRB): prepare 1-L fresh solution containing 100 ml of 10× RNA gel buffer, 20 ml of 37% (12.3 M) formaldehyde and 880 ml of RNase-free water in a fume hood.
8. RNA loading buffer (RLB): prepare 10 ml of a 5× stock solution in RNase-free water containing 4 ml of 10× RNA gel buffer, 20% glycerol, 33% formamide, 4-mM EDTA, pH 8.0, 0.2% bromophenol blue, 0.2% xylene cyanol. Store as 250-µl aliquots at –20°C or at 4°C for up to 3 months.
9. 0.5% SDS: 0.5% (w/v) sodium dodecyl sulfate in RNase-free water.
10. Ethidium bromide (EtBr): prepare 10-mg/ml stock in RNase-free water and store in dark bottle at 4°C. Caution - mutagenic (*see* **Note 1**).
11. Sodium acetate: prepare a 3-M stock solution in RNase-free water and adjust pH to 5.2 with acetic acid. Store as 0.5-ml aliquots at –20°C.
12. Cell lysis buffer (RLN, optional): 50-mM Tris–HCl, pH 8.0, 140-mM NaCl, 1.5-mM $MgCl_2$, 0.5% (v/v) Nonidet P-40. Prepare with RNase-free water.
13. RNase-free DNase 1: store reconstituted enzyme at 2–3 Kunitz units (KU)/µl in RNase-free water and 10× DNase 1 reaction buffer in small aliquots at –20°C.

3.2.2. First Strand cDNA Synthesis and PCR Amplification of Splice Variants

1. Qiagen Omniscript RT kit (Cat. no. 205111).
2. Random hexamer primers: prepare a 100-µM stock by re-suspending in RNase-free water. Prepare 10-µl aliquots and store at –20°C.

3. Oligo-dT primer: prepare a 10-µM stock by re-suspending in RNase-free water. Prepare 10-µl aliquots and store at –20°C.
4. RNA inhibitor (e.g. RNAsin from Promega, Cat. no. N2111): store at –20°C. Dilute to 10 U/µl with RNase-free water, immediately prior to use.
5. dNTP mix (dATP, dCTP, dGTP, dTTP): prepare 25-mM stock of each dNTP in RNase-free water. Prepare 10-µl aliquots and store at –20°C.
6. Taq DNA polymerase (Invitrogen, Cat. no. 18038-042): includes 10× PCR buffer, 50-mM $MgCl_2$ and Taq DNA polymerase.
7. Forward gene specific PCR primer: re-suspend in dH_20 and dilute to 10 pmol/µl. Store as 25-µl aliquots at –20°C.
8. Reverse gene specific PCR primer: re-suspend in dH_20 and dilute to 10 pmol/µl. Store as 25-µl aliquots at –20°C.
9. Autoclave RNase-free water.
10. DNA gel buffer (TBE) (10×): 0.89-M Tris base, pH 8.3, 0.89-M boric acid, 2-mM EDTA, pH 8.0. Autoclave and store at room temperature.
11. DNA loading buffer (10×): 50-mM Tris–HCl, pH 7.6, 60% glycerol and 0.25% (w/v) bromophenol blue. Store at room temperature in 1-ml aliquots.
12. SYBR® Safe DNA gel stain (10,000× concentrate, Invitrogen, Cat. no. S33102) store at room temperature in small aliquots.

3.2.3. Subcloning, Plasmid Amplification and Analysis of Splice Variant Amplicons

1. pCRII TOPO, or pCR2.1 TOPO cloning kit (Invitrogen, Cat. no. K4650-01 or K4500-01): includes TOPO vector and 6× TOPO Salt buffer (1.2-M NaCl and 0.06-M $MgCl_2$) with ligase.
2. Competent *E. coli* for transformation (*see* **Note 2**) (e.g. one shot chemical TOP 10 competent cells with TOPO cloning kit): store in 200-µl aliquots at –80°C.
3. LB (Luria Bertani) medium: combine 10 g of tryptone, 5-g yeast extract and 5-g NaCl in 1 L of dH_2O, Adjust pH to 7.4 using 1-M NaOH, divide into 250-ml fractions in glass bottles and autoclave.
4. LB-agar plates: add 3.75 g of bactoagar to 250 ml of LB broth in a glass bottle, autoclave to dissolve and sterilise. To prepare LB-agar plates with 100-µg/ml ampicillin heat the LB-agar in a microwave to melt, swirl the LB-agar to ensure that it is completely dissolved and allow it to cool to around 37°C. Add 250 µl of 100-mg/ml stock ampicillin and pour into 10-cm disposable Petri dishes, using the aseptic technique. Flame the surface of agar plates with a Bunsen burner to remove bubbles, cover and allow to set. Store the plates inverted and wrapped in nescofilm at 4°C for up to 2 weeks. Before use pre-warm to 37°C by inverting the Petri dish and placing it in a 37°C incubator, removing the condensate from the lid.

5. Ampicillin: prepare stock solution of 100 mg/ml in sterile dH_2O. Store in 0.5-ml aliquots at –20°C. Use at a final concentration of 100 μg/ml.
6. DNA miniprep plasmid purification: QIAprep spin miniprep kit (Qiagen, Cat. no. 27104).

3.3. Methods

3.3.1. General Design Considerations

3.3.1.1. Choice of Tissue/Cells

1. As pre-mRNA splicing is dynamically regulated, the choice of cell type, culture conditions, tissue type and physiological status of the host animal can all determine the splice variants identified.
2. The procedures given below are designed to allow parallel processing of multiple cell culture samples (e.g. from 6-well plates) or multiple tissues.

The procedures are optimised for handling < 25 mg of tissue or 1×10^5–1×10^6 cells to give < 50-μg total RNA. The tissues/cell lines contain different amounts of RNA, so pilot experiments with the system of interest to determine RNA content are useful in avoiding overloading of the RNA extraction method that can lead to RNA degradation and inefficient cDNA representation.

3.3.1.2. General Considerations to Minimise Risk of Contamination and Maintenance of an RNase-Free Environment

1. There is no substitute for good laboratory practice. Therefore ensure that the work area is tidy and clean and that waste is disposed of promptly. The lab bench should be swabbed with 70% ethanol on a regular basis.
2. Keep all stocks in sterile containers and in aliquots sufficient for a single experiment. Sterilisation of containers and bulk buffer solutions is routinely performed by autoclaving. For glassware used for RNA isolation wash in RNase-free water and autoclave.
3. Clean automatic pipettes regularly and use separate sets for PCR and RNA isolation.
4. Do not share stocks/aliquots between investigators/experiments.
5. Prepare all reagents with gloved (latex or nitrile) hands and ensure that gloves are replaced frequently. Wear a lab coat that is frequently laundered.
6. Use nuclease-free pipette tips with an integral filter to minimise cross-contamination.
7. Open Eppendorf and other tubes carefully. Avoid aerosols/leaks and clean immediately. For PCR tubes a PCR closing tool is useful to avoid gloved fingers coming into contact with the lid.
8. Wherever possible separate the following activities into different zones: RNA isolation and first strand cDNA synthesis, PCR, bacteria plate and growth.

3.3.1.3. Design of PCR Primers for Splice Variant Analysis

1. PCR primers should be designed (e.g. Using Vector NTI software, Invitrogen) within known exons and to span known introns. The choice of the primer location will depend on the splice site(s) under investigation (**Fig. 3.1**).
2. Aim to generate amplicons between 0.2 and 1 kb in size for the splice variants you might expect for efficient PCR and subsequent ligation into the cloning vector.
3. To facilitate downstream analysis (e.g. subcloning splice variant into full length channel construct for functional analysis) try and choose primers that flank two unique endonuclease restriction sites (*see* **Note 3**).
4. If primers do not span unique sites, engineer silent restriction sites, using unique restriction sites for endonucleases of high efficiency (e.g. *Kpn*I, *Bam*HI) in the respective forward and reverse primers.
5. Optimise primers based on the following criteria:
    1. Design forward and reverse primers from available Genbank sequences for species of interest with primer length between 19 and 25 bp, which prevents chances of cross-contamination (e.g. cloning a human when you are looking for mouse variants).
    2. Design primers to span several known exons – for example some tissues previously considered 'constitutive exons' may in fact be regulated by alternative pre-mRNA splicing (15).
    3. GC content should be between 40 and 60% and one should verify lack of secondary structure or primer dimer formation.
    4. Melting temperature (T_m) should be between 50 and 65°C, determined from the relationship $T_m = 4(G+C) + 2(A+T)$. Note: the primer and the T_m should be matched as closely as possible.
    5. Include a C or G nucleotide at the 3′ end of each primer.
    6. As amplicons will be subcloned into the TOPO vector do not use primers with 5′ phosphorylation.
    7. BLAST search (http://www.ncbi.nlm.nih.gov/BLAST/) your forward and reverse primers to verify the nucleotide sequence and specificity for the target gene.
6. Re-suspend primers in sterile autoclaved dH_2O to 10 pmol/µl. Store as small (20 µl) aliquots in sterile 0.5-ml Eppendorf tubes at –20°C. Do not reuse opened aliquots as inappropriate preparation/storage of primers is a major source of contamination.

3.3.2. Isolation of Total RNA from Tissues and Cells

3.3.2.1. Homogenisation of Small (<25 mg) Tissue Samples

1. Remove the tissue of interest rapidly, using aseptic techniques to minimise cross-contamination of tissue. If tissues are to be dissected, use fresh scalpel blades to generate a small block of tissue sample (<25 mg).
2. Freeze the tissue block by placing it on a single layer of tin foil placed on a bed of dry ice pellets (*see* **Note 4**).

3. If the tissue is not to be processed immediately, wrap the tissue loosely in labelled tin foil, place in pre-cooled plastic storage tube (50-ml Falcon tube) and store at −80°C until use (*see* **Note 5**).
4. Small frozen tissue sections can be conveniently crushed using a sharp blow from a small metal hammer, with the tissue wrapped in two layers of tin foil, and placed on a metal tray on a bed of dry ice.
5. (optional: if large >1-mm^3 fragments remain). Rapidly transfer tissue fragments by 'pouring' into a pre-cooled RNase-free pestle and mortar, using the tin foil as a funnel, and grind to a fine powder.
6. Add 600 µl of pre-cooled Qiagen tissue homogenisation buffer (RLT) to lyse the tissue. Optionally, or if the solution becomes very viscous with genomic DNA, shear the lysate through an RNase-free gauge 20 (20 g) needle and 1-ml syringe for 5–6 strokes.
7. Add 430-µl of 100% ethanol to the lysate and mix well by repeated pipetting using a 1-ml Gilson pipette.
8. Proceed to **Subheading 3.3.2.3** below to purify RNA using an RNeasy spin column.

3.3.2.2. Homogenisation of Cultured Cells in Monolayer

1. Remove all growth medium from the well (*see* **Note 6**) of 6-well plate (1×10^5–1×10^6 cells) by holding the plate at ~30° angle and aspirate by using a suction line with a 20-g needle placed at the intersection between the well floor and wall at the bottom of the plate (*see* **Note 7**).
2. Add 600 µl of Qiagen RNA extraction buffer (RLT), which includes guanidium thiocyanate salts that inhibit RNases (*see* **Note 8**), and repeatedly triturate the lysate over the well to remove all the lysed cells. Drain the lysate to the base of well as above (*see* **Note 9**), transfer the lysate to an RNase-free 1.5-ml Eppendorf tube and vortex vigorously for 10 s.
3. If the solution has visible cell clumps or becomes very viscous with genomic DNA, shear the lysate through an RNase-free 20-g needle and 1-ml syringe for 5–6 strokes.
4. Add 430-µl of 100% ethanol to the vortexed lysate and mix well by repeated pipetting, using a 1-ml Gilson pipette. DO NOT CENTRIFUGE. In some cell lines a small precipitate may result; if this is the case, transfer any precipitate with the lysate to the next step. This has no effect on the final RNA yield/purity.
5. Proceed to **Subheading 3.3.2.3** below to purify RNA using an RNeasy spin column.

3.3.2.3. Purification of RNA Using Qiagen RNeasy Mini Spin Columns

1. Transfer ~700 µl of the tissue (from **Subheading 3.3.2.1**) or cell (from **Subheading 3.3.2.2**) lysate into an RNeasy mini spin column by pipetting the lysate directly onto the filter.

Label the spin columns with a permanent marker on the side when processing multiple samples.

2. Place the spin column in the supplied 2-ml collection tube and place it carefully in the centrifuge rotor. Centrifuge at ~10,000×*g* for 15 s at room temperature (21–24°C) to bind the RNA to the silica membrane.
3. Carefully remove the filter from the collection tube, discard the flow through (*see* **Note 10**) and repeat **steps 2** and **3** for the remaining lysate using the same collection tube.
4. Add 700 µl of Qiagen RW wash buffer to the spin column. Centrifuge at ~10,000×*g* for 15 s at room temperature (21–24°C). Remove the filter carefully from the collection tube and discard the flow through.
5. Add 500 µl of Qiagen RPE wash buffer to wash the RNeasy spin column membrane. Centrifuge at ~10,000×*g* for 15 s at room temperature (21–24°C). Carefully remove the filter from the collection tube and discard the flow through.
6. Re-centrifuge spin column at 10,000×*g* for 2 min at room temperature (21–24°C). This step dries the spin column membrane to ensure that no RPE buffer or ethanol carries through which could otherwise inhibit downstream cDNA synthesis etc. Ensure that the spin column membrane and column are completely dry. Remove the spin column carefully to avoid any solution coming into contact with the spin column outflow.
7. Place the spin column in a fresh 1.5-ml collection tube. Add 20–40 µl RNase-free water to the centre of the spin column membrane and leave for 1 min. Centrifuge at 10,000×*g* for 1 min at room temperature (21–24°C) to elute the RNA.
8. (optional) Reload eluate onto the spin column and centrifuge as in **step 7**. This ensures complete RNA removal from the membrane and can increase concentration of the final eluate although the final total yield may be decreased, compared to using a second aliquot of RNase-free water.

3.3.2.4. Spectrophotometric Determination of RNA Quantity and Purity

1. Clean quartz cuvettes (path length 1 cm) with RNase-free water. Blank spectrophotometer absorbance at wavelength of 260 nm with 10-mM Tris–HCl, pH 7.0.
2. Dilute the RNA sample in 10-mM Tris–HCl, pH 7.0 in an RNase-free Eppendorf tube and vortex well. Place it in the same quartz cuvette used to blank spectrophotometer, ensuring that the cuvette has been washed extensively with RNase-free water and drained by inverting on a clean paper tissue.
3. Read absorbance at 260 nM and calculate the RNA concentration based on 1 absorbance unit at 260 nM = 40-µg RNA per ml (*see* **Note 11**).

4. Set the spectrophotometer to 280-nm wavelength and re-blank as in **step 1**.
5. Using the same dilution of RNA read absorbance at 280 nm as above.
6. Calculate the A260/A280 ratio. A ratio of between 1.9 and 2.1 indicates clean RNA, ratios considerably away from these values indicate contamination, e.g. by protein (*see* **Note 12**).

3.3.2.5. Quality of RNA Determined by Denaturing Gel Electrophoresis

This is highly recommended if you are new to RNA isolation or have concerns about the quality of RNA generated. Under most conditions the RNA generated is of very high quality and integrity and this step can be excluded once the procedure becomes routine, particularly if handling multiple samples.

1. Use a horizontal gel electrophoresis tank reserved for RNA analysis and clean it by rinsing in 0.5% SDS, wash extensively in RNase-free water, then rinse in 100% ethanol and allow to air dry.
2. To prepare 60 ml (sufficient for a standard 10 × 14 × 0.7 cm gel tray) of a 1.2% agarose gel place 6 ml of 10× RNA gel buffer (RGB) and 54-ml RNase-free water into an RNase-free 250-ml conical glass flask and sprinkle 0.72 g of ultrapure agarose onto the surface of the solution.
3. Loosely place a plastic cap onto the flask (to reduce evaporation) and heat in a microwave at 750 W for a total of 2–4 min until the agarose has completely dissolved. Approximately every 1-min swirl the flask, using thermal waterproof gloves, to ensure complete mixing. Ensure that the superheated agarose does not overspill the flask, or that the cap becomes too tight resulting in pressure build up.
4. Once the agarose is clear, with no visible lumps/grains, cool the flask under running water or in a water bath with constant swirling to ~65°C (should still be hand hot but one should be able to hold it comfortably for >10 s without thermal gloves).
5. Immediately upon cooling (*see* **Note 13**), in a fume hood, add 1.8 ml of 37% formaldehyde (12.3 M) and 1 µl of a 10-mg/ml ethidium bromide solution with constant swirling. Gently pour into the gel tray with appropriately sized comb to produce wells with ~30-µl capacity.
6. Place the gel tray on a flat surface, remove air bubbles from the comb and gel using an RNase-free 200-µl (yellow) Gilson pipette tip. Allow the gel to completely set (typically 30 min).
7. Place the gel in the electrophoresis tank, slowly pour in 1× RNA gel running buffer (RGRB, prepare a 1-L fresh solution containing 100 ml of 10× RNA gel buffer, 20 ml of 37% (12.3 M) formaldehyde and 880 ml of RNase-free water in a fume hood) so that the gel is just (1–2 mm) covered by the buffer. Carefully remove the comb ensuring that the well

bottoms are intact and gently wash wells using 1× RGRB buffer and an RNase-free Gilson pipette tip.

8. Let the gel equilibrate for ~30 min while preparing the RNA samples.
9. Dilute the RNA sample to approximately 10 µg/20 µl in RNase-free water and add 5 µl of 5× RNA loading buffer to the 20 µl of RNA sample, mix well, denature for 5 min at 65°C in a water bath and chill on ice for 5 min (*see* **Note 14**). Briefly centrifuge for 10 s at 10,000×*g* at 4°C before applying to the well of gel. Insert the pipette tip halfway into the gel and eject slowly to avoid spill over, while ensuring that the pipette does not pierce the gel.
10. Connect the electrodes so that the RNA will migrate towards the anode (positive, red lead).
11. Run the gel at ~100 V (5 V/cm) in a fume hood until the lower bromophenol blue dye has migrated approximately 2/3rds down the gel. Do not run at high voltages; this smears the RNA bands and can cause gel overheating resulting in release of formaldehyde and gel distortion (if the gel begins to overheat, reduce the voltage).
12. Visualise the gel on the UV transilluminator. The 28S and 18S ribosomal (rRNA) bands (**Fig. 3.2**) should be sharp with no evidence of smearing in between that indicates RNA degradation. The 28S band should have an intensity approximately twice that of the 18S band; the 28S rRNA is more labile, so equal intensities of 28S and 18S indicate RNA degradation.

3.3.2.6. Storage of RNA

Although RNA can be stored frozen in RNase-free water for up to a year at −80°C by avoiding freeze thaw cycles, we prefer to store RNA as a precipitate under ethanol.

1. To 20 µl of purified RNA add 140 µl of RNase-free water and 16 µl of 3-M sodium acetate, pH 5.2 in an Eppendorf tube.
2. Add 1 ml of 100% ethanol, stored at −20°C, and vortex vigorously for 10 s.
3. Leave in −20°C freezer for 1 h, centrifuge at >10,000×*g* and carefully discard the supernatant (*see* **Note 15**).
4. Add 0.5 ml of 100% ethanol and store in a −80°C freezer until use.
5. To reuse the RNA, centrifuge at >10,000×*g* and carefully discard the supernatant. Invert the tube and allow to air dry at room temperature to ensure that all the ethanol has evaporated (*see* **Note 16**).
6. Add 20 µl of RNase-free water and gently wash the back of the Eppendorf tube by rolling a bead of solution against the tube wall using the Eppendorf tip.
7. Place on ice until use.

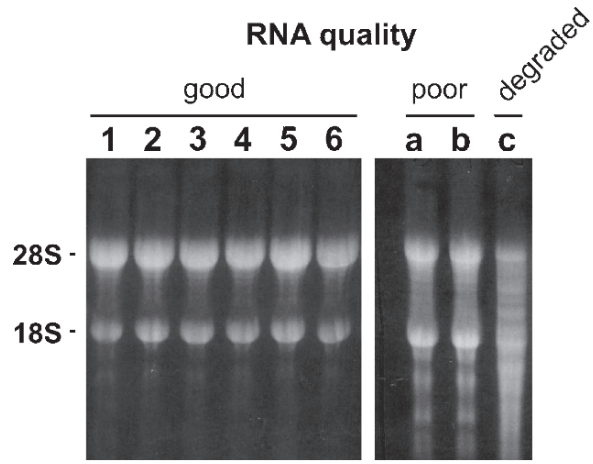

Fig. 3.2. Representative ethidium bromide stained denaturing agarose gel of total RNA purified from murine AtT20 corticotroph cells. *Lanes 1–6* indicate the reproducibility of high quality total RNA isolation following direct lysis of AtT20 cells from replicate wells of a 6-well cluster plate using Qiagen RNA extraction buffer RLT as described in **Subheading 3.3.2.2**. Note the prominent bands representing the 28S and 18S ribosomal RNA bands with the upper 28S band having increased intensity compared to the 18S band. *Lanes a–c* are from AtT20 cells assayed in parallel however cells were first lysed in cell lysis buffer (Qiagen buffer RLN; *see* **Note 8**) without any RNase inhibitors in the solution. Crude cell lysates were then left at room temperature for 5 min (*lanes a, b*) or 30 min (*lane c*) before subsequent addition of Qiagen RNA extraction buffer (RLT) to homogenise cells and inactivate RNase and RNA and then processed as above. In *a* and *b*, note the smearing of RNA resulting from ribosomal RNA fragmentation and decreased intensity of the 28S band relative to the 18S bands. In *panel c*, the 28S and 18S bands are indistinguishable and the RNA is badly degraded resulting in a near continuous smear of ribosomal RNA.

3.3.2.7. Eliminating Trace Genomic DNA from RNA Using DNase 1 (Optional)

For most subsequent applications this is not required, especially as you will be using primers that span introns. However, for high sensitivity techniques such as qRT-PCR, using primers that do not span introns and for very low mRNA abundance targets, this procedure may be required.

1. To a 0.5-ml RNase-free Eppendorf tube on ice add:

(a) 1 µg/µl of eluted RNA	10 µl
(b) 10× DNase 1 reaction buffer	2 µl
(c) RNA-free DNase 1	0.5 µl (~1 Kunitz unit)
(d) RNase-free water	to 20 µl

2. Incubate for 15 min at room temperature.
3. Heat inactivate DNase 1 at 65°C for 10 min (*see* **Note 17**), place on ice.
4. Use directly in reverse transcription reaction below (optionally can re-clean up RNA by going to **Subheading 3.3.2.2, step 2**).

3.3.3. First Strand cDNA Synthesis and PCR Amplification of Splice Variants

3.3.3.1. Reverse Transcription Using Qiagen Omniscript Reverse Transcriptase

Qiagen Omniscript reverse transcriptase (*see* **Note 18**) is optimised for generating cDNA from 50 ng to 2 µg of starting RNA. The protocol below uses a mix of oligo-dT and random primers to prime the reverse transcription reaction at high efficiency with good cDNA representation (*see* **Note 19**). Thaw all the reaction components at room temperature (apart from the Omniscript enzyme), vortex vigorously to mix, centrifuge for 10 s at 10,000×*g* to collect the liquid at the bottom of the tube and keep in ice/water bath.

1. Prepare RNA stock at 1 µg/µl using RNase-free water on ice (*see* **Note 20**). Denature at 65°C for 5 min in heating block, spin the condensate at 10,000×*g* for 10 s and store on ice.
2. Remove the Omniscript from the –20°C freezer and place it in a–20°C freezer block throughout to retain activity.
3. Prepare a master mix of reagents on ice in the order below (This is for a final volume of 20 µl/reaction. Make a 10% excess of the master mix, e.g. if the master mix is required for 10 reactions, make enough for 11 reactions.):

Component	Volume per reaction	Final
(a) 10× RT buffer	2 µl	1×
(b) 5-mM dNTP mix	2 µl	0.5-mM each dNTP
(c) 100-µM random hexamer	2 µl	10 µM
(d) 10-µM oligo-dT primer	2 µl	1 µM
(e) 10-U/µl RNAsin	1 µl	1 U/reaction
(f) 40-U/µl Omniscript RT	1 µl	4 U/reaction
(g) RNase-free water	9 µl	
Total	19 µl/reaction	

4. Mix the master mix well by vortexing for 5 s.
5. Distribute 19 µl of the master mix to individual 0.5-ml RNase-free Eppendorf tubes on ice, gently close caps after addition.
6. Add 1µg of the template RNA to each tube. Include a no template control to prevent contamination of any stock reagents used in the reverse transcription reaction. To minimise cross-contamination, when processing multiple samples, open the reaction tube only when the respective RNA aliquot is required; close the cap fully before opening a new RNA source.
7. Mix by vortexing for 5 s, centrifuge for 5 s at 10,000×*g* to collect the residual liquid.

8. Incubate in heating block (or thermocycler) at 37°C for 60 min.
9. Place on ice for 5 min, and centrifuge for 5 s at 10,000×*g* to collect the condensate.
10. Add 80-µl of nuclease-free water to each reaction tube to give a final volume of 100 µl (i.e. 1/5th dilution). Aliquot into 10-µl fractions on ice and place cDNA at –20°C for long term storage.

3.3.3.2. PCR Amplification of Splice Variant cDNAs from Reverse Transcribed RNA

In this assay, we use *Taq* DNA polymerase rather than a proofreading polymerase to amplify cDNA templates under the optimised condition because less than 1-kb amplicons are expected, and also because amplicons will be subsequently TOPO subcloned. This ensures that the amplicons have enough 3′ adenine overhangs (*see* **Note 21**).

1. Thaw all the reaction components at room temperature (apart from the *Taq* DNA polymerase enzyme), vortex vigorously to mix, centrifuge for 10 s at 10,000×*g* to collect the liquid at the bottom of the tube and keep on ice/water bath. Remove the *Taq* DNA polymerase from the –20°C freezer and place in a –20°C freezer block until use.
2. Prepare a PCR master mix on ice as given below for a reaction (*see* **Note 22**) (make enough master mix for the number of reactions required plus an extra 5%):

Component	Volume per reaction (µl)	Final
(a) 10× PCR buffer w/o Mg	2.0	1×
(b) 25-mM dNTP mix	0.5	0.2-mM each dNTP
(c) 50-mM $MgCl_2$	0.5	1.25 mM (*see* **Note 22**)
(d) 10-pmol/µl forward primer	0.5	5 pmol
(e)10-pmol/µl reverse primer	0.5	5 pmol
(f) 5-U/µl Taq DNA polymerase	0.5	2.5 U
(g) Sterile water	14.5	

3. Mix the master mix well by vortexing for 5 s.
4. Distribute 19 µl of the master mix to individual 0.2-ml thin-walled PCR tubes on ice, gently close caps after addition (*see* **Note 23**).
5. Add 1 µl of template (10–50 ng) first strand cDNA from stored RT reaction to each tube (i.e. ~1/100 dilution of the initial RNA prepared).

6. Including the following PCR controls:
   (a) No reverse transcription cDNA template to ensure that there is no genomic DNA or other cDNA contamination.
   (b) Purified RNA input to ensure that there is no genomic DNA or other cDNA contamination.
   (c) Positive control template (plasmid cDNA) to confirm PCR amplification (*see* **Note 24**).
7. Mix by vortexing for 2 s, centrifuge for 5 s at 10,000×g to collect the residual liquid.
8. Denature DNA at 94°C for 2 min in a thermal cycler (*see* **Note 25**).
9. Perform PCR using the following cycling parameters for 25–35 cycles (*see* **Note 22**):
   (a) Denature at 94°C for 40 s.
   (b) Anneal at 55°C for 45 s.
   (c) Extend at 72°C for 1 min (1 min/kb).
10. Final extension at 72°C for 7 min, then maintain cycler at 4°C until use (*see* **Note 26**).
11. For long term storage, store amplicons at −20°C.

3.3.3.3. DNA Agarose Gel Electrophoresis of Splice Variant Amplicons

The percentage of agarose used is dependent upon the amplicon sizes expected and the level of discrimination required between amplicon bands. For example, using a 1.5% agarose gel effectively separates amplicons between 0.5 and 1.0 kb. However, increasing agarose to 4% allows amplicons of ~5% difference in nucleotide length (in amplicons of around 0.5 kb) to be effectively discriminated.

1. Prepare 60 ml (sufficient for a standard 10 × 14 × 0.7 cm gel tray of a horizontal gel electrophoresis tank) of a 1.5% agarose gel by placing 6 ml of 10× DNA gel buffer (TBE) and 54 ml of distilled water into a 250-ml conical glass flask and sprinkle 0.9 g of ultrapure agarose onto the surface of the solution.
2. Loosely place a plastic cap onto the flask (to reduce evaporation) and heat in a microwave at 750 W for a total of 2–4 min. until the agarose has completely dissolved. Approximately every 1 min. swirl the flask, using thermal waterproof gloves, to ensure complete mixing and to ensure that the superheated agarose does not overspill the flask or that the cap does not become too tight resulting in a pressure build up.
3. Once the agarose is clear, with no visible lumps/grains, cool the flask under running water or in a water bath with constant swirling to ~65°C (should still be hand hot but one should be able to hold it comfortably for >10 s without thermal gloves).
4. After cooling, add dH_2O to 60 ml if the volume has decreased and add 6µl of SYBR® Safe (*see* **Note 27**) with constant swirling.

Gently pour into the gel tray with appropriately sized comb (to produce wells with ~30-µl capacity) to a depth of approximately 5 mm.

5. Place the gel tray on a flat surface, and immediately remove air bubbles from the comb and gel using a 200-µl (yellow) Gilson pipette tip. Allow the gel to completely set (typically 15–30 min).
6. Place the gel in the electrophoresis tank, slowly pour in 1× TBE buffer (prepared by diluting 10× TBE buffer in dH_2O) so that the gel is just (1–2 mm) covered by the buffer. Carefully remove the comb ensuring that the well bottoms are intact and gently wash the wells using TBE buffer and a yellow Gilson pipette tip.
7. Mix an aliquot (typically 10 µl) of each PCR reaction with 10× DNA loading buffer (*see* **Note 28**) using a pipette tip. Insert the pipette tip half way into the gel and eject slowly to avoid spill over, ensuring that the pipette does not pierce the gel.
8. Include an appropriate DNA marker ladder (e.g. range 100–1,000 bp in 100-bp steps) for determination of amplicon size.
9. Connect the electrodes so that the DNA will migrate towards the anode (positive, red lead).
10. Run the gel at ~100 V (5 V/cm) until the lower bromophenol blue dye has migrated approximately 2/3rd down the gel (typically for ~45 min for 10 × 14 cm gel). Duration will need to be modified according to the expected amplicon size and percentage of the agarose gel used.
11. Using gloved hands visualise the DNA gel on the UV transilluminator/imaging system. Ensure that the DNA is not overexposed as UV will nick DNA if amplicons are to be isolated/re-amplified from gel (*see* **Subheading 3.3.4.2**). Adjust brightness and contrast to optimise image. If DNA bands are not well separated the gel can be placed back in the electrophoresis tank and re-run further.

3.3.4. Subcloning, Plasmid Amplification and Analysis of Splice Variant Amplicons

To provide highly efficient and high throughput subcloning of amplicons we prefer to use a 'shot-gun' TOPO subcloning strategy – this allows efficient subcloning of multiple splice variant amplicons generated in a single PCR reaction without the need to separate individual amplicons by DNA gel electrophoresis. We do not recommend purifying DNA amplicons from DNA agarose gels as this significantly reduces TOPO cloning efficiency. Use fresh PCR reaction products wherever possible. However, smaller amplicons are more efficiently ligated into TOPO vectors than large amplicons. Amplicons of interest may be of very low abundance and hence, using the 'shot-gun' strategy may result in poor representation of these transcripts in the ligated plasmid

population. In this case we use a direct gel amplification/sub-cloning strategy (**Subheading 3.3.4.2**).

3.3.4.1. 'Shot-Gun' Cloning of PCR Amplicons Using TOPO Cloning

1. Set up the following reagents in a sterile 0.5-ml Eppendorf tube for each PCR product:

Component	Volume per reaction
(a) 6× TOPO cloning buffer	1 µl
(b) TOPO pCRII vector	1 µl
(c) PCR reaction	(1–4 µl)
(d) dH_2O	to 6-µl final volume

2. Mix gently with a pipette tip and incubate at room temperature for 15 min.
3. Proceed immediately to transformation of chemically competent *E. coli* (**Subheading 3.3.4.3**) (*see* **Note 29**).

3.3.4.2. Amplification and Cloning of Low Abundance or Large Amplicons

To avoid screening a large number of colonies, we use a separate strategy to clone fragments with apparent low abundance when visualised on DNA agarose gels (*see* **Note 30**).

1. Insert the tip of a sterile 20-µl (yellow) Gilson pipette into the DNA agarose gel with the isolated amplicon band visualised under brief UV illumination.
2. Move the tip up and down 2–3 times to capture the sample of amplicon.
3. Use this directly as a TOPO cloning template in **Subheading 3.3.4.1, step 1**.
4. Alternatively, use the amplicon/gel sample as a PCR template to re-amplify the fragment as described in **Subheading 3.3.3.2**. Subject the re-amplified products to TOPO cloning as above (*see* **Note 31**).

3.3.4.3. Transformation of Chemically Competent E. Coli TOP 10 Cells

1. Chemically competent cells are stored in a –80°C freezer as individual 200-µl aliquots in a 1.5-ml Eppendorf tube (*see* **Note 2**). Thaw competent cells on ice/water bath. DO NOT ALLOW TO THAW AT ROOM TEMPERATURE. Do not mix or vortex as competent cells are very fragile.
2. Transfer 1–4 µl of fresh TOPO reaction to an aliquot of competent cells, mix by stirring very gently using pipette tip on ice and incubate for 30 min on ice. Set up negative (no amplicon) and positive (10-ng circular plasmid with ampicillin resistance) reactions.
3. Heat shock cells at 42°C in a water bath (do not use heating block) to ensure good thermal equilibration for 45 s.

4. Immediately place tubes in ice/water bath for 2 min.
5. Add 250 µl of pre-warmed LB broth at 37°C. (Do not include selection antibiotic.)
6. Transfer capped tubes to a 37°C incubator for 1 h after shaking (220 rpm).
7. Spread (*see* **Note 32**) 50–200 µl of each transformation onto a pre-warmed (*see* **Note 33**) LB-agar plate containing 100-µg/ml ampicillin as selection.
8. Place the inverted LB-agar plate in an incubator overnight at 37°C.
9. Plates with colonies can be stored inverted, sealed with nescofilm at 4°C for a week. However it is best to continue immediately if possible.

3.3.4.4. PCR Screening of Bacterial Colonies to Identify Subcloned Amplicons

1. Select well separated colonies and identify them using a permanent marker to circle and number the colony on the underside of the LB-agar plate. Choose colonies of ~1-mm diameter with no satellite colonies.
2. Prepare PCR master mix and aliquot into PCR tubes as indicated in **Subheading 3.3.3.2**.
3. Carefully pick part of each selected colony using a sterile 10-µl pipette tip.
4. In place of adding cDNA aliquot carefully dip pipette tip with the selected colony into the PCR mix in the labelled PCR tube. Agitate the pipette tip up and down 3–4 times to mix.
5. Run the PCR (**Subheading 3.3.3.2**) and characterise amplicons by DNA agarose gel electrophoresis (**Subheading 3.3.3.3**).
6. Drop the pipette tip into 3-ml LB broth with ampicillin selection and incubate overnight for subsequent miniprep isolation of plasmid DNA (**Subheading 3.3.4.5**)
7. Choose splice variants based on different amplicon sizes to take the process forward for plasmid DNA amplification.

3.3.4.5. Plasmid DNA Miniprep Isolation of Positive Clones by Alkaline Lysis

1. The following protocol utilises the Qiagen QIAprep spin miniprep kit isolation based on alkaline lysis of bacteria and capture and purification of DNA on silica membranes.
2. Prepare 5-ml aliquots of LB broth containing 100-µg/ml of ampicillin as selection antibiotic in a 15-ml loose capped sterile tube.
3. Pick a single PCR positive colony from the LB-agar plate using a sterile 20-µl pipette tip (or a pipette tip from the PCR colony screen in **Subheading 3.3.4.4, step 4** above) and place the pipette tip in the LB broth.
4. Incubate overnight (maximum 16 h) in a 37°C incubator with shaking (220 rpm) or using a roller drum.
5. Place the LB broth on ice, remove the 1.5-ml aliquot into an Eppendorf tube and spin at 10,000×*g* for 30 s.

6. Carefully remove all the supernatant by aspiration (*see* **Note 34**) and re-suspend the bacteria pellet in 250 µl of buffer P1 by vigorously vortexing it for 10 s and incubate for 5 min at room temperature.
7. Add 250-µl of buffer P2 and mix by gently inverting the tube six times to lyse the bacteria, denature the plasmid and bacterial chromosomal DNA and solubilise the protein. DO NOT VORTEX as this will shear the chromosomal DNA.
8. Within 5 min of **step 7** add 350 µl of buffer N3 and mix immediately by inverting six times (*see* **Note 35**).
9. Centrifuge for 10 min at 14,000×*g* to pellet insoluble material.
10. Apply supernatant from **step 9** to a QIAprep spin column and centrifuge at 14,000×*g* for 1 min at room temperature. Discard the flow through.
11. Wash the column with 750-µl PE buffer followed by centrifugation at 14,000×*g* for 1 min at room temperature. Discard the flow through. Recentrifuge the spin column for 1 min to remove any residual wash buffer.
12. Elute the plasmid DNA by adding 50 µl of dH_2O to the centre of the silica membrane and allow it to stand for 1 min. Centrifuge at 14,000×*g* for 1 min at room temperature into a fresh, sterile 1.5-ml Eppendorf tube.
13. Determine plasmid DNA concentration in the eluate (**Subheading 3.3.4.6**) (*see* **Note 36**). Store plasmid DNA at 4°C, or –20°C for long term storage.

3.3.4.6. Determination of DNA Quality and Concentration for DNA Sequencing

1. Clean quartz cuvettes (path length 1 cm) with dH_20. Blank spectrophotometer absorbance at wavelength of 260 nm with 10-mM Tris–HCl, pH 7.0.
2. Dilute the DNA sample in 10-mM Tris–HCl, pH 7.0 in an Eppendorf tube and vortex well. Place in same quartz cuvette used to blank the spectrophotometer ensuring that the cuvette has been washed extensively with dH_2O and drained by inverting on a clean paper tissue.
3. Read absorbance at 260 nm and calculate the DNA concentration based on 1 absorbance unit at 260 nm = 50-µg double stranded DNA per ml.
4. Set the spectrophotometer to 280-nm wavelength and re-blank as in **step 1**.
5. Using the same dilution of DNA read absorbance at 280 nm as above.
6. Calculate the A260/A280 ratio. A ratio of between 1.7 and 2.0 indicates clean DNA, ratios considerably away from these values indicate contamination, e.g. by protein.
7. Prepare a 2-µg aliquot of DNA (typically at 100 ng/µl) for automated DNA sequencing (*see* **Note 37**).

3.4. Notes

1. Ethidium bromide (EtBr) is mutagenic; handle all solutions and gels with care using gloves. Solutions containing EtBr should be decontaminated (e.g. by passing through an activated carbon filter cartridge to remove the EtBr) before disposal.
2. Competent cell stocks can be prepared using the rubidium chloride method. Competent cells are very fragile so keep the cells and solutions on ice at all times and pipette slowly and carefully. Grow a 250-ml culture of *E. coli* to an OD_{600} of 0.4–0.6 in the presence of 20-mM $MgS0_4$. Pellet the cells by centrifugation at 4,500×*g* for 5 min at 4°C. Gently re-suspend cells in 100 ml of freshly prepared, ice cold TFB1 buffer (30-mM potassium acetate, 10-mM $CaCl_2$, 50-mM $MnCl_2$, 100-mM RbCl, 15% glycerol, pH 5.8 with 1-M acetic acid. Filter sterilise). Incubate the cells on ice for 5 min and re-pellet as above. Gently re-suspend the cells on ice in 10 ml of freshly prepared buffer TFB2 (10-mM MOPS, 75-mM $CaCl_2$, 10-mM RbCl, 15% glycerol, pH 6.5 with KOH. Filter sterilise). Incubate cells on ice for 30 min and gently aliquot 200 µl into pre-chilled 1.5-ml Eppendorf tubes. Snap freeze on dry ice/isopropanol bath and store immediately at –80°C. Cells should be competent for at least 3 months.
3. For example, when cloning splice variants at site C2 we took advantage of unique *Pac*I and *Blp*I restriction sites flanking the C2 splicing site.
4. This should only be used for tissue blocks 2–3 mm thick to ensure rapid freezing. If using thicker (e.g. 5 × 5 × 5 mm) tissue blocks it is best to freeze in liquid nitrogen. However, use of liquid nitrogen is not convenient when a large number of tissues are to be processed in parallel; in this case label a grid on tin foil placed on ice to freeze multiple tissues. For large tissue pieces (e.g. whole mouse brain) grind the tissue to a fine powder in liquid nitrogen using a RNase-free glass pestle and mortar that has been pre-chilled with liquid nitrogen. Only a small fraction of the powder (~25 mg) is required for RNA isolation using RNeasy mini columns that have a RNA binding capacity of 50–100 µg of RNA.
5. Wherever possible process the tissue immediately to reduce likelihood of RNA degradation. Once tissues are homogenised in the RNA extraction buffer, the RNases are inactivated. Commercially available RNA stabilisation solutions are available to allow tissue storage at 4°C (e.g. RNAlater from Qiagen). However we find freezing and rapid processing are as convenient and reliable.

6. It is essential to completely remove all growth medium; otherwise this can reduce RNA isolation and purification at later stages by interfering with efficient RNA binding to RNeasy membrane. An optional rapid wash step with PBS can be used, but again all PBS must be removed to avoid dilution.
7. We prefer to use the direct lysis method rather than removing cells by trypsinisation followed by pelleting. Not only does the latter take longer, and include more steps, but thedetachment of cells and rounding up can cause dramatic changes in RNA expression during the time required to pellet cells before lysis.
8. An alternative approach with tissue culture cells is to extract cytoplasmic RNA and remove genomic DNA by pelleting cell nuclei. This can help if genomic DNA contamination is an issue but the procedure results in cells being exposed to conditions under which RNase activity may affect the mRNA profile before the lysate is homogenised in guanidium thiocyanate containing buffer. For this procedure add 175 µl of pre-cooled Qiagen cell lysis buffer (RLN) to lyse the cell membranes. Triturate and repeatedly wash the RLN buffer across the well to ensure the complete removal of cells by holding the plate at a 30° angle to allow the solution to drain to the base of the plate. The solution should clear rapidly indicating immediate cell lysis. Transfer the lysate to an RNase-free Eppendorf tube pre-cooled on ice/water bath and incubate at 4°C for 5 min to ensure complete lysis of cells. Centrifuge the lysate at 300×*g* for 2 min at 4°C to pellet the nuclei and large cell debris. Transfer the supernatant to a fresh RNase-free Eppendorf tube and proceed from **Subheading 3.3.2.2, step 2**.
9. Many protocols recommend using a rubber policeman/cell scraper to remove lysed cells. We do not recommend this as highly efficient lysis/cell removal is achieved by triturating cells from wells and significant amounts of material can be lost in small wells by adherence to the scraper.
10. While discarding flow through, it is convenient to place the filter in an RNase-free Eppendorf in a rack for convenience while handling the collection tube. As RW1 and RPE buffer contain guanidium thiocyanate do not dispose of these buffers using bleach or strong acid.
11. This relationship is only valid at neutral pH in a low salt buffer. Typically dilute 4 µl of the final RNA eluate from an RNAeasy column in 996 µl 10-mM Tris–HCl, pH 7.0 to achieve an absorbance reading between 0.1 and 1.0. If the reading is above or below these values, adjust the RNA input to ensure reliability of measurements.

12. The ratio is influenced by pH and should be performed in low salt buffers. Ratio is optimally determined at pH 7.5 in these cases. However use of the same RNA dilution in neutral 10-mM Tris–HCl saves time and RNA and gives a reliable indication of purity.
13. Formaldehyde is toxic and is volatile. Ensure that the gel solution is cooled, but not starting to set, before addition.
14. RNA loading buffer is used to denature the RNA; increase the density of the sample to ensure that it sinks into the well (ensure that you do not have residual ethanol as this will cause the sample to float out of the well and furthermore ensure that wells are well washed) and add dyes that migrate through the gel to monitor the extent of electrophoresis. RNA gels are run at neutral pH, using MOPS buffer that has high buffering capacity at pH 7.0, as RNA is susceptible to degradation at high pH and RNA has a lower pKa than DNA. However, single stranded RNA can display a high secondary structure, which is why formaldehyde is used to keep the RNA denatured throughout.
15. RNA will tend to smear down the back of the Eppendorf tube and appear colourless. To aid orientation, place the Eppendorf so that the hinge is pointing to the outside of the rotor; the RNA will then smear down the wall of the tube below the hinge.
16. Avoid overdrying or heating to speed evaporation. Overdried RNA pellets can be difficult to re-suspend in water and elevated temperatures can accelerate RNA degradation.
17. Many protocols include addition of 2.5-mM EDTA final concentration to stop reaction. However, care must be taken while doing this, as too much EDTA can reduce the efficiency of subsequent reverse transcription reactions and heat inactivation is sufficient. Do not exceed the time/temperature of inactivation as otherwise the RNA may become degraded.
18. Omniscript reverse transcriptase is an RNA-dependent DNA polymerase (reverse transcriptase) enzyme that drives first strand cDNA synthesis. The enzyme also contains RNase H activity that degrades RNA in duplex with cDNA, thus removing the parental RNA template from the RNA:DNA hybrids. If we are isolating RNA from very small samples where recovered RNA may be <100 ng then we routinely use Sensiscript reverse transcriptase from Qiagen.
19. Three different types of primers can be used (1) oligo-dT primer that anneals to the 3′ polyA tail of mRNAs. However, subsequent analysis of splice variants at the 5′ end of the mRNA may be misrepresented due to reduced efficiency for long transcript length (especially if mRNAs for the target

of interest are >1.5 kb); (2) random primers are short (typically hexamers) sequences of DNA that bind along the RNA molecule and thus reverse transcribe polyA$^+$ and polyA$^-$ transcripts. In general random primers can produce shorter length cDNAs but with good coverage across the mRNA; (3) gene specific primers can be used if only one target is being amplified; this can improve sensitivity but careful choice of primer is necessary to ensure good representation of subsequent cDNA and besides other targets cannot be amplified in the subsequent PCR. If using gene specific primers, use a final concentration of 1 μM.

20. DEPC can inhibit the RT reaction. So ensure that if RNase-free water was treated with DEPC, that it has also been well autoclaved to remove any residual DEPC.
21. While *Taq* DNA polymerases do have a higher error rate as compared to proof reading polymerases such as *Pfu*, *Taq* polymerase is required to incorporate overhanging adenines to amplicons to facilitate efficient downstream TOPO cloning. It is possible to use a mix of *Taq* and proof reading enzymes. However, when amplifying amplicons of <1 kb, and analysing multiple amplicons followed by sequencing, we have not experienced any PCR error rate problems by using commercial *Taq* enzymes as compared to hybrid formulations.
22. Buffer and cycling parameters must be optimised prior to use. We typically design primers to have an annealing temperature (T_m) of 60°C and then run optimisation PCRs using 10–50 ng of an appropriate plasmid cDNA template at several different magnesium concentrations (e.g. final $MgCl_2$ of 5, 3.75, 2.5, 1.25 mM) and annealing temperatures below the T_m of the primers (T_m −3°C, T_m −5°C, T_m −7°C and T_m −10°C conditions).
23. Use a clean cap-closing tool rather than gloved fingers to significantly reduce chances of cross-contamination between tubes.
24. This is a useful control to ensure that PCR amplification has occurred. However considerable care must be taken as this plasmid stock is a major source of potential contamination. Inclusion of this control is an excellent way of also testing whether your experimental procedures are effectively preventing cross-contamination.
25. Use a thermocycler with a heated lid to avoid use of overlaying mineral oil. This significantly reduces the likelihood of cross-contamination. Whereever possible, arrange tubes with one tube spacing between neighbouring tubes across the PCR block to further reduce contamination crossover.
26. For high efficiency shot-gun subcloning into pCRII TOPO vector, do not freeze samples but use immediately. For very low abundance variants, an additional round of PCR amplification

may be required. In this case, use a 1/100 dilution of reaction from **step 10** above and use as template in a new PCR amplification from **step 2**. While the same primers can be used, a set of internally nested primers is preferred.

27. SYBR® Safe is a non toxic alternative to ethidium bromide and very useful for routine DNA amplicon screening. However, if you suspect low abundance amplicons use EtBr to stain the DNA gel using the precautions outlined in **Note 1**.
28. Ensure that you retain an aliquot of the fresh PCR reaction for downstream 'shot-gun' TOPO cloning. Do not mix all the PCR reaction with the DNA loading buffer. When processing multiple samples it is convenient to mix the PCR sample with the DNA loading buffer on top of a piece of nescofilm to avoid using additional Eppendorf tubes for mixing. Place multiple aliquots of DNA loading buffer in order of sample addition to well on nescofilm. Then using a fresh tip each time mix 10 µl of the PCR reaction with the DNA loading buffer on nescofilm by triturating several times and aliquot the mix into the respective well of the DNA agarose gel.
29. It is not necessary to set up a negative control (i.e. no TOPO reaction) for TOPO cloning, because a subsequent PCR screening of colonies will exclude false positive clones. TOPO reactions can be stored at –20°C for long term storage but from our experience, use of the fresh reaction for transformation generates fewer false-positive clones. We find the pCRII TOPO vector very efficient for subcloning amplicons <1 kb; however, if cloning amplicons larger than 2 kb, we find that the pCR2.1 TOPO vector gives improved cloning efficiency.
30. This approach can be used even when the amplicons are not well separated as the different amplicons are subsequently ligated and characterised in the pCRII TOPO vector. However, where possible, take samples from well isolated bands to improve the efficiency of direct TOPO cloning or re-PCR.
31. Some apparently low abundance high molecular weight DNA amplicons observed on DNA agarose gels may in fact be artefacts. For example, it is possible that heterodimerisation and hairpin looping of DNA fragments may occur, resulting in retarded migration of the DNA fragment. The presence of very large (i.e. several kb) DNA fragments in DNA agarose gels of PCR amplicons generally indicates genomic DNA contamination.
32. Pre-warm LB-agar plates (10-cm diameter petri dish containing 50-µg/ml of ampicillin as antibiotic selection) by inverting and placing in a 37°C incubator with the plate slightly overlapping the lid at one edge. Before use ensure that the condensate is shaken from the lid and place the plate upright.

33. A convenient spreader can be fashioned from a glass Pasteur pipette by bending the fine tip in a flame, so that the spreader is approximately half the diameter of the LB-agar plate. Slightly bend the tip upwards to prevent the spreader gouging into the agar. Store the spreader in 100% alcohol and flame between each use, allow to air cool under the aseptic technique (e.g. near a yellow Bunsen flame). It is often convenient to use two plates per transformation; plate one at 50 µl, the other at 200 µl to ensure that discrete well separated colonies are available after overnight incubation.
34. It is important to completely remove all supernatant, as otherwise the efficiency/purity of subsequent plasmid DNA is compromised. Invert the Eppendorf tube on a tissue paper to drain completely. The supernatant should be exposed to bleach before disposal.
35. The rapid neutralisation results in bacterial chromosomal DNA-forming insoluble aggregates while the plasmid DNA covalently closes via interstrand rehybridization and thus remains in solution. The potassium acetate also results in SDS precipitation, which pellets insoluble chromosomal DNA aggregates and protein. Rather than using a phenol/chloroform extraction, for the sake of convenience we routinely use a Qiagen QIAprep spin miniprep DNA filter to isolate the plasmid DNA from the supernatant, which is produced by precipitation of the insoluble aggregates.
36. Up to 5-ml of bacterial culture can be processed using this method if required, to produce sufficient DNA for downstream applications.
37. Using the alkaline lysis and the DNA miniprep spin column approach outlined in **Subheading 3.3.4.5** we find that the miniprep DNA is of high enough quality for automated DNA sequencing using the pCRII TOPO sequencing primers. Sequence multiple plasmid clones in which different sizes of splice variant amplicons have been determined. Sequence both strands to verify the sequence.

References

1. Matlin, A. J., Clark, F., and Smith, C. W. J. (2005) Understanding alternative splicing: towards a cellular code. *Nat Rev Mol Cell Biol* 6, 386–398
2. Black, D. L. (2003) Mechanisms of alternative pre-messenger RNA splicing. *Annu Rev Biochem* 72, 291–336
3. Blencowe, B. J. (2006) Alternative splicing: new insights from global analyses. *Cell* 126, 37–47
4. Xing, Y. and Lee, C. (2006) Alternative splicing and RNA selection pressure – evolutionary consequences for eukaryotic genomes. *Nat Genet* 7, 499–509
5. Li, Q., Lee, J.-A., and Black, D. L. Neuronal regulation of alternative pre-mRNA splicing. *Nat Rev Neurosci* 8, 819–831
6. Faustino, N. A. and Cooper, T. A. (2003) Pre-mRNA splicing and human disease. *Genes Dev* 17, 419–437

7. Garcia-Blanco, M. A., Baraniak, A. P., and Lasda, E. L. (2004) Alternative splicing in disease and therapy. *Nat Biotechnol* 22, 535–546
8. Licatalosi, D. D. and Darnell, R. B. (2006) Splicing regulation in neurologic disease. *Neuron* 52, 93–101
9. Butler, A., Tsunoda, S., McCobb, D. P., Wei, A., and Salkoff, L. (1993) mSlo, a complex mouse gene encoding 'maxi' calcium-activated potassium channels. *Science* 261, 221–224
10. Salkoff, L., Butler, A., Ferreira, G., Santi, C., and Wei, A. (2006) High-conductance potassium channels of the Slo family. *Nat Rev Neurosci* 5, 921–931
11. Shipston, M. J. (2001) Alternative splicing of potassium channels: a dynamic switch of cellular excitability. *Trends Cell Biol* 11, 353–358
12. Saito, M., Nelson, C., Salkoff, L., and Lingle, C. J. (1997) A cysteine-rich domain defined by a novel exon in a Slo variant in rat adrenal chromaffin cells and PC12 cells. *J Biol Chem* 272, 11710–11717
13. Lagrutta, A., Shen, K. Z., North, R. A., and Adelman, J. P. (1994) Functional differences among alternatively spliced variants of Slowpoke, a Drosophila calcium-activated potassium channel. *J Biol Chem* 269, 20347–20351
14. TsengCrank, J., Foster, C. D., Krause, J. D., Mertz, R., Godinot, N., Dichiara, T. J., and Reinhart, P. H. (1994) Cloning, expression, and distribution of functionally distinct Ca^{2+}-activated K^+ channel isoforms from human brain. *Neuron* 13, 1315–1330
15. Chen, L., Tian, L., Macdonald, S.H.F., Meclatterty, H., Hammond, M.S.L., Huibant, J.M., Ruth, P., Knaus, H. G., and Shipston, M. J. (2005) Functionally diverse complement of large conductance calcium- and voltage-activated potassium channel (BK) alpha-subunits generated from a single site of splicing. *J Biol Chem* 280, 33599–33609
16. Tian, L., Coghill, L. S., McClafferty, H., MacDonald, S. H. F., Antoni, F. A., Ruth, P., Knaus, H. G., and Shipston, M. J. (2004) Distinct stoichiometry of BK_{Ca} channel tetramer phosphorylation specifies channel activation and inhibition by cAMP-dependent protein kinase. *Proc Natl Acad Sci USA* 101, 11897–11902
17. Tian, L., Duncan, R. R., Hammond, M. S. L., Coghill, L. S., Wen, H., Rusinova, R., Clark, A. G., Levitan, I. B., and Shipston, M. J. (2001) Alternative splicing switches potassium channel sensitivity to protein phosphorylation. *J Biol Chem* 276, 7717–7720
18. Zhou, X. B., Arntz, C., Kamm, S., Motejlek, K., Sausbier, U., Wang, G. X., Ruth, P., and Korth, M. (2001) A molecular switch for specific stimulation of the BK_{Ca} channel by cGMP and cAMP kinase. *J Biol Chem* 276, 43239–43245
19. McCartney, C. E., McClafferty, H., Huibant, J. M., Rowan, E. G., Shipston, M. J., and Rowe, I. C. M. (2005) A cysteine-rich motif confers hypoxia sensitivity to mammalian large conductance voltage- and Ca-activated K (BK) channel alpha-subunits. *Proc Natl Acad Sci USA* 102, 17870–17875
20. Erxleben, C., Everhart, A. L., Romeo, C., Florance, H., Bauer, M. B., Alcorta, D. A., Rossie, S., Shipston, M. J., and Armstrong, D. L. (2002) Interacting effects of N-terminal variation and strex exon splicing on slo potassium channel regulation by calcium, phosphorylation, and oxidation. *J Biol Chem* 277, 27045–27052
21. Korovkina, V. P., Brainard, A. M., and England, S. K. (2006) Translocation of an endoproteolytically cleaved maxi-K channel isoform: mechanisms to induce human myometrial cell repolarisation. *J Physiol* 573, 329–341
22. Zarei, M. M., Eghbali, M., Alioua, A., Song, M., Knaus, H. G., Stefani, E., and Toro, L. (2004) An endoplasmic reticulum trafficking signal prevents surface expression of a voltage- and Ca^{2+}-activated K^+ channel splice variant. *Proc Natl Acad Sci USA* 101, 10072–10077
23. Xie, J. and McCobb, D. P. (1998) Control of alternative splicing of potassium channels by stress hormones. *Science* 280, 443–446
24. Xie, J. Y. and Black, D. L. (2001) A CaMK IV responsive RNA element mediates depolarization-induced alternative splicing of ion channels. *Nature* 410, 936–939
25. MacDonald, S. H. F., Ruth, P., Knaus, H. G., and Shipston, M. J. (2006) Increased large conductance calcium-activated potassium (BK) channel expression accompanied by STREX variant downregulation in the developing mouse CNS. *BMC Dev Biol* 6, 37

Chapter 4

Chemiluminescence Assays to Investigate Membrane Expression and Clathrin-Mediated Endocytosis of K_{ATP} Channels

Andrew J. Smith and Asipu Sivaprasadarao

Summary

Macroscopic ion channel currents (I) are a product of the channel open probability (P_o), the single channel current (i) and the number of channels present on the cell surface (N) at any given time ($I = P_o iN$). Endocytosis has been shown to be one of the key determinants of cell surface channel density and the defects of this process have been linked to diseases relating to ion channel dysfunction. Chemiluminescence-based techniques provide a rapid method for the examination of the rates of endocytosis and steady-state cell surface density of ion channels and have previously been used to investigate the endocytosis of pancreatic ATP-sensitive potassium (K_{ATP}) channels.

Key words: Endocytosis, Internalisation, Chemiluminescence, Surface density, K_{ATP} channels.

4.1. Introduction

It is becoming increasingly apparent that regulated trafficking pathways play a vital role in determining ion channel function. Clathrin-mediated endocytosis is known to be a key regulator of cell surface density for a wide range of channels including K_{ATP} *(1)* and CFTR *(2)* as well as a number of other Na^+ *(3)*, K^+ *(4)* and Ca^{2+} *(5)* channels. Defects in the process of endocytosis can also account for some of the deleterious effects associated with channel dysfunction in disease. Examples of this include impaired endocytosis of K_{ATP} channels associated with two mutations of Kir6.2, (the pore-forming subunit of pancreatic K_{ATP} channels), which causes permanent neonatal diabetes *(6)*.

Jonathan D. Lippiat (ed.), *Methods in Molecular Biology, Potassium Channels, vol. 491*

Book doi: 10.1007/978-1-59745-526-8

The rate of internalisation can be examined by chemiluminescence-based assays. For these approaches it is necessary to have antibodies that bind to the external portions of the channel to be examined. This allows antibody binding to a pool of channels on the cell surface while the cells are held in a state that is non-permissive to trafficking, achieved by cooling the cells to 4°C. When the cells are warmed back to temperatures permissive to protein trafficking, the channel/antibody complex is endocytosed from the cell surface. At an appropriate time, internalisation is halted by fixation and the proportion of labelled channels on the cell surface can be examined. Surface exposed channels are labelled with horseradish peroxidised (HRP)-conjugated antibodies allowing the use of a luminescence-based assay.

4.2. Materials

4.2.1. Chemiluminescence Techniques

1. Culture medium: Dulbecco's Modified Eagles Medium (DMEM) supplemented with 10% foetal bovine serum.
2. Culture plates: Sterile 24-well culture plates.
3. HEK cells stably expressing K_{ATP} channels (SUR1 and Kir6.2 bearing an extracellular HA-epitope – K_{ATP}-HA) *see* **ref.** *7*.
4. Transfection reagent: Fugene6 (Roche Diagnostics).
5. Phosphate buffered saline (PBS): 10-mM phosphate buffer, 2.7-mM KCl, 137-mM NaCl prepared from tablets (Sigma) by dissolving one tablet in 200-ml of water.
6. Antibodies targeted against external epitope: Rat anti-HA (clone 3F10) (Roche Diagnostics) (*see* **Note 1**).
7. Labelling medium: DMEM supplemented with 5% goat serum freshly prepared before each experiment.
8. HRP-conjugated antibodies: Anti-rat HRP-conjugated antibodies (Sigma).
9. Cell fixing solution: prepare 2% fresh paraformaldehyde (w/v) solution in PBS for each experiment. The solution should be carefully heated in a fume-hood to dissolve and then cooled to room temperature before use.
10. Cell solubilisation solution – 2% (w/v) sodium deoxycholate in 1× PBS.
11. Sensitive enhanced chemiluminescence (ECL) reagent (Pierce).
12. Automated microplate reader: e.g. POLARstar OPTIMA (BMG labtech) although other companies offer other options.

13. Modulators of endocytosis: Mammalian expression plasmids containing genes that disrupt clathrin-mediated endocytosis (e.g. dominant-negative (DN) forms of dynamin or μ2).

4.2.2. Cell Lysate Protein Determination Assay

1. BCA reagent: Mix 49 parts bicinchoninic acid solution (Sigma) and 1 part 4% (w/v) copper sulphate solution immediately before use.
2. Protein standards: Several samples of known protein concentration prepared by diluting 10-mg/ml BSA in the same buffer used to solubilise cells. The concentration of the protein standards should range from 0 to 10 μg/ml.
3. Cell lysates: Prepared as described in the individual protocols.

4.3. Methods

4.3.1. Endocytosis Kinetics by Chemiluminescence

The following protocol allows the determination of the rate of endocytosis of a channel from the cell surface. The internalisation of channels is investigated over a time course with samples taken at regular intervals. Each time-point is required to be performed in duplicate and therefore requires two wells of cells. A typical experiment will consist of at least five time-points (i.e. at least ten wells). An example of the data obtained form this type of experiment is shown in **Fig. 4.1a**.

1. Cells expressing K_{ATP}-HA are cultured to confluence in a 24-well culture plate under experimental conditions (*see* **Note 2**). Two wells are required for each time-point to be examined. In parallel, culture cells which do not express K_{ATP}-HA (*untransfected*) in a similar manner are to serve as negative controls.
2. Remove the culture medium and cool the cells to 4°C. Rinse three times with chilled PBS to remove the residual medium.
3. Overlay the cells in each well with 150 μl of chilled (4°C) labelling medium containing 0.2 μg/ml rat anti-HA antibodies and incubate at 4°C for 1 h to label channels on the cell surface.
4. Remove the labelling medium and rinse the cells six times with chilled PBS to remove any unbound antibodies.
5. Fix the cells in two of the wells by adding 100 μl of cell fixing solution. Incubate for 10 min at 4°C. These samples serve as zero time-point controls to which the extent of internalisation at other time-points will be compared.
6. Incubate the cells in pre-warmed (37°C) labelling medium containing no antibodies at 37°C for varying lengths of time to allow channel internalisation (*see* **Note 3**).

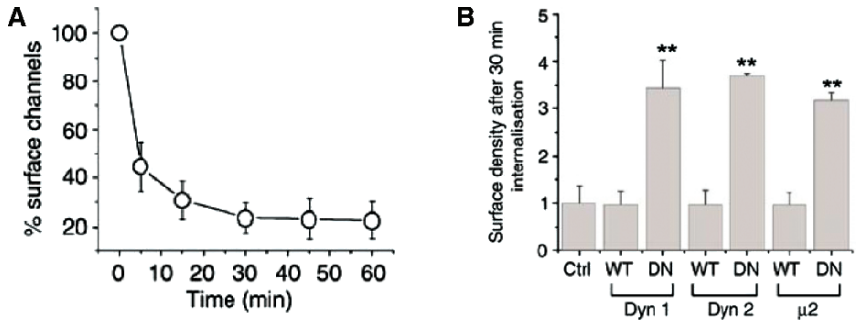

Fig. 4.1. Endocytosis and cell surface density of K_{ATP} channels in HEK293 cells. A time course of internalisation (**a**) and the steady-state surface expression (**b**) of K_{ATP} channels in HEK293 cells investigated by chemiluminescence-based methods. In (**b**) the surface density is increased by co-expression of dominant-negative (DN) forms of dynamin 1 (Dyn1), dymanin 2 (Dyn2) and μ2, each of which prevents clathrin-mediated endocytosis. (Reproduced from **ref. 6** with permission from the Nature publishing group).

7. Fix the cells by adding 100 μl of cell fixing solution. Incubate for 10 min at 4°C.
8. Rinse the cells three times with chilled PBS to remove residual fixative.
9. Incubate the fixed cells with labelling medium containing 1.2-μg/ml anti-rat HRP-conjugated antibodies at room temperature for 1 h.
10. Rinse eight times with PBS to remove any unbound antibodies.
11. Solubilise the cells by incubating with 150 μl of cell solubilisation solution for 20 min with gentle agitation.
12. Pipette two 50-μl aliquots of each solubilised cell sample into individual wells of a clear, flat-bottomed black-walled 96-well plate. Retain the remaining 50-μl sample on ice for future use.
13. Assay the HRP content of each lysate by adding 50 μl of high-sensitivity ECL reagent. Use an automated microplate reader to determine the luminescence. Allow the luminescence signal to reach a steady state, which typically takes between 5 and 10 s following addition of the ECL reagent.
14. Determine the total protein content of each lysate using the remaining lysate from step 10 (*see* **Subheading 4.3.3**).
15. Correct the luminescence readings for each sample relative to protein content (relative fluorescence units/μg protein).
16. Deduct the mean corrected luminescence readings for the untransfected control cells (which correspond to the background signals) from each of the luminescence readings for each test sample. This results in two background subtracted

readings for each lysate which is in turn one of two samples from the original 24-well culture plate.

17. Normalise each of the corrected readings to the signal at zero time, i.e. no internalisation. Perform the experiment in triplicate and express as mean ± SEM and plot vs. internalisation time. An example of the data is shown in **Fig. 4.1a**.

4.3.2. Steady-State Cell Surface Density Chemiluminescence-Based Assay

The above protocol (*see* **Subheading 4.3.1**) may be modified to allow the determination of the relative steady-state surface expression of channels at a given time. The protocol is identical except for the omission of **steps 5** and **6** (internalisation of labelled channels at 37°C). The channels on the cell surface are labelled at 4°C, at which temperature no trafficking will occur, and then the cells are fixed. The chemiluminescence protocol then continues and the channel cell surface density is quantified. The process of clathrin-mediated endocytosis may be disrupted by the expression of genetically encoded modulators (e.g. DN forms of dynamin 1, dynamin 2 and μ2). An example of the data is shown in **Fig. 4.1b**.

4.3.3. Cell Lysate Total Protein Assay

This protocol describes how the protein content of cell lysates is to be determined using the BCA method. Many alternative methods are available in kit form from numerous suppliers.

1. Pipette 10 μl of each cell lysate into individual wells of a flat-bottomed 96-well plate in duplicate.
2. Pipette 10 μl of each protein standard into individual wells of a flat-bottomed 96-well plate in triplicate.
3. Add 200 μl of BCA reagent to each well and incubate the plate at 37°C for 30 min.
4. Measure the absorbance of each sample at 550 nm using a plate reader.
5. Plot the mean absorbance values of the protein standards against protein concentration to create a calibration curve from which the mean protein content of the cell lysates can be extrapolated.

4.4. Notes

1. Antibodies targeted against extracellular regions of K_{ATP} are not commercially available. Therefore an extracellular HA-epitope was inserted into an extracellular loop of the Kir6.2 subunit using PCR-based techniques. It is vital that the insertion of epitopes is shown not to interfere with normal channel functions. The presence of extracellular HA

epitopes allows the use of well-characterised commercial anti-HA antibodies. It is important that the antibodies used contain no preservatives (e.g. sodium azide or thermosial) as these may harm the cells being investigated.

2. The adherence of cells may be improved by coating the bottom of each well with 0.0001% poly-L-lysine (>70,000 KDa) solution for 1 h. Each well should be rinsed with 1× PBS before seeding the cells into them.
3. The duration of the internalisation steps required will vary between different ion channels and should be determined empirically. For most applications 0, 15, 30 and 60 min should prove to be a good starting point.

Acknowledgment

The authors would like to thank Dr. Jamel Mankouri for the development of the chemiluminescence-based assays.

References

1. Hu, K., Huang, C. S., Jan, Y. N., and Jan, L. Y. (2003) ATP-sensitive potassium channel traffic regulation by adenosine and protein kinase C. *Neuron* **38**, 417–32.
2. Okiyoneda, T. and Lukacs, G. L. (2007) Cell surface dynamics of CFTR: the ins and outs. *Biochim Biophys Acta* **1773**, 476–9.
3. Herfst, L. J., Rook, M. B., and Jongsma, H. J. (2004) Trafficking and functional expression of cardiac Na+ channels. *J Mol Cell Cardiol* **36**, 185–93.
4. Steele, D. F., Eldstrom, J., and Fedida, D. (2007) Mechanisms of cardiac potassium channel trafficking. *J Physiol* **582**, 17–26.
5. Jarvis, S. E. and Zamponi, G. W. (2007) Trafficking and regulation of neuronal voltage-gated calcium channels. *Curr Opin Cell Biol* **19**, 474–82.
6. Mankouri, J., Taneja, T. K., Smith, A. J., Ponnambalam, S., and Sivaprasadarao, A. (2006) Kir6.2 mutations causing neonatal diabetes prevent endocytosis of ATP-sensitive potassium channels. *EMBO J* **25**, 4142–51.
7. Zerangue, N., Schwappach, B., Jan, Y. N., and Jan, L. Y. (1999) A new ER trafficking signal regulates the subunit stoichiometry of plasma membrane K(ATP) channels. *Neuron* **22**, 537–48.

Chapter 5

Investigation of K_{ATP} Channel Endocytosis by Immunofluorescence

Andrew J. Smith and Asipu Sivaprasadarao

Summary

Macroscopic ion channel currents (I) are a product of the channel open probability (P_o), the single channel current (i) and the number of channels present on the cell surface (N) at any given time ($I = P_o iN$). Intracellular trafficking pathways are proving to be of vital importance in regulating ion channel function since endocytosis, recycling and degradation all work in concert to maintain appropriate channel numbers on the cell surface. Immunofluorescence-based techniques provide a convenient and rapid method for the examination of these processes and have been used to investigate the intracellular trafficking of pancreatic ATP-sensitive potassium (K_{ATP}) channels.

Key words: Endocytosis, Immunofluorescence, K_{ATP} channels, Intracellular trafficking.

5.1. Introduction

Endocytosis is known to be a key regulator of cell surface density for a wide range of channels including K_{ATP} *(1)* CFTR *(2)* as well as a number of other Na^+ *(3)*, K^+ *(4)* and Ca^{2+} *(5)* channels. Defects in the process of endocytosis can also account for some of the deleterious effects associated with channel dysfunction in disease. Examples of this include impaired endocytosis of K_{ATP} channels associated with two mutations of Kir6.2, (the pore-forming subunit of pancreatic K_{ATP} channels), which causes permanent neonatal diabetes *(6)*. The fate of channels immediately following endocytosis can also have profound implications on the

Jonathan D. Lippiat (ed.), *Methods in Molecular Biology, Potassium Channels, vol. 491*

Book doi: 10.1007/978-1-59745-526-8

macroscopic currents of ion channels. Channels may be targeted for degradation in the lysosomes, stored at various sites within the cell or recycled back to the cell surface *(2, 5)*. Any perturbation of any of these processes will also affect the steady-state cell surface density of ion channels .

The rate of internalisation and subsequent subcellular destinations of ion channels can be examined by immunofluorescence. For these approaches it is necessary to have antibodies which bind to the external portions of the channel to be examined. This allows antibody binding to a pool of channels on the cell surface while the cells are held in a state which is non-permissive to trafficking, achieved by cooling cells to 4°C. When the cells are warmed back to temperatures permissive to protein trafficking, the channel/antibody complex is internalised from the cell surface and enters the endocytic pathway. At various time-points, internalisation is halted by fixation and the membrane/intracellular distribution of the labelled channels can be examined by fluorescence microscopy. The cells can also be treated to fluorescently label specific organelles so that the intracellular trafficking itinerary of an endocytosed channel can be determined.

5.2. Materials

5.2.1. Coverslip Preparation

1. Circular 13-mm diameter number 1 thickness borosilicate glass coverslips (BDH).
2. Poly-L-lysine: Sterile 0.01% poly-L-lysine (>70,000 KDa) solution.
3. 70% ethanol in water.
4. Sterile 24-well culture plate.
5. Sterile phosphate buffered saline (PBS): 10-mM phosphate buffer, 2.7-mM KCl, 137-mM NaCl prepared from tablets (Sigma) by dissolving one tablet in 200 ml of water and then autoclaved to sterilise.

5.2.2. Cell Culture

1. Culture medium: Dulbecco's Modified Eagles Medium (DMEM) supplemented with 10% foetal bovine serum. Warm to 37°C before using.
2. HEK cells stably expressing pancreatic K_{ATP} channels (sulphonylurea receptor 1 (SUR1) and Kir6.2 bearing an extracellular HA-epitope – K_{ATP}-HA) *(7)*.
3. Sterile phosphate buffered saline (PBS): 10-mM phosphate buffer, 2.7-mM KCl, 137-mM NaCl prepared from tablets (Sigma) by dissolving one tablet in 200 ml of water and autoclaved to sterilise. Warm to 37°C before using.

4. Trypsin–EDTA solution: Sterile 0.05% trypsin, 0.05% EDTA solution (Gibco BRL).

5.2.3. Immunofluorescence Techniques

1. Culture medium: Dulbecco's Modified Eagles Medium (DMEM) supplemented with 10% foetal bovine serum.
2. HEK cells stably expressing pancreatic K_{ATP} channels (sulphonylurea receptor 1 (SUR1) and Kir6.2 bearing an extracellular HA-epitope – K_{ATP}-HA) (*see* **ref.** *7*, also *see* **Note 1**).
3. Phosphate buffered saline (PBS): 10-mM phosphate buffer, 2.7-mM KCl, 137-mM NaCl prepared from tablets (Sigma) by dissolving one tablet in 200 ml of water.
4. Antibodies targeted against external epitope: Rat anti-HA (clone 3F10) (Roche Diagnostics) (*see* **Note 1**).
5. Labelling medium: DMEM supplemented with 5% goat serum freshly prepared before each experiment.
6. HRP-conjugated antibodies: Anti-rat HRP-conjugated antibodies (Sigma).
7. Poly-L-lysine coated coverslips are prepared by overlaying sterile 13-mm diameter borosilicate coverslips (number 1 thickness) with filter sterilised 0.0001% poly-L-lysine (>70,000 KDa) solution for 1 h. Rinse the coated coverslips three times with sterile 1× PBS prior to the seeding of cells onto them.
8. Cell fixing solution: prepare 2% fresh paraformaldehyde (w/v) solution in PBS for each experiment. The solution should be carefully heated in a fume-hood to dissolve and then cooled to room temperature before use (*see* **Note 2**).
9. Cell permeabilisation solution: Methanol/acetone (1:1, v/v) chilled to –20°C.
10. Blocking solution: 5% goat serum in 1× PBS. This may be stored at 4°C for up to a week following the addition of 0.05% (w/v) sodium azide.
11. Fluorophore-conjugated secondary antibodies: Anti-rat Cy3-conjugated IgG (Jackson ImmunoResearch) to label K_{ATP}-HA. Appropriate FITC-conjugated IgGs are required for organelle co-labelling.
12. Anti-fade reagent: Hard-set VECTAshield (Vector labs).
13. Organelle marker antibodies (*see* **Note 3**).
14. Laser-scanning confocal microscope: For Cy3 labelling a He/Ne laser fitted with 543-nm filters (or equivalent thereof) is required. For FITC labelling an argon laser fitted with 488-nm filters (or equivalent thereof) is required.

5.3. Methods

5.3.1. Preparation of Poly-L-Lysine Coated Coverslips

1. Soak a large piece of paper tissue with 70% ethanol and place in a laminar flow hood. Allow to dry.
2. Using forceps submerge coverslips in 70% ethanol to sterilise and place on tissue to air-dry.
3. Once dry, use forceps to place one sterile coverslip into each well of a 24-well plate.
4. Dilute 0.01% poly-L-lysine solution 1:100 with sterile PBS to give a 0.0001% solution.
5. Carefully overlay each coverslip with 150 µl of poly-L-lysine solution and leave for 30 min at room temperature.
6. Remove the poly-L-lysine solution and rinse the coated coverslips twice with sterile PBS.
7. Once all traces of PBS are removed the coated coverslips may be stored at 4°C until required.

5.3.2. Subculture of Cells and Seeding onto Coverslips

1. Culture cells expressing K_{ATP}-HA up to 70–80% confluence.
2. Remove culture medium and rinse with sterile PBS.
3. Add sufficient trypsin–EDTA solution to cover the cells and incubate for 2–3 min.
4. Once the cells detach themselves from the growth surface, add 10 volumes of pre-warmed culture medium and gently re-suspend the cells.
5. Add a single drop of cells to each poly-L-lysine coated coverslip in the 24-well plate and then add 0.5 ml of pre-warmed culture medium to each.
6. Culture the cells for a further 24 h or until they have adhered to the coverslip before labelling.

5.3.3. Examining Endocytosis by Immunofluorescence

The time-course of internalisation of K_{ATP} channels can be followed by labelling channels on the cell surface with an extracellularly targeted antibody and then following it up with its removal from the cell surface. To achieve this, several coverslips that have cells seeded onto them are required, one for each time-point. At several time-points internalisation is terminated by fixation and the distribution (cell surface or intracellular) of the channels can be examined. When the labelled samples are examined by confocal microscopy it is possible to see the redistribution of channels from the cell surface into intracellular structures as demonstrated in **Fig. 5.1a**.

1. Remove the culture medium and chill the cells to 4°C before rinsing three times with chilled labelling medium.
2. Pipette 150 µl of chilled labelling medium containing 0.2 µg/ml rat anti-HA antibody to each well and incubate at 4°C for 1 h to label extracellularly exposed channels.

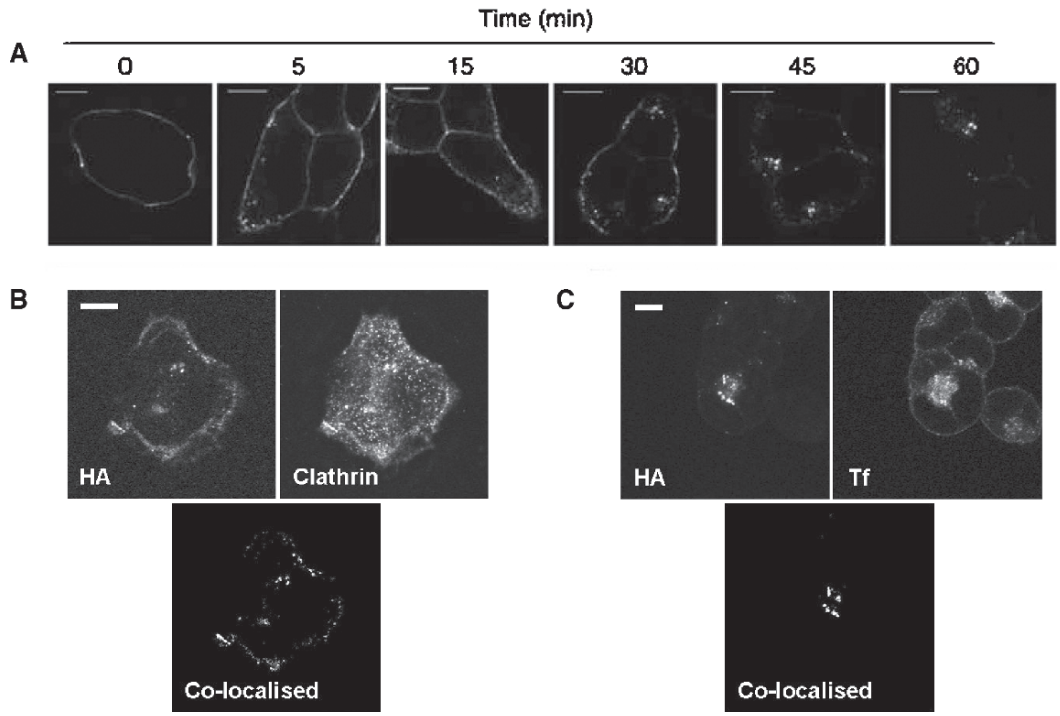

Fig. 5.1. Investigating endocytosis of K_{ATP} channels in HEK293 cells by immunofluorescence. (**a**) The time-course of internalisation shows the transit of anti-HA labelled K_{ATP}-HA channels from the cell surface into small cytoplasmic vesicular structures and finally into larger perinuclear aggregations. The intracellular distribution of endocytosed K_{ATP} channels may be examined by co-labelling cells with markers directed against organelles. In the example images shown, mouse anti-clathrin and anti-mouse Cy3-conjugated antibodies label clathrin-coated vesicles (**b**) and endocytosed FITC-conjugated transferrin (Tf) (which binds to transferrin receptors and is subsequently endocytosed) labels early endosomes (**c**). Anti-HA labelled K_{ATP} channels were labelled with contrasting fluorophores and imaged by confocal microscopy. The lower panels (co-localised) only show regions that display co-localisation between the two fluorophores. Scale bar = 10μm (reproduced from **ref.** *6* with permission from the Nature publishing group).

3. Remove the labelling medium (*see* **Note 4**) and rinse the cells six times with chilled 1× PBS to remove unbound antibodies.
4. Incubate the samples with 200 μl of labelling medium (pre-warmed to 37°C) for the desired length of time to allow internalisation to occur (*see* **Note 5**).
5. Terminate internalisation by replacing the warm labelling medium with chilled PBS followed by three further washes with chilled 1× PBS to remove excess labelling medium.
6. Fix the cells by adding 100 μl of cell fixing solution. Incubate for 10 min at room temperature and then rinse with 1× PBS.
7. Permeabilise the cells by incubating them with cell permeabilisation solution for 5 min. Rinse the cells three times with 1× PBS to remove residual permeabilisation solution.

8. Block non-specific binding sites in the cells by incubating them with blocking solution for 20 min at room temperature.
9. Incubate the cells with Cy3-conjugated secondary antibodies, diluted in blocking solution, for 1 h at room temperature to fluorescently label anti-HA antibody bound channels (*see* **Note 6**).
10. Wash the cells six times with 1× PBS to remove unbound antibodies.
11. Remove the coverslips from the 24-well plate using fine forceps and allow to air-dry (cell side up) for 5 min.
12. Mount the dried coverslips onto microscope slides using anti-fade reagent.
13. View the labelled samples by laser-scanning confocal microscopy. Example data are shown in **Fig. 5.1**.

5.3.4. Intracellular Localisation by Immunofluorescence and Subcellular Markers

To distinguish the identity of the intracellular compartments to which K_{ATP} channels are moved following endocytosis, it is necessary to label individual compartments using either highly specific antibodies or commercially available labelling reagents (e.g. mitotracker (Molecular probes) for mitochondria). When the endocytosed channels and organelles are labelled with fluorophores of different colours their distributions can be compared to each other. Examples of these data are shown in **Fig. 5.1b**, **c**.

1. Culture the cells expressing K_{ATP}-HA to confluence before passage. Seed the cells into 24-well plates containing poly-L-lysine coated 13-mm diameter coverslips so that a confluence of ~60% is obtained after 48 h of further culture.
2. Remove the culture medium and chill the cells to 4°C before rinsing three times with chilled labelling medium.
3. Pipette 150 µl of chilled labelling medium containing 0.2 µg/ml rat anti-HA antibody to each well and incubate at 4°C for 1 h to label extracellularly exposed channels.
4. Remove the labelling medium (*see* **Note 4**) and rinse the cells six times with chilled 1× PBS to remove unbound antibodies.
5. Incubate the samples with 200 µl of labelling medium (pre-warmed to 37°C) for the desired length of time to allow internalisation to occur (*see* **Note 5**).
6. Terminate internalisation by replacing the warm labelling medium with chilled PBS followed by three further washes with chilled 1× PBS to remove excess labelling medium.
7. Fix the cells by adding 100 µl of cell fixing solution. Incubate for 10 min at room temperature; then rinse with 1× PBS.
8. Permeabilise the cells by incubating them with cell permeabilisation solution for 5 min. Rinse the cells three times with 1× PBS to remove residual permeabilisation solution.

9. Block non-specific binding sites in the cells by incubating them with blocking solution for 20 min at room temperature.
10. Incubate the cells with antibodies raised against specific organelle marker proteins (*see* **Note 7**) diluted in blocking solution for 2 h at room temperature (*see* **Note 6**).
11. Rinse the cells extensively with PBS to remove excess organelle antibodies.
12. Incubate the cells for 1 h at room temperature with fluorophore-conjugated secondary antibodies ensuring that the channel and organelle are labelled with contrasting colours, e.g. use FITC (green) and Cy3 (red). These antibodies are diluted in blocking solution (*see* **Note 6**).
13. Rinse the cells extensively with PBS to remove excess secondary antibodies.
14. Remove the coverslips from the 24-well plate using fine forceps and allow to air-dry (cell side up) for 5 min.
15. Mount the dried coverslips onto microscope slides using a suitable anti-fade reagent.
16. Examine the labelled samples by laser-scanning confocal microscopy. Images obtained with Cy3 and FITC can be overlaid and the distributions of each protein of interest can be compared using image analysis software.

5.4. Notes

1. Antibodies targeted against extracellular regions of K_{ATP} are not commercially available. Therefore an extracellular HA-epitope was inserted into an extracellular loop of the Kir6.2 subunit using PCR-based techniques. It is vital that the insertion of epitopes is shown not to interfere with normal channel functions. The presence of extracellular HA epitopes allows the use of well-characterised commercial anti-HA antibodies. It is important that the antibodies used contain no preservatives (e.g. sodium azide or thermosial) as these may harm the cells being investigated.
2. Fixation with PFA leads to proteins becoming crosslinked with each other, which can lead to problems with antibody epitopes becoming inaccessible. This can also lead to the fragmentation of delicate structures within the cell. To solve these problems, cells can be fixed by incubating them with methanol (chilled to −20°C) for 5 min; however fixation by this method will also permeabilise cell membranes.

3. In order to selectively label intracellular organelles, the antibodies selected must be targeted against proteins which display a high degree of association with the organelle. Examples of such proteins are EEA1 (early endosomes), Mannose 6 phosphate receptor (late endosomes), Lamp1 (lysosomes), TGN38 (*trans*-Golgi network), Mannosidase II (Golgi network), calreticulin (endoplasmic reticulum) and nucleolin (nucleus). An alternative to labelling organelles with antibodies is to transfect cells with genetically encoded organelle markers such as the Clontech subcellular localisation vectors or to use compounds designed to label a particular compartment (e.g. Mitotracker from Invitrogen which labels mitochondria).
4. The labelling medium may be reused if necessary, although care should be taken to ensure that it does not become contaminated prior to reuse.
5. The duration of the internalisation steps required will vary between different ion channels and should be determined empirically. For most applications 0, 15, 30 and 60 min should prove to be a good starting point.
6. For antibody incubations with cells in 24-well plates, sufficient antibody labelling solution is required to submerge the coverslips, typically 150–200 µl. Smaller volumes of antibody labelling solution can be used by placing the coverslips cell-side up on a sheet of parafilm placed on a flat surface. This allows volumes of 30 µl per coverslip to be used since the hydrophobic surface of the parafilm ensures that all liquid remains on the coverslip.
7. The antibodies used to label organelles MUST be derived from a different species to the antibody used to label the internalised channel. This allows specific staining of the two primary antibodies with appropriate secondary antibodies. The fluorophores used must also be easily distinguished from each other (e.g. FITC – green and Cy3 – red).

Acknowledgments

The authors would like to thank Dr. Jamel Mankouri and Dr. Tarvinder Taneja for their contributions.

References

1. Hu, K., Huang, C. S., Jan, Y. N., and Jan, L. Y. (2003) ATP-sensitive potassium channel traffic regulation by adenosine and protein kinase C. *Neuron* **38**, 417–32.
2. Okiyoneda, T. and Lukacs, G. L. (2007) Cell surface dynamics of CFTR: the ins and outs. *Biochim. Biophys. Acta* **1773**, 476–9.
3. Herfst, L. J., Rook, M. B., and Jongsma, H. J. (2004) Trafficking and functional expression of cardiac Na+ channels. *J. Mol. Cell Cardiol.* **36**, 185–93.
4. Steele, D. F., Eldstrom, J., and Fedida, D. (2007) Mechanisms of cardiac potassium channel trafficking. *J. Physiol.* **582**, 17–26.
5. Jarvis, S. E. and Zamponi, G. W. (2007) Trafficking and regulation of neuronal voltage-gated calcium channels. *Curr. Opin. Cell Biol.* **19**, 474–82.
6. Mankouri, J., Taneja, T. K., Smith, A. J., Ponnambalam, S., and Sivaprasadarao, A. (2006) Kir6.2 mutations causing neonatal diabetes prevent endocytosis of ATP-sensitive potassium channels. *EMBO J.* **25**, 4142–51.
7. Zerangue, N., Schwappach, B., Jan, Y. N., and Jan, L. Y. (1999) A new ER trafficking signal regulates the subunit stoichiometry of plasma membrane K(ATP) channels. *Neuron* **22**, 537–48.

Chapter 6

Investigation of K_{ATP} Channel Endocytosis and Cell Surface Density by Biotinylation and Western Blotting

Andrew J. Smith and Asipu Sivaprasadarao

Summary

Macroscopic ion channel currents (I) are a product of the channel open probability (P_o), the single channel current (i) and the number of channels present on the cell surface (N) at any given time ($I = P_o iN$). Endocytosis has been shown to be one of the key determinants of cell surface channel density and defects of this process have been linked to diseases relating to ion channel dysfunction. Biotinylation allows the selective labelling and isolation of surface exposed proteins which can then be identified by Western blotting.

Key words: Endocytosis, Internalisation, Biotinylation, Western blotting, K_{ATP} channels.

6.1. Introduction

Alterations of trafficking processes have profound effects on ion channel cell surface densities *(1–3)*. These processes include endocytosis, recycling and biosynthetic delivery of channel proteins, all occurring in a coordinated manner to ensure an appropriate cell surface density *(4)*. An example of an ion channel where the biosynthetic delivery and endocytosis have been shown to influence channel numbers on the cell surface is the ATP-sensitive potassium (K_{ATP}) channel *(5–7)*. These processes have also been implicated in pathophysiological disorders; impaired biosynthetic delivery of K_{ATP} channels can lead to congenital hyperinsulinemia *(8, 9)* and reduced internalisation may lead to permanent neonatal diabetes *(6)*.

The steady-state surface density and internalisation rate of ion channels can be examined by biotinylation studies. Proteins

Jonathan D. Lippiat (ed.), *Methods in Molecular Biology, Potassium Channels, vol. 491*

Book doi: 10.1007/978-1-59745-526-8

on the cell surface, including the ion channel to be examined, are labelled with membrane-impermeable biotin at a temperature which is non-permissive to trafficking. The labelled proteins are then allowed to internalise for a period of time by incubating them at a temperature which is permissive to trafficking. Biotinylated proteins that remain on the cell surface are then chemically treated to remove the biotin, however, internalised proteins are not affected. The cells are then lysed and biotinylated proteins isolated by binding them to immobilised streptavidin. These isolated biotinylated proteins can then be resolved by SDS-PAGE and channel proteins identified by Western blotting. The steady-state cell surface density of channel proteins may be examined by omitting the internalisation and the biotin stripping steps.

6.2. Materials

6.2.1. Biotinylation of Cell Surface Proteins

1. Culture medium: Dulbecco's Modified Eagles Medium (DMEM) supplemented with 10% foetal bovine serum.
2. HEK cells stably expressing K_{ATP} channels (SUR1 and Kir6.2 bearing a FLAG epitope at the intracellular C-terminus).
3. Phosphate buffered saline (PBS): 10-mM phosphate buffer, 2.7-mM KCl, 137-mM NaCl prepared from tablets (Sigma) by dissolving one tablet in 200 ml of water.
4. Biotin labelling solution: 1.5-mg/ml Sulpho-*S*-*S*-biotin (Pierce) in 1× PBS (*see* **Note 1**) to be freshly prepared and stored on ice.
5. Glycine solution: 50-mM glycine in 1× PBS to be freshly prepared.
6. Internalisation buffer: 10-mM glucose in 1× PBS. Aliquots of this buffer (~2.5 ml per flask) need to be warmed to 37°C and chilled to 4°C prior to the experiment.
7. Glutathione buffer: 50-mM glutathione, 75-mM NaOH, 75-mM NaCl, 1-mM EDTA, 0.1% BSA, pH 9.0 to be freshly prepared and chilled to 4°C.
8. Iodoacetamide solution: 5-mg/ml iodoacetamide (Sigma) in 1× PBS to be freshly prepared and chilled to 4°C.
9. Extraction buffer: 50-mM Tris–HCl, pH 7.4, 2-mM EDTA, 2-mM EGTA, 100-mM NaCl, 1% (w/v) Triton X-100, 1× protease inhibitor cocktail (Roche diagnostics) freshly prepared and chilled to 4°C.
10. Neutravidin beads: Ultralink-neutravidin beads (50% slurry) (Pierce) were equilibrated by washing twice with extraction

buffer. 50 µl of 50% neutravidin bead slurry is required for each sample.

11. Reducing sample buffer: 25-mM sodium bicarbonate (pH 10.4), 4% SDS, 0.2% bromophenol blue, 20% glycerol. Add 100-mM DTT immediately prior to use.

6.2.2 Cell Lysate Protein Determination Assay

1. BCA reagent: Mix 49 parts bicinchoninic acid solution (Sigma) with 1 part 4% (w/v) copper sulphate solution immediately before use.
2. Protein standards: Several samples of known protein concentration are prepared by diluting 10-mg/ml BSA in the same buffer used to solubilise cells. The concentration of the protein standards should range from 0 to 10 µg/ml.
3. 96-well plates with clear flat bottoms.

6.2.3 SDS-PAGE and Western Blotting

1. Bio-Rad protean2 mini gel apparatus: Includes larger glass back casting plate with fitted spacers at the side, a smaller flat glass front casting plate and a plastic comb to form wells.
2. Gel running apparatus suitable for Bio-Rad protean2 gels: Includes gasket to hold gels in place and running tank.
3. Semi-dry Western blotting transfer cell (Bio-Rad).
4. Glycerol solution: 5% glycerol (w/v) in water. May be stored at room temperature.
5. Acrylamide mix: 30% acrylamide/bis-acrylamide solution (Sigma). This is a potent neurotoxin and care must be taken to limit exposure.
6. Resolving buffer: 1.5-M Tris–HCl, pH 8.8. May be stored at room temperature.
7. SDS solution: 10% SDS in water. May be stored at room temperature.
8. APS solution: 10% ammonium persulphate solution in water. This should be freshly prepared each day.
9. TEMED (Sigma). This should be stored at 4°C. Because of its long-term instability only small volumes should be purchased.
10. Stacking buffer: 0.5-M Tris–HCl, pH 6.8. May be stored at room temperature.
11. Water-saturated isobutanol: Isobutanol should be vigorously mixed with water and allowed to separate. Isobutanol will form the upper layer.
12. Running buffer: 25-mM Tris–HCl, pH 7.4, 192-mM glycine, 0.1% SDS in water. May be stored at room temperature.
13. Pre-stained protein standards: Broad-range pre-stained protein standard (Bio-Rad).

14. Transfer buffer: 25-mM Tris-HCl , 192-mM glycine, 0.1% SDS, 20% methanol in water, pH 7.4. Store at 4°C.
15. Supported nitrocellulose membrane (Hybond).
16. PBS-T: 1× PBS with 0.05% Tween-20.
17. Blocking solution: 5% non-fat dry milk in PBS-T (*see* **Note 2**).
18. Antibody dilution buffer: 0.5% non-fat dry milk in PBS-T (see Note 2).
19. Mouse anti-FLAG antibodies (Sigma).
20. Anti-mouse HRP-conjugated antibodies (Pierce).
21. X-ray film: Kodak Biomax XAR film (*see* **Note 3**).

6.3. Methods

6.3.1. Examining Endocytosis by Biotinylation

The rate of endocytosis of K_{ATP} channels has been examined through biochemical means by labelling cell surface channels with biotin. Biotinylated proteins that are internalised into cells by subsequent incubation at 37°C are protected from biotin removal by chemical treatment. The cells are then lysed and the remaining biotinylated proteins can be isolated by binding them to streptavidin-coated beads. The proteins can then be resolved by SDS-PAGE and identified by Western blotting. The relative abundance of biotinylated proteins can then be quantified. When several time-points of internalisation are performed the changes in internalisation can be appreciated. Examples of these data are shown in **Fig. 6.2**.

1. Culture cells expressing K_{ATP}-HA to confluence in 25-cm^2 culture flasks. One flask is required for each time-point to be investigated (*see* **Note 4**).
2. Remove the culture medium and rinse four times in 1× PBS.
3. Biotinylate cell surface channels with 2 ml per flask of chilled (4°C) biotin labelling solution for 20 min at 4°C.
4. Quench residual biotin by washing twice with chilled glycine solution, each for 5 min at 4°C.
5. Internalise labelled channels by incubating with pre-warmed (37°C) internalisation buffer at 37°C for the desired period of time.
6. Following the desired period, terminate internalisation by replacing the internalisation buffer with chilled internalisation buffer and keeping it at 4°C.
7. Replace the internalisation buffer with 2-ml of chilled glutathione buffer. This strips biotin from the surface exposed channels (but not from those which have internalised with the

biotin). Each flask requires two, 20-min washes with glutathione buffer at 4°C.

8. Remove the glutathione buffer and quench residual glutathione with 2 ml of iodoacetamide solution for 5 min at 4°C.
9. Remove the iodoacetamide buffer and lyse the cells in 1-ml of extraction buffer at 4°C with gentle agitation. Lysis is complete when cell clumps are no longer visible to the eye.
10. Transfer each lysate to a 1.5-ml microcentrifuge tube and centrifuge at 15,000 × *g* in a cooled (4°C) bench top microcentrifuge for 90 min. This clears the lysate of any residual cellular debris (*see* **Note 5**).
11. Determine the protein content of each lysate using a cell lysate total protein assay (*see* **Subheading 6.3.3**).
12. Dilute the lysates with extraction buffer so that they are all of the same concentration. The lysates should then be stored on ice.
13. Mix equal volumes of each lysate (containing equal quantities of total protein) with 50-µl of neutravidin beads in microcentrifuge tubes and incubate them with rotation at 4°C for 2 h. This allows the biotinylated proteins in the lysate to bind to the neutravidin beads.
14. Pellet the neutravidin beads by centrifugation and remove the supernatant (*see* **Note 6**).
15. Wash the neutravidin bead pellet four times with extraction buffer to remove any non-specifically bound proteins.
16. Elute the biotinylated proteins from the neutravidin beads by re-suspension of the washed neutravidin bead pellet in 50-µl of reducing sample buffer and incubate for 15 min at room temperature.
17. Pellet the neutravidin beads by centrifugation and resolve the eluted proteins contained within the reducing sample buffer by SDS-PAGE (*see* **Subheading 6.3.4**).

6.3.2. Examining Steady-State Cell Surface Density by Biotinylation

1. Culture cells expressing K_{ATP}-HA to confluence in 25-cm^2 culture flasks. One flask is required for each time-point to be investigated (*see* **Note 4**).
2. Remove the culture medium and rinse four times in 1× PBS.
3. Biotinylate cell surface channels with 2 ml per flask of chilled (4°C) biotin labelling solution for 20 min at 4°C.
4. Quench residual biotin by washing twice with chilled glycine solution, each for 5 min at 4°C.
5. Lyse the cells in 1-ml of extraction buffer at 4°C with gentle agitation. Lysis is complete when cell clumps are no longer visible to the eye.
6. Transfer each lysate to a 1.5-ml microcentrifuge tube and centrifuge at 15,000 × *g* in a cooled (4°C) bench top microcentrifuge

for 90 min. This clears the lysate of any residual cellular debris (*see* **Note 5**).

7. Determine the protein content of each lysate using a cell lysate total protein assay (*see* **Subheading 6.3.2**).
8. Dilute the lysates with extraction buffer so that they are all of the same concentration. The lysates should then be stored on ice.
9. Mix equal volumes of each lysate (containing equal quantities of total protein) with 50-µl of neutravidin beads in microcentrifuge tubes and incubate them with rotation at 4°C for 2 h. This allows the biotinylated proteins in the lysate to bind to the neutravidin beads.
10. Pellet the neutravidin beads by centrifugation and remove the supernatant (*see* **Note 6**).
11. Wash the neutravidin bead pellet four times with extraction buffer to remove any non-specifically bound proteins.
12. Elute the biotinylated proteins from the neutravidin beads by re-suspension of the washed neutravidin bead pellet in 50-µl of reducing sample buffer and incubate for 15 min at room temperature.
13. Pellet the neutravidin beads by centrifugation and resolve the eluted proteins contained within the reducing sample buffer by SDS-PAGE (*see* **Subheading 6.3.4**).

6.3.3. Cell Lysate Total Protein Assay

This protocol describes how the protein content of cell lysates is to be determined using the BCA method. Many alternative methods are available in kit form from numerous suppliers.

1. Pipette 10 µl of each cell lysate into individual wells of a flat-bottomed 96-well plate in duplicate.
2. Pipette 10 µl of each protein standard into individual wells of a flat-bottomed 96-well plate in triplicate.
3. Add 200 µl of BCA reagent to each well and incubate the plate at 37°C for 30 min.
4. The absorbance of each sample at 550 nm is measured using a spectrophotometer.
5. Plot the mean absorbance values of the protein standards against protein concentration to create a calibration curve from which the mean protein content of the cell lysates can be extrapolated.

6.3.4. SDS-PAGE and Western Blotting

These instructions relate to the use of Bio-Rad protean2 apparatus but can be easily modified for use with any other SDS-PAGE gel system. The following quantities are sufficient for the production of two 0.75-mm thick, 10% mini gels. The blotting protocol relates to the use of the Bio-Rad semi-dry transfer cell.

1. Clean the front and back gel casting plates with warm water and finally rinse with distilled water. Allow to dry.
2. Place the glass plates into the casting frame.
3. Prepare the separating gel mix: 4 ml of glycerol solution, 3.3-ml acrylamide mix, 2.5-ml resolving buffer, 100-µl SDS solution, 100-µl APS solution and 4-µl TEMED. Gently mix (*see* **Note 7**) and pipette into the gap between the two glass plates filling 3/4 of the way up (leaving sufficient room for the stacking gel and spacer comb). Finally overlay the mixture with water-saturated isobutanol. The gel should polymerise within 30 min.
4. Remove the isobutanol layer and rinse the top of the gel with water.
5. Prepare the stacking gel mix: 1.4 ml of glycerol solution, 330-µl of acrylamide mix, 250-µl of resolving buffer, 20-µl of SDS solution, 20-µl of APS solution and 2-µl of TEMED. Gently mix (*see* **Note 7**) and pipette into the gap between the two glass plates to the top. Immediately place the spacer comb into place to cast the sample wells. The gel should polymerise within 30 min.
6. Remove the gels from the casting apparatus and assemble the running tank (*see* **Note 8**). Fill the central buffer reservoir with the running buffer and carefully remove the combs.
7. Load equal amounts of each protein sample into individual lanes and a single lane with pre-stained protein standards.
8. Half fill the external tank with running buffer and place the lid on the tank.
9. Run the gel at 200 mV for 45 min or until the dye-fronts are run off the bottom of the gel.
10. Disassemble the gel running apparatus and remove one of the glass plates from the gel. Using a sharp blade, remove the stacking gel and discard.
11. Remove the gel from the glass plate and submerge it in chilled transfer buffer for no longer than 5 min.
12. Concurrently, soak nitrocellulose membrane cut to the same size as the resolving gel in chilled transfer buffer (*see* **Note 9**).
13. Cut two pieces of thick blotting paper to the same size as the resolving gel and soak in chilled transfer buffer.
14. Prepare the Western blot transfer stack as follows: (from the bottom) 1× soaked blotting paper, soaked nitrocellulose membrane, resolving gel and1× soaked blotting paper. This is summarised in **Fig. 6.1.**
15. Transfer proteins onto nitrocellulose using a Bio-Rad semi-dry transfer cell. Both electrodes must be wetted with transfer buffer. Once on the apparatus, use a sample tube to roll out any air bubbles which may be trapped within the

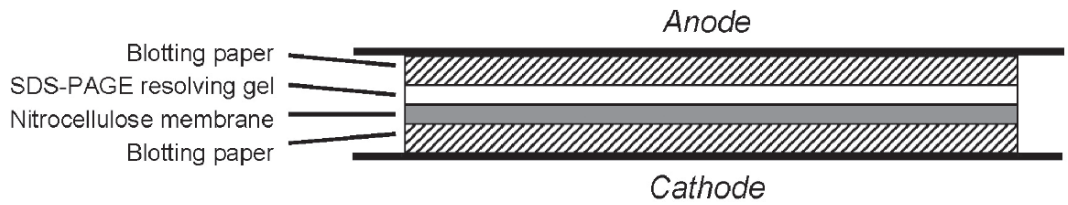

Fig. 6.1. Setting up for a Western blot transfer. These instructions assume the use of a Bio-Rad semi-dry transfer cell. The "Western blot stack" should be assembled as shown. A layer of pre-soaked thick blotting paper is laid flat onto the cathode. The soaked nitrocellulose is then carefully placed on top of this, followed by the soaked SDS-PAGE gel. The stack is completed by the addition of a final layer of soaked thick blotting paper. Air bubbles are then rolled out of the stack and the anode secured in place. When electrical current is passed through the stack, the SDS-coated proteins will migrate towards the cathode and become immobilised on the nitrocellulose membrane.

transfer stack. Assemble the transfer cell and run at 0.03 mA for 90 min.

16. Remove the nitrocellulose membrane from the apparatus and rinse twice with distilled water and twice with PBS-T.
17. Block the membrane by incubating with blocking solution for 1 h at room temperature with gentle agitation.
18. Incubate the membrane with mouse anti-FLAG antibody diluted in antibody dilution buffer overnight at 4°C with gentle agitation.
19. Wash excess antibody off the membrane with PBS-T at room temperature with gentle agitation. Four washes each of 5 min should be sufficient.
20. Incubate the membrane with anti-mouse HRP-conjugated antibodies.
21. Wash excess antibody off the membrane with PBS-T at room temperature with gentle agitation. Four washes each of 5 min should be sufficient.
22. During the final wash step prepare 1 ml of ECL reagent.
23. Place the washed membrane on a clean sheet of acetate and pipette the ECL reagent over the entire surface of the membrane. Incubate at room temperature for 2 min.
24. Drain the ECL reagent from the surface and cover the membrane with a second sheet of acetate.
25. The acetate containing the membrane is then placed in an X-ray cassette with X-ray film for an appropriate length of time (*see* **Note 10**). The film is then submerged in developing fluid until the signal has developed fully and then submerged in fixative fluid to preserve the signal. An example of the data obtained is shown in **Fig. 6.2**.

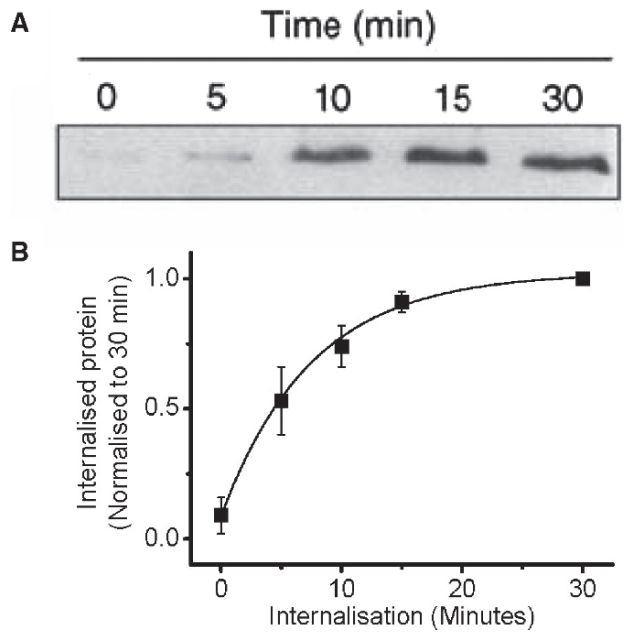

Fig. 6.2. An investigation of K_{ATP} channel internalisation by biotinylation. Cell surface exposed proteins were labelled with membrane impermeable biotin. Internalised, biotin labelled channels were protected from biotin cleavage by glutathione. An increase in signal therefore corresponds to an increase in internalised protein. The time indicates the duration of the internalisation step. (**a**) Kir6.2-HA was probed with mouse anti-FLAG and anti-mouse HRP-conjugated antibodies in the blot shown (reproduced from **ref. *6*** with permission from Nature publishing group). (**b**) The intensity of bands can be measured using image analysis software and plotted against internalisation time.

6.4. Notes

1. The Sulpho-*S*-*S*-biotin used is impermeable to cell membranes so only extracellularly exposed proteins will be labelled. Labelling with biotin also requires that lysine residues are accessible to the reagent, so some channel proteins may not be suitable for this type of labelling.
2. Solutions containing non-fat dry milk should be filtered through tissue paper to remove particulate matter. Failure to do this can lead to speckled background signals on the final blot.
3. Quantification of data may be achieved by digitally scanning blots although care must be taken during data acquisition not to saturate the signal. Alternatively automated systems may be used to capture the chemiluminescence signal.
4. The duration of the internalisation steps required will vary between different ion channels and should be determined empirically. For most applications 0, 15, 30 and 60 min should prove to be a good starting point.

5. Cell lysis provides a convenient point to halt the experiment. If this is to be the case, lysates should be stored at –80°C until required. Upon resumption of the experiment the lysates should be thawed slowly on ice. If the experiment is to be continued immediately, lysates should be kept on ice.
6. Whilst the supernatant is not required at any further stage of the biotinylation experiment it is often prudent to retain it for examination by SDS-PAGE and Western blotting at a later date should the biotinylation experiment fail. This sample should reveal whether the experiment failed during the biotinylation or because of problems at later stages.
7. The polymerisation of acrylamide gels is inhibited by exposure to air. Excessive mixing can aerate the mixture leading to poor polymerisation of the final gel. To further improve the quality of gels the starting solutions may be de-gassed.
8. Care must be taken when assembling the SDS-PAGE running tank to avoid any leaks between the central buffer reservoir and the external tank. Any such leaks cause the gel to run poorly.
9. Avoid handling nitrocellulose membranes with the hands as this may introduce background signals to the final blot. It is better to use clean forceps.
10. The length of exposure to X-ray film depends on the strength of the signal. Several exposures should be taken.

Acknowledgments

The Authors Would Like to thank Dr. Jamel Mankouri and Dr. Tarvinder Taneja for their Contributions.

References

1. Jarvis, S. E. and Zamponi, G. W. (2007) Trafficking and regulation of neuronal voltage-gated calcium channels. *Curr. Opin. Cell Biol.* **19**, 474–82.
2. Steele, D. F., Eldstrom, J, and Fedida, D. (2007) Mechanisms of cardiac potassium channel trafficking. *J. Physiol.* **582**, 17–26.
3. Lai, H. C. and Jan, L. Y. (2006) The distribution and targeting of neuronal voltage-gated ion channels. *Nat. Rev. Neurosci.* **7**, 548–62.
4. Pfeffer, S. (2003) Membrane domains in the secretory and endocytic pathways. *Cell* **112**, 507–17.
5. Zerangue, N., Schwappach, B., Jan, Y. N., and Jan, L. Y. (1999) A new ER trafficking signal regulates the subunit stoichiometry of plasma membrane K(ATP) channels. *Neuron* **22**, 537–48.
6. Mankouri, J., Taneja, T. K., Smith, A. J., Ponnambalam, S., and Sivaprasadarao, A. (2006) Kir6.2 mutations causing neonatal diabetes prevent endocytosis of ATP-sensitive potassium channels. *EMBO J.* **25**, 4142–51.
7. Hu, K., Huang, C. S., Jan, Y. N., and Jan, L. Y. (2003) ATP-sensitive potassium channel traffic regulation by adenosine and protein kinase C. *Neuron* **38**, 417–32.

8. Partridge, C. J., Beech, D. J., and Sivaprasadarao, A. (2001) Identification and pharmacological correction of a membrane trafficking defect associated with a mutation in the sulfonylurea receptor causing familial hyperinsulinism. *J. Biol. Chem*. **276**, 35947–52.

9. Taschenberger, G., Mougey, A., Shen, S., Lester, L. B., LaFranchi, S., and Shyng, S. L. (2002) Identification of a familial hyperinsulinism-causing mutation in the sulfonylurea receptor 1 that prevents normal trafficking and function of KATP channels. *J. Biol. Chem*. **277**, 17139–46.

Chapter 7

Lipid Microdomains and K^+ Channel Compartmentation: Detergent and Non-Detergent-Based Methods for the Isolation and Characterisation of Cholesterol-Enriched Lipid Rafts

Laura J. Sampson and Caroline Dart

Summary

The traditional view of the plasma membrane as a uniform cellular envelope formed from a homogenous mixture of lipids has been refined in recent years to reflect the heterogeneity of its composite lipids. The membrane can consist of upwards of 500 different types of lipids, which exhibit complex and dynamic interactions. Cholesterol and sphingolipids, in particular, partition away from the bulk of bilayer to form distinct microdomains or 'rafts'. Although controversial, lipid rafts have attracted considerable attention over recent years, firstly because of their apparent ability to selectively aggregate interacting signalling molecules, including ion channels and receptors, and secondly because of the implication that they may be involved in the spatial organisation of signalling pathways. Here we describe methods to isolate lipid rafts, assess their purity and determine the distribution of potassium channel proteins between raft and non-raft fractions.

Key words: Lipid microdomains, Lipid rafts, Caveolae, Cholesterol, K_{ATP} channels, Vascular smooth muscle, Detergent-resistant, Sucrose density centrifugation, SDS-PAGE, Western blot.

7.1. Introduction

Lipid microdomains or lipid rafts form within the bilayer and consist of tightly-packed aggregates of cholesterol and sphingolipids *(1–4)*. They represent a relatively rigid 'liquid-ordered' phase in contrast to the more fluid glycerophospholipid non-raft regions. Multiple types of rafts are likely to exist, based both on their lipid and protein composition *(5)*, but despite many years of study, lipid rafts remain controversial with little consensus on

Jonathan D. Lippiat (ed.), *Methods in Molecular Biology, Potassium Channels, vol. 491*

Book doi: 10.1007/978-1-59745-526-8

their size, composition, dynamics or physiological importance *(6–8)*. The only morphologically identifiable raft-like domain is a caveola where association with the protein caveolin causes the cholesterol and sphingolipid-enriched regions of the membrane to form small (50–100 nm) vesicular invaginations that are clearly visible in scanning or transmission electron microscopy *(9–11)*. The study of lipid rafts has been aided by the fact that their unusual composition gives them distinct biochemical properties. The tight packing of the lipid acyl chains in these regions results in a resistance to solubilisation by cold non-ionic detergents in which they form detergent-insoluble, glycolipid-enriched complexes, often referred to as DIGs *(12)*. The high lipid content of these complexes enables them to float to a low density during sucrose gradient centrifugation and allows the proteins associated with these regions to be isolated and characterised by Western blot analysis. Studies using these techniques have led to the identification of a wealth of signalling proteins that apparently aggregate in these regions, including a number of G-protein-coupled receptors, various classes of G-protein, voltage- and ligand-gated ion channels, protein kinase C, nitric oxide synthase, tyrosine kinases, H-ras and mitogen-activated protein kinase (reviewed by **refs.** *9, 10, 13*). This has led to the development of the idea that lipid rafts act to functionally compartmentalise cell-surface signalling *(2, 9, 10, 14)*. The protein components of rafts are however often contentious due to problems associated with raft isolation. Different detergents, and indeed different concentrations of the same detergent, produce rafts of differing protein and lipid composition *(5, 6)*. This may reflect the ability of some detergents to produce more 'pure' raft fractions by efficiently removing contaminating non-raft proteins and lipids, but this may equally suggest that some detergents selectively extract subsets of proteins and lipids from raft domains, leaving behind a domain that no longer resembles its "in vivo" form. Problems such as these have led to the development of non-detergent-based methods for the isolation of rafts *(15, 16)*. These essentially use sonication to disrupt the membrane followed by sucrose density centrifugation to separate the buoyant low-density raft component. While this method suffers from none of the selective extraction that plagues detergent-based methods, there is evidence that a number of contaminating non-raft proteins stay associated at the periphery of rafts and float with them to the low-density layers *(5, 17)*. Here we describe methods for both detergent and non-detergent-based extraction of lipid microdomains and suggest appropriate controls to assess the purity of the isolated fractions. The methods we describe were used to determine the compartmentalisation of the pore-forming Kir6.1 subunit of arterial ATP-sensitive potassium (K_{ATP}) channels in vascular smooth muscle caveolae *(18, 19)* and provide a useful

starting point in assessing the distribution of proteins between raft and non-raft regions. We would recommend that where possible fractionation experiments be followed up by functional and immunocytochemical studies.

7.2. Materials

7.2.1. Preparation of Arterial Homogenate: Detergent-Based (Triton-X 100) Method

1. 2-(*N*-Morpholino)ethanesulphonic acid (MES) buffered saline (MBS): 25-mM MES, 150-mM NaCl, pH 6.5. Store at 4°C.
2. Homogenisation buffer: MBS, 1% Triton-X 100 (v/v). Chill in refrigerator and keep on ice prior to use (*see* **Note 1**).
3. Pestle and mortar. Place in a –80°C freezer for several hours before use.
4. Liquid nitrogen.
5. Hand-held homogeniser.

7.2.2. Preparation of Sucrose Density Gradient: Detergent-Based (Triton-X 100) Method

1. MBS: 25-mM MES, 150-mM NaCl, pH 6.5. Store at 4°C.
2. MBS, 90% sucrose (w/v). Chill in refrigerator and keep on ice prior to use.
3. MBS, 35% sucrose (w/v). Chill in refrigerator and keep on ice prior to use.
4. MBS, 5% sucrose (w/v). Chill in refrigerator and keep on ice prior to use.
5. Centrifuge tubes.

7.2.3. Preparation of Arterial Homogenate: Non-Detergent-Based Method

1. 500-mM sodium carbonate (Na_2CO_3), pH 11. Store at 4°C.
2. Pestle and mortar. Place in a –80°C freezer for several hours before use.
3. Liquid nitrogen.
4. Hand-held homogeniser.
5. Probe sonicator.

7.2.4. Preparation of Sucrose Density Gradient: Non-Detergent-Based Method

1. 2-(*N*-Morpholino)ethanesulphonic acid (MES) buffered saline (MBS): 25-mM MES, 150-mM NaCl, pH 6.5. Store at 4°C.
2. MBS, 90% sucrose (w/v).
3. MBS, 250-mM Na_2CO_3, 35% sucrose (w/v).
4. MBS, 250-mM Na_2CO_3, 5% sucrose (w/v).
5. Polyethylene-terephthalate thin-walled ultracentrifuge tubes (for example Sorvall 12-ml polyclear Cat no. 06752).

7.2.5. SDS-Polyacrylamide Gel Electrophoresis (SDS-PAGE)

1. Resolving buffer: 1.5-M Tris–HCl, pH 8.8.
2. Stacking buffer: 0.5-M Tris–HCl, pH 6.8.
3. 30% acrylamide/bis solution (37.5:1) (this is a potential carcinogen when unpolymerised so care should be taken to avoid exposure).
4. *N*,*N*,*N*′,*N*′-Tetramethyl-ethylenediamine (TEMED).
5. 10% solution of SDS (w/v) in distilled water.
6. Ammonium persulphate: Prepare 10% solution (w/v) in distilled water immediately prior to use.
7. Isopropanol.
8. SDS Running buffer (×10): 250-mM Tris base, 1.92-M glycine, 1% SDS (w/v).
9. Pre-stained molecular weight markers such as Full Range Rainbow markers (Amersham Pharmacia Biotech) or pre-stained markers for molecular weights 27,000–180,000 (Sigma-Aldrich).

7.2.6. Western Blotting

1. Transfer buffer: 25-mM Tris base, 192-mM Glycine, 20% (v/v) methanol. No need to alter the pH. Chill prior to use.
2. Nitrocellulose membrane (Hybond ECL, Amersham Pharmacia Biotech).
3. Tris-buffered saline with Tween (TBS-T): 20-mM Tris–HCl, 137-mM NaCl, 0.1% (v/v) Tween 20, pH 7.6.
4. Blocking buffer: 5% (w/v) skim milk powder in TBS-T.
5. Primary antibody dilution buffer: 1% (w/v) skim milk powder in TBS-T.
6. Primary antibodies: mouse anti-adaptin, anti-caveolin 1, anti-flotillin 1, anti-flotillin 2 (BD Transduction Laboratories), mouse anti-transferrin receptor (Zymed Laboratories, Inc.), goat anti-Kir6.1 (R-14; sc-11224) and associated blocking peptide (sc-11224P) (Santa Cruz Biotechnology).
7. Secondary antibody dilution buffer: 1% (w/v) skim milk powder in TBS-T (this can be increased to 5% (w/v) skim milk powder if the secondary antibody produces high levels of background staining).
8. Secondary antibodies: Horseradish peroxidase-conjugated anti-mouse secondary (Jackson Immunochemical Laboratories). HRP-conjugated anti-goat secondary (Sigma-Aldrich).
9. Heavy weight blotting paper such as Whatman 3MM (0.34-mm thick).
10. Enhanced chemiluminescent (ECL) reagents and Hyperfilm ECL (both Amersham Pharmacia Biotech).

7.2.7. Measurement of Cholesterol and Sphingolipid (Ganglioside G_{M1}) Content

1. Amplex Red Cholesterol Assay Kit (Molecular Probes).
2. Horseradish peroxidase-coupled cholera toxin subunit B (Sigma-Aldrich).

7.3. Methods

The methods given below describe the procedure for isolating buoyant, cholesterol-enriched fractions (lipid rafts) from vascular smooth muscle cells using both detergent and non-detergent-based protocols. Both protocols use ultracentrifugation on discontinuous sucrose density gradients as a means of separating the low-density lipid rafts. It is particularly important that following ultracentrifugation all sucrose gradient fractions are characterised by Western blot analysis to assess the degree of separation of raft and non-raft regions. Useful markers for the raft regions are the proteins caveolin and flotillin. Markers for the non-raft regions are more problematic due to a lack of consensus over which proteins are universally excluded from rafts. Typically the transferrin receptor is used to indicate non-raft regions, although evidence suggests that even this receptor may be capable of partitioning into rafts under certain conditions *(20)*. β-adaptin, a subunit of the adaptor protein (AP) complex found in coated vesicles and clathrin-coated pits *(21, 22)* is another useful non-raft marker, although due to its involvement in vesicular trafficking it cannot be considered a definitive marker for the plasma membrane. As an additional means of identifying fractions containing lipid rafts, measurements of sphingolipid and cholesterol levels can be made. Sphingolipids (specifically ganglioside G_{M1}) can be determined by applying a small amount of each fraction to a nitrocellulose membrane and probing with horseradish peroxidase-coupled cholera toxin subunit B *(23)*. Cholesterol levels in each fraction can be quantified by fluorometric kit-based protocols such as the Amplex Red Cholesterol Assay Kit (Molecular Probes). Example results are shown in **Fig. 7.1**.

7.3.1. Preparation of Arterial Homogenate: Detergent-Based Method

1. Tissue, in this case, thoracic aorta (*see* **Note 2**), can either be processed immediately or frozen in liquid nitrogen for later use. 2–3 aortae should be used for each fractionation.
2. Place the aortae into a pestle that has previously been stored at −80°C (*see* **Note 3**). Pour a small quantity of liquid nitrogen over the aortae and crush with the mortar until the tissue is reduced to a powder.

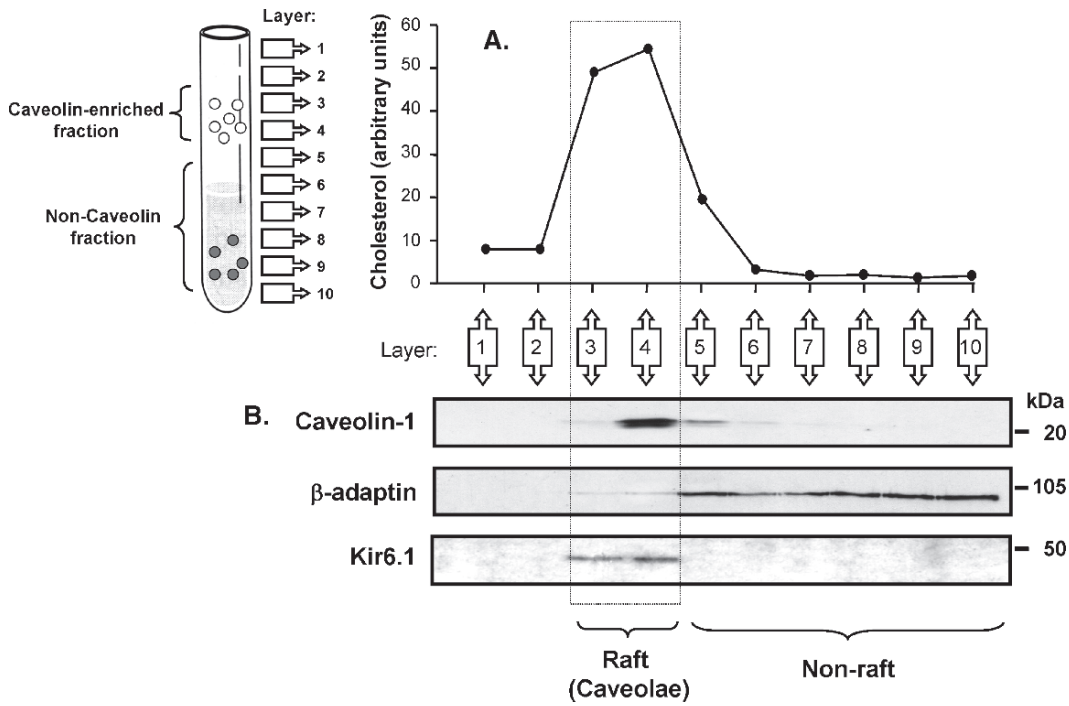

Fig. 7.1. Separation of caveolar and non-caveolar membrane fractions from rat aortic smooth muscle. (**a**) Relative cholesterol levels in each of ten 1-ml fractions collected from the top to the bottom of a discontinuous sucrose density gradient (shown schematically on *left*). (**b**) Western blot analysis of the fractions shown in A above to determine the localisation of the caveolae membrane marker, caveolin-1 (*top panel*), the non-caveolar, clathrin-coated pit protein, β-adaptin (*middle panel*) and the pore-forming subunit of the vascular K_{ATP} channel, Kir6.1 (adapted from **ref.** *18*).

3. Homogenise the powdered tissue in 2 mL of *ice cold* MBS (25-mM MES and 150-mM NaCl, pH 6.5) containing 1% Triton-X (*see* **Note 1**) on ice with a hand-held homogeniser, then incubate on ice for a further 10 min.
4. Make the homogenate up to 45% sucrose by the addition of an equal volume of ice cold 90% sucrose in MBS and load the resulting 4 mL into a thin-walled ultracentrifuge tube. This forms the bottom layer of the discontinuous sucrose density gradient.
5. Overlay the sample with 4 mL of ice cold 35% sucrose prepared in MBS and then 4 mL of ice cold 5% sucrose again prepared in MBS.
6. Separate the buoyant and non-buoyant membrane fractions by centrifugation of the sucrose gradient at ~260,000×*g* for 18 h at 4°C using an ultracentrifuge equipped with swing-out rotor (for example Sorvall TH-641). Remember to pre-cool the centrifuge before use and keep the gradients on ice until transferred to the centrifuge.

7. By carefully placing a pipette tip just under the surface at the very top of the gradient, collect consecutive 1-mL fractions and place these in pre-labelled tubes on ice. If the centrifuge tube is held up to light, the buoyant, cholesterol-enriched membranes are sometimes visible as a milky, light-scattering band at the 5–35% sucrose interface. Store the fractions at –20°C until required for SDS-PAGE.

7.3.2. Preparation of Arterial Homogenate: Non-Detergent-Based Method

1. Place 2–3 aortae into a pestle that has previously been stored at –80°C (*see* **Note 3**). Pour a small quantity of liquid nitrogen over the aortae and crush with the mortar until the tissue is reduced to a powder.
2. Homogenise the powdered tissue in 2 mL of 500-mM Na_2CO_3 pH 11 on ice with a hand-held homogeniser.
3. Disrupt the cell membranes by sonicating the homogenate (3 × 20 s bursts) on ice using a probe sonicator.
4. Make the homogenate up to 45% sucrose by the addition of an equal volume of ice cold 90% sucrose in MBS (25-mM MES and 150-mM NaCl, pH 6.5) and load the resulting 4 mL into a thin-walled ultracentrifuge tube. This forms the bottom layer of the discontinuous sucrose density gradient.
5. Overlay the sample with 4 mL of 35% sucrose prepared in MBS with 250-mM sodium carbonate and then 4 mL of 5% sucrose again prepared in MBS with 250-mM sodium carbonate.
6. Separate the buoyant and the non-buoyant membrane fractions by centrifugation of the sucrose gradient at ~260,000×g for 18 h at 4°C using an ultracentrifuge equipped with swing-out rotor (for example Sorvall TH-641).
7. By carefully placing a pipette tip just under the surface at the very top of the gradient, collect consecutive 1-mL fractions and place these in pre-labelled tubes on ice. If the centrifuge tube is held up to light, the buoyant, cholesterol-enriched membranes are sometimes visible as a milky, light-scattering band at the 5–35% sucrose interface. Store the fractions at –20°C until required for SDS-PAGE.

7.3.3. SDS-Polyacrylamide Gel Electrophoresis

1. These instructions assume the use of a Mini-PROTEAN 3 electrophoresis system (Bio-Rad).
2. Clean the glass plates with a 70% ethanol solution and dry before use.
3. Prepare a 0.75-mm thick, 10% resolving gel by mixing 2.5 mL of 1× resolving buffer with 3.33 mL of acrylamide/bis, 100 µL of 10% SDS and 3.97 mL of distilled water. To polymerise the gel add 100 µL of 10% ammonium persulphate solution and 5 µL of TEMED. Pour the gel up to approximately 3 cm from the top to leave space for the stacking gel and overlay with

isopropanol to prevent the top of the gel from drying out. The gel should polymerise in about 10–20 min depending on room temperature. (Keeping some of the gel mix in a universal tube is often a good idea to gauge the degree of polymerisation.)

4. Once the gel has set, pour off the isopropanol and rinse the surface of the gel well with distilled water. Remove any excess water by inserting a strip of filter paper between the plates taking care not to disturb the surface of the gel.
5. Prepare the stacking gel by mixing 2.5 mL of 1× stacking buffer with 1.3 mL of acrylamide/bis, 100 µL of 10% SDS, 6.0 mL of distilled water. To polymerise the gel add 100 µL of 10% ammonium persulphate solution and 10 µL of TEMED. Pour on top of the polymerised resolving gel to the top of the plates and insert the comb. The stacking gel should set within approximately 10 min depending upon the room temperature.
6. Prepare the running buffer by mixing 100 mL of 10× running buffer with 900 mL of distilled water.
7. Once the stacking gel has set, carefully remove the comb and wash several times with distilled water.
8. Assemble the gel into the running module, and clip the module into the running tank. Fill the central reservoir with 1× running buffer.
9. Load up to 30 µL (depending on the comb/well size) of each fraction from the sucrose gradient in consecutive lanes reserving the first and last lanes for pre-stained markers. It is often useful to load different markers at each end to delineate samples and to easily identify the orientation of gel.
10. Fill the outer reservoir with 1× running buffer and connect to the power supply. Run the gel for about 60–90 min at 100 V (~20–30 mA). The position of the pre-stained markers will give an indication of how far a protein of a particular molecular weight has migrated. The marker protein caveolin has a molecular weight of ~20 kDa. Therefore, ensure that the gel does not run for so long that these small proteins migrate off the bottom.

7.3.4. Western Blotting

1. Proteins that have been separated by SDS-PAGE are transferred to nitrocellulose membranes electrophoretically. These instructions assume the use of a Mini-PROTEAN 3 electrophoresis system (Bio-Rad) and wet transfer.
2. Prepare 1.5 L of transfer buffer and place in cold room/fridge to chill.
3. Cut four pieces of heavy weight blotting paper to the size of the fibre pads and place in a small volume of transfer volume to soak.

4. Cut the nitrocellulose membrane to the size of the resolving gel, wet with distilled water and then place along with filter paper to soak in the transfer buffer.
5. Disconnect the gel unit from the power supply and disassemble. Separate the glass plates and remove and discard the stacking gel.
6. Place one of the fibre pads onto a flat surface, lay two pieces of blotting paper on top of the pad and then place the gel carefully on top. Overlay the gel with the nitrocellulose membrane and roll over the surface of the membrane with something cylindrical (we typically use a plastic disposable stripette) to remove any bubbles and ensure good contact between the gel and membrane. Complete the sandwich by placing the remaining two pieces of blotting paper on top of the gel and overlay with the second fibre pad.
7. Clip into the gel holder cassette and insert into the transfer cell ensuring that the nitrocellulose membrane is between the gel and the anode. Place the transfer cell in the running tank and fill the tank with chilled transfer buffer. Surround the running tank with ice (or place the whole assembly in a cold room) and connect to the power supply.
8. Transfer proteins electrophoretically onto the nitrocellulose membrane at 100 mV (~300 mA) for approximately 1 h.
9. Disassemble the apparatus, carefully remove the membranes and rinse them briefly in TBS-T.
10. Block the membranes overnight at 4°C in blocking buffer.
11. Dilute the primary antibodies: anti-adaptin (1:1,000) anti-caveolin 1 (1:1,000), anti-flotillin 1 (1:250), anti-flotillin 2 (1:5,000), anti-Kir6.1 (1:500) in primary antibody dilution buffer and incubate with the membranes for 1–2 h at room temperature.
12. Wash the membranes for 3 × 10 min in TBS-T solution then incubate with horseradish peroxidase-conjugated secondary antibodies (1:20,000 dilution in secondary antibody dilution buffer) for a further hour at room temperature.
13. Visualise the labelled bands using enhanced chemiluminescence (ECL) (Amersham Pharmacia Biotechnologies) and exposure to light-sensitive film (Hyperfilm™ ECL™; Amersham).

7.4. Notes

1. Lipid raft regions are only resistant to solubilisation by *cold* detergents. It is therefore imperative that the detergent-based

isolation procedure is conducted with all reagents at 4°C and with the samples always on ice.

2. Obtained from male Wistar rats (~200 g) killed by stunning and rapid cervical dislocation. The care and euthanasia of animals conformed to the requirements of the UK Animals (Scientific Procedures) Act 1986.
3. Storage at –80°C reduces the chances of the pestle cracking upon exposure to liquid nitrogen.

References

1. Galbiati, F., Razani, B., and Lisanti M. P. (2001) Emerging themes in lipid rafts and caveolae. *Cell* **106**, 403–411.
2. Simons, K. and Toomre, D. (2000) Lipid rafts and signal transduction. *Nature Reviews Molecular Cell Biology* **1**, 31–39.
3. Simons, K. and Ikonen, E. (1997) Functional rafts in cell membranes. *Nature* **387**, 569–572.
4. van Meer, G. and Lisman, Q. (2002) Sphingolipid transport: rafts and translocators. *Journal of Biological Chemistry* **277**, 25855–25858.
5. Pike, L. J. (2004) Lipid rafts: heterogeneity on the high seas. *Biochemical Journal* **378**, 281–292.
6. Babiychuk, E. B. and Draeger, A. (2006) Biochemical characterization of detergent-resistant membranes: a systematic approach. *Biochemical Journal* **397**, 407–416.
7. Munro, S. (2003) Lipid rafts: elusive or illusive? *Cell* **115**, 377–388.
8. Douglass, A. D. and Vale, R. D. (2005) Single-molecule microscopy reveals plasma membrane microdomains created by protein-protein networks that exclude or trap signaling molecules in T cells. *Cell* **121**, 937–950.
9. Anderson, R. G. W. (1998) The caveolae membrane system. *Annual Review of Biochemistry* **67**, 199–225.
10. Razani, B., Woodman, S. E., and Lisanti, M. P. (2002) Caveolae: from cell biology to animal physiology. *Pharmacological Reviews* **54**, 431–467.
11. Parton, R. G. (2003) Caveolae – from ultrastructure to molecular mechanisms. *Nature Reviews Molecular Cell Biology* **4**, 162–167.
12. Brown, D. A. and Rose, J. K. (1992) Sorting of Gpi-anchored proteins to glycolipid-enriched membrane subdomains during transport to the apical cell-surface. *Cell* **68**, 533–544.
13. Martens, J. R., O'Connell, K., and Tamkun, M. (2004) Targeting of ion channels to membrane microdomains: localization of K-v channels to lipid rafts. *Trends in Pharmacological Sciences* **25**, 16–21.
14. Lisanti, M. P., et al. (1994) Characterization of caveolin-rich membrane domains isolated from an endothelial-rich source – implications for human-disease. *Journal of Cell Biology* **126**, 111–126.
15. Smart, E.J., et al. (1995) A detergent-free method for purifying caveolae membrane from tissue-culture cells. *Proceedings of the National Academy of Sciences of the United States of America* **92**, 10104–10108.
16. Song, K. S., et al. (1996) Co-purification and direct interaction of Ras with caveolin, an integral membrane protein of caveolae microdomains – detergent-free purification of caveolae membranes. *Journal of Biological Chemistry* **271**, 9690–9697.
17. Foster, L. J., de Hoog, C. L., and Mann M. (2003) Unbiased quantitative proteomics of lipid rafts reveals high specificity for signaling factors. *Proceedings of the National Academy of Sciences of the United States of America* **100**, 5813–5818.
18. Sampson, L. J., et al. (2004) Caveolae localize protein kinase A signaling to arterial ATP-sensitive potassium channels. *Circulation Research* **95**, 1012–1018.
19. Sampson, L. J., et al. (2007) Angiotensin II-activated protein kinase C targets caveolae to inhibit aortic ATP-sensitive potassium channels. *Cardiovascular Research* **76**, 61–70.
20. Batista, A., et al. (2004) Recruitment of transferrin receptor to immunological synapse in response to TCR engagement. *Journal of Immunology* **172**, 6709–6714.

21. Edeling, M. A., Smith, C., and Owen, D. (2006) Life of a clathrin coat: insights from clathrin and AP structures. *Nature Reviews Molecular Cell Biology* **7**, 32–44.
22. Robinson, M. S. (2004) Adaptable adaptors for coated vesicles. *Trends in Cell Biology* **14**, 167–174.
23. Hering, H., Lin, C. C., and Sheng, M. (2003) Lipid rafts in the maintenance of synapses, dendritic spines, and surface AMPA receptor stability. *Journal of Neuroscience* **23**, 3262–3271.

Chapter 8

Determination of Phosphoinositide Binding to K^+ Channel Subunits Using a Protein–Lipid Overlay Assay

Alison M. Thomas and Andrew Tinker

Summary

Phosphoinositides are an important component of the cell as they have a variety of roles that include cytoskeleton regulation, generation of second messengers, endosome trafficking, membrane transport and regulation of ion channels. The direct interaction between phosphatidylinositol-4,5-bisphosphate (PIP_2) and various inwardly rectifying potassium channels has been shown in recent years. Most of these studies have used existing electrophysiological methods. In this review, we describe a rapid and convenient biochemical assay that can be used to show direct binding of potassium channel subunits to anionic phospholipids. This method has been used to demonstrate the differences in affinity between members of the Kir3.0 family, where only the cytoplasmic C-terminal Kir3.1 domain and the N- and C-terminal domains of Kir3.4 have the ability to bind to anionic phospholipids.

Key words: K^+ channel, Phosphatidylinositol-4,5-bisphosphate, PIP strip, Phosphoinositides, Inward rectifier.

8.1. Introduction

Phosphoinositides play a variety of important roles within the cell. These include phosphatidylinositol-3-phosphate (PI3) that is involved in endosome trafficking *(1)* and phosphatidylinositol-4-phosphate (PI4) that is involved in membrane transport from the Golgi, where it is highly abundant, to the plasma membrane by the binding of proteins such as FAPP1 and FAPP2 *(2, 3)*. Phosphatidylinositol-4,5-bisphosphate (PIP_2) has been identified as being involved in various important processes including cytoskeleton regulation and the generation of second messengers *(4)*. In recent years, PIP_2 has also been shown to regulate transporters and ion channels. These include the Na^+/Ca^{2+} exchanger *(5)*, inwardly

Jonathan D. Lippiat (ed.), *Methods in Molecular Biology, Potassium Channels, vol. 491*

Book doi: 10.1007/978-1-59745-526-8

rectifying potassium channels, Kir *(6, 7)*, the voltage gated potassium channels, KCNQ *(8, 9)* and HERG *(10, 11)*, the transient receptor potential (TRP) superfamily of cation channels *(12)* and the epithelial sodium channel (EnaC) *(13)* amongst others.

The interaction between PIP_2 and potassium channels has been extensively studied in Kir. The presence of PIP_2 increases the open probability of the channels and its depletion via phospholipase C results in channel rundown *(14)*. Direct interactions between PIP_2 and Kir have been demonstrated using [^{3}H]-PIP_2 liposomes *(6)* and a PIP_2 antibody in inside-out patches *(15)*. Most of the above studies have used electrophysiology to show the link between PIP_2 and channel activation. However a more biochemical approach was required. To this end, a protein–lipid overlay assay was subsequently developed to allow direct interactions between potassium channel subunits and PIP_2 to be observed *(16)*. Our assay involved cloning and expressing the cytoplasmic channel subunit of members of the Kir3.0 family as a maltose-binding protein (MBP) tagged protein (N-terminal tag), using the protein–lipid overlay assay described here to investigate their differing abilities to bind to phosphoinositides. We have shown that the C-terminal cytoplasmic subunits of different members of the Kir3.0 family have differing specificities for phosphoinositides. This binding can also be influenced by mutating interesting residues, which has the effect of reducing binding, while the addition of the N-terminal cytoplasmic subunit results in increasing binding affinities *(16)*.

8.2. Materials

8.2.1. MBP Fusion Protein Expression and Purification

1. pMALc2x plasmid from New England Biolabs (Herts, UK).
2. *E. coli* BL21 (DE3) competent cell strain.
3. Growth Media (1 L): 10-g BactoTryptone, 5-g yeast extract, 5-g NaCl, 2-g Glucose. Autoclaved and stored at 4°C.
4. 1,000× Carbenicillin solution: 100 mg/mL; filter sterilised (0.2 µm) and stored at –20°C.
5. 0.1-M Isopropylthiogalactoside (IPTG); filter sterilised (0.2 µm) and stored at –20°C.
6. Amylose resin, supplied as 20% ethanol slurry (New England Biolabs, Herts, UK) and packed into polypropylene columns (Econo-Pac columns, Bio-Rad, Herts, UK).
7. Buffer A: 20-mM Tris–HCl, pH 7.5, 200-mM NaCl, 1-mM dithiothreitol (DTT), 1-mM ethylenediaminetetraacetic acid (EDTA). Add one tablet of protease inhibitors (Complete EDTA free, Roche Diagnostics, UK) to 50 mL of buffer A.

8. Elution buffer: buffer A + 10-mM maltose.
9. Buffer B: 50-mM Tris–HCl, pH 7.5, 200-mM NaCl, 1-mM DTT, 1-mM EDTA.
10. Centricon YM-30 centrifugal units (Millipore, UK).

8.2.2. Protein–Lipid Overlay Assay

1. PIP strips containing 16 different phosphoinositides (100 pmol per spot) from Echelon Biosciences (Salt Lake City, USA). Store at 4°C in the dark.
2. TBST: 10-mM Tris–HCl, pH 7.5, 150-mM NaCl, 0.1% Tween-20.
3. Blocking buffer A: TBST + 3% non-fatty acid Bovine Serum Albumin (BSA).
4. Anti-MBP antiserum (New England Biolabs, Herts, UK). Dilute 1:1,000 in blocking buffer A.
5. Blocking buffer B: TBST + 5% non-fat milk powder.
6. Secondary anti-rabbit IgG (GE Healthcare, Bucks, UK): dilute 1:5,000 in blocking buffer B.
7. ECL Western blotting System (GE Healthcare) used for chemiluminescent labelling and detection.
8. Hyperfilm ECL (GE Healthcare).

8.2.3. Analysis of Protein–Lipid Overlay

1. Scion Image (Scion Corporation, Maryland, USA) to analyse the relevant spot intensity.
2. GraphPad Prism version 4 (GraphPad Software, San Diego, CA, USA) for data analysis and presentation.

8.3. Methods

Eukaryotic Kir proteins, and membrane proteins in general, are difficult to obtain in a soluble form and in large quantities suitable for biochemical studies. The bacterial MBP expression system allows the production of large amounts of protein and easy purification through the presence of the MBP tag. In addition, MBP is a highly soluble protein that has been shown to increase the solubility of aggregation prone proteins when they are expressed as a fusion protein *(17)*. It is also thought that the presence of MBP encourages the correct folding of the fusion partner *(17, 18)*. For this reason, the MBP expression system was used in this method. As our channel subunits were shown to be highly unstable upon cleavage from MBP using Factor XA the entire fusion protein was used directly in the biochemical assay. This allowed us to use MBP as a control protein in all of the assays to ensure

that any binding that was observed was not due to the presence of MBP itself.

The use of nitrocellulose membranes containing different anionic phospholipids, such as the PIP strips used in this assay, provides a rapid and convenient method of determining binding to channel subunits. Additionally, PIP Arrays are available (Echelon, USA) that allow a dose-response curve to be determined. In this study, the cytoplasmic domain of Kir3.1 was able to bind to monophosphoinositols such as PI4 whereas the cytoplasmic domains of Kir3.2A and Kir3.4 were unable to bind any of the phosphoinositides present (**Fig. 8.2**). This reflects the functional data observed with the homomeric Kir3.1 that recovers from inhibition relatively quickly after stimulation of a Gq/11 receptor such as the M3 muscarinic receptor as compared to the homomeric Kir3.2, which does not.

8.3.1. Expression and Purification of MBP Fusion Proteins

1. *E. coli* BL21 (DE3) competent cells containing the desired MBP-Kir3.0 plasmid (*see* **Note 1**) are grown in Growth Media containing 1× carbenicillin until the OD_{600} is 0.6–0.8 nm.
2. IPTG is added to a final concentration of 0.3 mM and the cultures grown overnight at 25°C (*see* **Note 2**).
3. Cells are collected by centrifugation (4,000×*g* for 30 min at 4°C) and the resulting pellet resuspended in buffer A containing Protease Inhibitors (20 mL per 1 L of cell culture). Store the cell resuspension at –20°C until required.
4. Thaw the resuspended cells on ice and sonicate (5 × 60 s) to lyse the cell membranes (*see* **Note 3**).
5. Centrifuge (10,000×*g* for 30 min at 4°C) to separate the insoluble membranes and the soluble cytosolic fractions. Keep the supernatant on ice until required.
6. Resuspend the resulting pellet in 10 mL of buffer A containing protease inhibitors and repeat **steps 4** and **5** above (*see* **Note 4**). The supernatant was pooled with that from **step 5** and subsequently diluted fourfold.
7. A bed volume of 5–6 mL of amylose resin, packed into a chromatography column, is pre-equilibrated using 10 column volumes (CV) of buffer A (*see* **Notes 5** and **6**).
8. Load the diluted supernatant from **steps 5** and **6** onto the column.
9. The column is subsequently washed with 12 CV of buffer A to remove non-specifically bound proteins.
10. The desired MBP-Kir3.0 protein is eluted from the column using Elution buffer (*see* **Note 7**). Fractions of 1 mL are collected for a total of 3 column volumes. The fractions that contain protein (determined using BioRad Protein Assay

solution using the manufacturer's instructions) are pooled and concentrated using a centricon YM-30 (as per the manufacturer's instructions) until the protein concentration is determined to be greater than 5 mg/mL.

11. Protein is aliquoted and flash frozen in liquid nitrogen before storage at –80°C. An example of the purification of MBP-Kir3.4C is shown in **Fig. 8.1**. A total yield of 5–20 mg of protein was obtained per 500 mL of culture.

8.3.2. Protein–Lipid Overlay Assay

1. Incubate a PIP strip with blocking buffer A for 1 h at room temperature on a rocking platform shaker (*see* **Notes 8–10**).
2. Incubate the blocked PIP strip with blocking buffer A containing 1 µg/mL of the desired MBP fusion protein, rocking overnight at 4°C.
3. Wash the PIP strip with TBST for 10 min at room temperature before discarding the buffer and repeat to obtain a total of three washes.
4. Incubate the PIP strip with anti-MBP antiserum in blocking buffer A for 2–3 h at room temperature on a rocking platform shaker (*see* **Note 11**).
5. Wash the PIP strip for 15 min at room temperature and subsequently wash twice for 5 min with TBST.
6. Incubate the PIP strip with the desired secondary antibody, anti-rabbit immunoglobulin G (IgG), in blocking buffer B for 1 h at room temperature on a rocking platform shaker (*see* **Note 12**).

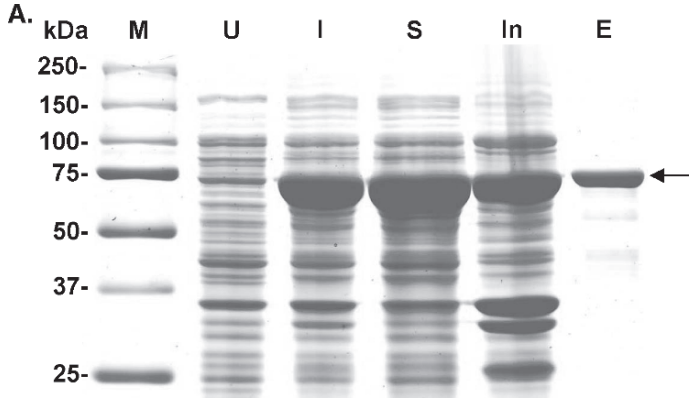

Fig. 8.1. Purification of MBP-Kir3.4C. A 10% SDS-PAGE showing purification of MBP-Kir3.4C fusion protein. *M* BioRad Precision plus Broad range SDS standards, *U* uninduced cells, *I* induced cells, *S* soluble protein, *In* insoluble protein, *E* eluted protein (2 µg). Marker sizes are indicated in kilodaltons (kDa) (reproduced from **ref.** *16* with kind permission from Springer Science and Business Media).

7. Wash the PIP strip once with TBST for 15 min followed by four washes of 5 min duration.
8. Detection of protein binding to the PIP strip: Mix 250 µL of detection reagent 1 and 250 µL of detection reagent 2 together. The PIP strip is placed on Clingfilm and the detection solution pipetted onto it. Fold the Clingfilm to ensure an even application of solution and leave at room temperature for 1 min.
9. Remove the PIP strip from the Clingfilm and remove excess solution using a tissue held to one corner before placing the PIP strip into the film cassette (*see* **Note 13**). In a dark room, the PIP strip is exposed to a sheet of Hyperfilm ECL for a few seconds before being processed with a Kodak X-Omat 1000 Processor.
10. The phosphoinositides that have bound to protein will show up as a visible spot and those that have not bound to protein

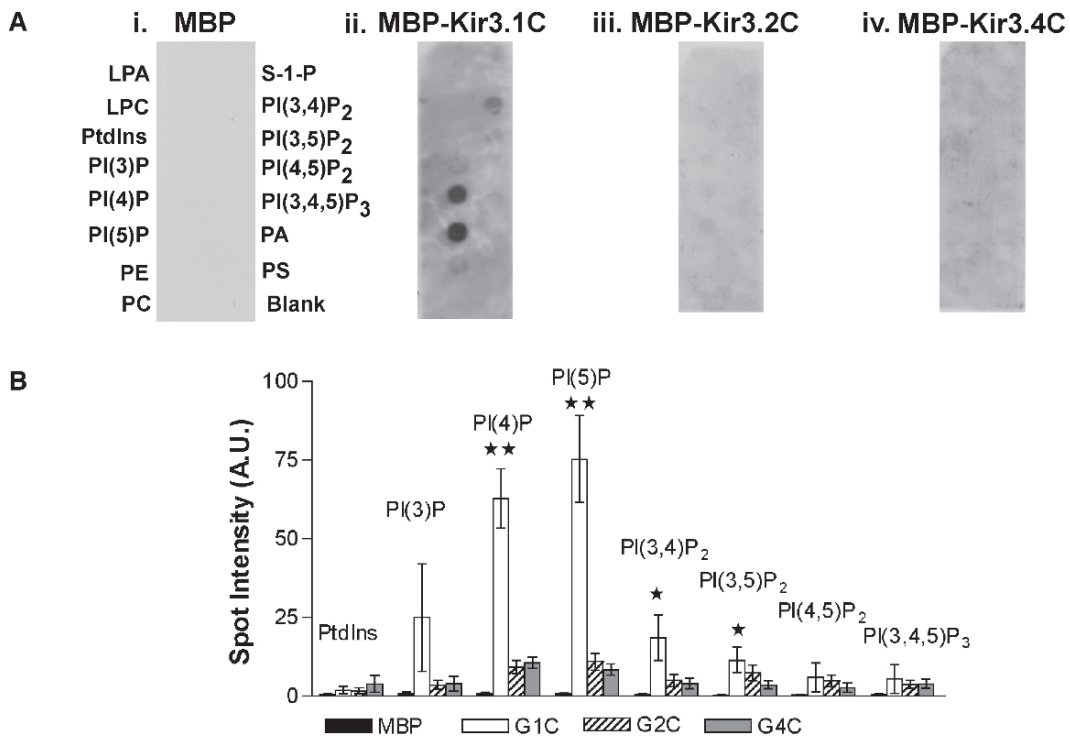

Fig. 8.2. Protein–lipid overlay assay with Kir3.0 C-terminal MBP proteins. (**a**) PIP strips with the various MBP fusion proteins bound: (*i*) MBP only, (*ii*) MBP-Kir3.1C, (*iii*) MBP-Kir3.2C, and (*iv*) MBP-Kir3.4C. *LPA* lysophosphatidic acid, *LPC* lysophsphatidylcholine, *PE* phosphatidylethanolamine, *PC* phosphatidylcholine, *S-1-P* sphingosine-1-phosphate, *PA* phosphatic acid, *PS* phosphatidylserine. (**b**) Graph showing the average spot intensity ($n = 4$) for the indicated phosphoinositides determined for each protein. Statistical significance was determined using one-way ANOVA and Dunnetts post-test and is represented as the following: $^{**}p < 0.01$ and $^{*}p < 0.05$ (reproduced from **ref.** *16* with kind permission from Springer Science and Business Media).

will not be visible. An example of this is shown in **Fig. 8.2a** with MBP alone, MBP-Kir3.1C, MBP-Kir3.2C and MBP-3.4C.

8.3.3. Analysis of Protein–Lipid Overlay Assay

1. Using Scion Image software, load file. Using a round spot to give 352 square pixels, measure the number of pixels within the spot (*see* **Note 14**).
2. The intensity of the background should then be subtracted from the sample spot (*see* **Note 15**).
3. Plot the values as a graph using GraphPad Software. An example of this is shown in **Fig. 8.2b**.
4. Analyse individual spots by comparing the sample spot to the control MBP spot using One-Way ANOVA and Dunnetts Multiple Comparison Post-Test (*see* **Note 16**).

8.4. Notes

1. Cloning of the desired Kir3.0 channel subunit was carried out using standard techniques. This generated a gene with MBP sequence at the N-terminus of the Kir3.0 C-terminal cytoplasmic channel subunit. The boundaries were determined using ScanProsite although any other similar program can be used.
2. Expression of the protein was carried out at 25°C overnight in order to ensure that the maximum amount of soluble protein was obtained. Lowering the temperature of growth cultures results in slower protein production and subsequently a larger proportion of the protein remains soluble and correctly folded *(19)*. As shown in **Fig. 8.1** the proportion of protein in a soluble form is >50% of the total protein.
3. During the sonication process to lyse the cell membranes it is important to keep the cell lysate on ice between each 60 s pulse. The sonication process generates a lot of heat and therefore the sample should be allowed to cool down between each pulse.
4. By repeated sonication and centrifugation the amount of soluble protein that is released from within the cells can be increased as sometimes the first round of lysis is not as efficient as expected.
5. All subsequent steps were carried out at 4°C to preserve protein function.
6. The chromatography columns used here were subjected to gravity flow chromatography. They are fitted with an upper bed support that prevents the column from running dry. However this method can also be adapted to suit any chromatography system.

7. The presence of maltose in the Elution buffer competes with the MBP portion of the fusion protein for binding to the Amylose resin to allow the elution of the MBP-Kir3.0.
8. Gloves and a pair of forceps must be used to handle the PIP strips to ensure that no contamination occurs. Plastic containers such as Petri dishes work well for washing the PIP strips.
9. On initial immersion into blocking buffer A the PIP strip must be fully submerged into the buffer. If necessary use a pair of forceps to ensure that it is submerged.
10. During all of the washing steps the PIP strip must be fully submerged in the blocking or washing buffers. The PIP strip should also have the phosphoinositides spots facing upwards (the cut upper left hand corner can be used for orientation) to ensure adequate washing and to subsequently reduce the amount of background observed.
11. In the method described here, the primary antibody used was the anti-MBP antiserum as we could show that this was a reliable antibody, which recognised both the MBP-Kir fusion proteins and the MBP control protein that was used as a negative control. However, any other reliable primary antibody could be used in this system.
12. An anti-rabbit IgG secondary antibody is used here as the primary antibody, anti-MBP, was raised in rabbits. The secondary antibody should be species specific for the primary antibody used.
13. When placing the PIP strip in the film cassette, again ensure that the cut corner is towards the top left of the cassette.
14. It is important to make sure that the selected circle encompasses as much of the spot as possible to ensure correct measurement of density per spot.
15. A measurement of the background intensity should also be taken, as this will ensure accurate measurements. A spot of the same size of the sample should be selected within the PIP strip that is representative of the overall background observed.
16. An *n* number of at least three is required for statistical analysis via ANOVA.

Acknowledgments

This work was supported by the British Heart Foundation.

References

1. Simonsen, A., Wurmser, A. E., Emr, S. D., and Stenmark, H. (2001) The role of phosphoinositides in membrane transport. *Curr. Opin. Cell Biol.* **13**, 485–492.
2. Godi, A., Di Campli, A., Konstantakopoulos, A., Di Tullio, G., Alessi, D. R., Kular, G. S., Daniele, T., Marra, P., Lucocq, J. M., and De Matteis, M. A. (2004) FAPPs control Golgi-to-cell-surface membrane traffic by binding to ARF and PtdIns(4)P. *Nat. Cell Biol.* **6**, 393–404.
3. De Matteis, M. A., Di Campli, A., and Godi, A. (2005) The role of the phosphoinositides at the Golgi complex. *Biochim. Biophys. Acta* **1744**, 396–405.
4. Toker, A. (1998) The synthesis and cellular roles of phosphatidylinositol 4,5-bisphosphate. *Curr. Opin. Cell Biol.* **10**, 254–261.
5. Hilgemann, D. W. and Ball, R. (1996) Regulation of cardiac Na_+, Ca_{2+} exchange and KATP potassium channels by PIP^2. *Science* **273**, 956–959.
6. Huang, C. L., Feng, S., and Hilgemann, D. W. (1998) Direct activation of inward rectifier potassium channels by PIP^2 and its stabilization by Gbetagamma. *Nature* **391**, 803–806.
7. Sui, J. L., Petit-Jacques, J., and Logothetis, D. E. (1998) Activation of the atrial KACh channel by the betagamma subunits of G proteins or intracellular Na_+ ions depends on the presence of phosphatidylinositol phosphates. *Proc. Natl Acad. Sci. USA* **95**, 1307–1312.
8. Zhang, H., Craciun, L. C., Mirshahi, T., Rohacs, T., Lopes, C. M., Jin, T., and Logothetis, D. E. (2003) $PIP^{(2)}$ activates KCNQ channels, and its hydrolysis underlies receptor-mediated inhibition of M currents. *Neuron* **37**, 963–975.
9. Loussouarn, G., Park, K. H., Bellocq, C., Baro, I., Charpentier, F., and Escande, D. (2003) Phosphatidylinositol-4,5-bisphosphate, PIP^2, controls KCNQ1/KCNE1 voltage-gated potassium channels: a functional homology between voltage-gated and inward rectifier K_+ channels. *EMBO J.* **22**, 5412–5421.
10. Bian, J., Cui, J., and McDonald, T. V. (2001) HERG $K_{(+)}$ channel activity is regulated by changes in phosphatidylinositol 4,5-bisphosphate. *Circ. Res.* **89**, 1168–1176.
11. Bian, J. S., Kagan, A., and McDonald, T. V. (2004) Molecular analysis of PIP^2 regulation of HERG and IKr. *Am. J. Physiol. Heart Circ. Physiol.* **287**, H2154–H2163.
12. Voets, T. and Nilius, B. (2007) Modulation of TRPs by PIPs. *J. Physiol.* **582**, 939–944.
13. Pochynyuk, O., Tong, Q., Medina, J., Vandewalle, A., Staruschenko, A., Bugaj, V., and Stockand, J. D. (2007) Molecular determinants of $PI(4,5)P^2$ and $PI(3,4,5)P^3$ regulation of the epithelial Na_+ channel. *J. Gen. Physiol.* **130**, 399–413.
14. Meyer, T., Wellner-Kienitz, M. C., Biewald, A., Bender, K., Eickel, A., and Pott, L. (2001) Depletion of phosphatidylinositol 4,5-bisphosphate by activation of phospholipase C-coupled receptors causes slow inhibition but not desensitization of G protein-gated inward rectifier K_+ current in atrial myocytes. *J. Biol. Chem.* **276**, 5650–5658.
15. Zhang, H., He, C., Yan, X., Mirshahi, T., and Logothetis, D. E. (1999) Activation of inwardly rectifying K_+ channels by distinct $PtdIns(4,5)P^2$ interactions. *Nat. Cell Biol.* **1**, 183–188.
16. Thomas, A. M., Brown, S. G., Leaney, J. L., and Tinker, A. (2006) Differential phosphoinositide binding to components of the G protein-gated K_+ channel. *J. Membr. Biol.* **211**, 43–53.
17. Kapust, R. B. and Waugh, D. S. (1999) *Escherichia coli* maltose-binding protein is uncommonly effective at promoting the solubility of polypeptides to which it is fused. *Protein Sci.* **8**, 1668–1674.
18. Nallamsetty, S. and Waugh, D. S. (2006) Solubility-enhancing proteins MBP and NusA play a passive role in the folding of their fusion partners. *Protein Expr. Purif.* **45**, 175–182.
19. Georgiou, G. and Valax, P. (1996) Expression of correctly folded proteins in Escherichia coli. *Curr. Opin. Biotechnol.* **7**, 190–197.

Chapter 9

Protein Complex Analysis of Native Brain Potassium Channels by Proteomics

Guillaume Sandoz and Florian Lesage

Summary

TREK potassium channels belong to a family of channel subunits with two-pore domains (K_{2P}). TREK1 knockout mice display impaired polyunsaturated fatty acid-mediated protection against brain ischemia, reduced sensitivity to volatile anesthetics, resistance to depression and altered perception of pain. Recently, we isolated native TREK1 channels from mouse brain and identified their specific components by mass spectrometry. Among the identified partners, the A-Kinase Anchoring Protein AKAP150 binds to a regulatory domain of TREK1 and acts as a molecular switch. It transforms low activity, outwardly rectifying TREK1 currents into robust leak conductances resistant to stimulation by arachidonic acid, membrane stretch and acidification. Inhibition of the TREK1/AKAP150 channel by Gs-coupled receptors is as extensive as for TREK1 alone (but faster) whereas inhibition of TREK1/AKAP150 by Gq-coupled receptors is reduced. Furthermore, the association of AKAP150 with TREK1 channels integrates them into postsynaptic scaffolds where G protein-coupled membrane receptors and channels dock simultaneously. This chapter describes the proteomic approach used to study the composition of native TREK1 channels and point out its advantages and limitations over more classical methods (two-hybrid screenings in the yeast and bacteria or GST-pull down).

Key words: Ion channels, Proteomics, Scaffolding proteins.

9.1. Introduction

TREK1 and TREK2 are closely related pore-forming subunits that belong to the family of two-pore domain potassium (K_{2P}) channels *(1, 2)*. They produce outwardly rectifying currents with low basal activity in classical conditions of heterologous expression *(3, 4)*. Mechanical stress and cell swelling, intracellular acidification, temperature, polyunsaturated fatty acids (PUFAs), including arachidonic acid, and lysophospholipids are natural stimulators of TREK channels (for a recent review *see* **ref.** *5*).

Jonathan D. Lippiat (ed.), *Methods in Molecular Biology, Potassium Channels, vol. 491*

Book doi: 10.1007/978-1-59745-526-8

On the other hand, neurotransmitters and hormones that activate Gq- or Gs-coupled receptors decrease their activity *(4, 6)*. In terms of pharmacology, TREK1 and TREK2 are opened by clinical concentrations of volatile anesthetics *(7)* and riluzole *(8)*, a drug used to protect motoneurones in amyotrophic lateral sclerosis. Mice with gene inactivation of TREK1 (TREK1$^{-/-}$) show an increased vulnerability to both epileptic seizures and brain ischemia *(9)*. They have lost neuroprotection by PUFAs, are more resistant to volatile anesthetics and display altered pain perception *(10)*. In addition, TREK1$^{-/-}$ mice present a depression-resistant phenotype *(11)*.

Ion channels are composed of hydrophobic pore-forming subunits often associated with auxiliary subunits. Growing evidence indicates that trafficking, addressing and functional properties of native ion channels depend on their lipidic and proteic environments *(12)*. In particular, the specificity and the speed of their regulations by membrane receptors require a promiscuous organization of the constitutive channel subunits with membrane receptors and complexes of intracellular molecules. Since their discovery in 1996, significant progress has been achieved in understanding the electrophysiological behaviours and physiological roles of TREK channels. However, nothing was known about their native proteic environment, in particular, in neuronal cells. Usually, the methods used to find partner proteins are the two-hybrid screenings in bacteria or yeasts, and the GST-pull down coupled to 2D-gel separation and mass spectrometry identification of precipitated proteins. The main concern is the number of false-positives generated by both techniques. They arise because observed interactions occur between partial sequences and not between full-length proteins, and also because interacting proteins are not in their original cellular context. Another major drawback is that rare partners such as true auxiliary subunits are not easily recovered. Rare RNAs are not systematically reverse-transcribed and cloned in cDNA libraries used for two-hybrid screening. By GST-pull down and 2D-gel separation of precipitated proteins, only abundant proteins can be spotted and further identified by mass spectrometry.

To overcome these limitations, we designed a proteomic approach based on immunoprecipitation and mass spectrometry (MS) analysis of native channel complexes *(13)*. Affinity-purified antibodies directed against TREK1 were covalently crosslinked to protein A-sepharose to produce anti-TREK1 immunobeads. These beads were incubated with brain synaptosomal proteins solubilized in a buffer containing a mild detergent, then briefly washed. Bound proteins were eluted and separated by SDS-PAGE. The nature of the precipitated proteins was determined by nanoLC-ESI-MS/MS (**Fig. 9.1**). From C57Bl6J wild-type (WT) mice, more than 110 different proteins were identified (**Table 9.1**). The precipitation of many of these proteins was due

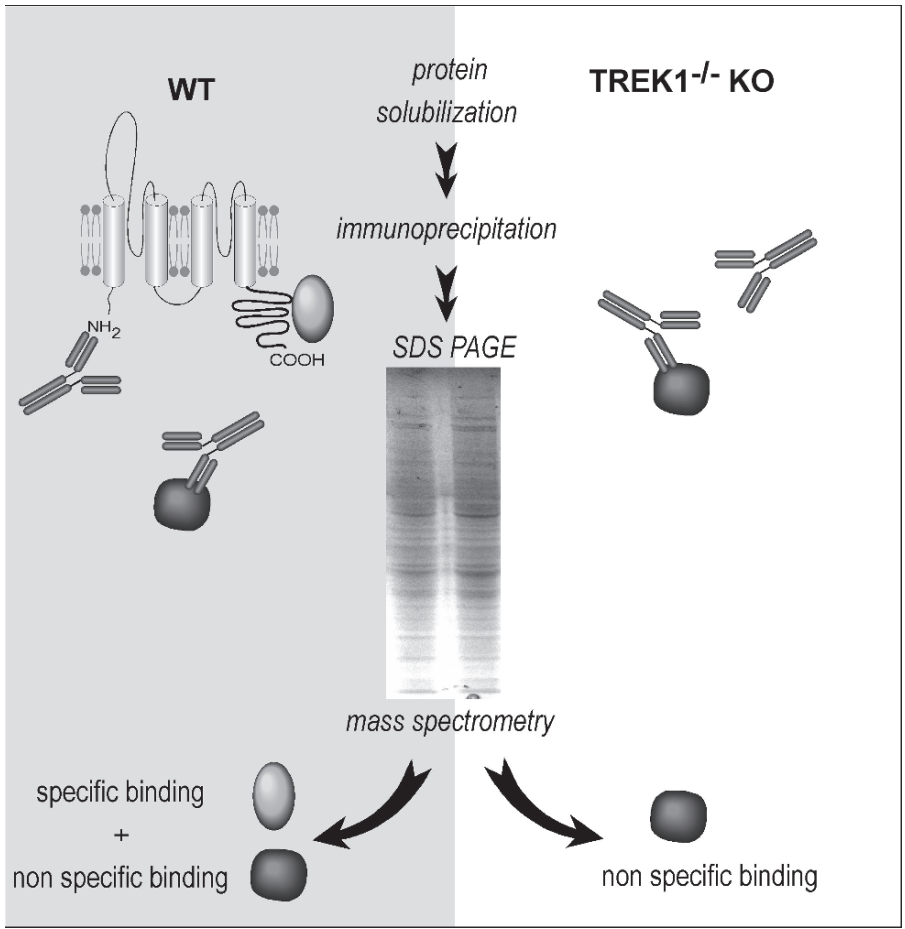

Fig. 9.1. Summary of the differential approaches used to identify proteins interacting with native TREK1 channels. Synaptosomal proteins were solubilized and then incubated with anti-TREK1 beads. Anti-TREK1 antibodies are directed against the amino-terminal region (N-ter) of TREK1. After a fast wash step, bound proteins were eluted and separated by SDS-PAGE then analyzed by mass spectrometry of tryptic peptides. In the absence of TREK1 (proteins prepared from TREK1$^{-/-}$ mice**, right panel**), only proteins binding nonspecifically to the beads or carrying epitopes related to the N-ter of TREK1 were precipitated. Proteins interacting with TREK1 from WT mice (**left panel**), are coprecipitated in addition to the proteins resulting from nonspecific binding.

to nonspecific binding to immunobeads and to crossreactivity of antibodies to epitopes unrelated to TREK1. A control immunoprecipitation was carried out by using solubilized synaptosomal proteins prepared from TREK1$^{-/-}$ mice. The vast majority of the proteins precipitated from WT mice were identical to the proteins isolated from TREK1$^{-/-}$ mice with the exception of four of them which were subsequently studied in detail. One of them, AKAP150, has a spectacular effect on TREK channel functional properties *(13)*. This result stresses the importance of this type of study for understanding ion channel function in the native cellular context.

Table 9.1
Proteins nonspecifically precipitated by anti-TREK1 beads and identified by mass spectrometry

Transport	*Metabolism*
Na/K-ATPase α1, 2, 3, β1	Glutamine synthase
K–Cl cotransporter	Pyruvate dehydrogenase
Calcium ATPase 1 and 2	Glutamate transaminase
Glial glutamate transporter 3	Malate dehydrogenase
Glutamate transporter 1 and 2	Lactate dehydrogenase
ATP synthase α-and β-subunits	Triose phosphate isomerase
ATPase, H^+ transporting, V1 subunit D	Cytochrome C
Cytoskeleton and cell structure	Carbonic anhydrase 2
β-spectrin homolog	NADH-ubiquinone oxidoreductase
α-spectrin	GAPDH
Tubulin α2 and β2	Pyruvate kinase
Dynamin	Glucose phosphate isomerase
α, β and γ actin	Adenine nucleotide translocase-1
Actin-related protein 2 and 3	Aconitase
Erythrocyte protein band 4.1	Hexokinase
14-3-3 ζ and γ	Creatine kinase
Clathrin, heavy polypeptide	α-enolase
AP1 β1	Manganese superoxide dismutase
AP2 α1 and β2	Glyceraldehyde-3-phosphate
NCAM 1 precursor	Dehydrogenase
Myelin proteolipid	Sdha protein
Spectrin α2	*Others*
Neurofascin	CTL serine protease 1
α-adaptin C	Preprogranzyme G

(continued)

Table 9.1
(continued)

CD47	Apolipoprotein A-IV precursor
Exocytosis, vesicle trafficking	TGF-β resistance-associated protein
SNAP-25	Picalm protein
Syntaxin 1B1	Adenine nucleotide translocase-1
Synaptotagmin	ADP, ATP carrier protein T2 – mouse
SNAP-91	Myelin proteolipid
Syntaxin binding protein	TBP-interacting protein
SV2	Picalm protein
Synaptophysin	Heat shock protein 1, 4 and 9
Endophylin	Valosin containing protein
AMPH	SHPS-1
VAMP2	Dm-20
Septin 5	CRMP1
Signaling	Septin 4
Go α2	Endophilin I
G β2	SIR2L2
RAC3	Slc25a4
CDC42	Harvey rat sarcoma virus oncogene
ARF3	Golli-myelin basic protein precursor
RAS homolog	Myelin proteolipid
RAB3, RAB6, RAB8 and RAB11	Dm-20
Protein phosphatase 3	Vasolin
PKAII α and β	Stxbp1
PDE1	*N*-ethylmaleimide sensitive fusion protein
Peroxiredoxin 1 and 5	NDR2
TRAG	Cell division cycle 10 homolog

9.2. Materials

9.2.1. Synaptosome Preparation and Protein Solubilization

1. Whole brains from WT and TREK1$^{-/-}$ adult mice.
2. Homogenization solution: 0.32-M sucrose, 100-µM CaCl2, 1-mM MgCl2.
3. 2-M sucrose solution: 2-M sucrose.
4. 1-M sucrose solution: 1-M sucrose, 100-µM CaCl2.
5. CaCl2 solution: 100-µM CaCl2.
6. Wash buffer: Phosphate Buffered Saline (PBS, Eurobio).
7. Solubilization buffer: PBS containing 1% Triton X-100 (Sigma), 2-mM EDTA and a mixture of protease inhibitors (Roche Diagnostics).

9.2.2. Affinity Column Preparation and Immunoprecipitation

1. Aminolink beads (Pierce).
2. Glycine buffer: 0.2-M glycine, pH 2.5 (HCl), 45 µm filtered.
3. Protein A-sepharose 4B fast flow beads (Sigma).
4. 0.5-M EDTA, pH 8 (NaOH); 45-µm filtered.
5. PBS (Eurobio); 45 µm filtered.
6. 1-M Tris–HCl, pH 7; 45 µm filtered.
7. 0.2-M triethanolamine (Sigma), pH 8.2 (NaOH).
8. 50-mM dimethyl pimelimidate (DMP) (Sigma) in 0.2-M triethanolamine, pH 8.2 (NaOH).
9. 50-mM ethanolamine, pH 8.2 (HCl).
10. Elution buffer: 50-mM diethylamine (DEA) (Sigma), 150-mM NaCl, pH 11.6.
11. SigmaPrep spin columns (Sigma).
12. Laemmli sample buffer (Bio-Rad).

9.2.3. Protein Separation by SDS-PAGE

1. Criterion XT Bis–Tris gel 12% (Bio-Rad).
2. Coomassie blue G250 (Bio-Rad).

9.3. Method

9.3.1. Preparation of Affinity-Purified Anti-TREK1 Antibodies

1. Immunize adult rabbits against a glutathion-*S*-transferase (GST) fusion protein (GST-TREK1) comprising the amino-terminal part of TREK1 (residues 1–44, Genbank accession number NP_034737) fused to GST (*see* **Note 1**).
2. Crosslink both GST and GST-TREK1 to amino beads following the manufacturer's protocol (Pierce).

3. Pre-absorb antibodies directed against the GST-tag by incubating 10 mL of serum with GST aminolink beads (1 mL at 5 mg/mL) during 2 h at 22°C. After centrifugation, collect the supernatant and incubate with GST-TREK1 aminolink beads (1 mL at 1 mg/mL) for 1 h at 22°C.
4. Wash the GST-TREK1 aminolink beads with 5-column volumes.
5. Elute the affinity-purified anti-TREK1 antibodies using 2 mL of glycine buffer.
6. Neutralize the pH of the solution containing the eluted antibodies using NaOH.
7. Determine the concentration of anti-TREK1 antibodies using a Bradford assay (Bio-Rad) (*see* **Note 2**).

9.3.2. Preparation of the Anti-TREK1 Affinity Column

1. Gently spin down 0.3 mL of protein A-sepharose beads (50/50 slurry) with a mini desktop centrifuge (1,000×*g*, 2 min) and wash twice with PBS.
2. Re-suspend the beads in 0.3 mL of PBS and add 0.3 mg of purified antibodies (here anti-TREK1 antibodies). Mix on a rocking table for 1 h at 22°C. Spin down (1,000g, 2 min) and save the supernatant for a Bradford assay to verify that all the antibodies have been adsorbed on the protein A-sepharose beads.
3. Wash the beads with 10 volumes of 0.2-M triethanolamine (twice) then spin down.
4. Re-suspend the beads in 20 volumes of freshly made 50-mM DMP in 0.2-M triethanolamine, pH 8.2 for covalent crosslinking of antibodies to protein A.
5. Gently rotate 45 min at 22°C, then spin down and suck off the liquid fraction.
6. For neutralization, re-suspend the beads in an equal volume of 50-mM ethanolamine, pH 8.2 and gently agitate on a rocking table 5 min at 22°C. Spin down and suck off the supernatant.
7. Re-suspend the beads in an equal volume of 50-mM ethanolamine pH 8.2 and keep for 1 h with gentle agitation at room temperature.
8. Spin down, exchange ethanolamine for PBS (twice) and remove the supernatant.
9. Wash twice with 10 volumes of elution buffer (pH 11.6) to eliminate the antibodies that are not covalently crosslinked. Immediately after, wash in PBS. The beads are ready to use.
10. Antichannel beads can be stored at 4°C for several weeks/months by adding sodium azide (final concentration: 0.05%) (s*ee* **Note 3**).

9.3.3. Synaptosomal Protein Preparation

1. Sacrifice five WT and five TREK1$^{-/-}$ mice by decapitation and rapidly collect the whole brains by dissection.
2. Drop the brains into ice-cold homogenization solution (around 6 mL for five brains, total volume of 10 mL).
3. Homogenize with a tissue grinder (Potter Elvehjem, total clearance 0.1 mm), 12 up-and-down strokes at 1,000 rpm.
4. Dilute with 28 mL of 2-M sucrose solution, then add 12 mL of CaCl2 solution. Mix. The final concentration of sucrose is 1.25 M. Transfer 25 mL into two SW28 (25 × 89 mm) centrifuge tubes (Beckman).
5. On this 25-mL layer carefully pour a 10-mL layer of 1-M sucrose solution, then a last layer of 5 mL of 0.32-M sucrose solution above to form a three-layer discontinuous gradient.
6. Spin for 3 h at 100,000×g and 4°C (Beckmann ultracentrifuge).
7. The first white upper band is mainly formed by myelin. The pinkish band at the interface between 1.25- and 2-M sucrose layers contains synaptosomes, while the red pellet contains mitochondria, blood cells, nuclei and cell debris.
8. The myelin layer was carefully discarded and then the synaptosomes were gently collected by pipetting.
9. The synaptosomes were diluted and gently homogenized in 30 mL of PBS and spun down 1for 5 min at 10,000×g to remove sucrose.
10. Finally, the synaptosomal pellets were re-suspended in 4 mL of PBS and used immediately or kept at −80°C after protein quantification using a Bradford assay (Bio-Rad).

9.3.4. Immunoprecipitation

1. Spin down 10 mg of synaptosomal proteins for 15 min at 10,000×g. Re-suspend the pellets in solubilization buffer (1 mL), gently agitate for 4 h at 4°C on a rocking table, then centrifuge for 30 min at 20,000×*g* at 4°C. Collect the supernatant containing the solubilized membrane proteins and keep at 4°C.
2. Wash 50 µL of the beads twice with 500 µL of PBS containing 0.1% Triton-100.
3. Load the solubilized proteins (1 mL of supernatant) onto the beads (50 µL corresponding to 100 µg of antichannel IgG) and incubate overnight at 4°C with gentle agitation (*see* **Note 4**).
4. Load the beads and supernatant into a SigmaPrep spin column connected to a vacuum apparatus for aspiration of the supernatant and wash buffer (Vac-Man laboratory vacuum manifold, Promega) (*see* **Note 5**).
5. Quickly wash the beads with 5 mL of ice-cold lysis buffer.
6. Remove the SigmaPrep spin column from the Vac-Man and place in an Eppendorf tube.

7. Elute the bound proteins by adding 25 µL of Laemmli sample buffer and incubating for 10 min at 22°C with gentle agitation (*see* **Note 6**).
8. Spin down (1,000×g, 5 min) and keep the eluate for gel separation.

9.3.5. SDS-PAGE and Protein Identification

1. Load the precipitated proteins onto a commercial denaturing gel and separate for 1 h at 150–200 V.
2. Stain the gel using coomassie blue (*see* **Note 7**).
3. Cut each lane into ten fragments and identify the precipitated proteins via direct nanoLC-ESI-MS/MS analysis of trypsin-digested gel fragments (*see* **Note 8**).

9.4. Notes

1. The cytosolic carboxy-terminal (C-ter) domain of TREK1, immediately following the fourth transmembrane segment (M4), plays a key structural role in channel activation suggesting that this region may be involved in protein-protein interaction and regulation. To prevent an eventual competition between the binding of the precipitating antibodies and the protein partners, we targeted the anti-TREK1 antibodies against the amino-terminal part of the channel.
2. Usually around 500 µg of specific antibodies are recovered from 10 mL of crude serum.
3. To check the quality of the affinity beads, different amounts of GST, GST-TREK1 and BSA proteins were incubated with 5 µL of beads. Precipitated proteins were analyzed by SDS-PAGE. The column was able to precipitate GST-TREK1 and to a minor extent, GST alone. The binding capacity was estimated to be close to 500 ng of GST-TREK1 per µL of beads.
4. By Western blot analysis, and using GST-TREK1 for comparison and quantification, we estimated that 10 ng of solubilizable TREK1 channel was present in 1 mg of the total synaptosomal proteins. 10 mg of synaptosomal proteins corresponds to 100 ng of solubilized TREK1 channel.
5. At this step it is important to avoid allowing the column to dry out.
6. The Laemmli sample buffer MUST NOT contain any reducing agent such as dithiothreitol (DTT) or β-mercaptoethanol (β-ME) to avoid reduction of interchain disulfide bridges and release of IgG chains in the eluate.

7. The maximal amount of precipitable TREK1 being 100 ng, coprecipitated partners are not visible after Coomassie blue protein staining. There were no staining differences between the lanes corresponding to control and test conditions.
8. With this method, 100 proteins were precipitated and identified. The vast majority of the proteins precipitated from WT mice were identical to the proteins isolated from TREK1$^{-/-}$ mice. Most of these proteins are abundant in the brain (**Table 9.1**). Only four proteins were specifically precipitated from WT mice and are good candidates as TREK1 protein partners. Two of them have a significant effect on the TREK1 current. The main advantage of this approach is to generate very few false-positives in comparison to the two-hybrid screenings. Its most obvious limitations are related to the solubilization and washing steps. If the binding affinity is low, the interaction between the channel and its protein partner will be lost during these steps. This can be only partially prevented by the mild conditions of solubilization (Triton X-100) and the unique and vacuum-assisted rapid wash of the beads. Finally, the very low abundance of TREK1 is another limitation. If some interactions are specific of discrete and reduced brain regions, the corresponding amount of precipitated complexes may not be sufficient for mass spectrometry detection and identification.

Acknowledgments

This work was supported by the Ligue Nationale Contre le Cancer (LNCC) and by a Japan–France Integrated Action Program SAKURA (06980UF).

References

1. Goldstein, S. A., Bayliss, D. A., Kim, D., Lesage, F., Plant, L. D., and Rajan, S. (2005) International Union of Pharmacology. LV. Nomenclature and molecular relationships of two-P potassium channels. *Pharmacol. Rev.* **57**, 527–540.
2. Lesage, F. and Lazdunski, M. (2000) Molecular and functional properties of two-pore-domain potassium channels. *Am. J. Physiol. Renal Physiol.* **279**, F793–F801.
3. Fink, M., Duprat, F., Lesage, F., Reyes, R., Romey, G., Heurteaux, C., and Lazdunski, M. (1996) Cloning, functional expression and brain localization of a novel unconventional outward rectifier K^+ channel. *EMBO J.* **15**, 6854–6862.
4. Lesage, F., Terrenoire, C., Romey, G., and Lazdunski, M. (2000) Human TREK2, a 2P domain mechano-sensitive K^+ channel with multiple regulations by polyunsaturated fatty acids, lysophospholipids, and Gs, Gi, and Gq protein-coupled receptors. *J. Biol. Chem.* **275**, 28398–28405.
5. Honore, E. (2007) The neuronal background K2P channels: focus on TREK1. *Nat. Rev. Neurosci.* **8**, 251–261.
6. Chemin, J., Girard, C., Duprat, F., Lesage, F., Romey, G., and Lazdunski, M. (2003)

Mechanisms underlying excitatory effects of group I metabotropic glutamate receptors via inhibition of 2P domain K^+ channels. *EMBO J.* **22**, 5403–5411.

7. Patel, A. J., Honore, E., Lesage, F., Fink, M., Romey, G., and Lazdunski, M. (1999) Inhalational anesthetics activate two-pore-domain background K^+ channels. *Nat. Neurosci.* **2**, 422–426.
8. Duprat, F., Lesage, F., Patel, A. J., Fink, M., Romey, G., and Lazdunski, M. (2000) The neuroprotective agent riluzole activates the two P domain K^+ channels TREK-1 and TRAAK. *Mol. Pharmacol.* **57**, 906–912.
9. Heurteaux, C., Guy, N., Laigle, C., Blondeau, N., Duprat, F., Mazzuca, M., Lang-Lazdunski, L., Widmann, C., Zanzouri, M., Romey, G., and Lazdunski, M. (2004) TREK-1, a K^+ channel involved in neuroprotection and general anesthesia. *EMBO J.* **23**, 2684–2695.
10. Alloui, A., Zimmermann, K., Mamet, J., Duprat, F., Noel, J., Chemin, J., Guy, N., Blondeau, N., Voilley, N., Rubat-Coudert, C., Borsotto, M., Romey, G., Heurteaux, C., Reeh, P., Eschalier, A., and Lazdunski, M. (2006) TREK-1, a K^+ channel involved in polymodal pain perception. *EMBO J.* **25**, 2368–2376.
11. Heurteaux, C., Lucas, G., Guy, N., El Yacoubi, M., Thummler, S., Peng, X. D., Noble, F., Blondeau, N., Widmann, C., Borsotto, M., Gobbi, G., Vaugeois, J. M., Debonnel, G., and Lazdunski, M. (2006) Deletion of the background potassium channel TREK-1 results in a depression-resistant phenotype. *Nat. Neurosci.* **9**, 1134–1141.
12. Levitan, I. B. (2006) Signaling protein complexes associated with neuronal ion channels. *Nat. Neurosci.* **9**, 305–310.
13. Sandoz, G., Thummler, S., Duprat, F., Feliciangeli, S., Vinh, J., Escoubas, P., Guy, N., Lazdunski, M., and Lesage, F. (2006) AKAP150, a switch to convert mechano-, pH- and arachidonic acid-sensitive TREK K^+ channels into open leak channels. *EMBO J.* **25**, 5864–5872.

Chapter 10

Xenopus Oocytes as a Heterologous Expression System for Studying Ion Channels with the Patch-Clamp Technique

Paolo Tammaro, Kenju Shimomura, and Peter Proks

Summary

Oocytes from the *Xenopus laevis* represent one of the most widely used expression systems for functional characterization of ion channels. Their large size facilitates both injection of heterologous cRNA and subsequent electrophysiological recordings of ion channel currents. Furthermore, *Xenopus* oocytes translate cRNA very efficiently, resulting in the generation of a large number of ion channels in the plasma membrane. In this chapter, we outline methods for oocyte preparation and maintenance and describe procedures for patch-clamping of oocytes, with a special focus on the macropatch technique. We discuss some common problems associated with patch-clamping of oocytes and their use as an expression system for ion channels.

Key words: *Xenopus laevis*, Oocytes, Ion channels, Patch-clamp, Macropatch, Inside-out, Outside-out, Patch-cramming, Heterologous expression.

10.1. Introduction

The South African frog *Xenopus laevis* has been used for a number of years as a laboratory animal and for its oocytes (*see* **Note 1**; *see also* **refs.** *1–3*). *Xenopus* oocytes provide several advantages in addition to their ability to efficiently translate heterologous cRNA into the respective protein, and to dock and insert functional membrane proteins of mammalian (or other) origin into their plasma membrane *(4)*. (1) *Xenopus laevis* is bred and kept in captivity at a relatively low cost *(1, 5)*. (2) Due to their large diameter (~1.1 mm) oocytes are particularly amenable to manipulations such as cRNA injection (*see* **Note 2**) and electrophysiological experiments. (3) Furthermore, since oocytes are naturally released into an adverse environment they are adapted for the

Jonathan D. Lippiat (ed.), *Methods in Molecular Biology, Potassium Channels, vol. 491*

Book doi: 10.1007/978-1-59745-526-8

efficient translation of proteins, independent of the necessity of absorbing nutrients from the environment.

Due to the efficient translation of injected cRNA, large-amplitude ion channel currents can be recorded from oocytes using the macropatch technique. A further advantage of the oocyte as an expression system is that amplitudes of endogenous currents are usually very small in comparison to those of heterologously expressed channels. Furthermore several cRNAs coding for different subunits can be coinjected in a defined ratio. This is of considerable importance when studying diseases associated with heterozygous mutations in ion channel genes, since this situation can be simulated by coinjecting an equal amount of wild-type and mutant subunits (*see* **Note 3**; *see also* **ref.** *6*).

It is important to keep in mind, however, that heterologously expressed polypeptides can sometimes upregulate endogenous channels in oocytes as well as endogenous proteins that may interfere with heterologously expressed proteins through the formation of heteromeric complexes (*see* **Note 4**). Likewise, differences in the lipid membrane composition between oocytes and native cells could modify the channel functional properties.

In this chapter, we describe the preparation and handling of *Xenopus* oocytes for the functional characterization of ion channels using the patch-clamp technique *(7*, *8)*. Several references are available that describe the electronics of the recording apparatus in detail (e.g., *see* **refs.** *9*, *10*) and therefore this will not be described here.

10.2. Materials

10.2.1. Oocyte Preparation and Maintenance

1. Collagenase type V.
2. MS222 (ethyl 3-aminobenzoate methanesulfonate salt).
3. OR-2 solution: 82.5-mM NaCl, 2-mM KCl, 5-mM HEPES, 1-mM $MgCl_2$ (adjust pH to 7.4 with NaOH).
4. Barth solution: 88-mM NaCl, 1.68-mM $MgSO_4$, 10-mM HEPES, 0.47-mM $Ca(NO_3)_2$, 2.4-mM $NaHCO_3$, 0.41-mM $CaCl_2$ (adjust pH to 7.5 with NaOH).
5. Shrink solution: 20-mM KCl, 10-mM HEPES, 200-mM K-aspartate, 5-mM EGTA (adjust pH to 7.4 with KOH).

10.2.2. mRNA Injection

1. Microinjector (e.g., Drummond Nanoject, Drummond, Scientific Co., Bromall, USA).
2. Glass capillaries for injection: e.g., 3-000-203-G; Drummond Scientific, Pennsylvania, USA.

3. cRNA.
4. RNAase-free water to dilute cRNA stock.
5. RNase-free pipette tips.
6. Plastic film.
7. Mineral oil.
8. 96-well plates (e.g., Microtest 96-well Assay Plate; BD Biosciences, Franklin Lakes, USA).

10.2.3. Patch-Clamp Recordings

1. One patch-clamp apparatus.
2. Pipette puller (e.g., Narishige PC-10, Narishige Scientific Instrument Lab, Tokyo, Japan).
3. Microforge (e.g., Narishige NF-900).
4. Capillary glass for macropatch pipette: e.g., 1.5-mm outer diameter, 0.86-mm inner diameter borosilicate glass.
5. Capillary glass for micropatch pipette: e.g., 1.6-mm outer diameter, 1.2-mm inner diameter (Aluminiumsilicate or borosilicate glass).
6. Mineral oil.
7. Sylgard (Dow Corning, Midland, MI).

10.3. Methods

10.3.1. Oocyte Preparation and Maintenance

1. Female *Xenopus laevis* are anesthetized by immersion in a solution of MS222 (1 g/l added to the water) or a similar anesthetic. It is good practice to place the animal on ice for surgery, to prolong the anesthetic effect. Through a small abdominal incision, a few ovary sacks are removed via a mini-laparotomy. The incision is then sutured and the animal is allowed to recover. Alternatively, the animal can be sacrificed. The procedure must conform to guidelines of the institution and country in which the procedure is carried out.
2. Immature stage V–VI oocytes (11) are incubated for 60–90 min with 1-mg/ml collagenase in divalent ion-free OR-2 solution at room temperature. A volume of ~5 ml of oocytes is digested in 15 ml of OR-2 (plus collagenase) solution. The flask is gently shaken during this period to ensure that enzymatic digestion occurs evenly. Some investigators report that addition of trypsin inhibitors can help improve the quality of the oocytes *(4)*. To stop the enzymatic reaction, the oocytes are repeatedly washed with Barth solution. After enzymatic digestion, the remaining follicular cell

layer is removed manually using two straight forceps (No. 5, Dumont, Switzerland). Oocytes showing evenly colored poles are selected and stored in Barth solution supplemented with 50 µg/ml of gentamycin and usually injected with cRNA on the same day or on the day after. Defolliculated oocytes should be transferred using a Pasteur pipette (plastic or glass with fire-polished sharp end).

10.3.2. cRNA Injection into Oocytes

1. cRNA is injected into the oocytes using a micromanipulator-mounted microinjector. To prevent cRNA degradation by RNAases, appropriate RNAase-free pipettes and DEPC water should be used. Gloves should be worn when handling cRNA samples. To prevent small particles blocking the injection capillaries it is recommended to briefly centrifuge cRNA samples so as to precipitate particles suspended in the solution.
2. Glass capillaries are pulled using a conventional pipette puller and the tip manually broken under a microscope to a diameter of ~20 µM. It is possible to smooth the edge of the needle using a microforge where the microfilament is covered with a drop of soda glass. The tip of the needle is put into contact with the melted glass and rapidly removed. This results in the formation of a beveled syringe needle-like pipette tip.
3. Injection needles are backfilled with mineral oil using a syringe needle to seal the pipette from air. They are then filled with 1–2 µl of cRNA solution (this volume is sufficient for injection of ~20–40 oocytes). To facilitate pipette filling, the drop is placed on a small piece of parafilm.
4. For injection, it is convenient to place the oocytes into a grooved plastic chamber filled with Barth solution, or to cover the bottom of the chamber with a plastic mesh with dimensions similar to those of the oocyte, to hold them in place during injection. Injection is done under a conventional stereomicroscope. A hand driven manipulator is used to guide the needle toward the oocytes. Each oocyte is injected with about 50 nl of solution containing ~2–20 ng of cRNA. If carefully observed under a microscope, it can be seen that the oocytes tend to swell when injected. This visual inspection may serve as an indication that injection has successfully occurred. This procedure described for cRNA injection can also be used to load oocytes with dyes or substances that modify the intracellular milieu (e.g., the Ca^{2+} chelator BAPTA or enzyme inhibitors) *(12)*.
5. After injection, the oocytes are stored in Barth's solution (supplied with gentamycin) at 14–18°C in small Petri dishes. The Barth solution should be replaced everyday and the damaged oocytes removed. To avoid damage of oocytes by

enzymes released by injured or dead oocytes, we found it beneficial to store them separately from each other. For this purpose, oocytes are stored in separate wells of 96-well plates (e.g., Microtest 96-well Assay Plate; BD Biosciences, Franklin Lakes, USA) with 200 µl of Barth solution in each well. The oocytes can be stored and used for electrophysiological experiments for as long as 8–14 days.

10.3.3. Distribution of Ion Channels in the Oocyte Membrane

1. Before conducting patch-clamp experiments it is important to consider that the distribution of heterologous ion channels is non-uniform on the oocyte membrane and may depend on the channel type *(8)*. Thus, in order to obtain large currents in macropatches, several regions might need to be explored with multiple patches in order to localize the area with the highest density of ion channels (*see* **Note 5**). A similar trial and error procedure is also necessary when micropipettes are used to search for single channels.
2. There is some batch to batch variability in the level of expression and distribution of *endogenous* ion channels and transporters. The predominant endogenous conductance in oocytes is due to Ca^{2+}-activated Cl– channels (13, 14). This may represent a serious problem when performing cell-attached recordings. In order to reduce activation of Ca^{2+}-activated Cl– channels on patch excision, the bath solution should contain a low Ca^{2+} concentration and appropriate chelators, such as EGTA. Cl^- ions can also be replaced by impermeable ions, such as methanesulfonic acid (15). Ca^{2+}-activated Cl^- conductances can also be blocked pharmacologically (e.g., with 0.3-mM niflumic acid) (*see* **Note 6**; *see also* **ref. 16**).
3. There are also endogenous cation channels that are normally blocked by extracellular divalent cations. These conductances display a characteristic outward rectification at potentials higher than 60–80 mV. Their activity can be limited by maintaining the extracellular Ca^{2+} and Mg^{2+} concentrations at values greater than 0.1 mM.
4. Some oocytes contain a large number of endogenous stretch-activated channels that have a single-channel conductance of 40 pS *(7)*. In excised patches, these channels can be identified by the application of positive or negative pressure to the patch, which stimulates their activity. The activity of these channels can be blocked by 100-µM gadolinium *(7)* (*see* **Note 6**).
5. For unknown reasons there is considerable seasonal variability in the quality of oocytes for heterologous expression studies. Better seal formation has been observed by several laboratories from late fall to middle spring.

10.3.4. Patch-Clamp Recording from Xenopus Oocytes

10.3.4.1. Skinning

In order to perform patch-clamp experiments, the oocyte vitelline layer has to be removed. This is done manually, with the aid of Type 5 straight forceps and working under a stereoscopic microscope. The *skinning* can be facilitated by exposing oocytes to a hypertonic solution (shrink solution) for a few minutes. Once the vitelline membrane is removed, the oocyte is transferred to the recording chamber. The oocyte should be handled with great care at this stage since, once the vitelline membrane is removed, the oocyte is quite fragile and sensitive to exposure to the air-water interface. Recording chambers are made of perspex or polycarbonate to favor the attachment of the oocyte to the bottom. It is good practice to wait for a few minutes before initiating experiments, to allow the oocyte to attach to the chamber and equilibrate with the bath solution.

10.3.4.2. Preparation of Patch Pipettes

1. Three types of glass capillaries can be used for different recording conditions. According to the melting temperature, the capillaries' glass can be classified as soft (soda glass), hard (borosilicate glass) and extra hard (aluminum glass) (17). Selection of the glass is made by balancing the requirement for low noise-recording characteristics (e.g., hard glass has a higher resistance and lower dielectric constant and therefore low noise) and the ease of working with each type of glass (e.g., with soft glass it is easier to achieve the desired profile of the pipette tip). It is important to be aware that soda glass releases heavy metals in the presence of divalent cation chelators, like EGTA or EDTA, and therefore should not be used when solutions contain these substances. Soda glass is also used for the injection needle. After being cut to an appropriate length, the edges of the glass capillary tubes are rounded using a Bunsen burner to mechanically protect the Ag/AgCl electrode in the pipette holder.
2. Pull the patch pipette in two stages. The first pull thins the capillary tube and will determine the characteristic of the shaft of the electrode, and in combination with the second pull it determines the tip diameter. We fabricate electrodes on the day of the experiment and store them in a closed container.

   To reduce the diameter of the pipette tip as well as to smooth and clean its surface, the tip of each patch pipette is fire-polished by bringing it close to a hot platinum wire of a microforge before use. Pipettes for macropatches are generally made from thick-walled borosilicate capillary glass. After polishing, they have an opening diameter of ~10–20 μM and an electrical resistance of 0.1–1.0 MΩ (**Fig. 10.1**).

   Pipettes for micropatches (characterized by an electrical resistance varying in the range of 2–20 MΩ and tip diameter

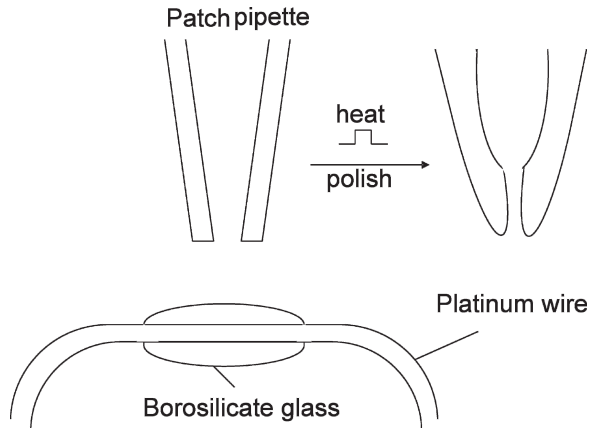

Fig. 10.1. Fabrication of macropatch electrodes. Soft soda glass is melted around the platinum wire (diameter of ~150 μM) of the microforge. Current is applied through the wire for a few seconds, until the pipette tip begins to melt and the desired final shape is achieved.

of ~1-μM diameter *(18)*) are made from aluminiumsilicate or borosilicate capillary glass. They may contain a thin filament to facilitate filling with the pipette solution. However, such a filament acts as a conduit which may cause the intracellular solution to creep up inside the pipette wall. This fluid that is near the filament may act as a noise source. Thus filamented capillaries should be avoided if the level of background noise has to be particularly low, such as during an experiment of "noise-analysis" or if the single-channel current amplitude is very small.

3. To improve the noise characteristics and reduce the tip capacity, pipette tips can be coated with a low dielectric and highly hydrophobic silicone polymer (Sylgard) *(17, 19)*. Sylgard should be manually applied as close as possible to the pipette tip, with the aid of a wire hook and working under a low-magnification microscope. A hot air stream from a heated coil, or a small "oven" made by a platinum coil, can be used to induce polymerization.

10.3.4.3. Ground Electrode

Ground electrodes are Ag ‖ AgCl electrodes, made with a chlorurated silver wire or Ag ‖ AgCl pellets. To avoid high and unstable electrode potentials, the bath solution has to contain at least 10–20 mM Cl^-. When it is necessary to use lower chloride concentrations, the electrode can be connected to the bath solution by an agar salt bridge, which comprises a capillary tube filled with 1–3% agar in bath solution. The use of an agar salt bridge also prevents contamination of the preparation by Ag^+ ions from the electrode. Agar bridges can be stored immersed in the bath recording solution at 4°C for several weeks.

10.3.4.4. Macropatch Recording

Sealing

1. In a patch-clamp setup specifically designed for patch-clamping of oocytes, the electrode holder should be mounted in order to approach the membrane at 45°. In this respect a setup designed for patching oocytes differs from ones designed for patch-clamping of mammalian cells, in which seal formation is easier if the pipette holder is positioned at a steeper angle. In some cases, a bend in the electrode may help to achieve the desired angle. Bending is achieved by placing a heating coil near the electrode tip *(20)*.
2. Both intracellular and extracellular solutions should be filtered with a 0.22-μM filter immediately before use. Electrodes can be back filled with a conventional syringe. Air bubbles that may be present in the electrode can be removed by gently tapping the electrodes. Inclusion of divalent cations, such as Mg^{2+} or Ca^{2+}, in either the pipette solution or the bath solution, facilitates formation of gigaohm seals. To improve the stability of the macropatch, the tip of the pipette is dipped briefly in an equal mixture of light and heavy mineral oil before it is filled with the pipette solution.
3. Using a microscope to observe the movements, the pipette tip is brought very close to the edge of the oocyte. The microscope could be either an inverted microscope or a stereoscopic microscope with high enough magnification (>30×). Seal formation is monitored electrically by measuring the resistance of the electrode before and during seal formation by applying a short (~10 ms) voltage step (~10 mV) to the pipette and measuring the resulting current amplitude.
4. A slight positive hydrostatic pressure should be continuously applied to the pipette while the tip is gently and slowly pushed into the oocyte without rupturing its membrane. The pipette is advanced slowly toward the membrane until a small increase in electrical resistance is observed. At this stage the positive pressure is released. This should result in a further increase in the electrical resistance. Seals with electrical resistance greater that 1 GΩ (gigaseals) can sometimes form simply by releasing the positive pressure.
5. If a gigaseal is not obtained following the release of positive pressure, negative pressure is applied to the pipette by gentle suction. The suction should be stopped when the seal resistance becomes greater than 1 GΩ. Intense or prolonged suction should be avoided as it may result in distortion of the membrane or formation of deep omega-patches or membrane vesicles. Recommended values for positive pressure before pressing the electrode into oocyte range are between 10–40 mm H_2O and for negative pressure (suction) during sealing formation between 100–200 mm H_2O (7).

6. Seal formation may become particularly slow when the seal resistance increases to above 10–20 MΩ. In such cases, negative pipette electrical potentials (up to 40 mV) may help promoting sealing. The formation of a gigaohm seal can take from a few seconds up to ~5 min.
7. Attention has to be paid when monitoring seal formation in oocytes injected with ion channels that are open at the patch holding potential. In this case, a tight seal might be achieved even if the patch electrical resistance does not reach GΩ values.

Excision

Excision of cell-attached patches is achieved by quickly removing the pipette tip from the oocytes, in a solution normally containing high K^+ and no Ca^{2+}. The speed of the pipette removal should be inversely proportional to the size of the membrane patch excised. Sometimes, when the patch is excised very slowly, membrane vesicles can form. Vesicles are sometimes difficult to see but they can be identified by the manifestation of a slow capacitive transient in response to a voltage pulse, observed after excision. Some researchers thus recommend compensation of capacitive transients before excision. In most cases, a vesicle is broken by the slow movement of the pipette toward a small silicone sphere until a change in the capacitive transient is observed *(7)*, or by crossing the water–air interface.

Leak and Capacity Subtraction

1. Unwanted currents may originate either from a leak arising from a poor seal between membranes and recording electrodes or by endogenous membrane currents. Endogenous current can be minimized by choosing correct solutions (*see* Step2 **Subheading 10.3.3**). Leaks and endogenous currents can be estimated by blocking the ion channel currents of interest using specific pharmacological blockers (if available).
2. When recording voltage-gated ion channels, leak currents and uncompensated capacitance can be effectively subtracted using a P/N voltage clamp protocol *(21)*. Briefly, at voltages below the activation threshold of the voltage-dependent channels, a number of voltage pulses that are scaled to a fraction of the test pulse (e.g., P/4) are applied N times (e.g., four times), and the resulting currents are averaged, scaled and subtracted from the current elicited by the test pulse.

Membrane Potential

With the patch-clamp technique, recordings can be obtained in cell-attached, inside-out (i.e., the intracellular side of the membrane is exposed to the bath solution) or outside-out membrane patches (i.e., the extracellular side of the membrane is exposed to the bath solution). The membrane patch potential (V_m) is under the control of the potential applied to the pipette (V_p). In cell-attached configuration, the $V_m = -V_p + V_r$, where V_r is the resting potential of the cell. Therefore, when $V_p = 0$, V_m is equal to the cell resting potential V_r. Depolarizing steps from this potential are obtained by applying a negative V whereas positive V_p voltages

correspond to hyperpolarization of V_m. In cell-attached configuration, inward membrane currents appear as positive signals at the current monitor outputs. Further, in the inside-out configuration, where $V_m = -V_p$, the sign of the control potential and the recorded current are inverted. In order to follow the standard electrophysiological convention (i.e., outward currents are positive and positive voltages are depolarizing), the acquisition software used must also be properly programmed, in order to invert digital stimulus and sampled values. Conversely, in the outside-out configuration, $V_m = V_p$, and currents have the conventional polarity.

10.3.4.5. Other Patch-Clamp Configurations

Micropatches

The basic technique for micropatch recording is similar to that which we have described for macropatch. The electrodes are pulled to a much smaller diameter than that typically used for macropatch pipettes. Formation of gigaseal with small pipettes is also very similar to that described for macropatches. Following initial contact with the membrane, suction is applied to form a tight gigaseal. Outside-out patches can be obtained by rupture of the patch after seal formation and slow removal of the pipette from the oocytes. Formation of outside-out patches with a macropipette is also possible, but the rate of success is considerably lower than with micropipettes. The intensity of the suction used in order to favor seal formation with micropipettes can be 2–5-fold greater than that used to assist macropatch formation.

Patch-Cramming

The large size of the oocyte is particularly suitable for *patch-cramming*, i.e., insertion of the patch-containing pipette into the oocyte (*see* **Fig. 10.2**). After excision of an inside-out patch, the pipette is pushed deep into the oocyte. We found that patch survival with this technique is quite high (80–90%); thus the patch can be repeatedly exposed to cytoplasmic and bath environments. For example, this approach has been used to demonstrate that cytoplasmic constituents (e.g., protein kinases) play a role in regulating the activity of certain ion channels *(22–25)*.

10.4. Notes

1. It should be noted that oocytes from other amphibians (such as oocytes from the cane toad *Bufo marinus (26, 27)*) have been successfully used as heterologous protein expression systems and may represent an alternative to *Xenopus* oocytes. This may be particular relevant in Australia, Asia and the Americas where *B. marinus* is widely available.
2. In the early days, receptors and ion channels were expressed in *Xenopus* oocytes by injection of total poly(A) mRNA

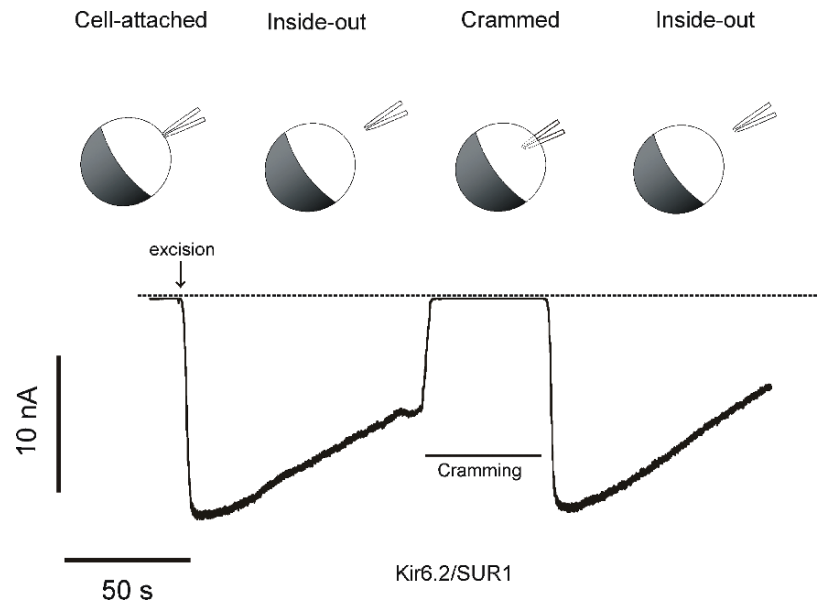

Fig. 10.2. Macroscopic K_{ATP} current recorded at −60 mV from a *Xenopus* oocyte coexpressing Kir6.2 and SUR1. The patch was excised in nucleotide-free solution at the time indicated by the arrow and reinserted into the oocytes (crammed) as indicated. The dashed *line* indicates the zero current level. Note that the current is virtually completely blocked in cell-attached or cramming mode, presumably because the high intracellular ATP level within the oocytes results in the complete blockage of the K_{ATP} channel.

extracted from tissue samples (e.g., *see* **refs.** *28, 29*). This method has the obvious disadvantage that all possible mRNA are translated into proteins. With the advent of gene cloning, the use of complementary RNA (cRNA) became predominant.

3. With respect to the expression of ion channels that are composed of two or more subunits, the amount of cRNA for each subunit that needs to be injected depends, in principle, on the stoichiometry of the subunits comprising the channel and the length of the cRNA encoding each subunit. However, different efficiency of RNA translation, or different posttranslational processing could modify this relationship. For example, the pancreatic beta cell K_{ATP} channel is formed by four Kir6.2 subunits, forming the channel pore, and an equal number of auxiliary subunits (SUR1). SUR1 is a protein of 1,581 amino acids whereas Kir6.2 is about five times shorter (390 amino acids). We found that the best K_{ATP} channel expression is achieved by injecting that five times more of the cRNA coding for SUR1 than coding for Kir6.2 RNA. Presumably, this results in the translation of approximately the same number of Kir6.2 and SUR1 subunits.
4. Examples include the IKs channel formed from the heterologously expressed IsK (minK) subunit and the endogenous KvLQT1 subunit *(30)*. Oocyte-specific interactions between

voltage-gated sodium channels and the cytoskeleton have also been reported *(31)*.

5. The expression levels are sometimes higher around the site of injection. For this reason, it can be useful to use a similar injection site in all oocytes, such as the centre of the animal hemisphere.
6. If blockers of endogenous channels are used, it is always important to check that they do not affect the activity of heterologously expressed ion channels. For example, of high concentration gadolinium might have electrical screening effects on the plasma membrane.

Acknowledgments

We wish to thank Drs. Oscar Moran and Tim Craig for their critical reading of the manuscript and helpful comments. P.T. holds a Junior Research fellowship at Wolfson College, Oxford.

References

1. Sive, H. L., Grainger, R. M., and Harland, R. M. (eds.) (2000) *Early development of Xenopus Laevis: a laboratory manual*. Cold Spring Harbor Laboratory, Cold Spring Harbor, NY.
2. Bodart, J. F. and Duesbery, N. S. (2006) *Xenopus tropicalis* oocytes: more than just a beautiful genome. *Methods Mol. Biol.* **322**, 43–53.
3. Gurdon, J. B., Lane, C. D., Woodland, H. R., and Marbaix, G. (1971) Use of frog eggs and oocytes for the study of messenger RNA and its translation in living cells. *Nature* **233**, 177–182.
4. Wagner, C. A., Friedrich, B., Setiawan, I., Lang, F., and Broer, S. (2000) The use of *Xenopus laevis* oocytes for the functional characterization of heterologously expressed membrane proteins. *Cell Physiol. Biochem.* **10**, 1–12.
5. Wu, M. and Gerhart, J. (1991) Raising *Xenopus* in the laboratory. *Methods Cell Biol.* **36**, 3–18.
6. Ashcroft, F. M. (2006) From molecule to malady. *Nature* **440**, 440–447.
7. Stuhmer, W. (1998) Electrophysiologic recordings from *Xenopus* oocytes. *Methods Enzymol.* **293**, 280–300.
8. Hilgemann, D. W. and Lu, C. C. (1998) Giant membrane patches: improvements and applications. *Methods Enzymol.* **293**, 267–280.
9. Sakmann, B. and Neher, E. (eds.) (1995) *Single-channel recording*. Plenum, New York.
10. Ogden, D. C. (ed.) (1994) *Microelectrode techniques*. The Plymouth Workshop Handbook, Cambridge.
11. Dumont, J. N. (1972) Oogenesis in *Xenopus laevis* (Daudin). I. Stages of oocyte development in laboratory maintained animals. *J. Morphol.* **136**, 153–179.
12. Oron, Y. and Dascal, N. (1992) Regulation of intracellular calcium activity in *Xenopus* oocytes. *Methods Enzymol.* **207**, 381–390.
13. Barish, M. E. (1983) A transient calcium-dependent chloride current in the immature *Xenopus* oocyte. *J. Physiol.* **342**, 309–325.
14. Hartzell, C., Putzier, I., and Arreola, J. (2005) Calcium-activated chloride channels. *Annu. Rev. Physiol.* **67**, 719–758.
15. Krafte, D. S. and Lester, H. A. (1992) Use of stage II–III *Xenopus* oocytes to study voltage-dependent ion channels. *Methods Enzymol.* **207**, 339–345.

16. Leonard, J. P. and Kelso, S. R. (1990) Apparent desensitization of NMDA responses in *Xenopus* oocytes involves calcium-dependent chloride current. *Neuron* **4**, 53–60.
17. Rae, J. L. and Levis, R. A. (1992) Glass technology for patch clamp electrodes. *Methods Enzymol.* **207**, 66–92.
18. Sakmann, B. and Neher, E. (1995) Geometric parameters of pipettes and membrane patches, in *Single-channel recording*, 2nd edition (Sakmann, B. and Neher, E., eds.), Plenum, New York, pp. 637–650.
19. Penner, R. (1995) A practical guide to patch clamping, in *Single-channel recording*, 2nd edition (Sakmann, B. and Neher, E., eds.), Plenum, New York, pp. 3–30.
20. Moody-Corbett, F. and Fry, M. (2002) Recordings from macropatches, in *Patch-clamp analysis, advanced techniques* (Walz, W., Boulton, A. A., and Baker, G. B., eds.), Humana, Totowa, NJ, pp. 287–299.
21. Heinemann, S. H. 1995. Guide to data acquisition and analysis, in *Single-channel recording*, 2nd edition (Sakmann, B. and Neher, E., eds.), Plenum, New York, pp. 53–90.
22. Tang, X. D. and Hoshi, T. (1999) Rundown of the hyperpolarization-activated KAT1 channel involves slowing of the opening transitions regulated by phosphorylation. *Biophys. J.* **76**, 3089–3098.
23. Krauter, T., Ruppersberg, J. P., and Baukrowitz, T. (2001) Phospholipids as modulators of K_{ATP} channels: distinct mechanisms for control of sensitivity to sulphonylureas, K^+ channel openers, and ATP. *Mol. Pharmacol.* **59**, 1086–1093.
24. Beck, E. J. and Covarrubias, M. (2001) Kv4 channels exhibit modulation of closed-state inactivation in inside-out patches. *Biophys. J.* **81**, 867–883.
25. Costantin, J. L., Qin, N., Waxham, M. N., Birnbaumer, L., and Stefani, E. (1999) Complete reversal of run-down in rabbit cardiac Ca^{2+} channels by patch-cramming in *Xenopus* oocytes; partial reversal by protein kinase A. *Pflugers Arch.* **437**, 888–894.
26. Markovich, D. and Regeer, R. R. (1999) Expression of membrane transporters in cane toad *Bufo marinus* oocytes. *J. Exp. Biol.* **202**, 2217–2223.
27. Vargas, R. A., Botero, L., Lagos, L., and Camacho, M. (2004) *Bufo marinus* oocytes as a model for ion channel protein expression and functional characterization for electrophysiological studies. *Cell Physiol. Biochem.* **14**, 197–202.
28. Sumikawa, K., Houghton, M., Emtage, J. S., Richards, B. M., and Barnard, E. A. (1981) Active multi-subunit ACh receptor assembled by translation of heterologous mRNA in *Xenopus* oocytes. *Nature* **292**, 862–864.
29. Miledi, R., Parker, I., and Sumikawa, K. (1982) Synthesis of chick brain GABA receptors by frog oocytes. *Proc. R. Soc. Lond. B Biol. Sci.* **216**, 509–515.
30. Sanguinetti, M. C., Curran, M. E., Zou, A., Shen, J., Spector, P. S., Atkinson, D. L., and Keating, M. T. (1996) Coassembly of K(V) LQT1 and minK (IsK) proteins to form cardiac I_{Ks} potassium channel. *Nature* **384**, 80–83.
31. Shcherbatko, A., Ono, F., Mandel, G., and Brehm, P. (1999) Voltage-dependent sodium channel function is regulated through membrane mechanics. *Biophys. J.* **77**, 1945–1959.

Chapter 11

Whole-Cell Recording Using the Perforated Patch Clamp Technique

Jonathan D. Lippiat

Summary

Many ion channels, particularly potassium channels, are regulated by intracellular substances, such as nucleotides or Ca^{2+}. These modulators are washed out of the cell during standard whole-cell patch clamp recordings, or maintained at a particular concentration if they are included in the pipette solution. Perforated patch clamp recording permits electrical access between the cell and the patch pipette using pore-forming antibiotics such as nystatin or amphotericin B. These are permeable to small monovalent ions but present a physical barrier to the larger impermeable ions and molecules. This maintains the integrity of many cytoplasmic components including soluble second messengers, and also helps to prevent channel "run down".

Key words: Amphotericin B, Nystatin, Patch clamp, Perforated patch, Potassium channels.

11.1. Introduction

One of the key advantages of the whole-cell patch clamp technique is the ability to determine the chemical environment on each side of the cell membrane through the careful design of both the bath and pipette solutions. Upon rupture of the patch of membrane enclosed by the tip of the patch pipette, the cell contents become a continuum with the pipette solution. As a result there is a two-way diffusion between the two compartments; for example, the ions and buffers (pH and calcium) invade the cell with a loss of nucleotides from the cell.

This aspect of patch clamp recording can also be a disadvantage when studying potassium channels that are dependent on the intracellular environment. Some channels are classified according

Jonathan D. Lippiat (ed.), *Methods in Molecular Biology, Potassium Channels, vol. 491*

Book doi: 10.1007/978-1-59745-526-8

to their intracellular modulators, such as ATP-sensitive K^+ channels (K_{ATP}), cyclic nucleotide-gated channels (K_{CNG}), or Ca^{2+}-activated K^+ channels (K_{Ca}), and the levels of these modulators change during normal cell functioning; a process that may be prevented by the whole-cell configuration. Many cells exhibit *run down*, where a loss of channel activity is observed over many seconds or minutes. This change in behaviour is attributed to the dialysis of substances that are required to maintain channel activity. In many cases this substance may be known, e.g. ATP that is required for channel or lipid phosphorylation by associated kinases can be added to the pipette solution, or it may be an unknown factor.

The perforated patch clamp technique is a variation of whole-cell recording, but instead of rupturing the membrane enclosed by the patch pipette by suction or "zapping" it is instead *perforated* by the incorporation of pore-forming substances supplied by the patch pipette. Perforation can be achieved using the antibiotics nystatin *(1)* or amphotericin B *(2)*, which are both permeable to the small monovalent ions Na^+, K^+, and Cl^-. These ion-permeable pores provide electrical access between the pipette and the cell due to the currents carried by these ions, but present a physical barrier to impermeable ions (e.g. Ca^{2+}) and molecules with a molecular weight above approximately 200 (e.g. ATP, glucose). The seal between the membrane and the pipette glass prevents the lateral diffusion of antibiotic away from the enclosed patch and maintains the integrity of the configuration *(3)*.

In this chapter, the perforated patch method that was used to record K^+ currents from mouse pancreatic β-cells *(4)* and HEK293 cells *(5)* is described, using perforation of the latter cell type with amphotericin B as an example. Amphotericin B is a polyene antibiotic that is commonly used as a fungicidal agent in tissue culture media (Fungizone). It has an affinity for ergosterols found in fungal membranes where it accumulates to form pores to disrupt cellular homeostasis. At the higher doses used in the pipette solutions amphotericin B invades the patch of membrane enclosed by the patch pipette through interactions with cholesterol.

11.2. Materials

11.2.1. Cell Culture

1. HEK293 cells.
2. Culture medium: DMEM + 10% FBS.
3. PBS.
4. Trypsin–EDTA cell dissociation solution.
5. 35 mm plastic Petri dishes.

11.2.2. Amphotericin Stock and Pipette Solutions

1. Amphotericin B (usually supplied as ≈80% purity).
2. Dimethylsulfoxide (DMSO).
3. Opaque or amber light-resistant microtubes.
4. Aluminium foil.

11.2.3. Electrophysiology

1. Patch clamp apparatus.
2. Pipette puller.
3. Microforge.
4. Capillary glass (thin-walled, unfilamented, *see* **Note 1**).
5. Glass 50 µl syringe with needle (e.g. Hamilton) to fill patch pipettes.
6. 1 ml plastic syringe.
7. Syringe filter disc, 20 µm holes.
8. Pipette solution: 70 mM K_2SO_4, 10 mM NaCl, 1 mM $CaCl_2$, 1 mM $MgCl_2$, 10 mM HEPES, pH 7.2 with KOH (*see* **Note 2**). This solution is stable at 4°C for several months, but check the pH before use.
9. Bath solution: 137 mM NaCl, 5.6 mM KCl, 2.6 mM $CaCl_2$, 1.2 mM $MgCl_2$, 10 mM HEPES, pH 7.4 with NaOH. This solution is stable at 4°C for several months, but check the pH before use.

11.3. Methods

11.3.1. Cell Culture

1. Wash cells twice with PBS and harvest using the trypsin–EDTA dissociation solution.
2. Add culture medium and centrifuge cells (200 g for 1 min).
3. Aspirate supernatant and re-suspend in the culture medium, diluting if necessary.
4. Add 2 ml of cell suspension to each of the 35 mm Petri dishes and incubate overnight (*see* **Note 3**).

11.3.2. Preparation of Amphotericin B Solutions

Amphotericin B is light-sensitive, so care must be taken to limit the exposure of the compound to both natural and artificial light.

11.3.2.1. Stock Solution

1. Measure 3 mg of amphotericin B powder into a light-sensitive microtube using an analytical balance.
2. Dissolve amphotericin B with 50 µl of DMSO using a sonicator to give a 60 mg/ml stock solution (*see* **Note 4**).
3. Use immediately or store at –20°C. This stock solution, if stored and handled correctly, can be used for 1 week.

11.3.2.2. Amphotericin Pipette Solution

1. Measure 2 ml of the pipette solution into a clean small glass beaker or vial of approximately 10 ml capacity (*see* **Note 5**).
2. Pipette and dissolve 8 µl of the 60 mg/ml stock amphotericin B in DMSO into the pipette solution to give a final concentration of 0.24 mg/ml (*see* **Note 6**).
3. Wrap the beaker with two layers of aluminium foil and place on ice until use (*see* **Note 7**). This solution is viable for 3–5 h.

11.3.3. Obtaining the Perforated Patch Configuration

Remove a dish of cells from the incubator, replace the culture medium with 1–2 ml of the bath solution and place on the microscope stage.

11.3.3.1. Loading Patch Pipette

A schematic of the following steps is shown in **Fig. 11.1**.

1. Pull patch pipettes from the glass capillaries using the puller and polish using the microforge. The resistance in the experimental solutions should be 3–5 MΩ (*see* **Note 8**).

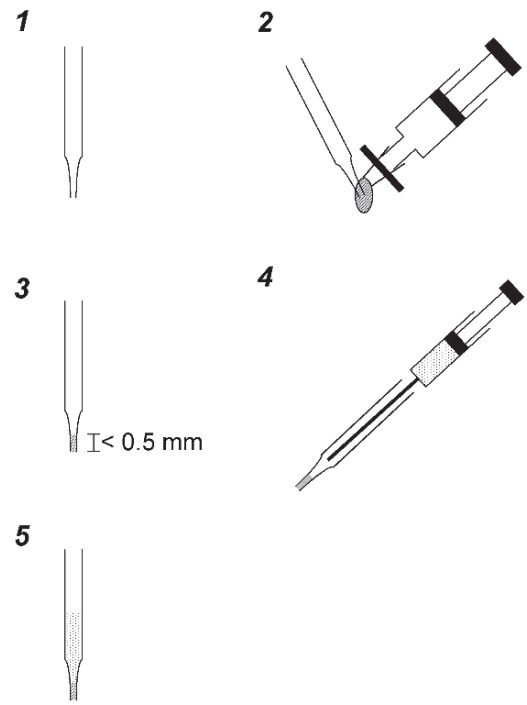

Fig. 11.1. Preparation and filling of patch pipettes. ***1*** Pull patch pipettes from capillary glass and polish using a microforge. ***2*** Place tip of patch pipette into a suspended droplet of amphotericin-free pipette solution for 5 s. ***3*** The antibiotic-free region should not extend more than 0.5 mm from the pipette aperture. ***4*** Back-fill patch pipette with amphotericin-containing pipette solution. ***5*** Ensure that no bubbles exist at the interface of the two solutions and proceed immediately to electrophysiology.

2. Load amphotericin-free pipette solution into a 1-ml plastic syringe and affix a filter disc.
3. Dispense pipette solution through the filter disc until a drop of filtered solution appears and is suspended from the filter disc.
4. Place the tip of the patch pipette into the drop of filtered pipette solution for 5 s (*see* **Note 9**).
5. Swirl the glass beaker or vial containing the amphotericin B pipette solution for several seconds (*see* **Note 10**).
6. Pierce the needle of the pipette-loading syringe through the foil and load the amphotericin-containing pipette solution. Repeat **steps 4–6** each time a patch pipette is used (*see* **Note 11**).
7. Immediately, back-fill the amphotericin pipette solution into the patch pipette and proceed to the electrophysiology (*see* **Note 12**).

11.3.3.2. Obtaining a Gigaohm Seal and Perforation

1. Place the patch pipette in the electrode holder.
2. Apply a very small amount of positive air pressure to the patch pipette via the side-port of the electrode holder (*see* **Note 13**).
3. Immerse the patch pipette into the bath and zero the offset potential (*see* **Note 14**) and Apply 1 mV test pulses from the 0 mV holding potential.
4. Select a single cell that does not make connections with neighbouring cells (*see* **Note 15**).
5. Position the patch pipette against the cell and apply negative pressure to the patch pipette to obtain a gigaohm (GΩ) seal (*see* **Note 16**).
6. Once a gigaohm seal has been obtained, change the test pulse to 10 mV, set the holding potential (usually −80 to −60 mV), and cancel the pipette capacitance using the amplifier fast capacitance cancellation settings.
7. Electrical access to the cell by perforation is indicated by the appearance of slow capacitance currents. The access resistance (R_a) decreases over time, as more amphotericin pores are formed in the membrane enclosed by the patch pipette. This can be observed by the change in the shape of the capacitance transients: from low amplitude that decays slowly (long time constant) to larger amplitude with a short decay time (**Fig. 11.2** *see also* **Note 17**). Monitor access resistance using the whole-cell (slow) capacitance cancellation settings on the amplifier and update the settings every minute. Once the resistance is below an acceptable value (e.g. <10 MΩ), series-resistance compensation circuitry may be engaged if required, and the experiment can commence. Access resistances that are 3–4 times the pipette resistance

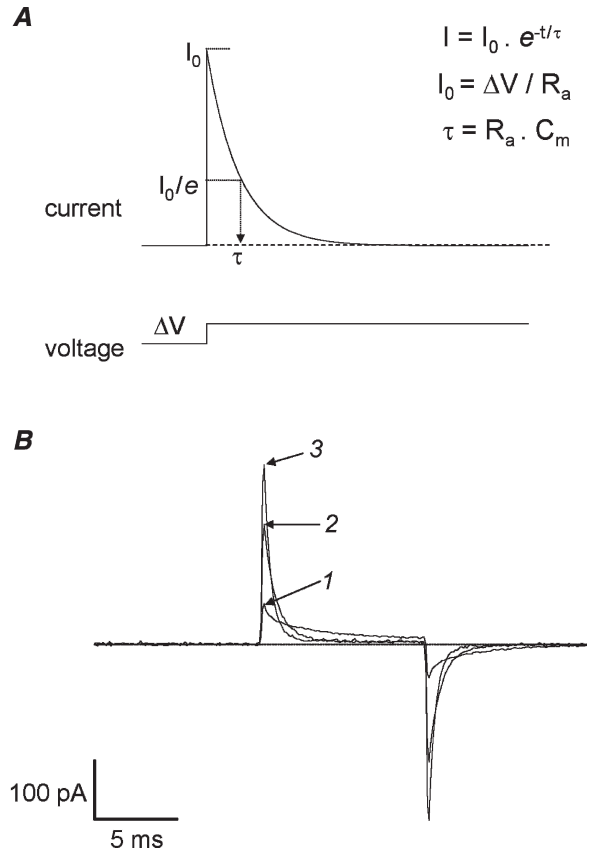

Fig. 11.2. (**A**) Representation of a transient capacitance current evoked by a voltage step. (**B**) Capacitance currents recorded from a HEK293 cell undergoing perforation by amphotericin B in the patch pipette. Representative currents at the start of the recording (*1*), after 100 s (*2*), and after 200 s (*3*). The decrease in the access resistance is indicated by the increase in the amplitude of the current and the rate of decay (shorter time constant).

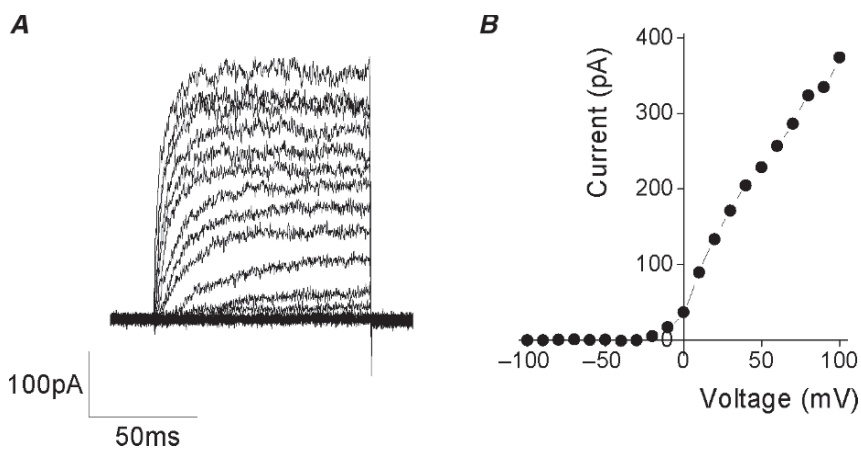

Fig. 11.3. Sample whole-cell perforated patch recordings from a HEK293 cell. Following perforation the whole-cell capacitance was cancelled and 80% series-resistance compensation was applied. (**A**) Representative currents were evoked by 100 ms pulses from −100 to +100 mV from a holding potential of −80 mV. The current–voltage relationship is shown in (**B**).

are typically obtained. A sample recording under these conditions is shown in **Fig. 11.3**.

11.4. Notes

1. Although filamented capillaries can be used, the lack of a filament in the capillary glass gives better "tipping" partitioning between amphotericin-containing and amphotericin-free solutions (*see* **Subheading 11.3.3.1**).
2. The pipette solution is designed to closely match the intracellular concentrations of K^+, Na^+, and Cl^-, which permeate amphotericin B pores. Whilst SO_4^{2-} is used here, other suitable impermeable counteranions, such as aspartate, may also be used. The gradual exchange of ions between cytosol and patch pipette to reach the Donnan equilibrium results in a voltage drift over time.
3. Cells can be plated onto glass cover slips if preferred and coating agents (e.g. poly-D-lysine) used if poorly adherent.
4. Do not attempt to mix with the pipette tip as the amphotericin B dissolved in DMSO will stick to the plastic tip. Flick the microtube to gather the contents to the bottom, dispense the DMSO along the side of the tube, and then sonicate.
5. The use of a glass container is recommended as the amphotericin–DMSO sticks to plastic.
6. This will appear as an apparently insoluble yellow "slug" at the bottom of the flask. Dissolve the "slug" by repeated pipetting with a 1 ml pipette (e.g. Gilson P1000).
7. The foil prevents destruction of the antibiotic by light.
8. Patch pipettes should be prepared as if they were to be used in standard whole-cell recording with relatively low resistances to reduce the membrane charging time constant and series-resistance errors. It is critical that patch pipettes are clean and polished to ensure optimal seal formation in as short a time possible, and it is worthwhile optimising the cell preparation and patch pipette fabrication.
9. The presence of amphotericin B in the pipette solution can prevent seal formation, and likewise any amphotericin B that leaks from the patch pipette near the cell can damage the membrane. By "tipping" the pipette tip with antibiotic-free solution, optimal seal formation should take place before the amphotericin reaches the tip where it invades the membrane. How much antibiotic-free solution should be loaded into the patch pipette tip (i.e. how long the patch pipette should

be held in the drop of antibiotic-free solution) requires optimising and depends on how quickly gigaohm seals are formed. The more a patch pipette is "tipped", the longer it takes for the amphotericin to arrive at the aperture and perforate the membrane. The antibiotic-free solution should not go beyond 0.5 mm from the aperture.

10. Amphotericin can readily come out of the solution or stick to the sides of the container. This is remedied by mixing by swirling the container prior to use.
11. This approach is preferred to using a conventional patch pipette filling syringe containing the amphotericin pipette solution as it enables the amphotericin to be mixed immediately prior to use, and avoids exposure to light, plastic, and filtering.
12. With the use of unfilamented capillary glass, there is a tendency for air bubbles to form at the interface between the two solutions. Dispense the amphotericin solution as close to the antibiotic-free "tip" as possible, and flick the pipette gently to remove bubbles from the taper.
13. This is usually done via tubing that is connected to a 1-ml syringe. Positive pressure is applied by pushing the plunger to the equivalent of 0.1 ml. The purpose is to maintain an outward flow of clean solution that prevents contamination from the bath solution and tissue. However, the pressure needs to be kept to a minimum so that the amphotericin-containing solution is not expelled over the tissue prior to seal formation.
14. The solutions described here give a junction potential of approximately +10 mV. The calculated or measured junction potential can be accounted for, prior to seal formation. This can be done automatically if the amplifier is computer driven, or manually by "zeroing" to the junction potential using the DC-offset with the amplifier in current clamp mode.
15. Contact between HEK293 cells results in electrical coupling via gap junctions, which will prevent single cell recording. Membrane currents from the additional cells will be conducted via gap junctions. Evidence for this can be observed from the whole-cell capacitance where additional components with a longer time constant (and therefore through higher access resistance) are observed.
16. Suction can be applied using a 1 ml syringe (*see* **Note 13**). Sealing can be assisted using negative holding potentials, but determining the optimum sealing procedure using the cells, patch pipettes, and solutions without amphotericin is strongly recommended.

17. The time-course of the capacitance transient follows the exponential function $I = I_0 e^{-t/\tau}$, where I_0 is the instantaneous current amplitude and τ is the time constant. I_0 follows Ohms Law, $I_0 = V/R_a$, where V is the amplitude of the test pulse and R_a is the access resistance (*see* **Fig. 11.2**). The time constant τ equates to $R_a C_m$, where C_m is the membrane capacitance. As R_a decreases with increased perforation, I_0 increases and τ decreases.

Acknowledgments

I thank Dr. Peter Proks (Oxford) and Dr. John Linley (Leeds) for helpful discussion regarding this technique, and the Welcome Trust and BBSRC for financial support.

References

1. Horn R. and Marty A. (1988) Muscarinic activation of ionic currents measured by a new whole-cell recording method. *J. Gen. Physiol.* **2**, 145–59.
2. Rae J., Cooper K., Gates P., and Watsky M. (1991) Low access resistance perforated patch recordings using amphotericin B. *J. Neurosci. Methods* **37**, 15–26.
3. Horn R. (1991) Diffusion of nystatin in plasma membrane is inhibited by a glass-membrane seal. *Biophys. J.* **60**, 329–33.
4. Toye A.A., Lippiat J.D., Proks P., Shimomura K., Bentley L., et al. (2005) A genetic and physiological study of impaired glucose homeostasis control in C57BL/6J mice. *Diabetologia* **48**, 675–86.
5. Tsuboi T., Lippiat J.D., Ashcroft F.M., and Rutter GA. (2004) ATP-dependent interaction of the cytosolic domains of the inwardly rectifying K^+ channel Kir6.2 revealed by fluorescence resonance energy transfer. *Proc. Natl Acad. Sci. USA* **101**, 76–81.

Chapter 12

Recording the Activity of ATP-Sensitive K^+ Channels in Open-Cell Cell-Attached Configuration

Andrei I. Tarasov

Summary

The functional activity of ion channels is affected by their local environment, and for certain types of channels this local effect is critical. This chapter describes a method of recording the activity of ATP-sensitive K^+ channels, expressed on the plasma membrane of pancreatic β-cells, without destroying the β-cell architecture. In the open-cell cell-attached patch-clamp configuration, ligands and effectors of these metabolism-dependent channels are delivered to their cytoplasmic side via pores in the plasma membrane produced by bacterial toxins.

Key words: ATP-sensitive K^+ channels, Patch-clamp, Open-cell cell-attached configuration, Membrane permeabilisation, Bacterial toxins.

12.1. Introduction

Permeabilisation of cell plasma membrane is widely used in cell biology to manipulate the concentrations of low-molecular weight (low-MW) soluble cytoplasmic components, without losing high-MW or non-soluble fraction. When applied to intact cells, this approach makes it possible to explore intracellular processes in what is believed to resemble physiological conditions. Axiomatically, permeabilisation of plasma membrane dissipates the energy stored in the form of the gradient of membrane potential. However, it does not have a direct effect on many membrane-bound phenomena, organelle homeostasis and vesicle dynamics.

Several methodologies of cell membrane permeabilisation have been developed. Early works used electroporation ("leaky cells"

Jonathan D. Lippiat (ed.), *Methods in Molecular Biology, Potassium Channels, vol. 491*

Book doi: 10.1007/978-1-59745-526-8

(1)) and mechanical shearing ("cell cracking" *(2)*). For single-cell studies, mechanical puncturing of the membrane is possible; however it is time-demanding and may cause systematic errors. The majority of authors therefore use chemical (saponin, digitonin) or biological (bacterial pore-forming toxins) agents for membrane permeabilisation. We have found that the latter approach works better for single-cell studies on pancreatic β-cells.

Bacterial toxin monomers bind to cell membrane, oligomerise and form pores, thus converting the membrane into a 'molecular sieve'. The toxins we deal with in this chapter do not interact with intracellular proteins or organelles and form pores strictly in the plasma membrane: the monomers of *S. aureus* α-toxin can not pass through the pores that they form and streptolysin-O from *S. pyogenes* binds specifically to cholesterol *(3)*. The pore size determines the selectivity of the permeabilised membrane and, together with the surface density of the pores, also determines the diffusion rates through the membrane. Thus, the cut-off molecular weight is determined only by the nature of the pore-forming toxin (**Table 12.1**) and does not depend on its concentration or experimental conditions. The experimental conditions, however, can affect the number of pores that are formed in the membrane and thereby the rate of the diffusion through the "molecular sieve". Fixed pore size and plasma membrane targeting help to interpret the experimental data unequivocally, minimising the artefacts related to diffusion or interaction with organelles. The disadvantages of pore-forming toxins are their price and the complexity of the concentration–effect relationship. The toxins are less stable in solutions than chemical detergents and quickly lose their activity at room temperature. The activity of toxins depends on the purity of the protein preparation and thus may vary from batch to batch. It is also important to remember that toxins introduce certain biological hazards.

Cell membrane permeabilisation can be applied in combination with the patch-clamp technique to study the function of ion channels and the kinetics of exocytosis in open-cell cell-attached patch-clamp configuration (henceforth "open-cell"). In essence, open-cell is a modified version of inside-out excised patch

Table 12.1
Comparative characteristics of bacterial protein toxins used as tools for cell permeabilisation

Toxin	Species	Working concentration	Pore radius (nM)	Cut-off MW (kDa)	Open-cell recording
Streptolysin-O	*S. pyogenes*	50–100 HU/ml	~30	150	**Ref.** *16*
α-Toxin	*S. aureus*	10–30 μg/ml	~1.5	3	**Ref.** *17*

configuration ("inside-out"), with the difference that, instead of the patch being excised from the cell surface, the cell membrane is rendered permeable to give direct access to the cytoplasmic side. As compared to inside-out patch, using open-cell configuration does complicate the experiments technically; the intactness of cellular architecture and local interactions however, can be critical for the function of ion channels and exocytotic machinery.

This chapter describes the protocol that we use to study the function of ATP-sensitive K^+ (K_{ATP}) channels in pancreatic β-cells, in open-cell patch-clamp configuration. Adenine nucleotides, the principal ligands of the K_{ATP} channel, block it when binding to its pore-forming subunit, Kir6.2. Their Mg^{2+}-dependent interaction with the regulatory subunit of the channel, SUR1, decreases the potency of the block. The levels of the two key metabolites, ATP and ADP, are thereby coupled to the electric potential of the β-cell plasma membrane. Binding of adenine nucleotides to the channel is affected by phosphocreatine and adenosine monophosphate, putatively via reactions catalysed by "local" creatine and adenylate kinases (*see* **ref.** *4* for review). In addition, membrane phosphatidylinositol phosphates and soluble esters of fatty acids upregulate the channel activity when binding to Kir6.2. The complexity of the metabolic regulation of the K_{ATP} channel as well as the effect of the "local" compartment make the use of open-cell configuration advantageous for its study.

In our experiments, we used bacterial toxins, *S. aureus* α-toxin and *S. pyogenes* streptolysin-O (SLO), to permeabilise the cells. α-Toxin is a better choice to study the effect of ligands with MW of ~1 kDa (**Table 12.1**): in our experience, cells permeabilised with α-toxin maintained morphology and had good diffusion rates for adenine nucleotides. However, bearing in mind the other applications of open-cell patch-clamp, we have also described the features of the protocol based on the use of SLO where they are different from that of α-toxin.

12.2. Materials

12.2.1. Reagents and Buffers

1. β-Cell isolation solution: 137 mM NaCl, 5.6 mM KCl, 1.2 mM $MgCl_2$, 2.56 mM $CaCl_2$, 1.2 mM NaH_2PO_4, 4.2 mM $NaHCO_3$, 10 mM HEPES (pH 7.4 with NaOH), 3 mM glucose, 100 units/ml penicillin, 100 μg/ml streptomycin; 0.5% BSA is added ex tempore.
2. 0.2 mg/ml Liberase RI (Roche) dissolved in albumin-free β-cell isolation solution.

3. Ca^{2+}-free solution: 137 mM NaCl, 5.6 mM KCl, 1.2 mM $MgCl_2$, 1.2 mM NaH_2PO_4, 4.2 mM $NaHCO_3$, 1 mM EGTA, 10 mM HEPES (pH 7.4 with NaOH), 3 mM glucose.
4. β-Cells are cultured in RPMI-1640 medium containing 11 mM glucose, 4 mM glutamine, 10% foetal bovine serum, 100 units/ml penicillin, 100 µg/ml streptomycin, at 37°C, 5% CO_2, absolute humidity.
5. Extracellular solution used in patch-clamp experiments: 137 mM NaCl, 5.6 mM KCl, 10 mM HEPES (pH 7.4 with NaOH), 1.1 mM $MgCl_2$, 2.6 mM $CaCl_2$, 3 mM glucose.
6. Intracellular solution: 30 mM KCl, 110 mM K-aspartate (*see* **Note 3**), 0.084 mM $CaCl_2$, 2 mM $MgSO_4$ (*see* **Note 7**), 0.5 mM EGTA, 10 mM HEPES (pH 7.2 with KOH), and MgATP as indicated.
7. Pipette solution: 140 mM KCl, 1.1 mM $MgCl_2$, 2.6 mM $CaCl_2$, 10 mM HEPES (pH 7.2 with KOH).

12.2.2. Dyes

Dyes are used to indicate cell membrane permeabilisation.

1. Propidium iodide (PI) is dissolved in intracellular solution to the stock concentration of 1 g/l (1.5 mM). Working solution is prepared by 1:300 dilution (5 µM).
2. Fluorescein diacetate (FDA) is dissolved in Me2SO (0.5 g/l = 1.2 mM) and used in 1:1,000 dilution (1.2 µM).
3. Trypan blue is purchased as 4 g/l solution and used in 1:1 dilution.

12.2.3. Toxins

The activities of the toxins vary from batch to batch; therefore they should be tested prior to experiments (*see* **Subheading 12.3.1**).

1. The α-toxin that we use in our experiments is a kind gift from Prof. Hagan Bayley, University of Oxford. Efficient β-cell permeabilisation has been reported with commercial preparations of α-toxin from PhPlate Stockholm *(5)* or Sigma *(6)*.
2. SLO is purchased from Sigma.

12.2.4. Patch-Clamp Apparatus

1. Grounded vibration-isolation table with Faraday cage (TMC).
2. Inverted microscope with ×10 and ×40 objectives (Nikon).
3. 3D micromanipulator, preferably electromechanical or piezoelectric (Luigs and Neumann).
4. Low-noise patch-clamp amplifier (HEKA or equivalent from Molecular Devices) with headstage, acquisition interface and software. Noise levels of connected and grounded system should not exceed 250 fA, with 1 kHz filtering.
5. Oscilloscope (Gould), connected in parallel to the Current Monitor of the amplifier. The recording times for open-cell

experiments may last 1 h, therefore monitoring the signal on two timescales is useful.

6. Peristaltic pump (Gilson).
7. Perfusion system can be easily manufactured from plastic tubing and syringes, and a 200 µl pipette tip can be used to join multiple perfusion channels into a single in-flow tube. The in-flow is driven by gravity; the rate of perfusion is in the range 0.8–2.0 ml/min. Both in-flow and out-flow tubes are attached to the microscope table with magnets. Optionally, coarse micromanipulators (Narishige) can be used.
8. Reference electrode (Harvard Apparatus).
9. The patch-clamp electrodes are pulled from thin-walled borosilicate filamented glass capillaries (Harvard Apparatus), fire-polished and coated with Sylgard to reduce the noise. The resistance of the electrodes filled with pipette solution and immersed into the extracellular solution is in the range 3–5 MΩ.
10. Optional. Four-pole Bessel filter (cut-off frequency 1–10 kHz, Frequency Devices) can be connected serially between the current monitor of the amplifier and the current channel of the acquisition interface.
11. Optional. Microinjector (Eppendorf or equivalent from General Valve or Narishige). The key requirement for the microinjector is vibration isolation; the injectable volume of toxin (~1 µl) does not, in any way, affect the precision.

12.3. Methods

12.3.1. Testing of the Toxin Activity

1. α-Toxin is:
   (a) Dissolved to a concentration of 500 µg/ml in the intracellular solution.
   (b) Activity of α-toxin is tested. β-Cells cultured overnight in a 24-well plate are incubated in 200 µl of intracellular solution containing 0, 0.17, 1.67, 5, 16.67, 41.67 and 83.33 µg/ml of α-toxin for 10 min at the temperature used in the patch-clamp experiments (22–25°C).
   (c) The toxin is removed; the cells are washed with 1 ml of intracellular solution, bathed in 200 µl of intracellular solution, stained with 200 µl of trypan blue solution and incubated for another 2 min. The numbers of "viable" (refractile, non-stained) and "non-viable" (inflated, stained) cells are counted under an inverted microscope (×10 magnification) and the percentage of permeabilised cells is calculated:

$$\text{Permeabilised cells}(\%) = \frac{\text{number of stained cells}}{\text{total number of cells}} \times 100\% \quad (12.1)$$

(d) The viability is plotted vs. the α-toxin concentration (**Fig. 12.1**, open circles, top axis), and the working concentration of the toxin is selected as roughly the one producing permeabilisation of 50% cells (13 µg/ml for the case represented in **Fig. 12.1**). *See* **Note 2** for discussion.

(e) The α-toxin is diluted to 20-fold of working concentration (i.e. to 260 µg/ml for the case given in **Fig. 12.1**), assuming an addition of 10 µl of the toxin solution into 200 µl of the bath solution during the experiment (*see* **Subheading 12.3.3**). The toxin is aliquoted in 100 µl volumes into plastic Eppendorf tubes and stored at −80°C.

2. Streptolysin-O (SLO) is:

(a) Dissolved to a concentration of 6,250 HU/ml in the intracellular solution.

(b) Activated by adding 0.14 ml of 1-M dithiothreitol into 4 ml of 6,250 HU/ml SLO (*see* **Note 5**) and incubating for 2 h at 37°C. SLO loses its activity when exposed to atmospheric oxygen and reduction with dithiotreitol helps to reactivate it *(7)*. This step is not required for α-toxin.

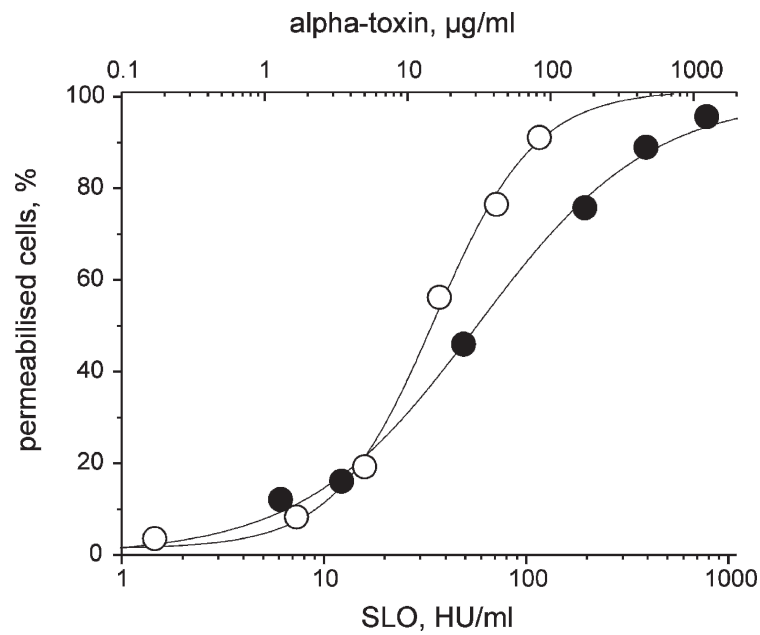

Fig. 12.1. Typical concentration–effect curves measured to determine the working concentrations of SLO (*solid circles*) and α-toxin (*open circles*). β-Cells were incubated with different concentrations of the toxins for 10 min at room temperature, and stained with trypan blue solution. The percentage of permeabilised cells is counted for every toxin concentration.

(c) The activity of SLO is tested in a similar way to that of α-toxin. SLO concentrations tested are 6, 12.2, 49, 195, 391 and 781 HU/ml.

(d) The working concentration of SLO is 57 HU/ml for the case represented in **Fig. 12.1** (solid circles, bottom axis).

(e) SLO is diluted to 1,200 HU/ml (for the case given in **Fig. 12.1**), aliquoted in 100 µl volumes into plastic Eppendorf tubes and stored at −80°C.

3. After thawing, the toxin aliquot should be kept on ice (+4°C) and used within the day. Re-freezing reduces the activity of the toxins.

12.3.2. β-Cell Isolation and Culture

1. All procedures are carried out under sterile conditions and (apart from digestion and washing in RPMI-1640) using ice-cold solutions.
2. Mice are killed by cervical dislocation.
3. The common bile duct is ligated at its exit to the duodenum and injected at its exit from the liver, with 2 ml of 0.2-mg/ml liberase solution using a syringe and a 30 G needle *(8)*.
4. The infused pancreata is then removed using watchmaker's forceps and incubated for 20 min in 10 ml of 0.2 mg/ml liberase solution, at 37°C. The digest is then washed three times in the isolation solution by centrifugation at 300×*g* for 1 min.
5. Islets of Langerhans are observed under a dissection microscope and hand-picked from the precipitate using 100-µl automatic pipette, washed in the dissociation solution, and gently aspirated 5–10 times in 2 ml of the dissociation solution with a fire-polished glass Pasteur pipette.
6. The dissociated islet cells are washed twice in RPMI-1640 and plated on 35-mm tissue-culture-treated Petri dishes or in 24-well plates. Alternatively, the cells can be cultured on glass coverslips.
7. β-Cells from dissociated islets are used for experiments between the second and fifth days in culture.

12.3.3. Open-Cell Cell-Attached Patch-Clamp Configuration

1. The pre-cultured β-cells are bathed in the extracellular solution (3 mM glucose) for 15–30 min before patching. This reduces the variation of the K_{ATP} channel activity observed before the permeabilisation, in cell-attached mode.
2. (Optional), FDA (0.5 mg/l) can be added to monitor the membrane permeabilisation (*see* **Subheading 12.3.4**). Within 1 min of addition and mixing the viable cells acquire bright green cytoplasmic fluorescence.
3. The patch-clamp electrode is filled with the pipette solution, introduced into the bath, and the giga-seal is made.

4. The volume of the bath solution is set to 100–200 µl by using a pre-designed perfusion chamber or a perspex insert fitting into a 35-mm Petri dish. Given the number of β-cells on each dish of around 100 and the mean osmotically active volume of a β-cell of 0.8 pl (at 300 mosmol/l) we get the total osmotically active volume of the β-cells on the dish of 80 nl. This is less than 0.1% of the total volume of the bath solution, which is sufficient for an efficient "concentration clamp".
5. In the cell-attached mode, at the pipette potential V_p = 0 mV ($V_m \approx$ –60 to –70 mV), single openings of K_{ATP} channels can be observed (**Fig. 12.2**). The extracellular solution is then replaced by the intracellular solution containing 100 µM MgATP (*see* **Note 8**), and V_m is set to –60 mV (V_p = 60 mV) to restore the gradient of electrochemical potential cancelled by symmetrical [K^+], [Na^+] and [Cl^-].
6. (Optional) Propidium iodide (PI; 3.3 mg/l) can be added into the bath solution either at this stage, or after the addition of

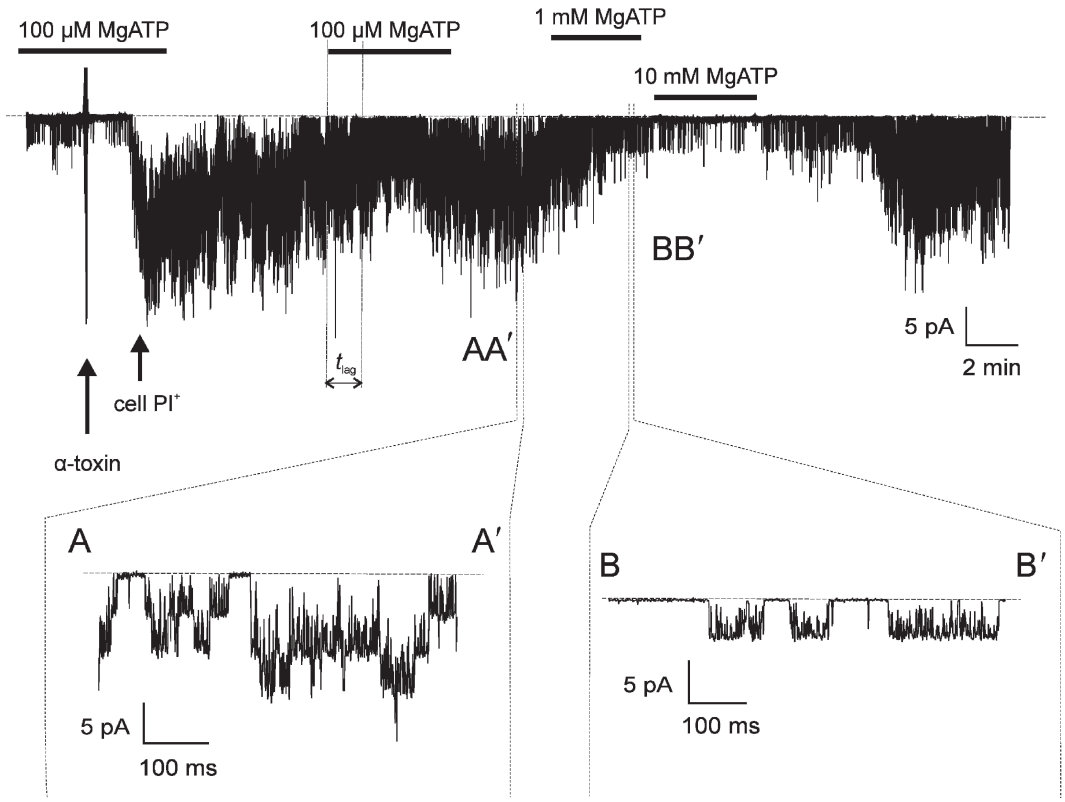

Fig. 12.2. Representative recording of the K_{ATP} channel activity in open-cell configuration. Addition of ligand (MgATP) is indicated by *horizontal bars*. Time points of addition of α-toxin and acquirement of PI-staining by the cell nucleus are indicated with *arrows*. The time required for diffusion of 100 µM MgATP into the cell is marked as t_{lag}. Parts of the trace marked as *AA′* and *BB′* are displayed on an expanded timescale in the *insets* below.

the toxin, to monitor the permeabilisation. We recommend adding the dye using an automatic pipette or injection system. Please note that frequent exposure to PI may result in non-specific staining of glass or plastic surfaces.

7. The toxin is then introduced into the solution. The perfusion is stopped, and 5–10 µl of the toxin is added into the bath solution with a 10 µl automatic pipette (Gilson), as a droplet, close to the patch electrode. The addition introduces a short noise transient into the recording (*see* **Fig. 12.2**); however it very rarely damages the seal. For other methods of adding toxin into the solution *see* **Note 1** and **Note 4**.
8. The toxin is left to diffuse, bind to the cell membrane and oligomerise, and within 1–2 min the first signs of permeabilisation can be observed. The activity of K_{ATP} channels may decrease, possibly due to the complete cancellation of $[Na^+]$ and $[K^+]$ gradients, which would reduce the utilisation of ATP by the sodium pump *(9)*, whilst the baseline shifts in a more positive direction and becomes less "noisy" (*see* **Note 6**).
9. The ensuing increase of PI (decrease of FDA) fluorescence and gradual restoration and increase of the K_{ATP} activity, due to the ATP wash-out, confirm the fact of permeabilisation (**Fig. 12.2**). If permeabilisation-related effects are not observed, one more 5 µl droplet of the toxin should be added to the solution, etc., until the cell is clearly permeabilised. Likewise, more of the toxin should be added if the onset of the permeabilisation is too slow.
10. 3–10 min after the permeabilisation, when the K_{ATP} activity has reached a stable level, the perfusion of the bath solution is re-started and the channel activity can be recorded in response to various agents. See however **Note 9**.

12.3.4. Visualisation of Cell Permeabilisation

The fluorescent dyes propidium iodide (PI) and fluorescein diacetate (FDA) are used to visualise the permeabilisation. The bright-field dye trypan blue is used to assay the toxin activity. Counting the cells by eye is technically easier in the bright field; therefore non-fluorescent staining has an advantage.

1. PI, a fluorescent DNA intercalant (λ_{ex} = 535 nm, λ_{em} = 615 nm, MW = 668; compare with 507 of ATP), is membrane-impermeant but does permeate through α-toxin pores. Upon the permeabilisation of the plasma membrane, the cell acquires nuclear red fluorescence, while the cell cytoplasm remains PI-negative. PI is dissolved in the intracellular solution to the working concentration of 3.3 mg/l either before application of the toxin or simultaneously or shortly after.
2. FDA is membrane permeant but in the cytoplasm it gets hydrolysed into non-permeant fluorescein (λ_{ex} = 494 nm,

λ_{em} = 517 nm, MW = 332). The working concentration for FDA is 0.5 mg/l. Intensive leakage of fluorescein through the toxin pores can also be taken as an indication of permeabilisation. One should bear in mind however, that fluorescein does (slightly) leak through the intact membrane and has a high rate of photobleaching.

3. Both PI and FDA have broad emission and excitation spectra, which makes it possible to visualise both of them simultaneously, using the same filter set. Combining a 470 ± 20 nm excitation filter, a 520 ± 20 nm emission filter and a 510 nm dichroic mirror allows one to observe bright green fluorescein emission and weaker but distinct emission of PI in the orange range of the spectrum.

12.3.5. Recording and Analysing the Ion Channel Activity in Open-Cell Configuration

1. The main driving force of the mass-exchange through the permeabilised membrane, in the open-cell experiments, is likely to be the gradient of chemical potential rather than the hydrostatic pressure.
2. A short lag-period (<60 s for experiments using α-toxin but longer in the case of SLO, *see* **Note 10**) is always observed between addition of the ligand (MgATP) and changes in the channel activity (t_{lag} in **Fig. 12.2**). The over-extension of the lag-period reflects insufficient permeabilisation, the lack of the lag-period means the patch is excised from the cell surface.
3. In contrast to what is observed in the inside-out patches *(10)*, the run-down of the K_{ATP} channel is quite small, in the open-cell configuration. The control (ligand-free) solution can therefore be applied only at the start and at the end of the experiment.
4. The duration of one open-cell experiment, which can be up to 1 h depends on the number of conditions tested. This sets limits for the acquisition rate. The acquisition software should be able to support long segments of continuous acquisition, with or without repeated stimulation, with on-line input of labels and comments. pClamp (Molecular Devices) is particularly recommended, Pulse (HEKA) requires insertion of a continuous segment and pre-loading of the solution database. Monitoring the recording on two timescales – "fast" for single-channel events and "slow" for the time-course of the channel activity – is a good idea.
5. Analysis of the continuous data assumes idealising the trace by counting the channel opening and closing events and further deriving the channel characteristics (Po, rate constants, etc.), in exactly the same way as is done for recordings from the inside-out configuration. The data corresponding to the diffusion of the ligand (t_{lag} in **Fig. 12.2**) should be excluded from analysis.

12.4 Notes

1. An efficient way to add the toxin to the solution is by dropping an aliquot with an automatic pipette. Adding via a perfusion system may produce a more uniform permeabilisation pattern due to better mixing but is much less cost-effective. Targeted addition of the toxin via the microinjection capillary minimises the amount of toxin needed for cell permeabilisation. However, it is technically more demanding as the capillary needs to be re-filled and re-positioned before each permeabilisation. The toxin is loaded into the injection pipette and injected into the solution, close to the patched cell, in a manner similar to that described above for the automatic pipette. The addition of the toxin can be visualised by pre-mixing it with 0.5 μg/ml rhodamine *(11)*. Keeping the toxin within the capillary (at room temperature) for long periods of time will result in a decrease of its activity. It is advisable not to reduce the total volume of the added toxin solution to below 1 μl.
2. Toxin and PI solutions do not mix well when injected or pipetted into the bath solution. Their local concentration in the area of addition will be higher than the average working concentration. The toxin concentration is therefore chosen that produces half-maximal permeabilisation of cells during the toxin testing.
3. Glutamate is frequently used as a substitute for chloride in the intracellular solution. However given its reported role in insulin exocytosis *(12)* we use aspartate. The rationale is to mimic the effect of intracellular anions and keep chloride at a low ("intracellular") level.
4. Oligomerisation of SLO monomers does not occur in hypothermic conditions *(7)*, binding to the membrane however does occur on ice (+4°C). In principle, this effect can be used to trigger the process of pore formation at will, however we have never attempted to do this. Millimolar Ca^{2+} causes resealing of SLO pores, which is used to deliver macromolecules into the cells by reversible permeabilisation *(13, 14)*. Employing permeabilisation with SLO would not be suitable for studies of Ca^{2+}-dependent effects. We are not aware of any inhibitory effects of low temperatures and Ca^{2+} on the formation and stability of α-toxin pores.
5. Concentrations of toxins are frequently given as HU (haemolytic units), μg/ml, or less frequently as IU (international units). HU and IU refer to the activity rather than the concentration. None of the three units would however give absolute reproducibility and therefore testing every batch of toxin prior to experiments is essential.

6. The process of membrane permeabilisation can be monitored by changes in the baseline noise and the increase of signal-to-noise ratio. The signal current I_s driven by command voltage V_p depends, in cell-attached mode (**Fig. 12.3a**, on the pipette resistance (R_{pip}), the resistance of the patch (R_{patch}), the resistance of the ion channels in the patch (R_{ic}), and the whole-cell resistance of K_{ATP} channels ($R_{whole\text{-}cell}$). An electromotive force E_{cell} produced by local depolarisation of the membrane by high-K^+ pipette solution contributes to the impedance as well *(15)*. Permeabilisation of the membrane (**Fig. 12.3b**) eliminates the two highly-variable effects: it cancels E_{cell} and dramatically reduces $R_{whole\text{-}cell}$. This decreases the noise levels of I_s, in response to V_p.
7. If the seals regularly develop leaks, in open-cell configuration, a reduction of the intracellular [Mg^{2+}] to 1.2 mM may help.
8. The presence of 0.1–3 mM of MgATP in the intracellular solution is critical. It is not recommended to expose the open-cell patch to ATP-free solutions for long periods as it causes run-down of the K_{ATP} channel activity, which is sometimes irreversible. With MgATP in the intracellular solution, the patch can maintain reasonably stable levels of K_{ATP} activity for several hours.
9. Permeabilisation weakens the attachment of the cell to the bottom of the dish. Lifting the electrode to excise the patch from the membrane of a permeabilised cell frequently results in removal of the whole cell. In this case, the inside-out patch configuration can be established by bringing the electrode tip to the air–water interface.
10. Apart from the gradient of ligand concentration, the duration of the lag-period for perfusion (*see* **Subheading 12.3.5**) depends on the number of pores in the membrane and on the pore size. The latter number is constant for each toxin but the former varies with toxin concentration. However it was difficult to increase the number of pores when using SLO as high concentrations of the toxin had a deleterious effect on the cell and resulted in the loss of the seal.
11. In the voltage-clamp recordings described here (open-cell and inside-out configurations) the membrane potential is taken as equal to $V_m = -V_p$, where V_p is the potential applied to the patch pipette. In the cell-attached configuration, V_m parametrically depends on the whole-cell conductance and $V_m \neq -V_p$.

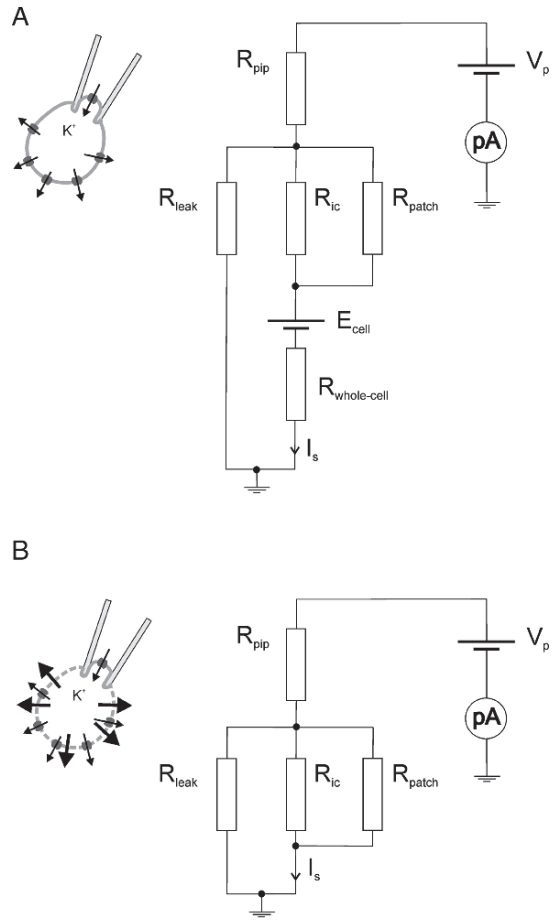

Fig. 12.3. Equivalent electrical circuits for cell-attached **(a)** and open-cell ***(b)*** voltage clamp configurations. V_p applied voltage, I_s "signal" current through the membrane patch, R_{pip} pipette resistance, R_{leak} resistance of the giga0hm seal, R_{patch} resistance of the patch excluding R_{ic} (resistance of the ion channels in the patch), $R_{whole\text{-}cell}$ whole-cell resistance of K_{ATP} channels. The electrogenic activity of the cell would be represented as two equal electromotive forces of opposite polarity connected serially and therefore will have no contribution to the circuit. However, the local depolarisation of the membrane due to high $[K^+]$ in the patch pipette creates an electromotive force E_c that opposes the applied voltage. Metabolism-dependent E_c and $R_{whole\text{-}cell}$ introduce additional noise in cell-attached recording. For open-cell mode (**b**), the permeabilisation of the membrane cancels E_c and reduces $R_{whole\text{-}cell}$ to a negligible value.

Acknowledgments

The author would like to thank Prof. Frances Ashcroft for hosting and being the driving force of the open-cell experiments, and Prof. Hagan Bayley for the gift of the α-toxin.

References

1. Baker, P. F. and Knight, D. E. (1981) Calcium control of exocytosis and endocytosis in bovine adrenal medullary cells. *Philos. Trans. R. Soc. Lond. B Biol. Sci.* **296**, 83–103.
2. Martin, T. F. and Walent, J. H. (1989) A new method for cell permeabilization reveals a cytosolic protein requirement for Ca2+-activated secretion in GH3 pituitary cells. *J. Biol. Chem.* **264**, 10299–10308.
3. Ahnert-Hilger, G., Bhakdi, S., and Gratzl, M. (1985) Minimal requirements for exocytosis. A study using PC 12 cells permeabilized with staphylococcal alpha-toxin. *J. Biol. Chem.* **260**, 12730–12734.
4. Tarasov, A., Dusonchet, J., and Ashcroft, F. (2004) Metabolic regulation of the pancreatic beta-cell ATP-sensitive K+ channel: a pas de deux. *Diabetes* **53**(Suppl. 3), S113–S122.
5. Thore, S., Wuttke, A., and Tengholm, A. (2007) Rapid turnover of phosphatidylinositol-4,5-bisphosphate in insulin-secreting cells mediated by Ca2+ and the ATP-to-ADP ratio. *Diabetes* **56**, 818–826.
6. Bhatt, H. S., Conner, B. P., Prasanna, G., Yorio, T., and Easom, R. A. (2000) Dependence of insulin secretion from permeabilized pancreatic beta-cells on the activation of Ca(2+)/calmodulin-dependent protein kinase II. A re-evaluation of inhibitor studies. *Biochem. Pharmacol.* **60**, 1655–1663.
7. Bhakdi, S., Weller, U., Walev, I., Martin, E., Jonas, D., and Palmer, M. (1993) A guide to the use of pore-forming toxins for controlled permeabilization of cell membranes. *Med. Microbiol. Immunol.* **182**, 167–175.
8. Wollheim, C. B., Meda, P., and Halban, P. A. (1990) Isolation of pancreatic islets and primary culture of the intact microorgans or of dispersed islet cells. *Methods Enzymol.* **192**, 188–223.
9. Ding, W. G. and Kitasato, H. (1997) Suppressing Na+ influx induces an increase in intracellular ATP concentration in mouse pancreatic beta-cells. *Jpn J. Physiol.* **47**, 299–306.
10. Ribalet, B., John, S. A., and Weiss, J. N. (2003) Molecular basis for Kir6.2 channel inhibition by adenine nucleotides. *Biophys. J.* **84**, 266–276.
11. Bienengraeber, M., Alekseev, A. E., Abraham, M. R., Carrasco, A. J., Moreau, C., Vivaudou, M., Dzeja, P. P., and Terzic, A. (2000) ATPase activity of the sulfonylurea receptor: a catalytic function for the KATP channel complex. *FASEB J.* **14**, 1943–1952.
12. Maechler, P. and Wollheim, C. B. (1999) Mitochondrial glutamate acts as a messenger in glucose-induced insulin exocytosis. *Nature* **402**, 685–689.
13. Barry, E. L., Gesek, F. A., and Friedman, P. A. (1993) Introduction of antisense oligonucleotides into cells by permeabilization with streptolysin O. *Biotechniques* **15**, 1016–1018.
14. Spiller, D. G., Giles, R. V., Grzybowski, J., Tidd, D. M., and Clark, R. E. (1998) Improving the intracellular delivery and molecular efficacy of antisense oligonucleotides in chronic myeloid leukemia cells: a comparison of streptolysin-O permeabilization, electroporation, and lipophilic conjugation. *Blood* **91**, 4738–4746.
15. Ogden, D. and Stanfield, P. (1994) Patch-clamp techniques for single channel and whole-cell recording. In *Microelectrode Techniques: The Plymouth Workshop Handbook* (Ogden, D., Ed.). Company of Biologists, Cambridge, pp. 54–78.
16. Tsuura, Y., Ishida, H., Hayashi, S., Sakamoto, K., Horie, M., and Seino, Y. (1994) Nitric oxide opens ATP-sensitive K+ channels through suppression of phosphofructokinase activity and inhibits glucose-induced insulin release in pancreatic beta cells. *J. Gen. Physiol.* **104**, 1079–1098.
17. Tarasov, A. I., Girard, C. A., and Ashcroft, F. M. (2006) ATP sensitivity of the ATP-sensitive K+ channel in intact and permeabilized pancreatic beta-cells. *Diabetes* **55**, 2446–2454.

Chapter 13

Planar Patch Clamp: Advances in Electrophysiology

Andrea Brüggemann, Cecilia Farre, Claudia Haarmann, Ali Haythornthwaite, Mohamed Kreir, Sonja Stoelzle, Michael George, and Niels Fertig

Summary

Ion channels have gained increased interest as therapeutic targets over recent years, since a growing number of human and animal diseases have been attributed to defects in ion channel function. Potassium channels are the largest and most diverse family of ion channels. Pharmaceutical agents such as Glibenclamide, an inhibitor of K_{ATP} channel activity which promotes insulin release, have been successfully sold on the market for many years. So far, only a small group of the known ion channels have been addressed as potential drug targets. The functional testing of drugs on these ion channels has always been the bottleneck in the development of these types of pharmaceutical compounds.

New generations of automated patch clamp screening platforms allow a higher throughput for drug testing and widen this bottleneck. Due to their planar chip design not only is a higher throughput achieved, but new applications have also become possible. One of the advantages of planar patch clamp is the possibility of perfusing the intracellular side of the membrane during a patch clamp experiment in the whole-cell configuration. Furthermore, the extracellular membrane remains accessible for compound application during the experiment.

Internal perfusion can be used not only for patch clamp experiments with cell membranes, but also for those with artificial lipid bilayers. In this chapter we describe how internal perfusion can be applied to potassium channels expressed in Jurkat cells, and to Gramicidin channels reconstituted in a lipid bilayer.

Key words: Ion channel, Potassium channel, Gramicidin, Planar patch clamp, Automated electrophysiology, Internal perfusion, Primary cells, Port-a-Patch.

13.1. Introduction

Ion channels are membrane proteins that act as gated pores for the movement of ions across cell membranes. They play an essential role in the physiology and pathophysiology of cells in the human body. Consequently, ion channels are important targets for the

Jonathan D. Lippiat (ed.), *Methods in Molecular Biology, Potassium Channels, vol. 491*

Book doi: 10.1007/978-1-59745-526-8

pharmaceutical industry, as well as for academic research, since their dysfunction is directly or indirectly involved in many severe disorders such as cardiac arrhythmia, diabetes, cancer, epilepsy, chronic pain, cystic fibrosis, and hypertension *(1)*.

The patch clamp technique developed by Erwin Neher and Bert Sakmann in the late seventies (Nobel Prize in Medicine 1991) is the gold standard for ion channel analysis *(2)*. A glass microelectrode is pressed against the cell surface and the ionic currents passing through the enclosed ion channels are measured in the "on-cell" configuration (*see* **Fig. 13.1**).

By applying further suction, the patch of membrane covering the pipette tip can be ruptured, which results in direct access to the cell's interior. This, so-called "whole-cell" configuration, allows voltage-control of the entire cellular membrane. The exchange of the external solution in this configuration is straightforward. The exchange of the internal solution, although possible, is quite tedious because it has to be accomplished through the pipette.

An easier alternative for exchanging the solution on the internal side of the cell membrane is given in the "inside-out" configuration. This configuration can be obtained by a quick retraction of the pipette from the cell membrane as shown in **Fig. 13.1**. A small membrane patch adheres to the tip of the pipette so that the inside of the membrane is now facing the bath solution. The bath solution can then be easily exchanged. The drawbacks of

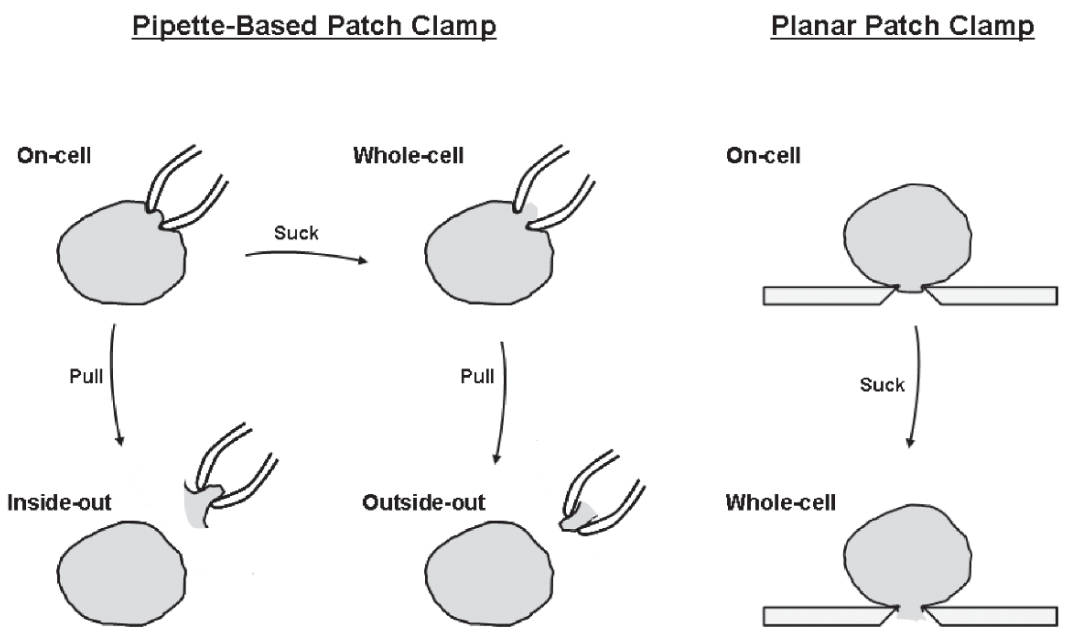

Fig. 13.1. Comparison of the different patch clamp configurations: between pipette-based and planar patch clamp (adapted from **ref.** *9*).

this method are that the external side of the membrane is now difficult to access, and that the number of channels remaining in the membrane patch is often low.

Figure 13.1 shows a comparison between the different patch clamp arrangements between pipette-based and planar patch clamp. The planar patch clamp technique allows only two configurations, "on-cell" and "whole-cell". However, because of the use of a planar chip substrate, the internal solution can be exchanged more easily. A few precautions must be taken into account, which will be discussed in this chapter.

13.2. Materials

13.2.1. Cell Culture for Planar Patch Clamp

1. Cell lines such as HEK 293, CHO, LTK, RBL, NIH 3T3 and Jurkat are typically used.
2. Neuroblastoma cell lines such as SHSY5Y, IMR 32 and NG108 have also been used with a high success rate for seal formation.
3. Primary cells such as Human Erythrocytes, human T-Lymphocytes, human Synoviocytes, human saphenous vein cells, human neutrophils, rat DRG neurons, DRG satellite cells, have also been used successfully.
4. Typical cell media used (PAA Laboratories, Linz Austria):
   (a) DMEM/Ham's F12 with L-Glutamine + 10% FCS.
   (b) RPMI 1640 with L-Glutamine + 10% FCS.
   (c) MEM with Hanks' salts with L-Glutamine + 10% FCS.

13.2.2. Cell Harvesting for Planar Patch Clamp

1. Washing buffer: 1× PBS without Ca^{2+} and Mg^{2+} (PAA Laboratories, Linz Austria).
2. Detachment buffer (PAA Laboratories, Linz Austria): 1× Trypsin–EDTA (1:250). Accutase or AccuMax can also be used (*see* **Note 1**).

13.2.3. Planar Patch Clamp Using the Port-a-Patch

1. Port-a-Patch (Nanion Technologies, Munich, Germany).
2. PatchControl software (Nanion Technologies, Munich, Germany).
3. Patch Clamp Amplifier: EPC10 (HEKA, Lambrecht, Germany).
4. Acquisition software: PatchMaster (HEKA, Lambrecht, Germany).
5. Borosilicate Patch Clamp Chips (Ø ~ 1 µm): NPC-1 (Nanion Technologies, Munich, Germany).
6. Internal K^+ buffer: 60-mM KF, 50-mM KCl, 10-mM NaCl, 2-mM $MgCl_2$, 20-mM EGTA, 10-mM Hepes, pH 7.2 (sterile filtered).

7. Internal Cs^+ buffer: 60-mM CsF, 50-mM CsCl, 10-mM NaCl, 2-mM $MgCl_2$, 20-mM EGTA, 10-mM Hepes, pH 7.2 (sterile filtered).
8. External buffer: 140-mM NaOH, 4-mM KCl, 2-mM $CaCl_2$, 1-mM $MgCl_2$, 10-mM Hepes, pH 7.4 (sterile filtered).

13.2.4. Preparation of Giant Unilamellar Vesicles

1. VesiclePrepPro (Nanion Technologies, Munich, Germany).
2. VesicleControl software (Nanion Technologies, Munich, Germany).
3. Indium Tin Oxide (ITO)-coated glass chamber (Nanion Technologies, Munich, Germany).
4. 1,2-Diphytanoyl-sn-Glycero-3-Phosphocholine (DPhPC) (Avanti polar lipids, Alabaster, AL).
5. Lipid solution: 5-mM DPhPC, 10% Cholesterol dissolved in Chloroform.

13.2.5. Planar Lipid Bilayer Formation

1. Port-a-Patch (Nanion Technologies, Munich, Germany).
2. PatchControl software (Nanion Technologies, Munich, Germany).
3. Patch Clamp Amplifier: EPC10 (HEKA, Lambrecht, Germany).
4. Acquisition software: PatchMaster (HEKA, Lambrecht, Germany).
5. Borosilicate Patch Clamp Chips (Ø ~ 1 µm): NPC-1 (Nanion Technologies, Munich, Germany).
6. Gramicidin solution: 100-nM Gramicidin dissolved in 70% ETOH.
7. KCl solution: 100-mM KCl, 10-mM Hepes (sterile filtered).
8. HCl solution: 100-mM HCl (sterile filtered).

13.2.6. Internal Perfusion Using the Port-a-Patch

1. Internal Perfusion System (Nanion Technologies, Munich, Germany).
2. Fused silica capillary (WPI, Sarasota FL, USA).

13.3. Methods

For pipette-based patch clamping a pipette is moved under the visual control of a microscope towards the cell using a micro-manipulator *(3)*. Since the contact between the cell and the pipette is very sensitive to any kind of movement between them, an anti-vibration table is required. **Figure 13.2a** shows a complete pipette-based patch clamp rig with the Faraday cage, the microscope, the anti-vibration table and the micro-manipulator.

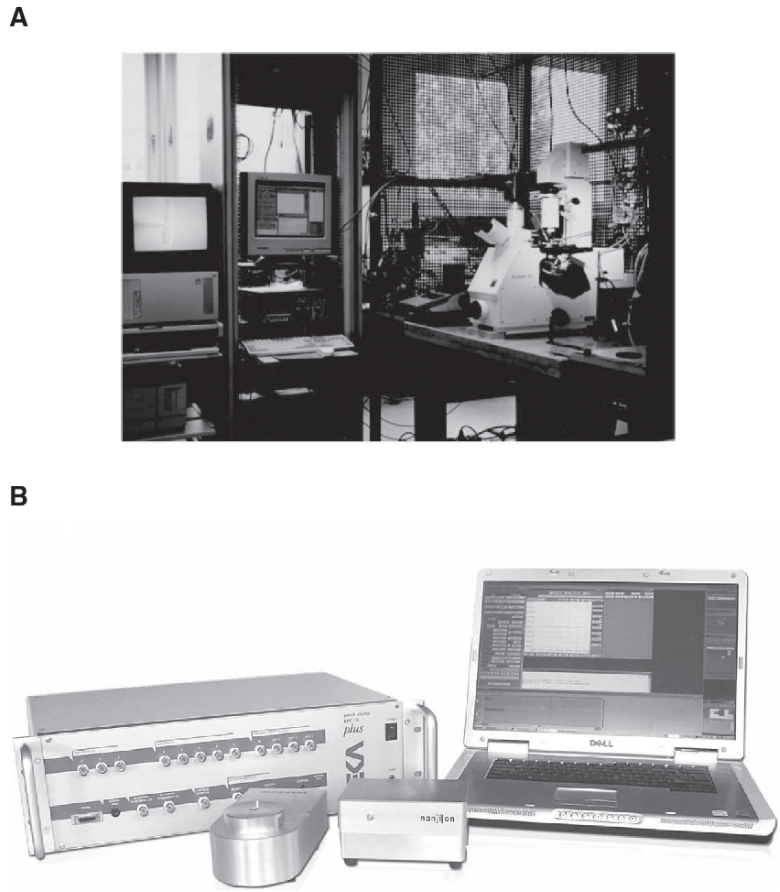

Fig. 13.2. Comparison of a typical pipette-based patch clamp rig on the *top* with a planar patch clamp rig on the *bottom*. (**a**) demonstrates the complexity of a pipette-based patch clamp rig, including an anti-vibration table, a microscope, micro-manipulators, an amplifier, a computer and a Faraday cage. (**b**) The planar patch clamp rig consists of a Port-a-Patch, an amplifier and a computer. It has a much smaller foot print than the conventional rig.

For planar patch clamp the situation is different. After adding a cell suspension onto the patch clamp chip with a ~1-μM hole, a cell is captured on top of the hole by applying suction. Since there is no relative movement between the sealed cell and the glass chip, no anti-vibration table, microscope or micro-manipulator is needed (**Fig. 13.2b**). Therefore, the Faraday cage can also be miniaturised.

Here we describe the functionality of the Port-a-Patch as an example for a planar patch clamp system. The Port-a-Patch (**Fig. 13.2b**) is a semi-automated patch clamp device providing data quality comparable to pipette-based patch clamping *(4–6)*. It utilises planar patch clamp chips (called NPC-1 chips), made from borosilicate glass, for the patch clamp recordings because of their excellent dielectric properties and clearly distinguishable stray capacitances. In the centre of the micro-machined glass chip is

an µm-sized aperture, onto which the cell is positioned automatically by application of suction (**Fig. 13.1**). Using a graphical user interface, the suction protocol is pre-programmed and computer controlled. The software adapts the applied negative pressure according to parameters such as pipette resistance, series resistance, and slow capacitance. In this way, the programme can determine if a cell has been sealed to the chip and whether the parameters correspond to the cell-attached or the whole-cell recording configuration.

13.3.1. Cell Culture

1. Typical cell lines, such as HEK 293 or Neuroblastoma cell lines, are grown in T75 flasks or plates of Ø = 96 mm and a surface of 60 cm^2. The plating of the cells has an influence on the seal behaviour (*see* **Note 2**).
2. The cells are split every 2–3 days. The cells are kept under a confluence of 60–80%. It is important to avoid cell clusters (*see* **Note 3**).

13.3.2. Cell Harvesting

1. Remove the medium from the cells and wash with PBS.
2. Add 2 ml of detachment buffer. Incubate for 2–5 min at 37°C.
3. Remove the cells with the medium from the plate and pipette them 3× gently up and down.
4. Centrifuge for 2 min at 100×*g*.
5. Discard the supernatant and re-suspend the cells in 1 ml of external buffer (resulting in a cell density of ~1×10^6–5×10^7 per ml).
6. In our experience, the cells in suspension remain viable for up to 4 h, stored at room temperature.

13.3.3. Planar Patch Clamp Using the Port-a-Patch

1. Add 5 µl of internal K^+ buffer to the inside of the borosilicate glass chip (**Fig. 13.3a**).
2. Screw the chip on top of the holder. The internal electrode makes an electrical contact with the internal solution.
3. Place the small Faraday cage in its designated space on top of the chip.
4. Add 5 µl of external buffer to the top of the chip. Now the external electrode (ground electrode) is electrically connected to the external buffer (**Fig. 13.3b**). The chip resistance and the offset can be measured.
5. When the PatchControl software is started, slight positive pressure is applied to the chip and the offset is corrected.
6. Before the application of 5 µl of the cell suspension, a slight suction of 50 mbar is applied. Once the suspension is added, a cell is attracted to the hole of the chip which leads to a small increase in the seal resistance.

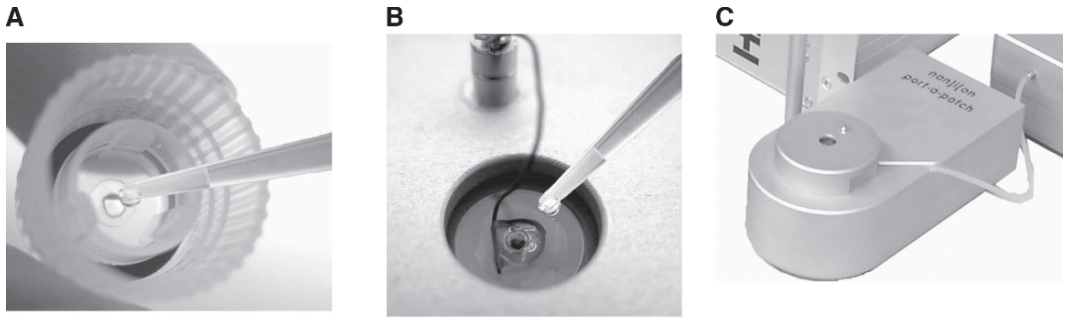

Fig. 13.3. (**a**) The bottom side of a patch clamp chip is filled with 5 µl internal K^+ buffer with the help of a pipettor. (**b**) 5 µl of external buffer makes contact with the bath electrode on top of the chip. (**c**) The Port-a-Patch is covered with a small Faraday cage and it is connected to a USB controlled suction pump.

7. The seal resistance is increased to a gigaseal by applying suction pulses and applying a negative voltage to the cells. This process runs automatically within the PatchControl software. It uses the same approach as an experienced patch clamper would do. A rinsing of the cells with external solution also often improves the seal resistance.
8. The whole-cell access is achieved by short suction pulses. For some cells it is helpful to support this process by zapping (*see* **Note 4**).

13.3.4. Preparation of Liposomes

1. Giant Unilamellar Vesicles (GUVs) are prepared using the electroformation method *(7)* in an ITO-coated glass chamber connected to the Nanion VesiclePrepPro setup.
2. 20 µl of the lipid solution is deposited on the ITO-coated glass surface.
3. After total evaporation of the solvent the lipids are assembled in a dehydrated lamellate phase.
4. A greased O-ring is placed around the dried lipid film and 300 µl of a non-ionic intracellular solution, sorbitol, with a concentration equal to 210 mM, is carefully added to the lipid film.
5. The second ITO-slide is placed on the top of the ring, with the ITO-layer facing downwards.
6. The process of electroformation is controlled by the Vesicle PrepPro setup and all parameters (amplitude, frequency, duration, etc.) for the electroformation are programmed in the *VesicleControl* software. Typically, an alternating voltage of 3-V peak-to-peak is applied with a progressive increase for the rise time and a decrease for the fall time to avoid abrupt changes, which might otherwise rupture the formed GUVs. The frequency of the alternating current is 5 Hz and is applied to the ITO-slides over a period of 2 h at room temperature.

7. After successful swelling, the vesicles were stable over weeks to months, refrigerated or frozen.

13.3.5. Planar Lipid Bilayer Formation and Gramicidin Incorporation

1. Add 5 µl of KCl solution to the inside of the borosilicate glass chip (**Fig. 13.3a**).
2. Screw the chip on top of the holder. The internal electrode forms an electrical contact with the internal solution.
3. Place the small Faraday cage in its designated space over the chip.
4. Add 5 µl of KCl solution to the top of the chip. Now the external electrode (ground electrode) is electrically connected to the external solution (**Fig. 13.3b**). The chip resistance and the offset can be measured.
5. By starting the Patch Control software a positive pressure is applied to the chip and the offset is corrected.
6. Before the application of 5 µl of the GUV suspension, a slight suction of typically 10–40 mbar, is applied. A GUV is attracted to the hole of the chip and as soon as it touches the glass surface, it bursts and forms a planar lipid bilayer with a typical seal resistance of tens of GΩ.
7. The additional GUVs are removed from the chip by washing twice with 20 µl of KCl solution.
8. The holding potential is set to 100 mV.
9. 1 µl of the Gramicidin solution is added to the chip. Incorporation of the Gramicidin channels is typically visible after 30 s to 2 min.
10. If no channel activity is visible after 3 min an additional µl of Gramicidin solution can be added.

13.3.6. Internal Perfusion Using the Port-a-Patch

The internal perfusion system consists of a special chip holder with an integrated internal perfusion and a perfusion system panel (**Fig. 13.4**). The internal perfusion system is an alternative head for the Port-a-Patch and can therefore be used with any Port-a-Patch. The perfusion system panel contains eight magnetic valves, which can be conveniently controlled by electrophysiological software.

1. For use of the internal perfusion with the Port-a-Patch, it is important that the internal electrode is connected to the ground (change the position of the switch on the back of the Port-a-Patch). This avoids noise and capacitance problems arising from the increased volumes of solutions for perfusion of the intracellular side (*see* **Note 5**).
2. The length of the fused silica capillary should be 1 mm above the inner plastic column as shown in **Fig. 13.4** (*see* **Note 6**).
3. Proceed for obtaining the whole-cell configuration or the lipid bilayer as described under **Subheadings 13.3.3** and **13.3.5**.

4. The internal buffer can now be exchanged.
5. **Figure 13.5** shows an example trace of Kv1.3 currents endogenously expressed in Jurkat cells. The speed of the internal solution exchange depends very much on the access resistance (*see* **Note 7**).

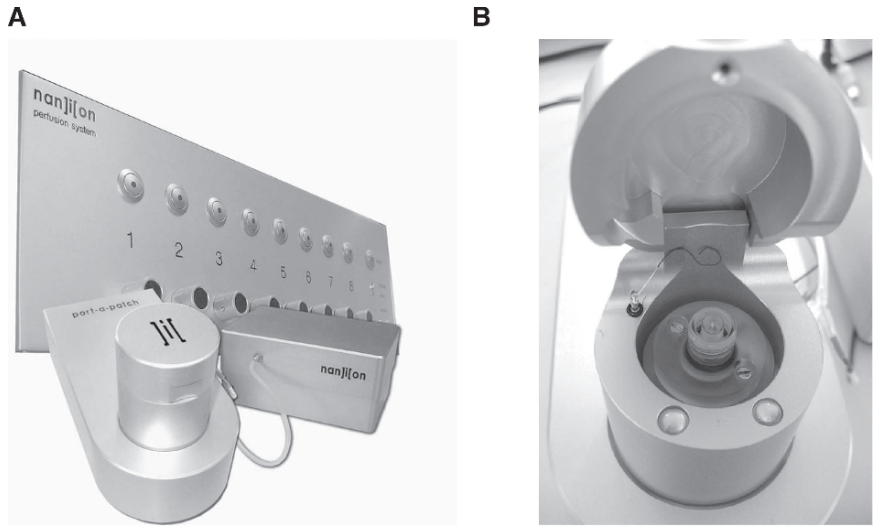

Fig. 13.4. (**a**) For the use of internal perfusion with the Port-a-Patch a special measuring top has to be used. (**b**) For effective noise reduction the internal perfusion is completely shielded.

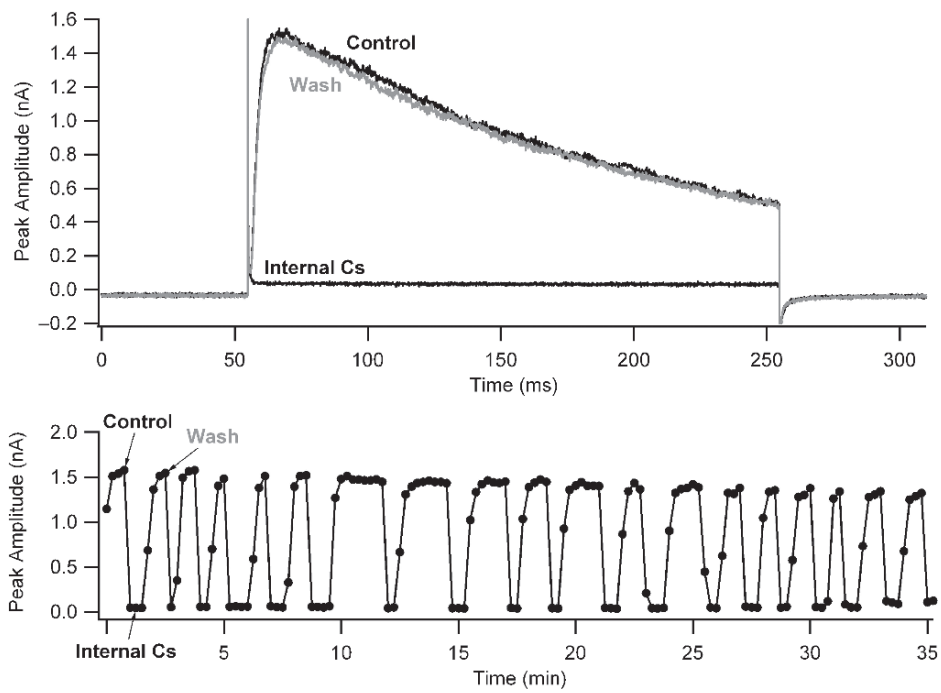

Fig. 13.5. Example traces for an internal solution exchange in the whole-cell configuration. Kv1.3 currents are recorded from Jurkat cells with an internal solution containing high potassium. By switching to a caesium containing solution, the outward current is inhibited. Wash-out and wash-in could be repeated many times.

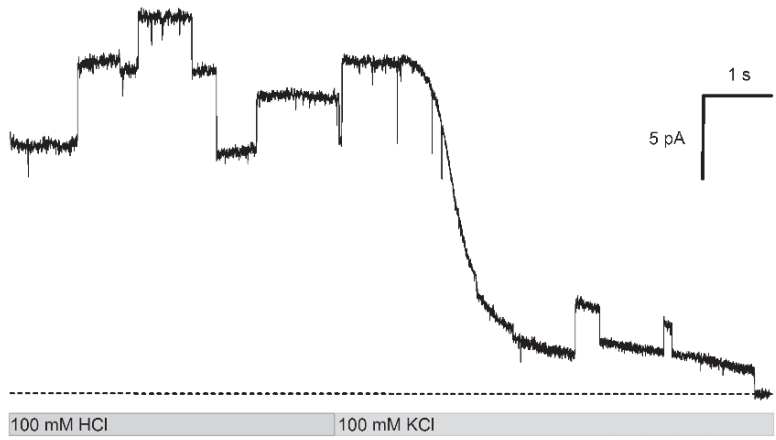

Fig. 13.6. Gramicidin recordings were performed from a lipid bilayer with the Port-a-Patch. The conductance of the single channels decreased remarkably by changing the internal solution from 100-mM HCl to 100-mM KCl.

6. **Figure 13.6** shows an example trace of Gramicidin currents in a lipid bilayer. In this case the internal perfusion is much faster.
7. It is important to mention that the final concentration of chloride ions should not be changed during an experiment without the use of an agar bridge or careful correction of the offset potential (*see* **Note 8**).
8. An exchange of the internal solution can also be done without the use of an internal perfusion system (*see* **Note 9**).

13.4. Notes

1. It is possible to use different detachment agents for harvesting the cells. In our experience, the standard trypsin/EDTA solution works very well. Some people prefer Accutase or AccuMax. Accutase is a mixture of a protease and a collagenase. It is supposedly gentler on the cells, since no inhibition of the protease is necessary. AccuMax is a more concentrated Accutase, plus it has additional DNAse activity. The protein expression is supposed to be higher while using this reagent.
2. Some cell lines are more difficult to seal than others. It is possible to improve the seal rates by optimising the cell culture. We see better results in seal rates by using T75 flasks instead of much smaller Petri dishes. The time between splitting and the confluency of the cells are also important parameters to adjust. If cells tend to be very fragile, it is better to harvest

them 3 days after plating. If they cannot go to the whole-cell configuration, it is better to use them just 1 day after plating.

3. Cell clusters are a considerable problem for planar patch clamp. Since the cells cannot be optically selected, the cell suspension should be as homogeneous as possible. For this reason the cells should be regularly split every 2–3 days with a trypsin treatment that ensures isolated cells.
4. Many cells are very sensitive to zapping pulses. A good starting point is 500 mV with a duration of 500 µs. Cells tolerate higher voltages, but seldom longer durations. If zapping alone does not result in a rupture of the membrane, it can be combined with a suction pulse.
5. The HEKA software (PatchMaster and Pulse) gives the option of switching the polarities by using the "on-cell" configuration. This is a very convenient feature, since the pulse protocols do not have to be adapted for the changed polarity.
6. The fused silica capillary should be approx. 1 mm above the inner plastic column (*see* **Fig. 13.7**). If the capillary is too long, it will touch the patch clamp chip and will be blocked. If the capillary is too short the internal solution will not reach up to the chip and dripping of the solution can be observed.
7. During a whole-cell experiment the speed of the internal solution exchange strongly depends on the series resistance. The

Fig. 13.7. The internal solution is applied through a fused silica capillary. The length of the capillary should be 1 mm above the inner plastic column.

difference in speed can be easily compared **Figs. 13.5** and **13.6**. The time-course of **Fig. 13.5** is in minutes with a series resistance of ~4 MΩ, whereas the time-course of **Fig. 13.6** is in seconds where the lipid bilayer does not induce an additional series resistance.

8. A change of the chloride concentration during an experiment results in a change of the offset. For more detailed information *see* **ref.** *8*.
9. It is also possible to change the internal solution without the use of an internal perfusion system. After obtaining the whole-cell configuration you can simply unscrew the patch clamp chip and turn it upside down. It is important that the solution on the top of the chip does not slide to the side, otherwise the cell will desiccate. The internal solution can be removed by a pipette and the new solution can then be added. 5 µl is sufficient. After screwing the chip back onto the chip holder the recording can be continued.

Acknowledgments

The Authors would like to thank Priv. Doz. Dr. Guiscard Seebohm for the development of the first prototype of the internal perfusion.

We acknowledge financial support from the European Union within the framework of the Marie Curie Training Network 019335 "Translocation" and from the Bundesministerium fuer Bildung und Forschung (BMBF 13N9110).

References

1. Ashcroft, F.M. (2000) *Ion Channels and Disease*. Academic, New York.
2. Neher, E. and Sakmann, B. (1976) Single-channel currents recorded from membrane of denervated frog muscle fibres. *Nature* **260**, 799–802.
3. Hamill, O.P., Marty, E., Neher, E., et al. (1981) Improved patch-clamp techniques for high-resolution current recording from cells and cell-free membrane patches. *Pflügers Arch* **391**, 85–100.
4. Fertig, N., Blick, R.H., and Behrends, J.C. (2002) Whole cell patch clamp recording performed on a glass chip. *Biophys J* **82**, 3056–3062.
5. Brüggeman, A., Stoelzle, S., George, M., et al. (2006) Microchip technology for automated and parallel patch-clamp recording. *Small* **2**, 840–846.
6. Farre, C., Stoelzle, S., Haarmann, C., George, M., Brüggemann, A., and Fertig, N. (2007) Automated ion channel screening: patch clamping made easy. *Expert Opin Ther Tagerts* **11**, 557–565.
7. Angelova, M.I. (2001) Liposome electroformation. In *Giant Vesicles* (Luisi, P.L. and Walde, P. Ed.). Wiley, Chichester, pp. 27–36.
8. Neher, E. (1995) Voltage offsets in patch-clamp experiments. In *Single-Channel Recording* (Sakmann, B. and Neher, E. Eds.). Plenum, New York, pp. 147–153.
9. Hille, B. (1992) *Ionic Channels of Excitable Membranes*. Sinauer Associates, Sunderland, MA, p. 89.

Chapter 14

Analysing Steroid Modulation of BK_{Ca} Channels Reconstituted into Planar Lipid Bilayers

Heidi de Wet, Jonathan D. Lippiat, and Marcus Allen

Summary

A number of recent studies have described the activation of BK_{Ca} channels by steroid hormones such as estrogen. The proposed mechanisms are diverse and include both the direct interaction with the ion channel subunits and the stimulation via receptor activation and cell signalling pathways. To investigate the activation of BK_{Ca} channels by estrogen we devised a cell-free system by incorporating recombinant channels of known subunit composition into artificial bilayers and recorded single channel currents. This chapter describes the methods used to prepare purified membrane fractions from cultured cells and the construction of artificial phospholipids bilayers for the incorporation and recording of ion channels.

Key words: BK_{Ca}, Maxi-K, Planar lipid bilayer, Estrogen, Membrane purification.

14.1. Introduction

Large conductance Ca^{2+}- and voltage-sensitive K^+ channels (BK_{Ca} or Maxi-K) regulate smooth vascular muscle tone by conducting hyperpolarising spontaneous transient outward currents (STOCs) in response to cytosolic Ca^{2+} sparks *(1)*. The ion channel is formed by a tetramer of Sloα1-subunits, and the function and pharmacology are fine-tuned by the association with regulatory β-subunits, Sloβ1–4 (reviewed in **ref.** *2*).

Estrogen (17β-estradiol) relaxes smooth muscle cells by opening BK_{Ca} channels, but there is much debate over the precise mechanism as there is evidence for both the direct activation of the channel via the Sloβ1-subunit *(3)* and via the stimulation of cytoplasmic estrogen receptors *(4)*. The use of a cell-free ion

Jonathan D. Lippiat (ed.), *Methods in Molecular Biology, Potassium Channels, vol. 491*

Book doi: 10.1007/978-1-59745-526-8

channel preparation can therefore assist in distinguishing between these effects. As the name suggests, the BK_{Ca} channel has a distinctly large unitary conductance (~300 pS in symmetrical K^+). This makes BK_{Ca} channel currents amenable to analysis in impure membrane fractions without the need for further purification. Planar lipid bilayer recordings were carried out by allowing membrane fractions purified from cells expressing recombinant BK_{Ca} channels comprised of Sloα alone or Sloα1 + β1 to incorporate into an artificial planar lipid bilayer.

This technique has several advantages: purified membrane fractions are cell-free, making it possible to investigate the effect of estrogen and other steroids on the BK_{Ca} channel activity in isolation from the genomic and cellular effects whilst the lipid environment is not disturbed by solubilisation and reconstitution. Drugs can be added to either side of the membrane to investigate the location of drug binding sites and the use of recombinant channels allows easy genetic manipulation and control over subunit composition. Furthermore, single channels incorporated into planar bilayers are amenable to optical investigation that could take place concurrently with current measurements (e.g. *see* **ref.** *5*).

14.2. Materials

14.2.1. Cell Culture

1. Human embryonic kidney (HEK) cell line stably expressing BK_{Ca} channels (e.g. *see* **ref.** *6*) or another cell line expressing an ion channel of interest (*see* **Note 1**).
2. Cell culture medium: DMEM supplemented with 10% foetal bovine serum and antibiotics to maintain the selection of stably expressing cells (e.g. 5 μg/ml blasticidin to select for Slo 1 expression and 1 mg/ml G418 to select for Sloβ1-subunit expression; *see* **ref.** *6*).
3. Phosphate-buffered saline (PBS), pH 7.0 at room temperature (RT).
4. Trypsin–EDTA cell dissociation solution.
5. 25, 75 and 175 cm^2 tissue culture flasks.

14.2.2. Membrane Preparation

1. Chilled phosphate-buffered saline (PBS) with 1 mM EDTA, pH 7.0.
2. Protease inhibitors.
3. 5, 10 and 25 ml serological pipettes.
4. Buffer 1: 10 mM Tris–HCl pH 7.4, 250 mM sucrose, 200 mM $CaCl_2$ – stable at 4°C for several months.

5. Buffer 2: 10 mM Tris–HCl pH 7.4, 25 mM sucrose, 1-mM EDTA – stable at 4°C for several months.
6. Buffer 3: 10 mM Tris–HCl pH 7.4, 35% (w/v) sucrose, 1 mM EDTA – stable at 4°C for several months.
7. Buffer 4: 10 mM Tris–HCl pH 7.4, 250 mM sucrose – stable at 4°C for several months.
8. Buffer 5: 150 mM NaCl, 1.5 mM $MgCl_2$, Tris–HCl pH 7.0, 20% Glycerol – stable at 4°C for several months.
9. 22 and 25 G syringe needles.
10. 5 and 10 ml plastic syringes.
11. 1.5 ml microtubes.
12. 50 ml tubes.
13. Nitrogen cavitation apparatus.
14. Ultracentrifuge with swing bucket rotor (e.g. Beckman SW28) and appropriate ultracentrifuge tubes.

14.2.3. Bilayer Recording

Schematics of the apparatus are shown in **Figs. 14.1** and **14.2**. A bilayer recording system can be constructed by anyone familiar with the patch clamp apparatus.

1. Lipid bilayer cup/chamber for bilayer formation (e.g. Warner Instruments chamber BCH-13A and cup CP13A-250).
2. Ag/AgCl electrodes.
3. Vibration-isolated platform (e.g. an air table).
4. Faraday cage to enclose the recording chamber.
5. Light source.
6. Magnetic stirrer.
7. Patch clamp amplifier that is capable of bilayer recordings (e.g. Warner Instruments PC-501A or Bio-logic BLM-120).
8. (Optional) Signal generator that can generate a triangular wave form to measure membrane capacitance (some bilayer amplifiers, such as the BLM-120, have this as a built-in feature).
9. Analogue to digital converter (e.g. CED micro1401 MkII).
10. Computer for data acquisition and analysis.
11. Single channel analysis software (e.g. WinEDR, University of Strathclyde, UK).
12. Data storage device (e.g. portable hard drives).

14.2.4. Agar Bridges

1. Glass capillaries.
2. 2 M KCl.
3. Agar.

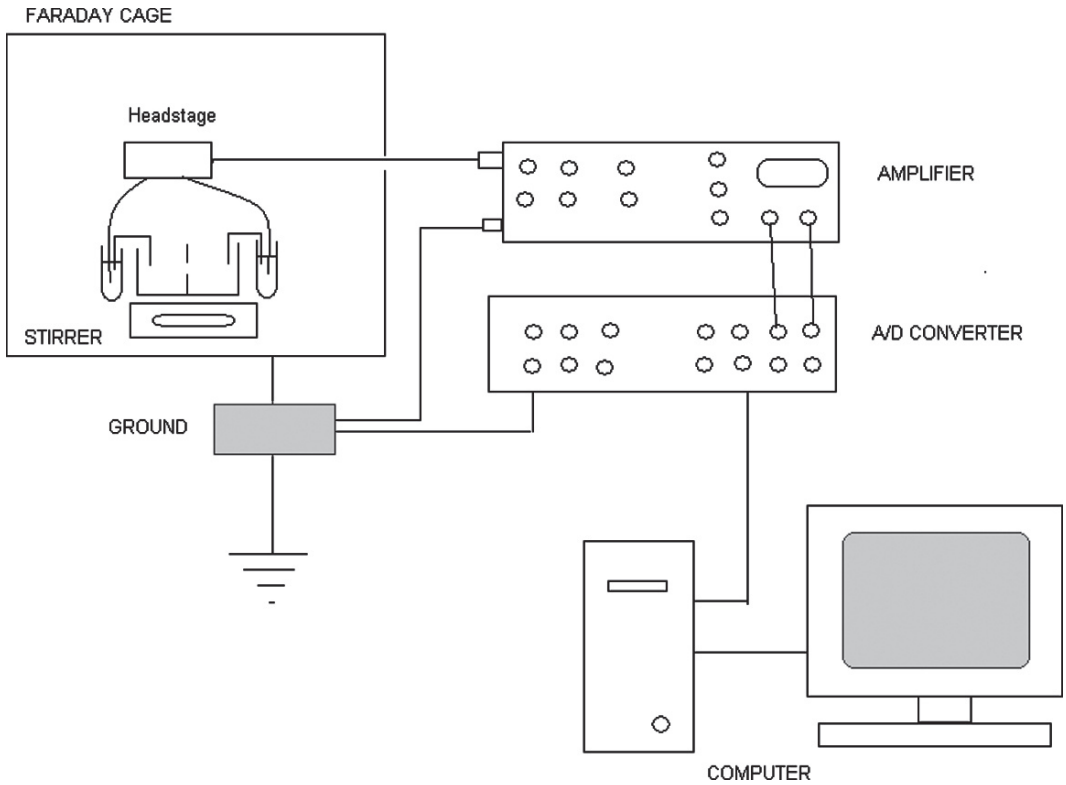

Fig. 14.1. Artificial bilayer recording apparatus.

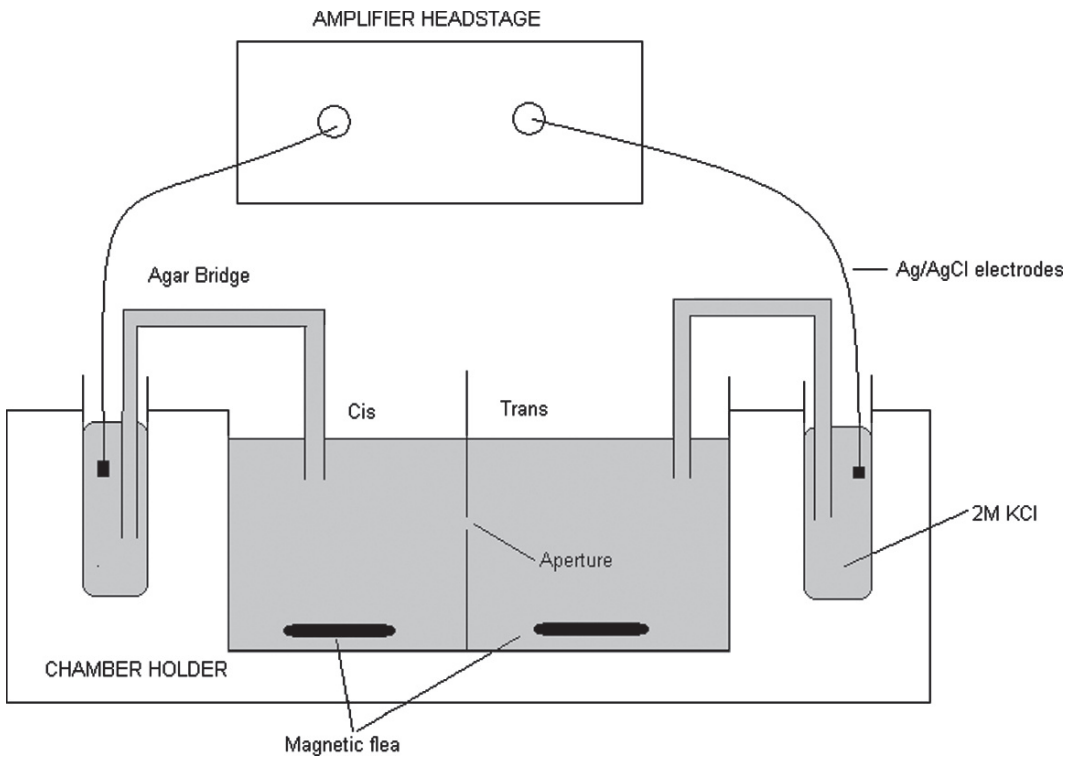

Fig. 14.2. Bilayer chamber and recording bath setup.

14.2.5. Lipid Preparation

1. POPE:1-Palmitoyl-2-Oleoyl-*sn*-glycero-3-phosphoethanolamine (Avanti Polar Lipids).
2. POPS: 1-Palmitoyl-2-Oleoyl-*sn*-glycero-3-[phosphor-L-serine] (Avanti Polar Lipids).
3. Chloroform.
4. Nitrogen gas supply.
5. *n*-Decane.

14.2.6. Experimental Solutions

1. High Free Calcium (50 µM) buffer: 150 mM KCl, 1 mM EGTA, 1 mM $MgCl_2$, 1.05 mM $CaCl_2$, 10 mM HEPES pH 7.2 with KOH.
2. Low Free Calcium (0.5 µM) buffer: 150 mM KCl, 1 mM EGTA, 1 mM $MgCl_2$, 0.75 mM $CaCl_2$, 10 mM HEPES pH 7.2 with KOH.
3. 10 mM estrogen in DMSO.

14.3. Methods

14.3.1. Cell Culture

1. If the HEK cell lines are seeded from frozen stock, thaw the cells at 37°C until just thawed and place on ice immediately.
2. Add 1 ml of the thawed cell suspension to a 25 cm^2 culture flask and allow cells to adhere for 3 h.
3. Gently wash the cells with 2 ml of cell culture media and carefully aspirate all dead cells.
4. Grow cells until completely confluent.
5. Wash confluent cells twice with phosphate-buffered saline.
6. Detach cells using trypsin–EDTA solution and harvest by centrifugation at 200×*g*.
7. Aspirate supernatant and resuspend in 9 ml fresh selective culture medium.
8. Seed 3-ml resuspended cells in 75 cm^2 culture flasks and add 10–12 ml selective culture media. Grow cells until confluent.
9. Repeat **steps 6–8** and seed the cells in 175 cm^2 culture flasks.
10. Grow until confluent and increase the cell culture to 20 × 175 cm^2 confluent cells.

14.3.2. Membrane Preparation

1. Aspirate the culture medium from the tissue culture flasks.
2. Detach cells with 5–10 ml of cold PBS with 1 mM EDTA. Shake cells loose by tapping the side of the flask smartly.
3. Meanwhile, cool the nitrogen cavitation apparatus on ice.
4. Harvest cells by centrifugation at 500×*g* for 15 min at 4°C.
5. Resuspend the pellet in 5× the pellet volume of Buffer 1 containing protease inhibitors using a serological pipette.
6. Load the cavitation apparatus with the cell suspension and seal.
7. Fill the cavity with nitrogen gas to a pressure of 1,000–1,500 psi and leave on ice for 15 min (*see* **Note 2**).
8. Bleed the apparatus and collect the burst cells in a 50-ml tube and repeat the bursting step once more.
9. Dilute the cell lysate to 25 ml with ice-cold Buffer 2.
10. Centrifuge the diluted suspension at 500–1,000×*g* for 10 min to collect cell debris and unbroken cells.
11. Add 10 ml of Buffer 3 to the ultracentrifuge tube to create a sucrose cushion.
12. Gently layer the supernatant from **step 9** carefully on top of the sucrose cushion using a serological pipette set.
13. Balance the weight of the ultracentrifuge tubes using Buffer 2 to within 0.1 g of each other. Handle the tubes very carefully so as not to disturb the sucrose cushion.
14. Centrifuge at 30,000×*g* for 30 min at 4°C.
15. Remove 5–10 ml of the supernatant at the top of the tube using a serological pipette.
16. Collect the cloudy suspension resting on the top of the sucrose cushion using a 10 ml plastic syringe.
17. Transfer the collected interface to a fresh ultracentrifuge tube. Dilute the collected interface with Buffer 4 to fill the ultracentrifuge tube (*see* **Note 3**).
18. Balance the weight of the tubes to within 0.1 g of each other and centrifuge at 100,000 *g* for 45 min at 4°C.
19. Discard the supernatant and resuspend the glassy-appearing pellet in 1.5 ml of Buffer 5 containing the protease inhibitors using a 22-G syringe needle and then a 25-G needle on a 5-ml syringe until the suspension is lump-free.
20. Store in 50–100 µl aliquots at –80°C.

14.3.3. Agar Bridge Fabrication

1. Form U-shaped bridges from the capillary glass by melting gently over a Bunsen burner flame.
2. Prepare 4% agar in 2 M KCl by adding 4 g of agar to 100 ml 2 M KCl while heating and stirring.

3. Fill bridges with molten agar/KCl, ensuring that no bubbles appear.
4. Store bridges in 2 M KCl solution at 4°C.
5. Excess agar/KCl can be stored at 4°C.

14.3.4. Bilayer Construction

Figure 14.2 shows a schematic of the bilayer cups.

1. Reconstitute POPS and POPE in chloroform at 50 mg/ml. These solutions should be stored in the dark at −20°C.
2. Add 7.5 µl of POPS and 7.5 µl of POPE to a sealable 2 ml glass volumetric flask.
3. Evaporate the chloroform under a stream of nitrogen gas. Seal the volumetric flask with the stopper to minimise contact with air.
4. Resuspend the dried lipid with 25 µl of *n*-decane.
5. The lipid is ready to use. This preparation is useable for 3–4 h, but avoid contact with air.
6. Place 1 µl of the reconstituted lipid carefully spread around the aperture of the recording cup and over the aperture to form a bilayer (*see* **Note 4**).
7. Insert the cup into the chamber holder and add 1 ml of the recording buffer to the cup and 1 ml of the appropriate recording buffer to the chamber holder.
8. Connect the *cis* and *trans* side of the bath to the amplifier head stage via the agar bridges as indicates in **Fig. 14.2**. The *cis* side should normally be at ground potential.
9. Assess bilayer formation by applying 1–10 mV square or triangular voltage pulses (*see* **Note 5**).
10. The bilayer can have a voltage clamped between −150 and 150 mV and should have a leak conductance of less than 10 pS and a capacitance of greater than 150 pF (*see* **Note 5**).

14.3.5. Channel Incorporation and Modulation by Steroids

Once a stable bilayer has formed BK_{Ca} channels can be incorporated.

1. Add 2 µl of the membrane preparation to the *cis* side of the chamber. It is important to stir the bilayer occasionally as membranes can sink to the bottom of the recording chamber.
2. Hold the bilayer potential at ± 50 mV and wait for channel insertion by observing single channel activity on the oscilloscope.
3. If no channels have inserted after 20 min then a further 2 µl samples of the membrane preparation should be added.
4. Once channels have been inserted it is important to estimate how many channels are present. This can be done by changing

the membrane potential to raise the open probability and by observing the number of multiple openings (*see* **Fig. 14.3**; *see also* **Note 6**).

5. Once a stable recording of channel activity is observed pharmacological agents such as steroids can be added to either side of the bilayer.

14.3.6. Data Analysis

1. Data analysis can be done off-line. It is advisable to get a back-up data onto a portable hard drive.
2. WinEDR can be used to analyse single channel data. Amplitude histograms and dwell time histograms, including burst analysis, can be constructed. In addition, data can be exported into other software packages, such as QuB, or a programme to present the data in a statistical form, if required.

14.4. Notes

1. Channels with a small conductance will not be well suited for this work, as contaminating channels that are endogenous to HEK cells are sometimes observed during recordings.
2. Any other pressure based bursting apparatus may be used, e.g. a French press. Cell lysis by sonication tends to result in higher levels of protein degradation.
3. This is important, as a half-filled tube will collapse.
4. Artificial (or "black") lipid bilayer formation often needs to be "encouraged". Painting the lipid onto a cup may fail to

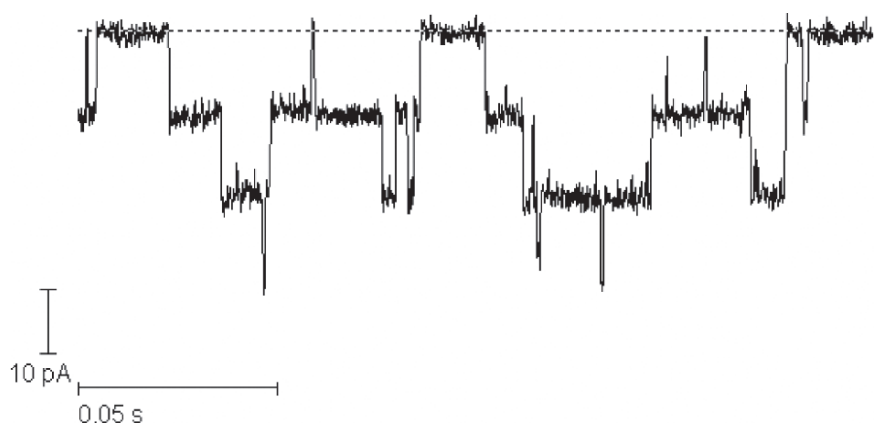

Fig. 14.3. A typical single channel recording. This bilayer has at least three individual BK_{Ca} channels inserted, as evidenced by the multiple downward current levels from the zero current level (*dashed line*).

form a bilayer. Either the lipid is absent from the aperture and the amplifier can not pass enough current to clamp the voltage, or it is blocked by multiple layers of lipid and the membrane capacitance is too low. There are a number of ways to encourage bilayer formation:

(a) "Lifting a bilayer": Gently suck up the recording buffer in the *cis* chamber using a 1-ml pipette and then gently return to the recording chamber. Dragging the surface of the recording solution across the aperture encourages a redistribution of lipid and bilayer formation.

(b) "Painting a bilayer": This is done using a ball of glass formed on the end of capillary tubing by heating the glass with a Bunsen burner. This clean glass probe can then be dipped in the stock lipid and applied directly to the hole and this is often enough to encourage bilayer formation.

5. The passive bilayer properties are easy to evaluate under voltage clamp conditions. The conductance is equal to current deflection divided by the voltage step (e.g. conductance = 1 pA/100 mV = 1×10^{-12} A/0.1 V = 1×10^{-11} S or 10 pS). The capacitance of a membrane is described by the equation $C = \varepsilon A / d$, where C is the capacitance in Farads, ε is the dielectric constant of the lipid, A is the area of the bilayer, and d is the thickness. Current flow onto a capacitor (e.g. a lipid bilayer membrane) is given by the equation $i = C(\mathrm{d}V / \mathrm{d}t)$. We can combine both equations to give $i = (\varepsilon A / d)(\mathrm{d}V / \mathrm{d}t)$. A triangular wave form has a constant rate of change and if we change the voltage across our bilayer in a triangular manner then $\mathrm{d}V/\mathrm{d}t$ will be constant. More importantly the dielectric constant of the lipid is fixed and the thickness of the bilayer is determined by the lipid tail length. Therefore, the equation can be simplified to $i = kA$, where $k = (\varepsilon / d)(\mathrm{d}V / \mathrm{d}t)$. Using a triangular pulse, the current output of the amplifier is therefore directly proportional to the area of the bilayer. The current output can be calibrated to capacitance by placing a 100-pF capacitor between the input and ground of the patch clamp amplifier head stage. Take care when handling patch clamp amplifier head-stages as they are extremely sensitive to static electricity and can be easily damaged. Capacitance can also be monitored and measured from the capacity transients evoked by square-wave voltage pulses.

6. Changing membrane potential to fully activate channels will only work with those channels that are gated by voltage. Other stimuli may need to be applied to activate other types of channel, e.g. Ca^{2+}.

References

1. Brenner, R., Perez, G.J., Bonev, A.D., Eckman, D.M., Kosek, J.C., Wiler, S.W., Patterson, A.J., Nelson, M.T., and Aldrich, R.W. (2000) Vasoregulation by the beta1 subunit of the calcium-activated potassium channel. *Nature* **407**, 870–876.
2. Orio, P., Roja, P., Rerreira, G., and Latorre, R. (2002) New disguises for an old channel: MaxiK channel beta-subunits. *News Physiol. Sci.* **17**, 156–161.
3. Valverde, M.A., Rojas, P., Amigo, J., Cosmelli, D., Orio, P., Bahamonde, M.I., Mann, G.E., Vergara, C., and Latorre, R. (1999) Acute activation of Maxi-K channels (hSlo) by estradiol binding to the beta subunit. *Science* **285**, 1929–1931.
4. Han, G., Yu, X., Lu, L., Li, S., Ma, H., Zhu, S., Cui, X., and White, R.E. (2006) Estrogen receptor alpha mediates acute potassium channel stimulation in human coronary artery smooth muscle cells. *J. Pharmacol. Exp. Ther.* **316**, 1025–1030.
5. Ide, T., Takeuchi, Y., Aoki, T., and Yanagida, T. (2002) Simultaneous optical and electrical recording of a single ion-channel. *Jpn. J. Physiol.* **52**, 429–434.
6. DeWet,H.,Allen,M.,Holmes,C.,Stobbart,M., Lippiat, J.D., and Callaghan, R. (2006) Modulation of the BK channel by estrogens: examination at single channel level. *Mol. Membr. Biol.* **23**, 420–429.

Chapter 15

Using Bioluminescence Resonance Energy Transfer to Measure Ion Channel Assembly

Gina M. Whitaker and Eric A. Accili

Summary

Bioluminescence Resonance Energy Transfer (BRET) measures protein interactions within 10 nm of each other. Aside from its ability to probe for interactions at high resolution, this technique operates in live, intact cells, and offers a high throughput method of detection. Thus far, BRET has been widely used in measuring G protein receptor dimerization. In this chapter, we describe the BRET methodology in detail and apply this technique to the measurement of ion channel assembly. In addition, we discuss how BRET can be used to compare the extent of homomeric and heteromeric channel assembly.

Key words: Bioluminescence Resonance Energy Transfer, Ion channel assembly, Protein–protein interactions, Heteromer, Homomer, Tetramer, Subunit.

15.1. Introduction

It is widely accepted that the majority of potassium channels assemble as tetramers to form functional channels. Channels can self-assemble from four identical subunits to form homomers, or can form heteromers by coassembly of structurally homologous subunits. Functional coassembly is traditionally addressed by electrophysiology, which can also provide information on subunit stoichiometry *(1, 2)*. Physical assembly of ion channel subunits has been directly examined by crystal structure analysis, which has perhaps provided the clearest picture of channel structure thus far *(3, 4)*. Nevertheless, the ability to crystallize ion channels has proven to be extremely difficult and thus these studies are few and far between. More commonly, indirect measurements using

Jonathan D. Lippiat (ed.), *Methods in Molecular Biology, Potassium Channels, vol. 491*

Book doi: 10.1007/978-1-59745-526-8

techniques such as in vitro translation or coimmunoprecipitation are used to measure interactions between subunits *(5)*. However, the rigorous biochemical manipulation involved in such techniques, as well as removal of channels from their membrane environment, can alter the native channel structure as well as putative intersubunit interactions. In addition, these techniques cannot easily distinguish between direct and indirect protein interactions within larger complexes. One can circumvent some typical issues associated with traditional biochemical techniques by using Fluorescence Resonance Energy Transfer (FRET) *(6, 7)*. FRET measures protein interactions at a high resolution, within 10 nm, whilst in their membrane environment, resulting in precise information pertaining to the subcellular location of interaction. Nonetheless, FRET measurements can be difficult to interpret since the assay requires initial excitation by an external light source which can result in photobleaching, autofluorescence, or direct excitation of the acceptor molecule, thereby producing erroneous signals or high signal-to-background ratios.

Similar to FRET, Bioluminescence Resonance Energy Transfer (BRET) also measures energy transfer in live cells, between proteins of interest located less than 10 nm from one another. To measure BRET, two putatively interacting proteins of interest are fused with either Renilla-Luciferase (R-Luc, a bioluminescent donor molecule) or Green Fluorescence Protein (GFP, a acceptor molecule) and coexpressed in a heterologous expression system. A substrate (coelenterazine), which is added to the cells, is oxidized by R-Luc, which in turn emits bioluminescent energy at a wavelength of 395 nm. GFP is excited at this wavelength, thereby emitting fluorescence at 510 nm provided that the interacting partners are in close enough proximity (**Fig. 15.1**). The efficiency of energy transfer can then be quantified as a BRET ratio of emission intensity at 510 nm to that at 395 nm. The magnitude of a BRET signal varies inversely with the sixth power of distance up to 10 nm, thus providing high resolution for measuring interacting proteins *(8)*. By using the coelenterazine substrate rather than an external light source to excite the donor molecule, the issues associated with fluorescence excitation can be avoided. Further, BRET measurements are taken on large populations of cells, thus providing a high throughput method of detection of protein interactions.

BRET is widely used to measure dimerization of G protein-coupled receptors (GPCR) as well as dynamic changes in GPCR interactions, and has also been used to quantify the extent of homo- and heterodimerization of GPCRs *(9, 10)*. We have recently adapted this technique to measure self- vs. coassembly of different Hyperpolarization-activated Cyclic Nucleotide-modulated (HCN) channel subunit isoforms (HCN2 and HCN4) *(11)*. In this chapter, we elaborate on how BRET can be used to

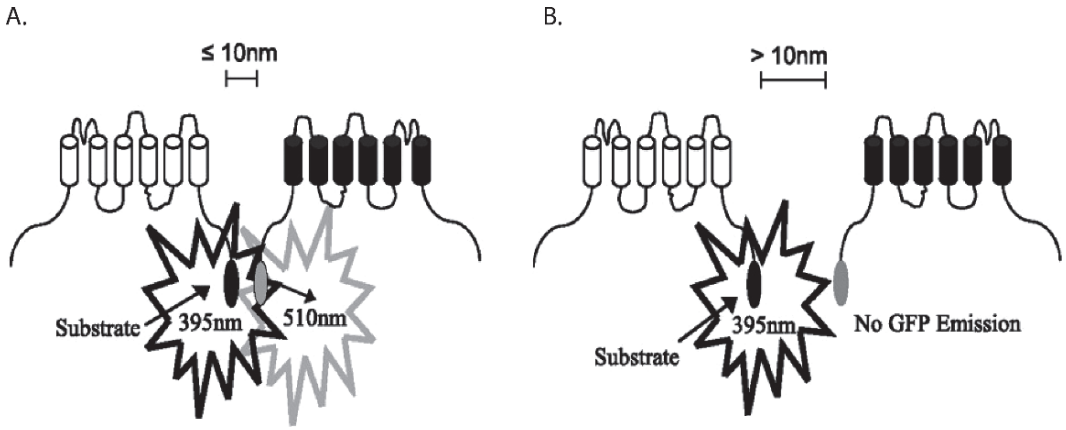

Fig. 15.1. BRET measures protein interactions within less than 10 nm apart. (**a**) Upon degradation of its substrate (DeepBlueC coelenterazine), RLuc emits light at 395 nm. Emission at this wavelength will excite GFP if it is located within 10 nm of the RLuc protein. The GFP will then emit light at 510 nm. The intensity of GFP emission depends on the proximity of GFP to RLuc. (**b**) If RLuc and GFP are greater than 10 nm from each other, the emission from RLuc will not excite GFP, and the calculated BRET ratio will be low. BRET ratios are calculated by dividing the recorded GFP emission (relative fluorescent units) by RLuc emission (relative luminescent units) (reproduced from **ref.** *11* with permission from the American Society for Biochemistry and Molecular Biology, Inc.).

measure and compare homomeric and heteromeric ion channel assembly in live Chinese Hamster Ovary (CHO) cells.

15.2. Materials

15.2.1. Cell Culture and Transfection

1. Fusion protein expression vectors: pGFP^2-N, pGFP^2-C, pRLuc-N and pRLuc-C (Perkin Elmer).
2. cDNA encoding ion channel subunits of interest.
3. Chinese Hamster Ovary (CHO) cells (American Type Culture Collection) (*see* **Note 1**).
4. Cell culture medium: F12 Nutrient Mixture (1×) containing L-glutamine, supplemented with 5% fetal bovine serum (FBS) and 0.25% Penicillin-Streptomycin (Invitrogen Canada, Inc.).
5. FuGENE 6 Transfection Reagent (Roche Diagnostics Canada).
6. Transfection Media: F12 Nutrient Mixture (1×) containing L-glutamine, supplemented with 5% FBS (Invitrogen Canada, Inc.).
7. 60-mm cell culture-treated dishes.

15.2.2. BRET Assay

1. Dulbecco's phosphate-buffered saline (D-PBS): 8-g/L NaCl, 2.16-g/L $Na_2HPO_4 \cdot 7H_2O$, 0.2-g/L KCl, 0.2-g/L KH_2PO_4,

0.1-g/L $CaCl_2$, 0.1-g/L $MgCl_2 \cdot 6H_2O$, 1-g/L D-glucose, 0.036-g/L sodium pyruvate (Invitrogen Canada, Inc.).

2. 0.05% Trypsin with EDTA-4Na (1×) (Invitrogen Canada, Inc.).
3. F12 Nutrient Mixture (1×) containing L-glutamine, supplemented with 5% FBS (Invitrogen Canada, Inc.).
4. BRET buffer: D-PBS supplemented with 2 ug/mL of aprotinin.
5. DeepBlueC coelenterazine substrate (PerkinElmer, Inc.) reconstituted to 1 mM in absolute ethanol and diluted to 15 uM in BRET buffer just prior to use (*see* **Note 2**).
6. 96-well white optiplates (PerkinElmer, Inc.).
7. Victor V Plate Reader (PerkinElmer, Inc.) including the following additions:
   - Optical Excitation filter: 405/5 nm (for GFP fluorescence quantification).
   - Optical Emission filters: 410/80 nm and 515/30 nm.
   - 1–3 channel injectors.
   - Wallac 1420 workstation software.

15.3. Methods

15.3.1. Cell Culture and Transfection

1. Make cDNA fusion constructs of interest using standard subcloning techniques such that each cDNA partner is tagged with a GFP or RLuc at either the N- or C-termini (*see* **Notes 3** and **4**).
2. Culture CHO cells in Cell Culture Media, in 60-mm cell culture-treated dishes at 37°C with 5% CO_2 injection until they are approximately 50% confluent. Include one dish as an untransfected background control.
3. In 1.5-mL eppendorf tubes, mix cDNA (either RLuc-tagged construct alone, or optimized combinations of RLuc- and GFP-tagged constructs) (*see* **Notes 5** and **6**) with 100 µl of F12 media (without antibiotics) and FuGENE 6. transfection reagent. Use a 3:1 ratio of FuGENE 6 Transfection Reagent to total cDNA amount added. Incubate tubes at room temperature for 30 min.
4. Replace Cell Culture Media from cultured cells with Transfection Media, and then add transfection mixture from eppendorf tubes to cells. Agitate gently, and then incubate for 24 h at 37°C with 5% CO_2 injection.

15.3.2. BRET Assay

15.3.2.1. Cell Preparation

1. 24-h post-transfection, wash cells twice with 3 mL of D-PBS at room temperature.
2. Add 1 mL of 0.05% Trypsin–EDTA and incubate cells for 5 min with occasional agitation.

3. Add 3 mL of Transfection Media to inactivate the 0.05% trypsin–EDTA, and then collect the cell mixture in appropriate centrifuge tubes.
4. Centrifuge cells at 500–700×*g* for 5 min.
5. Remove supernatant and resuspend cells in 100 ul of BRET buffer.
6. Add 50 ul of well-mixed cells (approximately 100,000 cells) in duplicate to individual wells of a 96-well white optiplate.
7. Incubate cells for 30 min at room temperature in the dark.
8. Just prior to proceeding with BRET measurements, prepare a sufficient amount of 15-uM DeepBlueC in BRET buffer and keep it on ice in the dark.

15.3.2.2. Measurement of GFP Fluorescence

1. Place the 96-well plate into the Victor V plate reader.
2. Set up and run the protocol for measurement of GFP fluorescence using the Wallac 1420 workstation software (*see* **Note 7**):
   (a) Shake the entire plate for 5 s at medium speed.
   (b) Use the 405/5-nm excitation filter and 515/30-nm emission filter to measure relative GFP fluorescence units for each well that contains cells.
3. Calculate the fold over background of GFP fluorescence according to the following equation, where background is the relative fluorescence units from the well containing untransfected cells:
   – Relative Fluorescence Units at 510 nm of well *x*
   – Relative Fluorescence Units at 510 nm of background

15.3.2.3. Measurement of BRET

Design a protocol for BRET using the Wallac 1420 workstation software as follows, such that machine runs through the entire protocol for each well before proceeding to subsequent wells.

1. Add 25 µL of 15-µM DeepBlueC in BRET buffer to the first well using the injector installed on the Victor V plate reader, such that the final concentration of DeepBlueC in the well is 5 µM.
2. Shake the optiplate for 5 s at medium speed in the plate reader.
3. Immediately measure emission intensity at 395 nm (relative luminescence units) followed by emission intensity at 510 nm (relative fluorescent units) in the first well.
4. Repeat **steps 1–3** for subsequent wells until all wells are read.

15.3.2.4. BRET Analysis

1. Use the following equation to calculate BRET ratios for each well (*see* **Note 8**)

   (Emission at 510 nm – Emission at 510 nm of control well)

   (Emission at 395 nm – Emission at 395 nm of control well)
2. Determine the mean BRET values from duplicate wells.

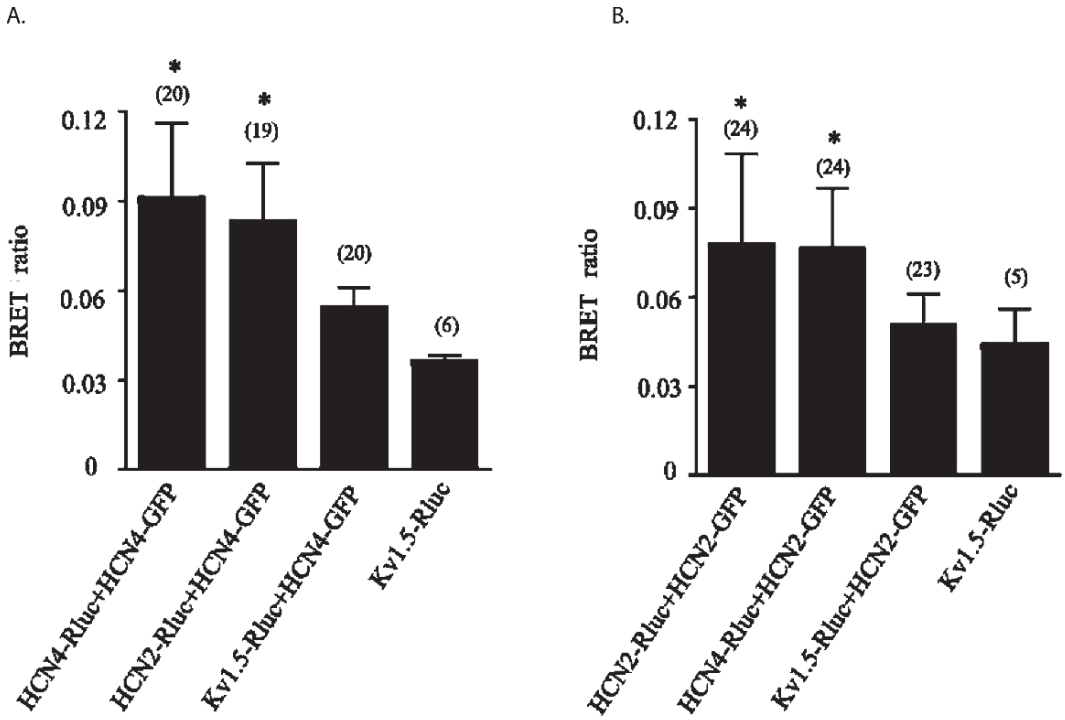

Fig. 15.2. BRET ratios support similar levels of self-assembly and coassembly of HCN2 and HCN4 isoforms in live CHO cells. (**a**) and (**b**) Bar graphs of BRET values determined from cells cotransfected with different channel construct combinations. Values represent means ± SD for each set of constructs, and (*n*) values depict the number of cell populations used to determine mean values over 3–6 independent transfections. Experiments were performed in duplicate at four different RLuc/GFP cDNA ratios. Statistical comparisons were carried out using a one-way analysis of variance followed by Bonferroni's multiple comparison post-test comparing all pairs. The asterisks indicate significant differences from the BRET ratios produced by cotransfection of Kv1.5-RLuc and HCN2-GFP or HCN4-GFP or Kv1.5-RLuc transfected alone. All combinations of HCN isoforms are significantly greater than negative controls ($p < 0.01$) but are not different from each other ($p > 0.05$). Kv1.5-RLuc + HCN2-GFP and Kv1.5-RLuc + HCN4-GFP BRET ratios are not significantly greater than the Kv1.5-RLuc background BRET ratio ($p > 0.05$) (reproduced from **ref.** *11* with permission from the American Society for Biochemistry and Molecular Biology, Inc.).

3. Repeat the experiment and plot *n* number of duplicates as a bar graph of BRET ratios including standard error. Compare the test pairs to negative and positive controls using one-way ANOVA followed by a post-test to compare all pairs (*see* **Fig. 15.2**; *see also* **Note 9**).

15.4. Notes

1. The cell culture and transfection protocol and reagents described in this chapter have been optimized for a CHO cell heterologous expression system. However, other mammalian

expression systems and transfection reagents would also be appropriate and have been used for BRET assays *(12, 13)*.

2. DeepBlueC is air and light sensitive, thus store vial tightly sealed in the dark at −20°C and allow it to equilibrate to room temperature prior to opening.
3. In our experiments, the following cDNA constructs were made: HCN2-GFPN and HCN2-GFPC, as well as HCN2-RLucN and HCN2-RLucC such that HCN2 is expressed on the N- and C-terminal ends respectively, of either GFP or RLuc. These constructs were also made using HCN4 (HCN4-GFPN, HCN4-GFPC, HCN4-RLucN and HCN4-RLucC). We also made a construct in which Kv1.5 is expressed on the C-terminal end of the RLuc tag, to be used as a negative control (*see* **Note 6**). All tagged combinations (both N and C) should be made in order to determine the optimal combination for efficient energy transfer. Once the optimal RLuc- and GFP-tagged combination is determined, this should be kept constant across all compared partners and controls in order to accurately compare BRET ratios.
4. Once constructs are made, it is important to verify that folding, assembly or trafficking of the channel is not inhibited by the fused protein tags. In our case, we used patch-clamp electrophysiology to measure currents of expressing constructs in CHO cells, ensuring that the tagged constructs produced currents similar to their wild type counterparts.
5. The magnitude of BRET increases with increasing GFP expression to a saturating level if the expressing RLuc- and GFP-tagged constructs are interacting within 10 nm. Thus, in order to obtain optimal BRET ratios, it is important to transfect variable amounts of GFP-tagged cDNA with a constant and optimized amount of RLuc-tagged cDNA. For our experiments, we transfected 0.5 ug of RLuc-tagged cDNA in all conditions. For GFP-tagged constructs, we transfected the following amounts: 0.5, 1.0, 1.5, 2.0 and 2.5 µg. Expression levels are measured as "fold-over-background" of relative luminescence and fluorescence units, using the plate reader (*see* **Note 6**).
6. When analyzing BRET data, it is important to compare the results to appropriate controls. In our case, we felt it important to choose a negative control which is similar in structure and function to, but does not coassemble with, HCN2 or HCN4 subunits. Thus we coexpressed RLuc-tagged Kv1.5 (Kv1.5-RLuc) with either HCN2-GFP or HCN4-GFP as our negative control. In addition, we transfected Kv1.5-RLuc alone, as a control for background BRET levels. For positive controls, we cotransfected differently tagged homomeric combinations: HCN2-RLuc with HCN2-GFP, or HCN4-RLuc with HCN4-GFP, since HCN2 and HCN4 channels form functional homotetrameric channels *(14)*.

7. Direct measurement of GFP fluorescence (by exciting GFP at the correct wavelength) gives information about the level of GFP-tagged protein expression. With increasing GFP expression (while maintaining RLuc expression constant), BRET values consequently increase to eventually saturating levels if the protein interaction is specific. This can be plotted as a graph of BRET ratio vs. GFP/RLuc fold over background and fitted with a saturation curve. However, in our experiments, GFP-tagged protein expression levels remained relatively constant despite increasing the amount of transfected GFP-tagged cDNA. Thus, in our case we used a bar graph to accurately compare BRET values.
8. The emission from control wells is the background luminescence and the resulting fluorescence is either from untransfected cells (as performed in our experiments) or from cells that have only been transfected with RLuc-tagged construct.
9. In our experiments, we compared homomeric RLuc- and GFP-tagged HCN2 and HCN4 combinations (our positive control) with the coexpression of differently tagged HCN2 and HCN4 subunits. Within the limits of BRET sensitivity, the magnitudes of BRET ratios were not significantly different between all homomeric and heteromeric combinations of HCN2 and HCN4. Thus, we concluded that HCN2 and HCN4 subunit isoforms are able to self-assemble and coassemble with equal preference in CHO cells (**Fig. 15.2**).

References

1. Isacoff, E.Y., Jan, Y.N., and Jan, L.Y. (1990) Evidence for the formation of heteromultimeric potassium channels in *Xenopus* oocytes. *Nature* **345**, 530–534.
2. MacKinnon, R. (1991) Determination of the subunit stoichiometry of a voltage-activated potassium channel. *Nature* **350**, 232–235.
3. Doyle, D.A., Morais Cabral, J., Pfuetzner, R.A., Kuo, A., Gulbis, J.M., Cohen, S.L., Chait, B.T., and MacKinnon, R. (1998) The structure of the potassium channel: molecular basis of K+ conduction and selectivity. *Science* **280**, 69–77.
4. Long, S.B., Campbell, E.B., and Mackinnon, R. (2005) Crystal structure of a mammalian voltage-dependent shaker family K+ channel. *Science* **309**, 897–903.
5. Babila, T., Moscucci, A., Wang, H., Weaver, F.E., and Koren, G. (1994) Assembly of mammalian voltage-gated potassium channels: Evidence for an important role of the first transmembrane segment. *Neuron* **12**, 615–626.
6. Zheng, J. and Zagotta, W.N. (2004) Stoichiometry and assembly of olfactory cyclic nucleotide-gated channels. *Neuron* **42**, 411–421.
7. Jares-Erijman, E.A. and Jovin, T.M. (2006) Imaging molecular interactions in living cells by FRET microscopy. *Curr. Opin. Chem. Biol.* **10**, 409–416.
8. Wu, P. and Brand, L. (1994) Resonance energy transfer: methods and applications. *Anal. Biochem.* **218**, 1–13.
9. Gales, C., Van Durm, J.J., Schaak, S., Pontier, S., Percherancier, Y., Audet, M., Paris, H., and Bouvier, M. (2006) Probing the activation-promoted structural rearrangements in preassembled receptor-G protein complexes. *Nat. Struct. Mol. Biol.* **13**, 778–786.
10. Goin, J.C. and Nathanson, N.M. (2006) Quantitative analysis of muscarinic acetylcholine receptor homo- and heterodimerization in live cells: regulation of receptor down-regulation by heterodimerization. *J. Biol. Chem.* **281**, 5416–5425.

11. Whitaker, G.M., Angoli, D., Nazzari, H., Shigemoto, R., and Accili, E.A. (2007) HCN2 and HCN4 isoforms self-assemble and co-assemble with equal preference to form functional pacemaker channels. *J. Biol. Chem.* **282**, 22900–22909.
12. Lisenbee, C.S. and Miller, L.J. (2006) Secretin receptor oligomers form intracellularly during maturation through receptor core domains. *Biochemistry* **45**, 8216–8226.
13. Lavoie, C., Mercier, J.F., Salahpour, A., Umapathy, D., Breit, A., Villeneuve, L.R., Zhu, W.Z., Xiao, R.P., Lakatta, E.G., Bouvier, M., and Hebert, T.E. (2002) Beta 1/beta 2-adrenergic receptor heterodimerization regulates beta 2-adrenergic receptor internalization and ERK signaling efficacy. *J. Biol. Chem.* **277**, 35402–35410.
14. Ludwig, A., Zong, X., Stieber, J., Hullin, R., Hofmann, F., and Biel, M. (1999) Two pacemaker channels from human heart with profoundly different activation kinetics. *EMBO J.* **18**, 2323–2329.

Chapter 16

The Use of FRET Microscopy to Elucidate Steady State Channel Conformational Rearrangements and G Protein Interaction with the GIRK Channels

Adi Raveh, Inbal Riven, and Eitan Reuveny

Summary

While X-ray crystallography provides extremely high-resolution snapshot of protein structure, it lacks the ability to provide dynamic information on the processes involving conformational rearrangements of the protein. Methods to record protein conformational dynamics are present, in particular those that are based on fluorescence measurements, and are now more and more utilized in studying proteins in their natural environment. Here we describe the use of fluorescence resonance energy transfer (FRET) technique to monitor the conformational rearrangements associated with the gating of the G protein-coupled potassium channel (GIRK/Kir3.x), and its relation with the G protein subunits. The FRET technique is combined with total internal fluorescence (TIRF) microscopy, and allows the dissection of the signal originating from channel proteins that reside exclusively in the plasma membrane. Since most of the components associated with GIRK channel gating are intracellular, that involve various biochemical steps, proteins were labeled with genetically encoded variants of the green fluorescence protein and signals were acquired from live cells in culture. Using these methodologies we were able to show that gating conformational rearrangements, i.e. the opening of the channel, involve the rotation and expansion of the channel subunits cytosolic termini, along the channel's central axis. In addition, the G proteins that trigger this process reside very close to the channel, to ensure high signaling specificity and to provide temporal precision of the gating process.

Key words: TIRF microcopy, FRET, GIRK, GPCR, Fluorescence spectroscopy, Anisotropy measurements.

16.1. Introduction

Fluorescence resonance energy transfer (FRET) is a process in which energy is nonradiatively transferred from an excited fluorophore (the donor) to a nearby chromophore (the acceptor). This process depends on the dipole–dipole coupling between the two

Jonathan D. Lippiat (ed.), *Methods in Molecular Biology, Potassium Channels, vol. 491*

Book doi: 10.1007/978-1-59745-526-8

and on the distance between the donor and the acceptor molecules. In general these two variables will determine the efficiency of transfer. In more practical situations, where the donor and the acceptor are free to rotate around a certain axis, the distance between the donor and the acceptor is the main determinant influencing the efficiency of resonance transfer *(1)*. The dependence of the transfer efficiency on distance is very high, e.g., raised to the sixth power. Thus minute change in the distance between the donor and the acceptor chromophores is translated to a big change in FRET efficiency. For this reason the FRET techniques has been used as an inter- and/or intramolecular ruler, operating in the range between 1 and 10 nm *(2)*. The FRET technique also has its limitations and various considerations have to be taken once quantitation is in mind *(3–5)*. One of the ways to estimate the FRET efficiency between two fluorophores is to rely on the amount of donor emission, the closer the fluorophores the larger the dequenching (reduction in emitted photons) of the donor *(5)*. Once one has the mean of eliminating the acceptor molecule, the ratio of donor emission in the presence of the acceptor to a condition where the acceptor is nonfunctional, e.g., bleached, will determine the FRET efficiency *(6, 7)*.

There are many ways to detect the emitted fluorescence; the most conventional one is to use a specific emission filter to allow only photons within a certain wavelength to pass through, and to be detected by a photomultiplier or by an avalanche photodiode. This arrangement has a high temporal resolution, but lacks the spectral information. This may be important when information is required regarding the spectral characteristics of the emitted photons. In our studies we used a spectrometer and a back illuminated CCD array to capture spectral information from our sample. The signal intensities at the expected emission peak of the donor were measured before and immediately after photo-bleaching of the acceptor, and then were used to calculate the FRET efficiency (E). Distances between the donor and the acceptor chromophores were then calculated based on $E = R_0^6/(R_0^6+R^6)$, where R_0 (Förster distance) is the distance when $E = 0.5$. $R_0=(9.7\times10^3 J\phi_D n^{-4}\kappa^2)^{1/6}$, 50.4 Å for CFP/YFP pair *(8)*. In our previous studies *(9, 10)* we utilized the advantages of FRET microscopy to study the rearrangement of G protein-coupled potassium channels (GIRK/Kir3.x) upon their gating and their mode of interaction with G proteins. GIRKs are inwardly rectifying K^+ channels that generate slow, inhibitory postsynaptic potentials upon activation by *Pertussis*-toxin-sensitive G protein-coupled receptors (GPCRs) *(11)*.

GIRK activation requires the binding of Gβγ to the channel. Upon neurotransmitter release from the presynaptic cleft and GPCR stimulation at the postsynaptic site, GTP is exchanged for GDP on the Gα subunit of the G protein. This, in turn, leads to the dissociation of a Gβγ subunit from the Gα subunit, to freely

interact with the channel's Gβγ binding domains. The binding of Gβγ induces a conformational change of the channel promoting the opening of the permeation pore to allow the selective flux of K^+ ions through it. The flow of ions is mainly in the outward direction which then hyperpolarizes the postsynaptic membrane, to produce a reduction in excitation.

There is no full length three-dimensional structure of the GIRK channel. Nevertheless, the structure of the conserved regions (regions that are shared by other inwardly rectifying channels from bacteria to vertebrates, of both the N- and C-terminal cytosolic domains) have been solved by X-ray crystallography *(12–14)*. These structures of the cytosolic domains in conjunction with solved structures of the membrane core of other similar transmembrane potassium selective channels, KcsA, MethK and KirBac, provide a general static view of the channels presumably in the closed and open conformations *(12, 15–17)*; for a review *see* **ref.** *18*. Despite the knowledge accumulated as described above, we still do not have a detailed mechanistic understanding of the conformational changes that allow channel gating of inwardly rectifying potassium channels, in particular those that are activated by intracellular modulators, like G proteins.

We took advantage of the known stoichiometry of the GIRK channels and the fact that one of the subunits, GIRK1, is unable to form homotetramers. In our work we used the cardiac version of GIRK channels, mainly heterotetramers of GIRK1/GIRK4 in a 1:1 ratio, thought to be arranged in a fourfold symmetry *(19–21)*. This turns out to be of a great advantage, since FRET pairing of known stoichiometry allows quantitative interpretation of the FRET signals. We chose to tag both the cytoplasmic N- and C-termini of these subunits by the fluorescent FRET pair CFP (the donor) and YFP (the acceptor) *(8, 22)*. CFP and YFP are a good FRET pair, having a relatively large overlap between CFP emission spectrum and YFP absorption spectrum, which is crucial for efficient energy transfer. In addition, their absorption spectra enable selective excitation of the donor with minimal or complete absence of acceptor excitation. It is very important to test the functionality of the tagged channel subunits. All fused constructs were thus imaged to validate proper translocation to the plasma membrane, and tested electro-physiologically for their functionality *(10)*.

Measuring FRET between tagged neighboring subunits in each combination (two termini for each of the subunits) allowed us to measure the distances between the neighboring subunits and to translate each distance to a point in X, Y, Z space.

Two kinds of FRET measurements were performed, to elucidate structural changes associated with channel gating and to understand the relationship between the channel and the G protein subunits, at rest and during activation. The former measurements were conducted for both closed and open channels (by both

over-expression of Gβγ or following activation of the A1 adenosine receptor). Comparison of the space representation of the channel's cytosolic ends in its closed, vs. open states enabled us to create a model that predicts the general vectorial change associated with channel gating. The relationships between the GIRK channel and the G proteins subunits were studied by tagging the channel subunit with the donor fluorophore and the appropriate G protein subunits with the acceptor. In both types of measurements, the technicality of the experiment is similar and thus will be discussed without referring to any particular set of experiments independently. In some cases, we will describe the detailed calculation methodology which is specific for the specific type of experiment presented.

To increase the confidence that changes seen in FRET efficiency are indeed due to changes in the distance between the fluorophores, one has to verify that the relative mobility of the donor and/or the acceptor is not changing during the conformational transitions. We thus also describe the methodologies used to record the acceptor fluorescence anisotropy. Fluorescent anisotropy, *r*, is a measure of the extent of polarization of the sample. Upon excitation with polarized light, the emission from many samples is polarized. However, rotational diffusion of the fluorophores can lead to depolarization of the emission and thus to a reduced excitation of the neighboring acceptor *(1)*. In our experiments, after correcting for the microscope polarization characteristics (see below), the apparent acceptor anisotropy values were similar for both unstimulated and stimulated cells, indicating that although the acceptor is attached to the channel, fluorophores' free mobility is not affected following channel gating. Hence, constraints on dipole orientation are unlikely to substantially affect the FRET efficiency or account for FRET efficiency changes detected upon channel activation.

In most cases when intracellular fluorescent tags are utilized, they are encoded genetically as fusion to the protein of interest. This approach introduces a complication when used on membrane proteins, or any proteins that have a well-defined subcellular distribution. To specifically image those proteins in their target location, means of spatial control of either the excitation or the emission is desired. In the case of the GIRK channels the spatial control becomes very important, mainly due to the fact that a substantial amount of the mature fluorescently tagged channels are already present in many intracellular compartments. Therefore, to specifically monitor channel residing exclusively in the plasma membrane, we used total internal fluorescence (TIRF) *(23)*. In TIRF microscopy, on reaching the critical angle (and beyond), the excitation beam totally changes its direction and is reflected from the cover glass. This process is mainly due to the difference of the refraction index of the cover glass and the water (for more reading *see* **refs.** *23* and *24*). Once the excitation beam is reflected from the glass, it generates an electromagnetic standing wave, the evanescent wave (perpendicular to the cover

glass), that has the exact spectral characteristics of the excitation light. The power of this evanescent wave drops exponentially within 100–200 nm, depending on the excitation angle and wavelength of the excitation beam. This useful characteristic of the evanescent wave allows the selective excitation of objects very close to the cover glass, such as the plasma membrane of cells.

Using the described methods we were able to monitor the conformational rearrangements of the GIRK channels during gating and the intricate relationship of this channel with the G proteins, both at rest and during activation *(9, 10)*.

Following is a detailed description of the methodology used to obtain these results as well as points that require special attention.

16.2. Materials

16.2.1. Preparation of Poly-L-Lysine Coated Cover Slips

1. Ø24 mm number 0 cover slips (*see* **Note 1**).
2. 1-M NaOH (keep safety precautions and work in chemical hood).
3. 0.01% Poly-l-lysine. Store at 4°C.
4. Borate buffer solution: Boric acid (3.1 g/l), Borax (4.75 g/l). Store at 4°C.
5. Sterile double-distilled water (DDW).
6. 0.22-µm syringe filter, syringe.
7. 6-well plates.
8. Aluminum foil.
9. Autoclaved glass pipettes and 2-, 5-, and 10-sterile plastic pipettes.

16.2.2. Cell Culture

1. Human embryonic kidney (HEK 293) cells.
2. T-25 Tissue culture flasks.
3. 0.25% Trypsin–EDTA.
4. Dulbecco's Modified Eagle's Medium (DMEM), HEPES modification, without L-Glutamine.
5. DMEM/F-12 (HAM) 1:1 without L-Glutamine.
6. L-Glutamine solution, 200 mM.
7. Pen-Strep solution (penicillin 10,000 units/ml; Streptomycin 10 mg/ml).
8. Fetal calf serum (FCS).
9. 15-ml conical centrifuge tubes, 1.5-ml eppendorf tubes.
10. 35-mm tissue culture dishes.
11. Autoclaved glass pipettes and 2-, 5-, and 10-sterile plastic pipettes.

16.2.3. Transfection

1. Plasmids of GIRK1 and GIRK4 subunits tagged with CFP or YFP on their N- or C-termini. The subunits are fused to pCMV-CFP/YFP N1 or C1 vectors (Clontech). (Available on request) (*see* **Note 2**).
2. cDNA of Adenosine type 1 receptor (A1r) or any other alternative Gi/o GPCR.
3. Fugene transfection reagent (Roche). Store at –20°C and keep capped.
4. Dulbecco's Modified Eagle's Medium (DMEM), HEPES modification, without L-Glutamine.
5. 1.5-ml eppendorf tubes.

16.2.4. TIRF Microscopy and Spectroscopy

1. In-house designed chamber suitable for inverted-microscopy imaging (or any other commercial alternative).
2. Dulbecco's Phosphate Buffered Saline (PBS) with $MgCl_2$ and $CaCl_2$: 0.133-g/l $CaCl_2$, 0.1-g/l MgCl, 0.2-g/l KCl, 0.2-g/l KH_2PO_4, 8.0-g/l NaCl, 1.15-g/l Na_2HPO_4 (pH 7.1–7.5).
3. Olympus 60X/1.45NA objective or equivalent from Zeiss or Nikon.
4. Olympus IX70 inverted microscope (any inverted microscope is suitable).
5. Dichroic mirrors: 465DCLP, 520DCLP; Emission filters: HQ485/30M, HQ535/30M and E470LP (all from Chroma) or alternative filter sets that match the spectral requirements for CFP-YFP FRET imaging and laser excitation.
6. Argon laser for CFP excitation using the 454-nm laser line. 440- or 405-nm diode lasers are also suitable for the CFP/YFP pair.
7. TILL-TIRF microscope condenser (TILL photonics).
8. Oriel MS127i 1/8 m Imaging Spectrograph attached to the microscope side port via C-mount adaptor (light was collimated and refocused into the spectrograph).
9. 16-bit back illuminated CCD detector 256 × 1024 pixels (Andor, Belfast).
10. Xenon arc light source or an Argon laser for acceptor photobleaching with its 514-nm line.
11. Polychrome II monochromator (Till Photonics).
12. MCD software (Andor, Belfast) for control and data acquisition from the CCD detector.
13. Single mode, polarizing maintaining fiber (Point Source) matched to 400–500 nm wavelength.

16.2.5. Anisotropy Measurements

1. Polarizing beamsplitter cube. Light was collimated before entering the polarizing cube using the appropriate lenses and later refocused into the photomultipliers.
2. Two H7711-03 photomultiplier tubes (Hamamatsu Photonics) or equivalent. The photomultipliers gain factor was calibrated using the same light source reflected from glass.
3. Digidata 1322A digitizer (Axon).

16.2.6. Data Analysis

1. Excel or an equivalent electronic spreadsheet.
2. Matlab (The Mathworks).

16.3. Methods

16.3.1. Preparation of Clean Poly-L-Lysine Coated Cover Slips (see Note 3)

1. Soak Ø24 mm number 0 cover slips for 3 h in 1-M NaOH solution (*see* **Note 4**).
2. Carefully wash the cover slips with DDW for 1 h.
3. Repeat **step 2** three times, remove the DDW, cover with foil and let the cover slips dry over night in an oven set to a temperature of 250°C.
4. Dissolve Poly-L-lysine (PLL, 0.01%) in the borate buffer solution (1:4 ratio). Filter the PLL solution in a 0.22-µm syringe filter, and pipette 200 µl of it on the center of each cover slip, placed in 6-well plates (*see* **Note 5**). Wrap the 6-well plates with aluminum foil and store overnight outside the hood to avoid PLL evaporation.
5. Add 2 ml of sterilized autoclaved DDW to each well and use suction to wash out the excess PLL fluid. Wash with 4 ml of sterilized DDW for 2 h and remove the DDW. Repeat the last wash once more, remove the water and dry the cover slips in the hood. Wrap the 6-well plate with aluminum foil and store in a clean place (*see* **Notes 6** and **7**).

16.3.2. Cell Culture (see Notes 8 and 9)

1. *Day 1.* Prepare growth-medium composed of DMEM containing 10% FCS, 1% L-Glutamine, and 2% Pen-Strep solution. Aspirate the media from T-25 tissue culture flasks grown to ~90% confluence of HEK293 cells. Treat the cells with 0.5 ml of 0.25% Trypsin–EDTA for 1–2 min in a 37°C incubator. Observe under binocular that the cells become rounded and detach from flask bottom. Gently tap the flask to help cell displacement and then immediately block trypsinization by applying 7 ml of growth-medium to the flask. Re-suspend the cells by gently pipetting them in the medium using sterilized glass pipette to obtain a single

cell suspension. Transfer the cell suspension to a sterile 15-ml conical centrifuge tube. Spin the cells down at 150×*g* for 7 min, discard the supernatant without disturbing the cell pellet. Re-suspend the cells in 3 ml of fresh growth-medium, pipetting gently to dissociate pellet to a single cell suspension. Count the cells using a hemocytometer. Plate 3×10^5 cells/plate homogenously in 35-mm tissue culture dishes containing 3-ml fresh growth-medium for each transfection planned. Maintain overnight at 37°C in a humidified atmosphere of 95% air, 5% CO_2.

2. *Day 2*. Transfect the cells with the plasmids of study (*see* **Subheading 16.3.3**).
3. *Day 3*. Prepare serum-free medium (*see* **Note 10**): DMEM/F-12 containing 1% L-Glutamine and 2% Pen-Strep solution. Aspirate the medium from the 35-mm tissue culture dishes containing the transfected cells. Treat the cells with ~150 µl (4–5 drops) of 0.25% Trypsin–EDTA for 1 min in 37°C incubator. Gently tap the tissue culture dishes to help cell displacement from the dish and immediately block trypsinization by applying cells with 1 ml of growth-medium. Re-suspend the cells by gently pipetting the cells in the medium to obtain a single cell suspension. Transfer the cell suspension to a sterile 1.5-ml eppendorf tube. Spin the cells down at 150×*g* for 7 min. Discard the supernatant without disturbing the cells pellet. Re-suspend the cells in 1 ml of fresh serum-free medium. Pipette gently to dissociate pellet to a single cell suspension. Apply 150 µl of the serum-free medium in the center of each cover slip, and then add homogenously 15–20 µl (*see* **Notes 11** and **12**) of the cells containing media to achieve moderate density of cells on the cover slips. Incubate the 6-well plates, with cells plated on the cover slips, for ~10 min in the 37°C humidified incubator. Clarify under binocular the desired density of cells per cover slip, and gently apply 2 ml of serum-free medium in each well. Maintain overnight at 37°C in a humidified atmosphere.

16.3.3. Transfection (Day 2) (see Note 13)

1. Plan GIRK transfections in different subunit combinations so that while one subunit is tagged by CFP the second is tagged by YFP (*see* **Notes 14–16**). Pipette the plasmids mixture to a sterile eppendorf tube (tube A) per transfection. Add a GPCR of the Gi/o subfamily for activating the channel. Riven et al. ***(10)*** used the Adenosine 1 receptor (A1r) for this purpose.
2. Prepare a sterile tube (tube B) for each transfection containing DMEM (*see* **Note 17**) and add Fugene directly into it. The DNA:Fugene:DMEM ratio for reaction should be 2 (in µg):5(in µl):100(in µl), respectively. Incubate tube B for 5 min at room temperature.

3. Add the content of tube B to tube A dropwise, with gentle vortexing. Incubate for 15 min at room temperature.
4. Aspirate the medium from the cell culture dishes containing the cells from day 1 and add 2 ml of 37°C prewarmed DMEM (*see* **Note 17**).
5. Add the content of tube A from **step 3** to the cells dropwise. Swirl the dish to ensure even dispersal. Incubate the cells for 5 h at 37°C in a humidified atmosphere.
6. Aspirate the DMEM (containing transfection mixture) from the tissue culture dishes containing the transfected cells. Add 2 ml of preheated growth-medium.

16.3.4. TIRF Microscopy and Spectroscopy (Day 4)

1. Turn on the laser to let it stabilize (for at least 15 min) and cool down the spectrograph CCD to –30°C to minimize dark noise.
2. Mount a cover slip in the imaging chamber; wash the cells carefully twice with PBS and place on the microscope stage. Image the cells using a 60X/1.45NA (*see* **Note 18**) and focus on the cells using transmitted light.
3. A cell with a defined cytoplasm should be chosen and magnified using the 1.5× magnification tube lens to have an effective magnification of 90× (*see* **Note 19**).
4. To validate cell transfection, illuminate the cell with the 454-nm line of the Argon laser for CFP excitation. CFP fluorescence is selectively inspected using 465DCLP dichroic and HQ485/30M emission filters (*see* **Note 20**).
5. Focus the TIRF system: After focusing the object on the desired plane, laser beam should be focused into the back focal plane of the object using the focusing wheel of the TIRF condenser. Set the laser beam in the epi configuration and focus the TIRF condenser to produce a parallel beam (leading to a minimal spot when projected on a distant surface like the ceiling) (*see* **Note 21**). Turn the angle adjustment screw on the TIRF condenser until the laser beam is eventually totally internally reflected, and signal fluorescence is limited to the depth of evanescence wave excitation. Out of focus laser will not produce the appropriate TIRF image.
6. Spectroscopy: Switch to 465DCLP dichroic and E470LP emission filters for spectroscopic measurements using the 454-nm Argon line.
7. Set the spectral calibration of the spectrograph and determine the data type in the software to be background subtracted.
8. Determine the exposure time for data collection to 50–200 ms in the software (*see* **Note 22**) and use the lowest possible laser intensities to minimize bleaching and yet provide a reliable fluorescence emission spectra.

9. Collect background spectra. The best way to collect background spectra is to move to an area in the cover glass containing an untransfected cell.
10. Collect a spectrum from a transfected cell.
11. Switch to the 520DCLP dichroic and HQ535/30M emission filters and illuminate the sample in the epi configuration with 514 ± 5 nm for 500 s using the Polychrome II monochromator to bleach the acceptor (*see* **Notes 23–25**). This can also be done with a 514-nm argon laser in a much shorter time (exposure time should be determined on individual basis, depending on the laser power/optical path). Switch back to 465DCLP dichroic and E470LP emission filters.
12. Collect cell emission spectrum immediately following the acceptor bleaching.
13. To evaluate the conformational changes following GPCR activation, expose cover slips containing transfected cells to 0.5–2 mM of adenosine (in PBS) (*see* **Note 26**). Then estimate FRET efficiencies in the same procedures as described above (*see* **Note 27**).

16.3.5. Anisotropy Measurements

1. Use polarizing cube beamsplitter to split the collimated emission signal from the sample to its parallel and perpendicular components (*see* **Note 28**).
2. Record simultaneously the parallel and perpendicular components of the acceptor emission signal using the two photomultiplier tubes.
3. Collect background signals from an area with cells not expressing the construct and subtract the two background components from the appropriate main signal.
4. Calculate the anisotropy, r, according to $r=(I_{||}-I_{\perp})/(I_{||}+2I_{\perp})$, where the $I_{\perp}$ and $I_{||}$ are the perpendicular and the parallel emitted light (background corrected) with respect to the polarized excitation light, respectively.
5. Repeat the procedure for both unstimulated and stimulated cells to check for changes in the extent of donor-acceptor random mobility under the two gating modes of the channel.

16.3.6. Data Analysis

1. Measure the intensity of the peak of CFP emission (at 490 nm) from spectra taken before (I_{DA}) and after (I_{D}) acceptor photobleaching.
2. Calculate FRET efficiency, E, using the equation $E = 1 - I_{DA}/I_{D}$.
3. Calculate the distance R between donor and acceptor, using the Förster equation where $E = 1/(1 + (R/R_0)^6)$ or $E = 1/(1 + (R/R_0)^6/2)$ in cases where donor is assumed to have equal distance to both acceptors in the tetrameric arrangement (in the

combinations of 4N-*Cy*/1N-*Yl* and 4C-*Cy*/1C-*Yl*) (*see* **Note 29**). R_0 (Förster distance) is 50.4 Å in the case of CFP/YFP pair *(8)*.

4. Do the same calculations for agonist treated and nontreated cells.
5. The three-dimensional vector coordinates of the tagged fluorophores were computed using the Euclidean distances between the chromophores (calculated from the FRET efficiency) and an in-house computer program (MatLab 6.1 release 12.1), with convergence within a 1% error in distance. The model assumes (1) a fourfold symmetry for channel assembly and (2) the distance of the C-terminal end from the membrane is greater than the distance of the N-terminal end.

16.4. Notes

1. We found it necessary to work with a reliable brand of cover slips to achieve good TIRF images. Many cheap brands claim for the appropriate refractive index of their cover slips but yielded poor TIRF images. It is very important to have a perfect match between the objective lens, the immersion oil and the cover glass. We found that Marienfeld microscope cover glass and Olympus nonfluorescence immersion oil (nd = 1.516) is a perfect combination with our Olympus objective (1.45NA 60X-first generation).
2. The nomenclature is consistent with Riven et al. *(10)* such that 4N-*Cy* stands for a GIRK4 subunit tagged by CFP on its N-Terminus, etc.
3. This step is crucial to get a tight attachment between the cells and the cover slips. Hence, it is important for obtaining high-quality TIRF images of the membrane, and to minimize the background level of the cover slip.
4. Since NaOH is a strong base, work in a chemical hood using safety precautions.
5. From this step on work is done under sterile conditions.
6. PLL wash is important since excess PLL is toxic to cells. The extended DDW wash periods are needed since the wash is mostly through a diffusion process.
7. It is possible to use the coated cover slips also a few days after their preparation if kept sterile and closed in a clean place.
8. Trypsin and media should be prewarmed to 37°C.
9. Sterile techniques should be maintained. All liquid should be filtered using 0.22-μm filters and all glassware has to be autoclaved before used.

10. Serum-free medium is used in order to avoid auto fluorescence. Cells maintained in serum-free medium tend to appear less round and to demonstrate many membrane projections.
11. The exact volume of cells added to a cover slip should be evaluated taking into consideration the need to achieve the final cell's density such that the field recorded through-the-objective will include a single cell in most cases.
12. Some portion of the transfected cells can be transferred to tissue culture dishes with the growth-medium, and be maintained in 37°C humidified incubator. The cells will grow in the presence of serum and can be plated on cover slip on *day 4* and imaged on *day 5*.
13. We described here transfection protocol using Fugene reagent that worked successfully. However, other transfection methods can be used as well. Besides the obvious need for low toxicity level and high transfection efficiency, check also for transfection effect on cells autofluorescence. For example, after calcium chloride transfections, cells contained many intracellular autofluorescent spots.
14. Keep subunit transfection ratio of GIRK1:GIRK4 of 1:5, respectively. This ratio was achieved empirically. GIRK1 contains ER retention signal and therefore cannot translocate to the membrane without the assembly with GIRK4. On the contrary, GIRK4, which does not have an ER retention signal, can translocate on its own to the membrane and form functional GIRK4 homotetramers, biasing the FRET evaluations.
15. The following plasmids amounts were transfected in the study by Riven et al. ***(10)*** (plasmid weight in μg is in parentheses): 4N-Cy(0.2)/1C-Yl(1)/A1r(1); 4N-Cy(0.2)/1N-Yl(1)/A1r(1); 4C-Cy(0.2)/1N-Yl(1)/A1r(1); 4C-Cy(0.2)/1C-l(1)/A1r(1) (*see* **Note 2** for nomenclature).
16. For efficient transfections we recommend addition of at least 2 μg of total weight of plasmids, and not to exceed 15-μl total volume of DNA in the transfection reaction.
17. Transfections should be made in serum-free medium. Both DMEM and Optimem successfully worked for this purpose.
18. We recommend comparing different immersion oils for obtaining the best TIRF images. Pay attention to matching immersion oil that has minimum fluorescence and the best match of refractive index for your objective under the excitation wavelength of use.
19. If cells were plated at a moderate density, using 90× total magnification will result in a single cell within the field of detection. Since the detection is through-the-objective, care is given such that each spectrum will represent a single cell.
20. For selective inspection of YFP emission and for YFP bleaching use 520DCLP dichroic and HQ535/30M emission filters.

21. If the laser beam exiting the objective is not parallel, part of the laser light might not be totally internally reflected causing background fluorescence.
22. Short exposure time is desired to minimize donor bleaching. Bleached donor will underestimate FRET efficiency values.
23. Eliminate detector exposure to the extended strong Xenon or Argon illumination during acceptor photobleaching.
24. The time needed for total acceptor bleaching should be determined for each setup beforehand by monitoring acceptor emission intensity during its continuous illumination by the Xenon or with an equivalent laser source.
25. It is important to establish that the CFP is not affected by this procedure.
26. The appropriate exposure time of cells to the agonist should be determined empirically. In our experimental setup, 1-h exposure to 0.5–2 mM of adenosine was necessary to allow full equilibration of the GPCR situated in close proximity to the cover slip.
27. Alternatively, the activation of the GIRK channel can be evaluated by cotransfecting Gβγ subunits to constitutively activate the channel *(25)*.
28. Align the polarizing cube properly. The laser reflections from a glass cover slip can be used to examine the alignment. The parallel axis should have the maximal intensity, where the perpendicular line should be at minimum. Typically, polarization cube (Thor Labs) can polarize light at 98 and 2% for the parallel and perpendicular line, respectively.
29. In the case of 4N-*Cy*/1N-*Yl* and 4C-*Cy*/1C-*Yl*, a correction to the equation is needed since the donor resonance energy is transferred to two acceptors located in identical distances from the donor. In the other combinations the distance between the donor and the closer acceptor dominates in terms of the FRET *(10)*.

References

1. Lakowicz, J. R. (2006) Principles of fluorescence spectroscopy, 3rd Edition. Springer, Berlin.
2. Stryer, L. (1978) Fluorescence energy transfer as a spectroscopic ruler. *Annu. Rev. Biochem.* **47**, 819–846.
3. Wallrabe, H. and Periasamy, A. (2005) Imaging protein molecules using FRET and FLIM microscopy. *Curr. Opin. Biotechnol.* **16**, 19–27.
4. Nguyen, A. W. and Daugherty, P. S. (2005) Evolutionary optimization of fluorescent proteins for intracellular FRET. *Nat. Biotechnol.* **23**, 355–360.
5. Jares-Erijman, E. A. and Jovin, T. M. (2003) FRET imaging. *Nat. Biotechnol.* **21**, 1387–1395.
6. Miyawaki, A. and Tsien, R. Y. (2000) Monitoring protein conformations and interactions by fluorescence resonance energy transfer

between mutants of green fluorescent protein. *Methods Enzymol.* **327**, 472–500.

7. Bastiaens, P. I., Majoul, I. V., Verveer, P. J., Soling, H. D., and Jovin, T. M. (1996) Imaging the intracellular trafficking and state of the AB5 quaternary structure of cholera toxin. *EMBO J.* **15**, 4246–4253.
8. Tsien, R. Y. (1998) The green fluorescent protein. *Annu. Rev. Biochem.* **67**, 509–544.
9. Riven, I., Iwanir, S., and Reuveny, E. (2006) GIRK channel activation involves a local rearrangement of a preformed G protein channel complex. *Neuron* **51**, 561–573.
10. Riven, I., Kalmanzon, E., Segev, L., and Reuveny, E. (2003) Conformational rearrangements associated with the gating of the G protein-coupled potassium channel revealed by FRET microscopy. *Neuron* **38**, 225–235.
11. Luscher, C., Jan, L. Y., Stoffel, M., Malenka, R. C., and Nicoll, R. A. (1997) G protein-coupled inwardly rectifying K^+ channels (GIRKs) mediate postsynaptic but not presynaptic transmitter actions in hippocampal neurons. *Neuron* **19**, 687–695.
12. Kuo, A., Gulbis, J. M., Antcliff, J. F., Rahman, T., Lowe, E. D., Zimmer, J., Cuthbertson, J., Ashcroft, F. M., Ezaki, T., and Doyle, D. A. (2003) Crystal structure of the potassium channel KirBac1.1 in the closed state. *Science* **300**, 1922–1926.
13. Nishida, M. and MacKinnon, R. (2002) Structural basis of inward rectification, cytoplasmic pore of the G protein-gated inward rectifier GIRK1 at 1.8 A resolution. *Cell* **111**, 957–965.
14. Pegan, S., Arrabit, C., Zhou, W., Kwiatkowski, W., Collins, A., Slesinger, P. A., and Choe, S. (2005) Cytoplasmic domain structures of Kir2.1 and Kir3.1 show sites for modulating gating and rectification. *Nat. Neurosci.* **8**, 279–287.
15. Doyle, D. A., Cabral, J. M., Pfuetzner, R. A., Kuo, A., Gulbis, J. M., Cohen, S. L., Chait, B. T., and MacKinnon, R. (1998) The structure of the potassium channel, molecular basis of K^+ conduction and selectivity. *Science* **280**, 69–77.
16. Jiang, Y., Lee, A., Chen, J., Cadene, M., Chait, B. T., and MacKinnon, R. (2002) Crystal structure and mechanism of a calcium-gated potassium channel. *Nature* **417**, 515–522.
17. Nishida, M., Cadene, M., Chait, B. T., and MacKinnon, R. (2007) Crystal structure of a Kir3.1-prokaryotic Kir channel chimera. *EMBO J.* **26**, 4005–4015.
18. Bichet, D., Haass, F. A., and Jan, L. Y. (2003) Merging functional studies with structures of inward-rectifier K^+ channels. *Nat. Rev. Neurosci.* **4**, 957–967.
19. Tucker, S. J., Pessia, M., and Adelman, J. P. (1996) Muscarine-gated K^+ channel, subunit stoichiometry and structural domains essential for G protein stimulation. *Am. J. Physiol.* **271**, H379–H385.
20. Silverman, S. K., Lester, H. A., and Dougherty, D. A. (1996) Subunit stoichiometry of a heteromultimeric G protein-coupled inward-rectifier K^+ channel. *J. Biol. Chem.* **271**, 30524–30528.
21. Sadja, R., Alagem, N., and Reuveny, E. (2002) Graded contribution of the Gbeta gamma binding domains to GIRK channel activation. *Proc. Natl Acad. Sci. USA* **99**, 10783–10788.
22. Heim, R. and Tsien, R. Y. (1996) Engineering green fluorescent protein for improved brightness, longer wavelengths and fluorescence resonance energy transfer. *Curr. Biol.* **6**, 178–182.
23. Axelrod, D. (1989). Total internal reflection fluorescence microscopy. *Methods Cell Biol.* **30**, 245–270.
24. Axelrod, D., Thompson, N. L., and Burghardt, T. P. (1983) Total internal inflection fluorescent microscopy. *J. Microsc.* **129**, 19–28.
25. Reuveny, E., Slesinger, P. A., Inglese, J., Morales, J. M., Iniguez-Lluhi, J. A., Lefkowitz, R. J., Bourne, H. R., Jan, Y. N., and Jan, L. Y. (1994) Activation of the cloned muscarinic potassium channel by G protein beta gamma subunits. *Nature* **370**, 143–146

Chapter 17

The Voltage-Clamp Fluorometry Technique

Chris S. Gandhi and Riccardo Olcese

Summary

Ion channels are the cell's gatekeepers. These proteins selectively allow ionic current to flow down its electrochemical gradient. In some cases, specialized chemical or voltage sensing domains respond to environmental changes and signal the cell to adjust its internal chemistry in response to its surroundings. Because of their importance in cell function, channels have been the focus of intense study at the functional and structural level. Here we describe the optical technique voltage-clamp fluorometry (VCF) which is used to monitor the functional state and probe the structural rearrangements that take place as ion channels are activated by voltage. VCF combines electrophysiology, molecular biology, chemistry, and fluorescence into a single technique. Our focus is on voltage-gated ion channels, but the technique described can be applied to other proteins. We describe the cut open vaseline gap configuration (COVG) for VCF recording.

Key words: Ion channel, Electrophysiology, Voltage-clamp, Cut open voltage-clamp, Voltage-clamp fluorometry, TMRM, PyMPO, Cysteine labeling, Conformational change.

17.1. Introduction

Biophysicists have traditionally used a combination of electrophysiology, molecular biology, and chemistry to study ion channels. Voltage-clamp fluorometry (VCF) was originally developed in the Isacoff laboratory *(1)* and is the descendant of two important techniques (1) traditional oocyte-based two-electrode voltage clamp (TEVC) and (2) scanning cysteine accessibility mutagenesis (SCAM).

TEVC is a standard and straightforward electrophysiology technique widely used for studying channels expressed in *Xenopus* oocytes. Stefani, in collaboration with Bezanilla, has subsequently improved and modified the oocyte voltage-clamp in the

Jonathan D. Lippiat (ed.), *Methods in Molecular Biology, Potassium Channels, vol. 491*

Book doi: 10.1007/978-1-59745-526-8

cut open vaseline gap (COVG) variation *(2)*. Although COVG is more complicated to implement than TEVC, it offers faster and more uniform control over voltage as well as a low noise, high frequency response (1.2 nA rms at 5 KHz and 24 μS time constant) making it an ideal recording method to capture fast kinetics (e.g., gating current) and to use when a large signal-to-noise ratio is important.

The SCAM approach was developed by the Karlin laboratory and used to probe the topology of the nicotinic acetylcholine receptor *(3)*. Briefly, the reactivity of a small thiol specific reagent to an introduced cysteine is measured while the conformation of the protein is controlled either by application of ligand or voltage. A reactive site is interpreted to be "accessible" and a nonreactive site is interpreted to be "inaccessible" to the probe. Numerous groups have applied this technique to study the voltage-dependent rearrangements of ion channels, and their combined results *(4)* are the basis for the proposed outward movement of the voltage sensing membrane segment S4 during channel activation. The optically based measurement VCF *(1)* is a natural extension of this chemical approach.

The idea behind VCF is relatively simple. A channel of interest is engineered to include a single reactive cysteine residue and expressed in *Xenopus* oocytes. The cysteine is then selectively modified with an organic thiol-reactive fluorophore probe (**Fig. 17.1**). Structural rearrangements during channel gating are assayed via differences in fluorescence emission caused by changes in the probe exposure to solvent (e.g., moving from aqueous to lipid phases) and/or proximity to quenching groups. The fluorescence is typically monitored at a fixed wavelength with a photomultiplier tube, CCD camera, or photodiode while the gating state of the channel is controlled with a voltage-clamp. In practice, a change in protein structure near the probe is reported as a dimming or brightening of fluorescence (ΔFs). These reports occur in real-time and monitor the kinetics of protein motion. For example when a fluorophore is attached to the S4 segment of K_v channels, the kinetics of the change in fluorescence intensity reflect the kinetics of S4 movement *(5, 6)*. Additionally, since a fluorophore reports changes in structure near its attachment site, the optical signal can help determine the contribution of different parts of the protein to distinct steps in the kinetic pathway *(6, 7)*. In spite of some technical limitations (e.g., in general only extracellularly exposed cysteines are accessible to form covalent bonds with thiol-reactive probes), VCF has proven to be a successful approach to explore conformational changes in voltage and ligand-gated channels and has produced invaluable information about the dynamic processes underlying ion channel operation. Several pioneering examples can be found in the references *(1, 5–12)*. Importantly, VCF can resolve conformational changes

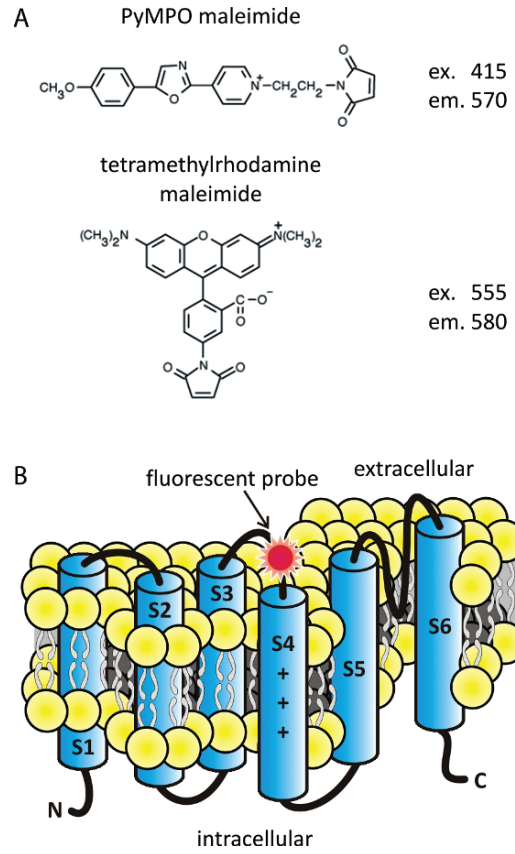

Fig. 17.1. Thiol-reactive fluorophores label unique cysteines placed at strategic positions in the channel protein. These fluorophores, sensitive to the surrounding environment, can report conformational changes of the channel. (**a**) Two commonly used fluorophores used in voltage-clamp fluorometry (VCF) and their excitation (ex.) and emission (em.) maxima. (**b**) A schematic of one channel subunit embedded into the plasma membrane. A single labeled cysteine, substituted in the S3–S4 loop, reports voltage dependent rearrangements of this region (*see* **Fig. 17.6**).

of noncharged regions of a protein, thereby providing complementary information to electrophysiology studies.

17.2. Materials

17.2.1. Oocyte Isolation and Culture

1. 10× Ca^{2+}-Free Solution for oocyte defoliculation. 830 mM NaCl, 20 mM KCl, 10 mM $MgCl_2 \cdot 6H_2O$, 100 mM HEPES. Dissolve the above in 800 mL of ddH_2O. Adjust pH to 7.6 with NaOH. Adjust final volume to 1 L. Sterilize through 0.2 µM filter. Dilute to 1× Ca^{2+}-Free as needed. Store both solutions at room temperature.

2. Collagenase II and III Cocktail for oocyte defolliculation. To 30 mL of 1× Ca^{2+}-Free add 15 mg of Type II collagenase and 25 mg of Type III collagenase. Store collagenase stocks at −20°C. Prewarm bottles to room temperature before opening. Use cocktail immediately, and do not store.
3. 10× ND96 Solution for oocyte culture. 960 mM NaCl, 18 mM $CaCl_2 \cdot 2H_20$, 10 mM $MgCl_2 \cdot 6H_20$, 100 mM HEPES. Dissolve the above in 800 mL of ddH_2O. Adjust to pH 7.6 with NaOH and adjust volume to 1 L. Sterilize through 0.2 µM filter. Dilute to 1× ND96 as needed. Store both solutions at room temperature.

17.2.2. Oocyte Incubation, Endogenous Cysteine Preblock, and Channel Labeling

1. ND96. 96 mM NaCl, 2 mM KCl, 1.8 mM $CaCl_2$, 1 mM $MgCl_2$, 10 mM HEPES pH 7.6 plus gentamycin and pyruvate. Take 200 mL of 10× ND96 and add 1,800 mL of ddH_2O. Add 2 mL of gentamycin (50 mg/mL) and 5 mL of 1 M pyruvate. Sterilize through 0.2 µM filter. Store at 18°C.
2. High Potassium Labeling Solution (depolarizing). 120 mM K-methanesulfonate (KMES), 2 mm $CaCl_2$, 10 mM HEPES, pH 7.0.
3. Low Potassium Labeling Solution (hyperpolarizing). 120 mM Na-methanesulfonate (NaMES), 2 mM $CaCl_2$, 10 mm hepes, pH 7.0.
4. *(optional)* Tetraglycine maleimide (TGM) for cysteine preblock. Aliquot and store at −20°C.
5. 100 mM stock of tetramethylrhodamine maleimide (5′-TMRM; T-6027, Molecular Probes, Eugene, OR) in DMSO or DMF anhydrous. Dissolve 5 mg of 5′-TMRM in 104 µL of DMSO or DMF. Keep away from light. Store at −20°C. Avoid contact with moisture (*see* **Note 1**).
6. 20 mL scintillation vials for oocyte labeling (Perkin Elmer, Waltham, MA).
7. MiniFridge II, Model 260009 (Boekel Scientific, Feasterville, PA) or equivalent temperature controlled incubator. The small size of the MiniFridge allows the temperature to be rapidly adjusted and can house several 20 mL scintillation vials at the recording station.

17.2.3. Recording Solutions and Agar Bridges

Prepare recording solutions from isotonic (~240 mMol/kg) stock solutions of NMGMES (*N*-methylglucamine methanesulfonate), KMES, $Ca(MES)_2$, etc., and mix according to your needs. Typical recording solutions are given below.

1. Internal Solution (total K^+ = 120 mM) for bottom chamber. 110 mM potassium glutamate, 10 mM K-HEPES, pH 7.0
2. External Sodium Solution (total Na^+ = 120 mM) for middle and upper chamber. 110 mM NMGMES, 10 mM Na-HEPES, 2 mM $Ca(MES)_2$, pH 7.0.

3. External Potassium Solution (total K^+ = 120 mM) for middle and upper chambers. 110 mM KMES, 10 mM K-HEPES, 2 mM $Ca(MES)_2$, pH 7.0.
4. Permeabilizing Solution. 0.1% saponin in internal solution. 2–5 mL of concentrated 10% saponin stock can be prepared in distilled water and stored at 4°C. Take care as the stock is easily contaminated with bacteria. The permeabilizing solution should be prepared fresh every 2–3 days as it loses strength rapidly.
5. Vaseline. Coating the rims of the oocyte chambers improves the seal between the oocyte and the chambers. Although pure Vaseline® can be used, we prefer a mixture of Parafilm and heavy mineral oil (Sigma-Aldrich, St. Louis, MO). Cut several small pieces of Parafilm (0.3 g total) and place in a small beaker. Overlay with 2 ml heavy mineral oil and warm on hot plate, stirring until the Parafilm is completely dissolved and the solution appears as thick oil. Let it cool to room temperature. The consistency will be similar to honey, slightly less viscous than the original Vaseline®. We will refer to this Parafilm/oil mixture as vaseline.
6. Agar bridges. Thread a thin Pt wire through six glass capillaries (previously bent on a Bunsen flame to the proper shape) and fill with external recording solution in 3% agar. Store the bridges in the recording solution at 4°C. Keep the bridges as short as possible. When dealing with large currents (>1–5 μA), fill the bridges with either 1 M NaMES or KMES in 3% agar. Store in same buffer (*see* **Note 2**).

17.2.4. Equipment

Use equipment and consumables appropriate for a standard oocyte voltage-clamp experiment with the exception of the following.

1. A Faraday cage located in a dark room or equipped with black out curtains (e.g., black rubberized fabric (Thorlabs, Newton, NJ)) (*see* **Note 3**).
2. An active vibration isolation table or passive air mounts placed under a heavy breadboard, supporting a stereoscope, fluorescence microscope, recording chambers, and micromanipulators.
3. CA-1/CA-1B Cut Open Voltage Clamp Amplifier (Dagan Corp., Minneapolis, MN). This amplifier can be operated in TEVC as well as COVG mode. Methods section assumes that a CA-1B is used.
4. Recording chambers. Use a COVG plastic chamber assembly similar to the ones provided by Dagan Corp. The upper recording chamber should have a length of at least 25 mm to allow the positioning of the water immersion objective in the center of the chamber while leaving enough room to

place three agar bridges. Depending on the working distance of the objective, the lateral walls of the upper (recording) chamber may need to be lowered to allow focusing on the oocyte upper dome. *(optional)* The underside of the upper chamber can be painted with black nail polish to minimize reflection and background light.

5. An upright fluorescence microscope outfitted with a 5× air immersion objective (to aid oocyte impairment) and a 40× water immersion objective (for fluorescence recording). Equivalent results were obtained with an Achroplan 40x 0.8W (working distance (wd) = 3.6 mm) (Zeiss, Thornwood, NY) or a LUMPL FL 40x 0.8W (wd = 3.3 mm) (Olympus, Center Valley, PA) (*see* **Note 4**).
6. High quality fluorescence filter sets (excitation/dichroic/emission) appropriate for the fluorophore used. For example, use the 41002 filter cube set for TMRM, Exciter = 535/50 nm, Emitter = 610/75 nm, Dichroic 565 long pass or a 31048 filter cube set for PyMPO, Exciter = 390/22 nm, Emitter = 515/30 nm, Dichroic 425 DCLP (Chroma, Rockingham, VT).
7. A TTL triggered shutter to avoid unnecessary bleaching of the fluorophore. The shutter is opened a few ms before starting the acquisition via a shutter driver (e.g., Uniblitz shutter driver VMM D1 (Vincent Associates, Rochester, NY)).
8. PhotoMax 200 PIN diode current amplifier (Dagan Corp., Minneapolis, MN) or equivalent detector to measure the fluorescence intensity of the site directed florescent probe.

17.3. Methods

The key to a successful VCF experiment is proper sample preparation. Both the quality of cells and fluorophore labeling conditions are crucial. It is imperative that oocytes be completely defolliculated. Labeling conditions have to be empirically determined for each cysteine mutant; the included protocol provides the most common and successful starting conditions (*see* **Note 5**).

17.3.1. (Optional) Tetraglycine Maleimide Synthesis and Purification

TGM is a nonfluorescent, sulfhydryl specific small molecule. It is used to selectively label the oocyte's surface exposed endogenous cysteines before channel expression at the plasma membrane *(1)*. TGM prelabeling can significantly reduce background fluorescence, but in many cases is not necessary.

1. In a 20 mL scintillation vial, dissolve 30 mg of tetraglycine (TG; Sigma-Aldrich, St. Louis, MO) in 5 mL of 0.1 M NaCl,

0.1 M NaPhosphate, pH 7.25. This gives a 25 mM TG solution.

2. Add slowly (drop by drop) 0.25 mL of 200 mM SMCC in DMF (S-1534; Molecular Probes, Eugene, OR) to the TG solution while continuously stirring.
3. Incubate for 1 h at 37°C while stirring slowly.
4. Purify TGM from unreacted components by HPLC. Use a semipreparative C18 reversed phase column and an acetonitrile gradient (+0.1% TFA). TGM is eluted by 15–16% acetonitrile as a single, sharp peak.
5. Divide the eluted TGM solution into 1.5 mL centrifuge tubes, and dry overnight in a speed-vac. Do not use heat.
6. To determine the TGM concentration, dissolve the content of a tube and determine the maleimide concentration by measuring the reactivity of TGM to a known amount of free cysteine using Ellman's reagent *(13, 14)*.

17.3.2. Cell Isolation, Injection, Incubation, and Labeling

Xenopus oocytes may be isolated using standard protocols; however, it is imperative that cells be completely free of their follicular layer as the layer is nonspecifically labeled by fluorophores and interferes with the high resistance vaseline seal between the oocyte and the upper and middle COVG chambers. Treat oocytes with the Collagenase II and III cocktail in 1× Ca^{2+}-free solution to remove the follicular layer (*see* **Note 6**).

1. Choose twenty to forty stage V–VI oocytes for mRNA microinjection. Oocytes should be completely defoliculated and have a uniformly pigmented animal pole. Batches of oocytes with very dark animal poles usually have lower background fluorescence and give the best results. Smaller oocytes should also be avoided as they do not fit properly in the COVG chambers.
2. Microinject each oocyte with 50 nL cRNA (0.02–1 µg/µL) using a Drummond nanoinjector (Drummond Scientific, Broomall, PA). Inject near the equator of the oocyte to avoid the nucleus and use the smallest injection pipette tip possible that allows successful injection without pipette clogging. Avoid large injection pipettes as they damage the oocytes leading to cell death, poor expression, and/or injection scars which contribute to background fluorescence.
3. After cRNA injection, place 20–40 oocytes in sterile, tissue culture grade 25 mm Petri dishes (for example Falcon 353002). Incubate in ND96 solution for 1–9 days at 12 or 18°C. Incubation at 12°C traps newly synthesized channels in the ER and prevents surface expression. This allows endogenous surface cysteines to be preblocked with TGM in order to reduce the background fluorescence *(optional)*.

Incubation at 18°C allows newly synthesized channels to traffic to the plasma membrane. Cells incubated at 18°C cannot be preblocked.

4. *(optional)* 12–18 h before recording, wash cells once in ND96 and transfer to a 20 mL scintillation vial containing 0.5–1 mM TGM in ND96. Incubate for 30 min at 12°C. Wash three times in ND96 to completely remove unreacted TGM. Proceed to **step 5** and incubate at 18°C overnight. The higher temperature should allow your channel to traffic out of the ER (*see* **Note 7**).
5. 12–18 h before recording, wash cells once in ND96 and replace with ND96 solution supplemented with 200 μM DTT (to break potential disulfide bonds) and 10 μM EDTA (to remove heavy metals). Incubate at 18°C overnight.
6. Immediately prior to recording, thoroughly rinse the oocytes with labeling solution to remove excess DTT and transfer to a 20 mL scintillation vial containing 2 mL of labeling solution spiked with TMRM to a final concentration of 5–10 μM. Incubate for 30–40 min in the dark. Keep cells on ice or at room temperature. Wash three times in recording solution and incubate in the dark at 12°C (*see* **Note 8**).

17.3.3. Voltage-Clamp Fluorometry in COVG Mode

COVG recordings are performed under an upright fluorescence microscope. Recordings are performed in a dark room or in a Faraday cage equipped with black out curtains. All cell handling is done in as low light as possible. Oocyte mounting within the COVG recording chambers is performed underneath a dissection stereoscope mounted adjacent to the fluorescence microscope (**Fig. 17.2c**). The entire chamber is then moved under the fluorescence microscope. A 5× objective with a long working distance is used for inserting the intracellular electrode (V_1) into the center of the oocyte dome before switching to the 40× water immersion objective (*see* **Note 9**).

The cut open chamber consists of three compartments (**Fig. 17.3**). The upper or recording chamber electrically isolates the oocyte upper domus (~1/5 of the total oocyte surface). Fluorescence and current is recorded from this chamber. The middle chamber voltage-clamps the middle part of the oocyte, serving as a guard shield. The bottom chamber isolates the oocyte lower domus which is permeabilized with 0.1% saponin to reduce the access resistance to the oocyte interior. The bottom chamber contains the intracellular solution and hosts a current injecting agar bridge (I) to actively clamp the oocyte interior to $V = 0$ mV (via feedback with the intracellular glass electrode V_1). The upper and middle chambers are actively clamped to the command potential. Each chamber is connected to a 6 well block via agar bridges. When assembling

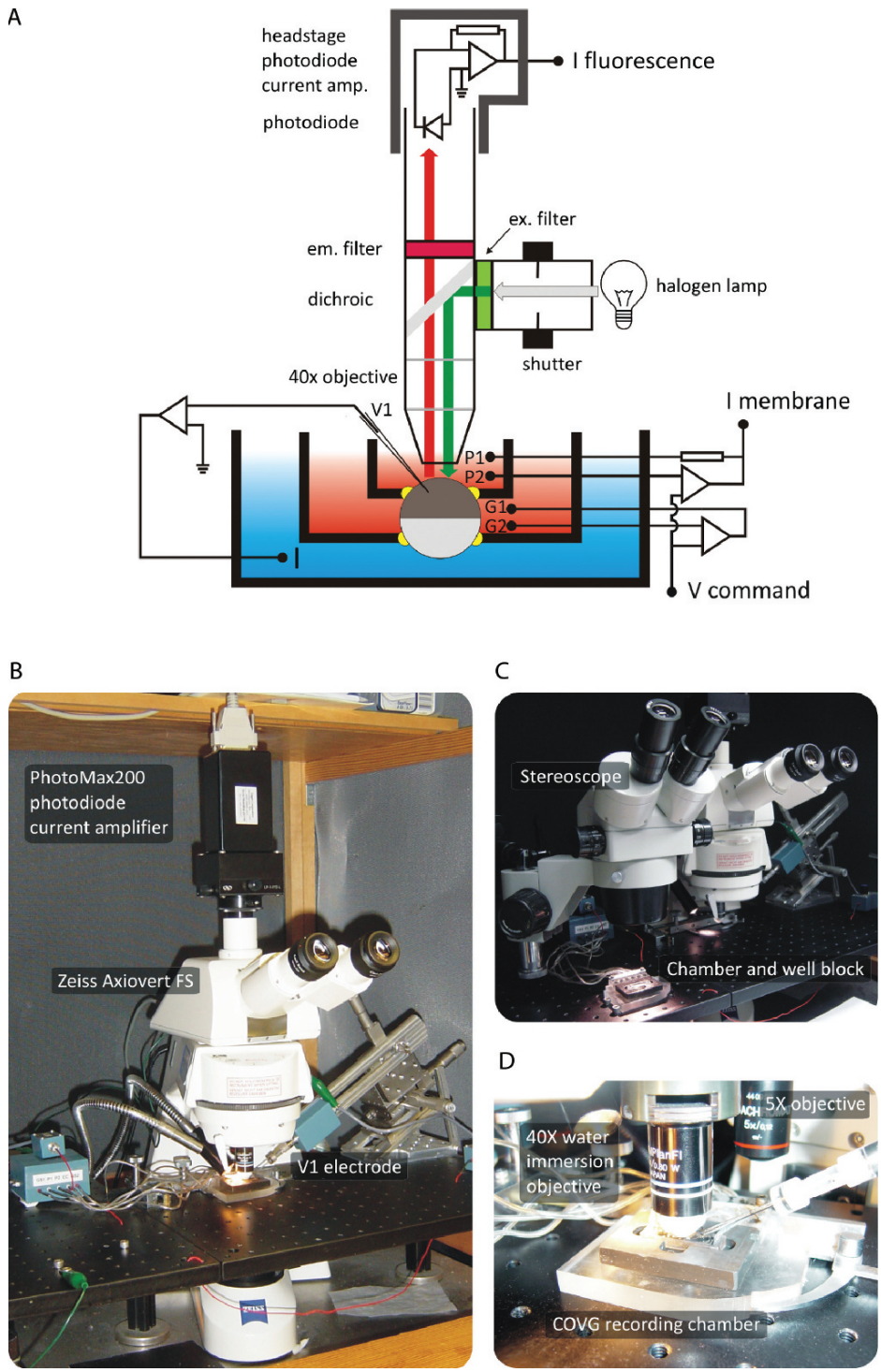

Fig. 17.2. The voltage-clamp fluorometry light path/circuit and COVG circuit. (**a**) Schematic of the recording chamber, fluorescence light path, photodetector circuit, and COVG circuit. The bottom chamber (filled with internal solution) is held at ground, and the middle chamber and upper chambers (filled with external solution) are clamped to the command voltage. Fluorescence and current is recorded only from the upper chamber. Light is detected by a top mounted photodiode whose output is connected to a low noise current amplifier. (**b**) A typical VCF/COVG setup. (**c**) Side mounted dissection scope used for chamber assembly and oocyte mounting. (**d**) Close up of the COVG chamber mounted on a fluorescence microscope.

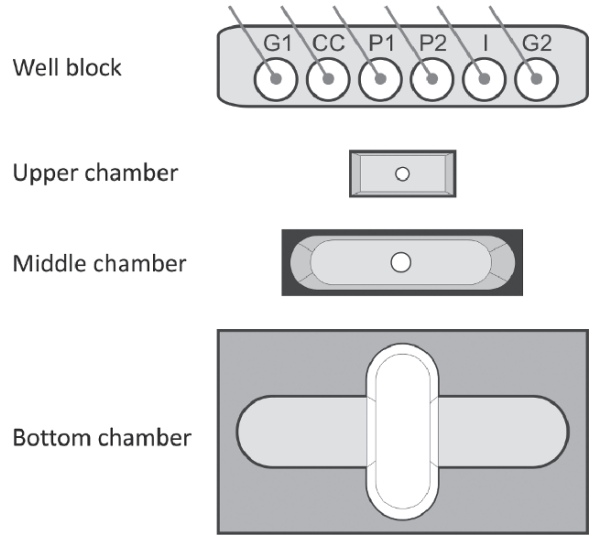

Fig. 17.3. COVG well block and chambers. Electrical and fluorescence recordings take place in the upper chamber.

the chamber and bridges, ensure that solutions do not form contacts between the bridges, wells, or sides of the chambers. In particular do not overfill the chambers.

17.3.3.1. Mounting the Oocyte

1. Set the CA-1B amplifier to Cut Open mode. Adjust front panel controls according to **Fig. 17.5** (*see* **Note 10**).
2. Using computer controls, set the holding potential to 0 mV. Maintain the holding potential at 0 mV unless otherwise instructed in the Notes section.
3. Remove bridges from storage solution and blot off excess solution. Fill the 6 well bridge block with 1 M NaCl and position the bridges and middle chamber as shown in **Fig. 17.4a** (*see* **Note 11**).
4. Using a fine capillary pipette glass stick, coat the rim of the middle chamber hole with a small amount of vaseline ensuring that that the hole remains clear. Clear the hole with suction if necessary.
5. Fill both bottom and middle chambers with external solution. Ensure that the hole is clear (i.e., no vaseline, no air bubbles). The two chambers should now be in electrical contact.
6. Set software to apply a repetitive 10 mV test pulse (i.e., a 7 ms pulse repeating at 30 Hz) and check the capacity transient. The pulse should last 7 ms with a steady state amplitude of 10 mV as in **Fig. 17.4a.** Leave the test pulse running until the mounting procedure is complete.

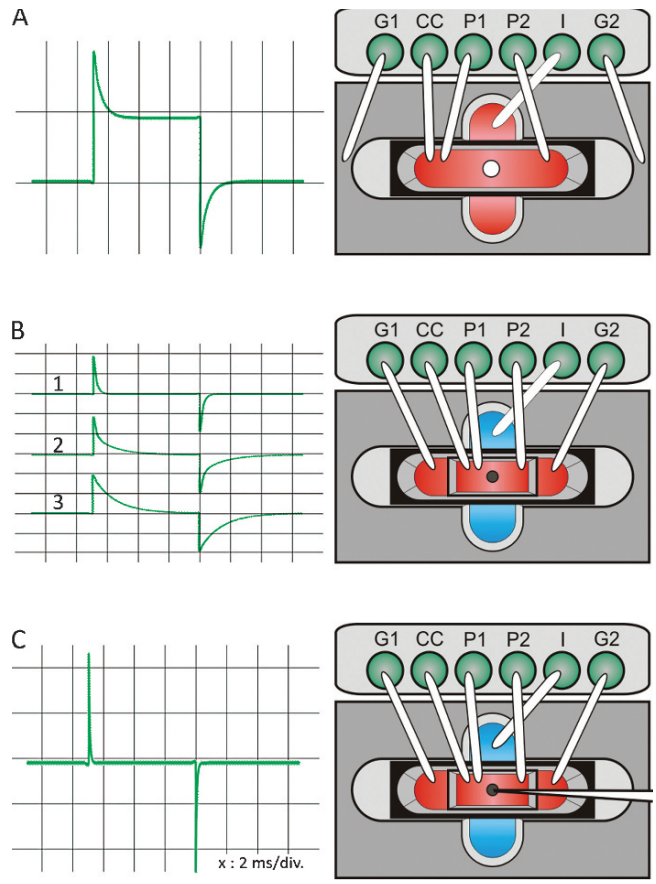

Fig. 17.4. Oocyte mounting and chamber circuit testing in COVG mode. The well block is filled with 1 M NaCl and electrically connected to the chambers via agar bridges. (**a**) The hole in the middle chamber is coated with vaseline, and the middle chamber is inserted into the bottom chamber. Both chambers are filled with external solution and are in electrical contact via the central hole. The bath/guard is set to PASSIVE, and the clamp is OFF. A 10 mV test pulse generated by the CA-1B amplifier produces the oscilloscope trace shown *left*. (**b**) Oocyte permeabilization. After oocyte mounting, the bottom chamber is filled with internal solution + 0.1% saponin. Middle and upper chambers are filled with external solution. The bath/guard is set to ACTIVE, and the clamp is OFF. The test pulse will initially appear as a fast single exponential decay (*1*). In time the test pulse becomes slower reflecting partial permeabilization (*2*). Permeabilization is complete when the test pulse appears as a slow single exponential decay (*3*). Permeabilization of the oocyte takes 30–60 s. (**c**) Final recording configuration. Saponin is removed and the bottom chamber is filled with internal solution. An intracellular electrode has been inserted into the oocyte. Bath/guard is set to ACTIVE, and the clamp is ON.

7. Using a glass transfer pipette, place one labeled oocyte on the vaseline coated hole with the animal (dark) pole facing up.
8. Apply quick suction to remove a small amount of solution from the bottom chamber. This maneuver will "suck" the oocyte into the hole, improving the seal between the oocyte

A

	Control	Setting		Control	Setting
1	Mode	Cut open	7	Filter command	30 μs
2	Clamp source	Headstage	8	Holding voltage/toggle	0 turns (0 mV)/Off
3	Clamp	Off	9	Im Gain (a)	1.0
4	Bath/Guard	Passive	10	Capac. & Resist. Comp.	Off
5	External command	On	11	Gain (b)	1.0
6	Test command	Off	12	Bessel filter	2-5 kHz

B

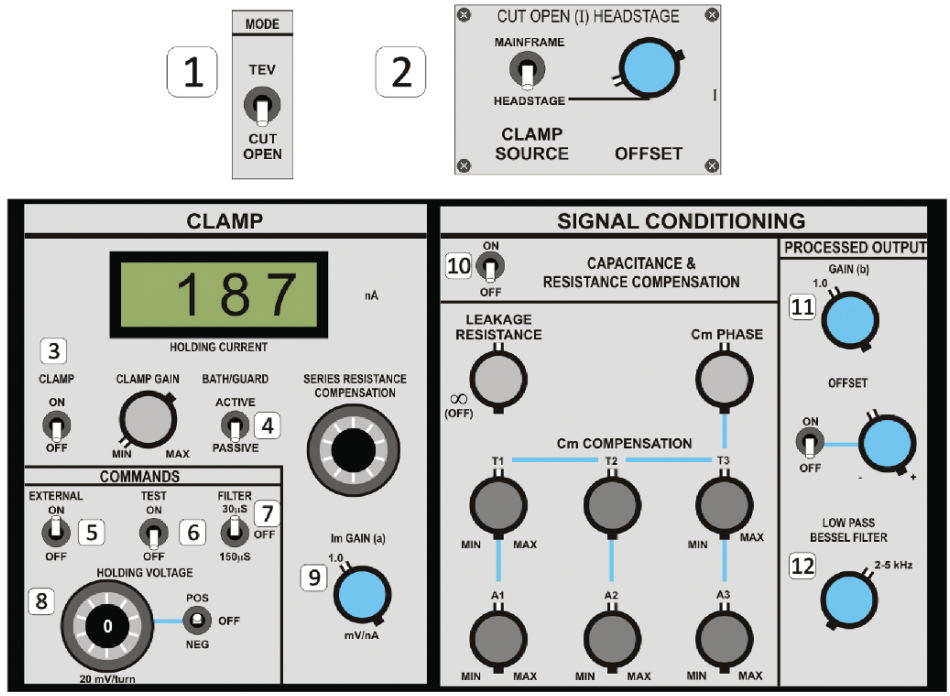

Fig. 17.5. (**a**) Initial CA-1B voltage-clamp amplifier settings for a typical COVG experiment. (**b**) Schematic of the cut open headstage and front panel controls of the CA-1B voltage-clamp amplifier. Numbered controls refer to panel (**a**).

and the vaseline coated hole of the bottom chamber. The current amplitude during the test pulse (i.e., the leak current) should decrease slightly but clearly.

9. Apply a thin film of vaseline (almost invisible) to the underside of the upper chamber and clear the hole by applying suction.
10. Gently push the upper chamber down into the middle chamber so that a small dome of the oocyte is isolated from the middle chamber and peeks through the upper chamber. This is the patch of membrane from which current and fluorescence will be recorded (*see* **Note 12**).
11. Place the bridges in the recording configuration as shown in **Fig. 17.4b**.

12. Switch the Bath/Guard toggle to ACTIVE. The leak current should be close to zero (**Fig. 17.4b, 1**) (*see* **Note 13**).
13. Remove solution from the bottom chamber and refill with permeabilizing solution, paying attention not to produce bubbles. Monitor the permeabilization process by following the capacitative current elicited by the test pulse. The leak current should not increase, while the capacity transient should become progressively slower (**Fig. 17.4b**, 2–3). Permeabilization is complete when the transient no longer changes and appears as a single, slow exponential decay (**Fig. 17.4b**, 3). The permeabilization process typically takes 30–60 s.
14. Remove the permeabilizing solution from the bottom chamber. Wash and refill the bottom chamber with the internal solution, paying attention not to produce bubbles. Move the entire chamber/well assembly under the fluorescence microscope. Be careful not to disturb the bridges, chamber, or oocyte.
15. Using a low magnification objective (5×) immerse the voltage sensing electrode (V_1) into the external solution (upper chamber) and adjust the offsets for V_1 and V_2 so that they read the inverse of the holding potential (HP) applied (i.e., adjust offset to +90 mV if the applied HP is –90 mV). After the adjustment, the front panel V_m (i.e., $V_1 - V_2$) meter should read 0 mV.
16. Impale the cell to the right of the center of the upper domus with the glass pipette (V_1) (R = 0.5 MΩ) maintaining a shallow angle to leave enough clearance for the microscope objective. Track oocyte impalement by noting the front panel V_m meter. STOP IMMEDIATELY as soon as V_1 reaches the other side of the membrane and reads the membrane potential.
17. Toggle the Clamp to ON. The capacity transient will become very fast (**Fig. 17.4c**).
18. Adjust the membrane potential to the correct holding potential by adjusting the offset knob on the cut open headstage clamp source (**Fig. 17.5**).
19. (optional) Toggle ON Capacitance & Resistance Compensation. Compensate the leak current first. Next, compensate the capacitance transients starting from the slowest component (rightmost knobs) and moving towards the faster components. In the process you will need to readjust all the components backwards and forwards to achieve a complete compensation of the capacity transient. Good capacity compensation with COVG usually requires more tweaking than with patch clamp amplifiers.

17.3.3.2. Simultaneous Recording of Fluorescence and Ionic and/or Gating Currents

Fluorescence and channel current are acquired as two separate inputs monitored by an electrophysiology software package. Any package that can acquire from two analog inputs is suitable.

1. Illuminate and focus the upper domus of the oocyte using the 40× water immersion objective. The field of the suggested objectives will cover most of the oocyte upper domus (~600 µM in diameter).
2. Insert an appropriate filter cube into the fluorescence light path of the microscope, according to the fluorophore used for labeling (*see* **Note 14**).
3. Set software to acquire data from analog inputs 1 (oocyte current) and 2 (photodiode current).
4. Power on the PhotoMax diode amplifier or an equivalent detector and synchronize the shutter operation with the voltage-clamp protocol (*see* **Note 15**). Simultaneously acquire the oocyte ionic (or gating) current and the photodiode current (*see* **Fig. 17.6**; *see also* **Note 16**). For some fluorophore labeled positions the background fluorescence (F) can be very large and the measurable ΔF very small ($\Delta F/F$ 0.1% or less). In these cases it is necessary to subtract the basal fluorescence "online." The PhotoMax system can measure and digitally store the basal fluorescence level, imputing an equal subtraction current into the headstage, thus holding the DC current close to zero. This track and hold feature allows the use of high gain without saturating the amplifier, significantly improving the signal-to-noise ratio (*see* **Note 17**).

17.4. Notes

1. The choice of fluorophore is application dependent. TMRM and PyMPO are used strictly as an example. A variety of thiol-reactive fluorophores are commercially available and some experimenting can be useful. For example we found that some positions in the hSlo channel were accessible to TMRM but not to PyMPO and vice versa *(15)*, possibly due to the different molecular sizes and shapes of these probes. Additionally, different isomers of the same fluorophore

Fig. 17.6. (continued) channel opening. Adapted from **ref. *16*** (Copyright 2007 The Rockefeller University Press). (**c**) A nonconducting Shaker mutant (W434F) fluorescently labeled at position 356C (S3–S4 linker) with TMRM in either the "wild-type" or inactivation removed (IR) background. Gating current and fluorescence are recorded simultaneously. The fluorescence tracks the motion of position 356 which in turn follows the gating current. Both the return gating current and fluorescence are slowed in the IR background indicating that the return of position 356 to the resting state is immobilized in IR relative to "wild-type" (adapted from **ref. *16***).

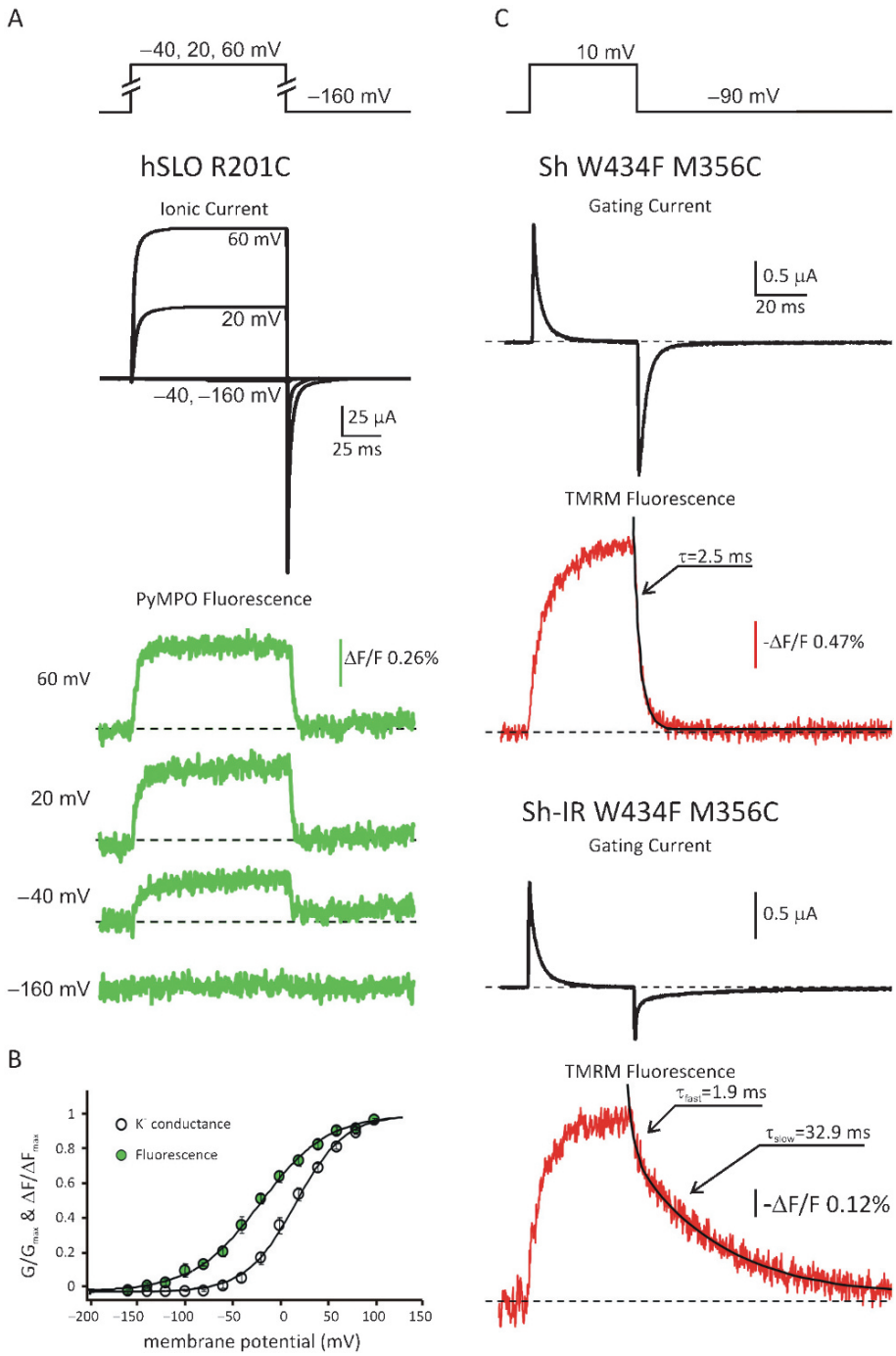

Fig. 17.6. Examples of VCF data from the hSlo and Shaker channels. (**a**) Simultaneous recording of ionic current and Pympo fluorescence from the human BK channel (hSlo). A *Xenopus* oocyte was injected with cRNA encoding an hSlo channel containing a single extracellularly exposed cysteine at position 201 located in the S4 transmembrane segment. The oocyte was incubated for 40 min in 10 mM PyMPO maleimide. The K^+ current elicited by depolarization to the indicated potentials from a holding potential of -160 mV and corresponding fluorescence traces are shown. As the channel open probability increases with each depolarizing step, the fluorescence intensity increases revealing conformational changes of the channel. Notice the significant ΔF elicited by the voltage step to -40 mV, which is not sufficient to open the channel. (**b**) The steady state conductance and fluorescence vs. voltage curves for hSlo R201C. Note that the fluorescence curve is left shifted relative to the conductance revealing that a conformational change occurs in S4 prior to

sometimes change the amplitude (magnitude and sign) of the fluorescence signal ***(6)***. Make all fluorophore stocks at as high a concentration as practically possible to minimize oocyte exposure to DMSO or DMF. High exposure results in leaky cells.

2. The suggested chambers are extremely compact. Bridges should be as short as possible and allow easy placement and movement in the oocyte chambers. Several bridge lengths should be tested for optimal placement within the chamber taking into account both the needs of the optical path and manipulators.
3. We recommend using black out curtains attached directly to the Faraday cage. However, be aware that the temperature in the cage can increase steadily throughout the day due to the heat produced by the fluorescence lamp. If temperature control is an issue, mount the lamp outside the cage or cut a vent in the top of the cage. It is also helpful to place a small DC powered fan near the lamp to circulate hot air away from the microscope.
4. The microscope can be extremely simple since VCF only collects photons; it does not acquire images. However, microscopes with low loss light paths are preferable. In particular, make sure that 100% of the light can be output to the detector port and that the light path is properly aligned. Mounting the photodiode to a three-axis micropositioner helps maximize light gathering. We use Halogen lamps (100 W or more) for the excitation source as they are quiet (low noise introduced into recordings) and do not interfere with the voltage-clamp recording. Since the change in fluorescence emission (ΔF) can be minimal, it is imperative to power the halogen lamp with a very well regulated DC power supply to avoid fluctuation in the light intensity. We have had reproducible success using a model IF15-15 12V–16A (International Power, Oxnard, CA) to power 100-W 12-V halogen lamps by Zeiss and Osram (Xenophot). Higher light intensity can be achieved with Xenon arc lamps (especially if more power toward the blue region of the spectrum is needed).
5. Be aware that additional molecular biology beyond cysteine substitution may be required to produce VCF suitable channels. Wild-type cysteines may have to be removed to prevent unwanted labeling and to decrease the fluorescence background. Additionally, labeling efficiency depends on the location of the cysteine substitution. In general, external loops are the easiest to label. The external facing ends of helices can also be labeled relatively easily. Deeper positions generally require higher fluorophore concentrations

or longer labeling times. Cytoplasmic positions cannot be labeled using this protocol, since the suggested fluorophores are membrane impermeant.

6. There is significant batch to batch variability in collagenase activity. Collagenase treatment times need to be empirically determined and may take as long as 45 min with continuous brisk shaking at room temperature. After collagenase treatment, the oocytes will have to be visually inspected and sorted to remove lysed and/or nondefoliculated cells. Allow the cells to recover for 1 day in ND96 before proceeding, and change the solution at least once during that time.
7. Lowering the temperature to trap newly synthesized channels in the ER is both construct/clone and oocyte batch specific. Do not assume that lower temperature always prevents surface expression. When testing new constructs, always check expression levels at several temperatures before attempting to preblock cells.
8. The choice of the labeling solution is channel and site dependent. For voltage-gated channels use High K^+ (depolarizing) labeling solution for cysteines that are expected to be extracellularly exposed in the open state. Use Low K^+ (hyperpolarizing) labeling solution for cysteines that are expected to be extracellularly exposed at rest.
9. VCF was initially developed for recording in TEVC mode and may be easier for some labs to implement in this configuration. To perform VCF in this mode, use an inverted fluorescence microscope and an oocyte chamber that can accommodate a bottom, glass coverslip. The oocyte should always be presented animal (dark) pole down (i.e., towards the objective) and may be held in place with the help of a small nylon mesh as the oocyte tends to naturally rotate animal pole up.
10. The controls on the CA-1B may be labeled slightly different depending on the manufacture date.
11. The cut open chamber and the 6 well block for the bridges are very compact. The space can be very cramped, and the bridges may be close to each other or even touching. This is especially true of the current injecting bridge *I* and P2 which need to cross each other. It is imperative that no electrical shorting occurs between the 6 wells. Coating the area around the wells with silicone grease can be used to prevent shorting. Short circuits (e.g., salt bridges) may form between bridges or between wells, and they are a major source of complications for investigators new to the COVG technique. Attention should be paid so that of the bridges

are dry before positioning and that they do not displace solution from the wells.

12. Be careful not to trap air under the upper chamber. One way to ensure that no air is trapped is to bring the chamber down at a slight angle and then level the chamber as the top of the oocyte begins to show through the chamber hole. The top of the oocyte should peek out of the upper chamber. It should not bulge out under tension. The agar bridges may be temporarily removed from the middle chamber during this step. Replace the bridges once the upper chamber is in place.
13. For some voltage-gated channels, the test pulse from holding potential = 0 mV may produce an apparent leak current if the channel is highly expressed and conducting. The apparent leak should disappear by lowering the holding potential to a sufficiently negative voltage. Be careful not to change the holding potential until after the oocyte is mounted and sealed to the chamber. This passes less current through and prolongs the life of the bridges.
14. Several fluorophores undergo photodestruction over the course of an experiment resulting in progressive loss in signal. If the fluorescence signal is strong, photodestruction can be reduced by inserting neutral density filters in the excitation path. Alternatively, a free radical scavenger such as mercaptoethylamine (MEA) may be used in the recording solution to slow photodestruction.
15. If possible, use a TTL pulse generated by the electrophysiology software package to control the shutter. To prevent photodestruction, open the shutter as briefly as possible (i.e., do not collect fluorescence during preconditioning voltage pulses).
16. In some cases, relatively small fluorescence signals will require averaging multiple fluorescence recordings (typically 3–20) in order to reduce noise. If averaging for long amounts of time, pay special attention not to photodestroy the fluorophore during the recording.
17. The headstage of a regular patch clamp amplifier can be modified to be used for photometry. A photodiode (e.g., PIN-020A photodiode (UDT Technologies, Torrance, CA)) in photovoltaic configuration can be connected to the headstage input of a patch clamp amplifier for the amplification of the photocurrent. However, in this case an external, offsetting circuit (more powerful than the one present on the amplifier) is required to null the background photocurrent.

Acknowledgments

We thank Medha Pathak, Sandra Wiese, Nicoletta Savalli, and members of the Olcese and Isacoff laboratories for helpful suggestions.

References

1. Mannuzzu, L.M., M.M. Moronne, and E.Y. Isacoff. (1996) Direct physical measure of conformational rearrangement underlying potassium channel gating. *Science* **271**, 213–216.
2. Stefani, E. and F. Bezanilla. (1998) Cut-open ocyte voltage-clamp technique. *Methods Enzymol* **293**, 300–318.
3. Akabas, M.H., et al. (1992) Acetylcholine receptor channel structure probed in cysteine-substitution mutants. *Science* **258**, 307–310.
4. Gandhi, C.S. and E.Y. Isacoff. (2002) Molecular models of voltage sensing. *J Gen Physiol* **120**, 455–463.
5. Cha, A. and F. Bezanilla. (1997) Characterizing voltage-dependent conformational changes in the Shaker K+ channel with fluorescence. *Neuron* **19**, 1127–1140.
6. Gandhi, C.S., E. Loots, and E.Y. Isacoff. (2000) Reconstructing voltage sensor-pore interaction from a fluorescence scan of a voltage-gated K+ channel. *Neuron* **27**, 585–595.
7. Pathak, M.M., et al. (2007) Closing in on the resting state of the Shaker K(+) channel. *Neuron* **56**, 124–140.
8. Loots, E. and E.Y. Isacoff. (1998) Protein rearrangements underlying slow inactivation of the Shaker K+ channel. *J Gen Physiol* **112**, 377–389.
9. Zheng, J. and W.N. Zagotta. (2000) Gating rearrangements in cyclic nucleotide-gated channels revealed by patch-clamp fluorometry. *Neuron* **28**, 369–374.
10. Bannister, J.P., et al. (2005) Optical detection of rate-determining ion-modulated conformational changes of the ether-a-go-go K+ channel voltage sensor. *Proc Natl Acad Sci USA* **102**, 18718–18723.
11. Gandhi, C.S. and E.Y. Isacoff. (2005) Shedding light on membrane proteins. *Trends Neurosci* **28**, 472–479.
12. Bruening-Wright, A. and H.P. Larsson. (2007) Slow conformational changes of the voltage sensor during the mode shift in hyperpolarization-activated cyclic-nucleotide-gated channels. *J Neurosci* **27**, 270–278.
13. Sedlak, J. and R.H. Lindsay. (1968) Estimation of total protein-bound and nonprotein sulfhydryl groups in tissue with Ellmans reagent. *Anal Biochem* **25**, 192–205.
14. Kitagawa, T., et al. (1981) Preparation and characterization of hetero-bifunctional cross-linking reagents for protein modifications. *Chem Pharm Bull* **29**, 1130–1135.
15. Savalli, N., et al. (2006) Voltage-dependent conformational changes in human Ca(2+)- and voltage-activated K(+) channel, revealed by voltage-clamp fluorometry. *Proc Natl Acad Sci USA* **103**, 12619–12624.
16. Savalli, N., et al. (2007) Modes of operation of the BKCa channel beta2 subunit. *J Gen Physiol* **130**, 117–131.

Chapter 18

Identification of Mutations in the Kir6.2 Subunit of the K_{ATP} Channel

Sarah E. Flanagan and Sian Ellard

Summary

The beta-cell ATP-sensitive potassium channel is a key component of stimulus–secretion coupling in the pancreatic beta-cell. The channel consists of four subunits of the inwardly rectifying potassium channel Kir6.2 and four subunits of the sulfonylurea receptor 1. Loss of function mutations in the *KCNJ11* and *ABCC8* genes that encode for Kir6.2 and SUR1 can cause over-secretion of insulin and result in hyperinsulinism of infancy, while gain of function mutations in *KCNJ11* and *ABCC8* have recently been described that result in the opposite phenotype of diabetes.

Genetic testing is important for patients with hyperinsulinism or neonatal diabetes, as identification of a K_{ATP} channel mutation confirms a diagnosis of their disorder. This genetic information may direct the clinical management; for example, patients with neonatal diabetes may transfer from insulin to sulfonylureas with an improvement in glycaemic control. The genetic diagnosis can also help to predict the likely course of the disease and may allow accurate counselling in terms of recurrence risk for these families.

This chapter focuses on the methodology used for the analysis of the *KCNJ11* gene by direct sequencing. The same principles can be employed for *ABCC8* analysis although the polymerase chain reaction (PCR) primers will differ. Details on DNA extraction from peripheral blood leukocytes, amplification of the *KCNJ11* gene by the PCR, sequencing, and mutation detection are provided.

Key words: DNA extraction, Polymerase chain reaction, Sequencing, *KCNJ11*, Neonatal diabetes, Hyperinsulinism.

18.1. Introduction

The beta-cell ATP sensitive K^+ channel (K_{ATP}) consists of two essential subunits Kir6.2 and sulfonylurea receptor 1 (SUR1). Kir6.2, encoded by the *KCNJ11* gene, is the pore-forming subunit and belongs to the inwardly rectifying potassium channel

Jonathan D. Lippiat (ed.), *Methods in Molecular Biology, Potassium Channels, vol. 491*

Book doi: 10.1007/978-1-59745-526-8

family. SUR1 is encoded by the *ABCC8* gene and belongs to the ATP-binding cassette (ABC) transporter family. The channel is an octameric complex of four Kir6.2 and four SUR1 subunits. The channels couple glucose metabolism to membrane electrical activity and insulin release in pancreatic beta-cells. When blood glucose levels rise, the consequent increase in glucose metabolism results in an alteration in the ratio of cytosolic nucleotides (ADP/ATP), and this causes K_{ATP} channel closure and membrane depolarisation. This subsequently activates voltage-dependent calcium channels leading to an influx of calcium. The increase in intracellular calcium concentration triggers insulin granule exocytosis.

Given the central role of the K_{ATP} channel in insulin secretion it is not surprising that mutations in the genes, *KCNJ11* and *ABCC8*, can result in both hypo and hyperglycaemia *(1–4)*. Homozygous, compound heterozygous or more rarely heterozygous dominant inactivating mutations in the *KCNJ11* and *ABCC8* genes are the most common cause of hyperinsulinism (OMIM 256450). Missense, nonsense, and frameshift mutations have been reported, which result in either a reduction or complete loss of K_{ATP} channel activity at the surface membrane *(5–7)*.

Activating *KCNJ11* and *ABCC8* mutations have been shown to cause neonatal diabetes (OMIM 600937) *(3, 4, 8)*. To date, only dominantly acting missense *KCNJ11* mutations have been described in patients with neonatal diabetes: this is in contrast to *ABCC8* where diabetes may result from heterozygous activating mutations, homozygous activating mutations, or compound heterozygosity for both an activating and inactivating mutation *(9)*. The majority (~80%) of *KCNJ11* mutations reported have arisen 'de novo' in the proband, so there is no family history of neonatal diabetes *(4, 10–13)*.

The identification of an *ABCC8* or *KCNJ11* mutation in a patient with hyperinsulinism or neonatal diabetes is important, as it provides a firm diagnosis of their disorder and also confirms the subtype. This information helps to predict the likely course of the disease and will influence the clinical management of the patient. For example, identification of a K_{ATP} channel mutation in a patient with neonatal diabetes can have a major impact on treatment, as the beta-cell K_{ATP} channel can be pharmacologically regulated by sulfonylurea drugs, which work by binding to and closing the K_{ATP} channel thereby restoring insulin secretion. Many patients have transferred from insulin injections to sulfonylurea tablets with an improvement in glycaemic control *(8, 11, 14–16)*. For autosomal dominant neonatal diabetes, the identification of a disease-causing mutation in a proband has implications for other family members. The recurrence risk is dependent of the mode of inheritance. For de novo mutations, there is a small risk due to the possibility of germline mosaicism in a parent *(17, 18)*, whereas for dominantly inherited mutations the risk is 50%. In contrast, siblings of probands with recessively acting mutations

will have a 25% risk of inheriting both mutations and developing the disease. For patients with hyperinsulinism, identification of recessive *ABCC8* or *KCNJ11* mutations allows the option of prenatal testing in future pregnancies.

This chapter focuses on the methodology used for the analysis of the *KCNJ11* gene. The same principles can be employed for *ABCC8* analysis although polymerase chain reaction (PCR) primers will differ (for details of primer sequences *see* **ref.** *9*). Sequencing is the 'gold standard' method for mutation screening and therefore our method of choice for the analysis of the *KCNJ11* gene. Briefly, following DNA extraction the single exon of the *KCNJ11* gene is amplified by the PCR in three overlapping fragments. Successful amplification can be confirmed by agarose gel electrophoresis, which allows visualisation of the PCR products. Purified PCR products are sequenced by the dideoxy chain termination sequencing method. The sequencing reactions are then separated by size on a capillary sequencer. Computer software generates the DNA sequence, which is depicted as an electropherogram that can then be analysed by various software packages.

18.2. Materials

18.2.1. Collecting Samples

1. EDTA (ethylenediamine tetraacetic acid) (7.5 mL) in anticoagulant blood tube.

18.2.2. DNA Extraction from Whole Blood

1. Wizard Genomic DNA Purification kit (Promega, Wisconsin, USA). Store at room temperature.
2. Ethanol (99.7–100%). Dilute to 70% with distilled water. Store at room temperature.
3. Isopropanol. Store at room temperature.
4. DNA rehydration solution (0.1 mM EDTA): 10 mL of 10× rehydration buffer (supplied in Wizard Kit), 2 mL of 1 M Tris–HCl, pH 7.6, and 88 mL double distilled (dd) water. Store in 50-mL aliquots at room temperature.

18.2.3. Amplification of the KCNJ11 Gene by the Polymerase Chain Reaction

1. Megamix Double (Microzone, Haywards Heath, UK). Store at –20°C.
2. DNA 10 ng/μL. Store at –20°C.
3. Double distilled water (ddH_2O). Store at room temperature.
4. Primers complementary to three overlapping fragments of the single exon of *KCNJ11*. The primers sequences are as follows: fragment 1 (forward primer) GTGCCCACCGAGAGGACT (reverse primer) GAGCCCCACGATGTTCTG; fragment 2

(forward primer) CACCAGCATCCACTCCTTCT (reverse primer) GTTTCCACCACGCCTTCC; fragment 3 (forward primer) CTACCATGTCATTGATGC (reverse primer) CCACATGGTCCGTGTGTA. All primers are M13-tailed (*see* **Note 1**). Primers are generally shipped lyophilised. Stock primers should be made to 100 pmol/μL by adding the given volume of dd H_2O. Primers should be stored in 100 μL aliquots at a working concentration of 2 pmol/μL at −20°C. The diluted primer mix includes both forward and reverse primers.

18.2.4. PCR Check Gel

1. Running buffer: 10× Tris–Borate–EDTA (TBE): 0.89 M Tris borate, 0.02 M EDTA, 0.89 M boric acid pH 8.3. Store at room temperature.
2. Agarose. Store at room temperature.
3. Bench top PCR DNA 1,000 bp ladder. Store at room temperature.
4. Ethidium bromide (this is a mutagen and so care should be taken with storage and handling). Store at room temperature and shield from light.
5. Gel loading solution (Sigma Aldrich, MO, USA). Store at room temperature.

18.2.5. Purification of the PCR Products

1. Exonuclease I (New England Biosciences, MA, USA). Store at −30°C.
2. Shrimp alkaline phosphatase (Promega, Wisconsin, USA). Store at −30°C.
3. Double distilled water (ddH_2O). Store at room temperature.

18.2.6. Sequencing Reactions and Sequencing Clean-Up

1. 5× Big Dye Dilution buffer (Applied Biosystems, Warrington, UK). Store at 2–8°C.
2. Big Dye Terminator V3.1 (Applied Biosystems, Warrington, UK). Store at −30°C.
3. M13 forward sequencing primer (2.5 pmol/μL). The primer sequence is TGTAAAACGACGGCCAGT. Store at −30°C.
4. Performa DTR Gel Filtration Cartridges VH Bio (Edge Biosystems, MD, USA). Store at 2–8°C.
5. Double distilled water. Store at room temperature.

18.2.7. Electrophoresis of Sequencing Reactions and Sequence Analysis

1. ABI 3730 48 capillary DNA analyser (Applied Biosystems, Warrington, UK).
2. POP7 (Applied Biosystems, Warrington, UK).
3. Mutation Surveyor Software V2.61 (SoftGenetics, PA, USA).

18.3. Methods

18.3.1. Collecting Samples

Ideally, DNA should be extracted from peripheral blood leukocytes. EDTA tubes should be filled with the appropriate volume of blood and then inverted several times to ensure mixing with the anti-coagulant (*see* **Note 2**).

18.3.2. DNA Extraction from Whole Blood

High-quality DNA can be extracted from peripheral blood leukocytes using the Wizard Genomic DNA Purification Kit (*see* **Note 3**).

1. To lyse the erythrocytes, take 1–7.5 mL of blood and transfer to a 50-mL centrifuge tube. To this add 9 mL of cell lysis solution for every 3 mL of blood. Invert the tube twice to mix and incubate at room temperature for 10 min. Invert a further two to three times during this period. Following incubation, centrifuge at 2,000×g for 10 min.
2. Pour off the supernatant without disturbing the visible white pellet and add 5 mL of cell lysis solution. Vortex to mix and then centrifuge at 2,000×*g* for 10 min.
3. To lyse the nuclei and leukocytes, pour off the supernatant carefully without disturbing the visible white pellet and add 5 mL nuclei lysis solution and pipette.
4. When viscous, add 1.65 mL of protein precipitation solution to the nuclear lysate and vortex to mix. Centrifuge at 2,000×*g* for 10 min.
5. Transfer the supernatant to a 15-mL tube containing 5 mL of isopropanol. Gently mix the solution by inversion. Strands of DNA should become visible.
6. Centrifuge at 2,000×*g* for 2 min and then decant the supernatant into waste.
7. Add 1 mL of 70% ethanol to the DNA pellet and centrifuge for 2 min at 2,000×*g*. Decant the ethanol into a sterile universal and air-dry the DNA pellet for 10–15 min.
8. Add 500 µL of DNA rehydration solution (0.1 mM EDTA) (*see* **Note 4**) and rehydrate the DNA by incubating at 37°C until dissolved. This will take approximately 10–12 h.
9. Store the DNA at –20°C.

18.3.3. Amplification of the KCNJ11 Gene by the Polymerase Chain Reaction

This method results in the generation of millions of copies of the *KCNJ11* gene generated from the original DNA template.

1. Remove the Megamix Double, DNA, and primers from the –20°C freezer (see **Note 5**) and label 3 × 0.2 mL sterile PCR microfuge tubes for each patient and a negative control. If

amplifying a number of patient samples, it may be preferable to use a 96-well plate.

2. To each of the tubes add 10 µL of Megamix Double, 5 µL of 10 ng/µL DNA (or ddH_2O for the negative control), and 2.5 µL of forward and 2.5 µL of reverse primer. Centrifuge the tubes briefly.
3. Place PCR microfuge tubes in a thermocycler, making sure that caps are properly closed, and run the following programme:

1 Cycle	95°C	3 min
30 Cycles	95°C	30 s
	60°C	1 min
	72°C	1 min
1 Cycle	72°C	10 min

4. On completion, the PCR samples should be stored at 2–8°C.

18.3.4. PCR Check Gel

Agarose gel electrophoresis is used to visualise PCR products (*see* **Note 6**). These instructions assume the use of an ABGene Electrofast Wide gel system although they are easily adaptable to other formats.

1. Prepare a 5-mM thick 2% agarose gel by mixing 2 g agarose with 100 mL of 1× TBE running buffer.
2. Microwave for approximately 1.5 min to dissolve the agarose. Run cold water over the flask to cool the molten agarose to approximately 60°C.
3. Add 5.0 µL ethidium bromide and swirl to mix carefully avoiding bubbles.
4. Pour agarose into the pre-assembled electrophoretic rig, making sure the comb is correctly positioned. The gel should polymerise within 30–40 min.
5. Prepare a 1: 10 dilution of the 10× running buffer.
6. Pour approximately 50 mL of the 1× TBE running buffer into the gel tank and remove the casting gates and comb.
7. Add 2 µL gel loading buffer to 5 µL of each sample. Load samples and controls and 2 µL of the benchtop PCR DNA ladder to the marker well.
8. Close the gel tank and connect to the power supply. The gel should be run at 120 V for 15 min (200 mA).
9. Following electrophoresis, the PCR products can be visualised on a transilluminator. The presence of the DNA size standard allows confirmation that the correct size products have been amplified (*see* **Note 7**).

18.3.5. Purification of the PCR Products

1. Prepare 1 µL of a 1:1:1 mix of Exonuclease I, Shrimp alkaline phosphatase and ddH_2O for each of the PCR products and

mix by vortexing. Add 1 µL of the mixture to three labelled 0.2-mL sterile microfuge tubes. To each of these add 1.5 µL of the corresponding PCR product. Centrifuge the tubes briefly (*see* **Note 8**).

2. Incubate at 37°C for 30 min then deactivate the enzymes by incubation at 80°C for 15 min. Centrifuge the tubes briefly (*see* **Note 9**).

18.3.6. Sequencing Reactions and Sequence Clean-Up

1. Prepare the sequencing master mix for each purified PCR product as follows: 0.37 µL of Big Dye Terminator Sequencing Mix, 1.83 µL of Big Dye Dilution Buffer, 2 µL of M13 tailed forward sequencing primer (at 2.5 pmols/µL), and 3.3 µL of water (*see* **Note 10**). Add 7.5 µL of this sequencing mix to each of the microfuge tubes containing the 2.5 µL of purified PCR product. Centrifuge the tubes briefly and place in the thermocycler (*see* **Note 11**).
2. Run the following programme:

25 Cycles	96°C	10 s
	50°C	5 s
	60°C	2 min

Following completion of the sequencing programme, carry out the following:

3. Centrifuge the filtration cartridges at 850×*g* for 3 min (*see* **Note 12**) and transfer the inner column to a clean, labelled 1.5 mL microfuge tube. Discard the outer tube containing the buffer.
4. Apply the sequencing reactions directly to the gel bed, making sure not to touch the gel or the side of the tube with the pipette tip.
5. Centrifuge the tube at 850×*g* for 3 min then discard the inner column and transfer samples to a 96-well non-skirted plate ready for sequencing.

18.3.7. Electrophoresis of Sequencing Reactions and Sequence Analysis

These instructions assume the use of an ABI 48 capillary 3730 DNA analyser although they are easily adaptable to other formats.

18.3.7.1. Electrophoresis

1. A septa should be put onto the 96-well non-skirted plate which can then be placed into a plate retainer and loaded into the ABI 3730. The sequencer should be run as per the manufacturer's protocol.
2. Following electrophoresis, the samples can be analysed on sample collection software (*see* **Note 13**).

18.3.7.2. Sequence Analysis

Mutation Surveyor software can be used for mutation detection. Analysis requires a reference file to define the exon boundaries, amino acid and nucleotide numbering and regions of interest (*see* **Note 14**), and normal sequence from a patient with no mutations

or polymorphisms within the region of interest for comparison with the patient sequences. The software will highlight any differences in sequence between the control and patient samples. It is possible to annotate polymorphisms in Mutation Surveyor so that common polymorphisms can be distinguished from other variants identified. Quality can be monitored using the program's quality score (a noise:signal ratio) or by assessment of Phred scores. Phred is a base-calling program that assigns scores based on the probability that the base call is correct. Hence a Phred score of 20 represents 99% likelihood that the call is correct, 30 = 99.9%, and 40 = 99.99%.

18.3.8. Mutation Confirmation and Pathogenicity of Unknown Variants

It is recommended that any mutations identified are confirmed prior to reporting. This should involve repeating the PCR of the fragment harbouring the mutation using a fresh dilution of stock DNA, followed by re-sequencing. Mutation testing for affected family members can be carried out at the same time as mutation confirmation. If there is no family history of diabetes or hyperinsulinism, unaffected parents should also be screened for the mutation. In the case of hyperinsulinism, this testing would confirm carrier status for the parents and would allow accurate genetic counselling in regards to the likelihood of future affected pregnancies. For patients with neonatal diabetes and a novel *KCNJ11* mutation, the presence of a de novo mutation, as shown by its absence in the unaffected parents, lends support to the variant being pathogenic (*see* **Note 15**).

18.4. Notes

1. PCR primers complementary to the forward strand should start with the M13 sequence, 5′ TGTAAAACGACGGCCAGT, while primers targeting the reverse strand should start with 5′ CAGGAAACAGCTATGACC. These sequences act as a target sequence for the universal primer which is used for sequencing.
2. To ensure high-quality DNA, it is advised that if immediate extraction is not possible then blood be stored at 2–8°C. It is recommended that DNA extraction is carried out within 5 days of sample collection.
3. This method for DNA extraction involves lysis of the erythrocytes in the Cell Lysis Solution, followed by lysis of the leukocytes and their nuclei in the Nuclei Lysis Solution. The cellular proteins are then removed by a salt-precipitation step;

this precipitates the proteins leaving the high-molecular-weight genomic DNA in solution. Finally, the genomic DNA is concentrated and desalted by isopropanol precipitation.

4. Following transfer of the supernatant to 5 mL of isopropanol and gentle inversion, strands of DNA should become visible. If DNA has not been seen at this stage, then it is recommended that 100 µL rather than 500 µL of DNA rehydration solution is used to dissolve the DNA pellet.
5. We have found Megamix to be a very convenient and efficient means for DNA amplification. The PCR mix contains all of the fixed components needed for PCR amplification and the mix is very stable and can be freeze/thawed many times without any noticeable loss in enzyme activity.
6. The PCR products are loaded onto the gel and subjected to an electric field by applying an electric voltage across the gel by means of a buffer (electrolyte) solution (TBE). The negatively charged DNA fragments migrate to the positive electrode. Low-molecular-weight DNA or small PCR products will migrate faster than high-molecular-weight DNA or large PCR products and this allows the samples to be separated by size. The PCR products are visualised in the agarose gel by addition of ethidium bromide. Although this step is not crucial, it is recommended, as sequencing a 'failed' PCR product will result in unnecessary expenditure due to wasted sequencing reagents.
7. The running buffer solution should be run through a commercially available charcoal filter or treated with charcoal-activated 'tea bags' prior to drain disposal.
8. The exonuclease I degrades excess single-stranded primer oligonucleotides from the PCR reaction mixture in a 3′–5′ direction. Shrimp alkaline phosphatase (SAP) is added to catalyse the dephosphorylation of 5′ phosphates from the DNA. Alkaline phosphatases are used for the dephosphorylation of 5′ phosphorylated ends of DNA for subsequent labelling with dideoxynucleotides (ddNTPs).
9. If it is not possible to proceed with sequencing reactions following the PCR purification, then it is recommended that the purified PCR products be stored at –30°C. We have found that sequencing quality is occasionally reduced if the samples are left for an extended period of time.
10. PCR products require single direction sequencing. The sequencing produced by this method is of high quality which provides confidence that any mutations will be detected by sequencing just the forward strand. In our experience unidirectional sequence analysis has a sensitivity of >99%.

11. This method utilises a single-stranded purified PCR product that acts as a template for the synthesis of a complementary strand of DNA. The Big Dye Terminator contains a DNA polymerase and four ddNTPs which lack a 3′ hydroxyl group. Each ddNTP is labelled with a base-specific fluorescent dye. The absence of the 3′ hydroxyl group prevents phosphodiester bonding, resulting in the formation of many hundreds of oligonucleotide fragments which differ in length.
12. Gel Filtration Cartridges are used to remove excess Big Dye Terminator, salts, and other low-molecular-weight material. If there are large numbers of sequencing reactions to purify, then it is recommended that 96-well gel filtration plates be used as per the manufacturer's instructions (Edge Biosystems, MD, USA).
13. Capillary electrophoresis separates the sequencing reactions by size, which allows the order of nucleotides within the sequence to be determined.
14. Further information regarding installation and user information for Mutation Surveyor software can be found in the manual that accompanies the software package.
15. When novel variants of unknown functional significance are identified in the *KCNJ11* gene, it is important to obtain information to support or refute their role in the given phenotype. It is useful to screen ethnically matched normal chromosomes, as the absence of the variant in 298 normal chromosomes allows 95% confidence that the frequency of the change is less than 1%. This provides support to the variant being a disease-causing mutation rather than a rare polymorphism. It is also useful to check whether the mutated residue is conserved across species. A mutation at a highly conserved residue would suggest that the residue is crucial for the proper function of the protein. A number of web sites can be used to check conservation (e.g. the University of Santa Cruz Web site: http://genome.ucsc.edu/). Web sites are also available to analyse the effect of mutations on splicing, all of which are freely available on the Web.

References

1. Thomas PM, Yuyang Y, and Lightner E (1996) Mutation of the pancreatic islet inward rectifier, Kir6.2 also leads to familial persistent hyperinsulinemic hypoglycemia of infancy. *Hum Mol Genet* 5:1809–1812.
2. Thomas PM, Cote GJ, Wohilk N, Haddad B, Mathew PM, Rabel W, Aquilar-Bryan L, Gagel RF, and Byran J (1995) Mutations in the sulphonylurea receptor and familial persistent hyperinsulinemic hypoglycemia of infancy. *Science* 268:426–429.
3. Proks P, Arnold AL, Bruining J, Girard C, Flanagan SE, Larkin B, Colclough K, Hattersley AT, Ashcroft FM, and Ellard S (2006) A heterozygous activating mutation in the sulphonylurea receptor SUR1 (ABCC8) causes neonatal diabetes. *Hum Mol Genet* 15:1793–1800.

4. Gloyn AL, Pearson ER, Antcliff JF, Proks P, Bruining GJ, Slingerland AS, Howard N, Srinivasan S, Silva JM, Molnes J, Edghill EL, Frayling TM, Temple IK, Mackay D, Shield JP, Sumnik Z, van Rhijn A, Wales JK, Clark P, Gorman S, Aisenberg J, Ellard S, Njolstad PR, Ashcroft FM, and Hattersley AT (2004) Activating mutations in the gene encoding the ATP-sensitive potassium-channel subunit Kir6.2 and permanent neonatal diabetes. *N Engl J Med* 350:1838–1849.
5. Nestorowicz A, Inagaki N, Gonoi T, Schoor KP, Wilson BA, Glaser B, Landau H, Stanley CA, Thornton PS, Seino S, and Permutt MA (1997) A nonsense mutation in the inward rectifier potassium channel gene, Kir6.2 is associated with familial hyperinsulinism. *Diabetes* 46:1743–1748.
6. Ashcroft FM (2005) ATP-sensitive potassium channelopathies: focus on insulin secretion. *J Clin Invest* 115:2047–2058.
7. Huopio H, Reimann F, Ashfield R, Komulainen J, Lenko HL, Rahier J, Vauhkonen I, Kere J, Laakso M, Ashcroft F, and Otonkoski T (2000) Dominantly inherited hyperinsulinism caused by a mutation in the sulfonylurea receptor type 1. *J Clin Invest* 106:897–906.
8. Babenko AP, Polak M, Cave H, Busiah K, Czernichow P, Scharfmann R, Bryan J, Aguilar-Bryan L, Vaxillaire M, and Froguel P (2006) Activating mutations in the ABCC8 gene in neonatal diabetes mellitus. *N Engl J Med* 355:456–466.
9. Ellard S, Flanagan SE, Girard CA, Patch AM, Harries LW, Parrish A, Edghill EL, Mackay DJ, Proks P, Shimomura K, Haberland H, Carson DJ, Shield JP, Hattersley AT, and Ashcroft FM (2007) Permanent neonatal diabetes caused by dominant, recessive, or compound heterozygous SUR1 mutations with opposite functional effects. *Am J Hum Genet* 81:375–382.
10. Massa O, Iafusco D, D'Amato E, Gloyn AL, Hattersley AT, Pasquino B, Tonini G, Dammacco F, Zanette G, Meschi F, Porzio O, Bottazzo G, Crino A, Lorini R, Cerutti F, Vanelli M, and Barbetti F (2005) KCNJ11 activating mutations in Italian patients with permanent neonatal diabetes. *Hum Mutat* 25:22–27.
11. Sagen JV, Raeder H, Hathout E, Shehadeh N, Gudmundsson K, Baevre H, Abuelo D, Phornphutkul C, Molnes J, Bell GI, Gloyn AL, Hattersley AT, Molven A, Sovik O, and Njolstad PR (2004) Permanent neonatal diabetes due to mutations in KCNJ11 encoding Kir6.2: patient characteristics and initial response to sulfonylurea therapy. *Diabetes* 53:2713–2718.
12. Vaxillaire M, Populaire C, Busiah K, Cave H, Gloyn AL, Hattersley AT, Czernichow P, Froguel P, and Polak M (2004) Kir6.2 mutations are a common cause of permanent neonatal diabetes in a large cohort of French patients. *Diabetes* 53:2719–2722.
13. Flanagan SE, Edghill EL, Gloyn AL, Ellard S, and Hattersley AT (2006) Mutations in KCNJ11, which encodes Kir6.2, are a common cause of diabetes diagnosed in the first 6 months of life, with the phenotype determined by genotype. *Diabetologia* 49:1190–1197.
14. Zung A, Glaser B, Nimri R, and Zadik Z (2004) Glibenclamide treatment in permanent neonatal diabetes mellitus due to an activating mutation in Kir6.2. *J Clin Endocrinol Metab* 89:5504–5507.
15. Pearson ER, Flechtner I, Njolstad PR, Malecki MT, Flanagan SE, Larkin B, Ashcroft FM, Klimes I, Codner E, Iotova V, Slingerland AS, Shield J, Robert JJ, Holst JJ, Clark PM, Ellard S, Sovik O, Polak M, and Hattersley AT (2006) Switching from insulin to oral sulfonylureas in patients with diabetes due to Kir6.2 mutations. *N Engl J Med* 355:467–477.
16. Codner E, Flanagan SE, Ugarte F, Garcia H, Vidal T, Ellard S, and Hattersley AT (2007) Sulfonylurea treatment in young children with neonatal diabetes: dealing with hyperglycaemia, hypoglycaemia and sickdays. *Diabetes Care* 30:e28–e29.
17. Gloyn AL, Cummings EA, Edghill EL, Harries LW, Scott R, Costa T, Temple IK, Hattersley AT, and Ellard S (2004) Permanent neonatal diabetes due to paternal germline mosaicism for an activating mutation of the KCNJ11 Gene encoding the Kir6.2 subunit of the beta-cell potassium adenosine triphosphate channel. *J Clin Endocrinol Metab* 89:3932–3935.
18. Edghill EL, Gloyn AL, Goriely A, Harries LW, Flanagan SE, Rankin J, Hattersley AT, and Ellard S (2007) Origin of de novo KCNJ11 mutations and risk of neonatal diabetes for subsequent siblings. *J Clin Endocrinol Metab* 92:1773–1777.

Chapter 19

Modulation of Potassium Ion Channel Proteins Utilising Antibodies

Mark L. Dallas, Susan A. Deuchars, and Jim Deuchars

Summary

The application of antibodies to living cells has the potential to modulate the function of specific proteins by virtue of their high specificity. This specificity has proven effective in determining the involvement of many proteins in neuronal function where specific agonists and antagonists do not exist, e.g. ion channel subunits. We discuss a way to utilise subunit specific antibodies to target individual channel subunits in electrophysiological experiments to determine functional roles within native neurones. Utilising this approach, we have investigated the role of the voltage-gated potassium channel Kv3.1b subunit within a region of the brainstem important in the regulation of autonomic function. We provide some useful control experiments in order to help validate this method. We conclude that antibodies can be extremely valuable in determining the functions of specific proteins in living neurones in neuroscience research.

Key words: Antibody, Neurone, Ion channel, Patch clamp, Brainstem, Potassium channel.

19.1. Introduction

Antibodies by their very nature provide a high level of specificity to their target molecules (antigens). In this context, antibodies are widely used in ion channel research for the purposes of immunohistochemistry (*1,2*). In a somewhat different approach, we undertook experiments to evaluate the use of protein-specific antibodies as tools in an electrophysiological setup. In particular, we wanted to address the functional role of specific ion channel subunits in native neurones. We focussed on a family of voltage-gated potassium (Kv) ion channels, the Kv3 subfamily, which shows a widespread distribution throughout the central nervous system *(3)*. Splice variants, accessory subunits, and the assembly of homomeric/heteromeric tetramers increase the complexity

Jonathan D. Lippiat (ed.), *Methods in Molecular Biology, Potassium Channels, vol. 491*

Book doi: 10.1007/978-1-59745-526-8

of this family of channels *(4)*. These channels have a unique biophysical fingerprint that sets them apart from other voltage-dependent channels. Most mammalian Kv channels activate at relatively negative voltages (–60 to –30 mV), but in the case of the Kv3 channels the activation is more positive at approximately –10 mV *(5)*. This is significant since this high activation threshold will only be crossed during the firing of an action potential.

The ability to unambiguously dissect out functional roles for Kv3 channel proteins depends on the availability of specific pharmacological tools. Although broad-spectrum channel blockers exist (e.g. tetraethlyammonium (TEA)), individual subunit blockers remain scarce. In order to address this, we undertook electrophysiological experiments utilising an antibody targeting the Kv3.1b subunit in the intracellular patch solution. By using this approach, we have shown a functional role for the Kv3.1b subunit in the repolarisation of action potentials within native neurones *(6)*.

19.2. Materials

19.2.1. Brain Slice Preparation

1. Sucrose artificial cerebral spinal fluid (aCSF): 217 mM sucrose, 26 mM $NaHCO_3$, 3 mM KCl, 2 mM $MgSO_4$, 2.5 mM NaH_2PO_4, 2 mM $CaCl_2$, 10 mM glucose (adjust to pH 7.4). This solution should be made up fresh and stored at 4°C.
2. Normal aCSF: 124 mM NaCl, 26 mM $NaHCO_3$, 3 mM KCl, 2 mM $MgSO_4$, 2.5 mM NaH_2PO_4, 2 mM $CaCl_2$, 10 mM glucose (adjust to pH 7.4). This solution should be made up fresh and stored at room temperature.
3. A solution of agar (3%) made up in normal aCSF (see above).
4. Mixed-gas cylinder (95% O_2, 5% CO_2).

19.2.2. Electrophysiology

1. Intracellular solution: 110 mM K-gluconate, 11 mM EGTA, 2 mM $MgCl_2$, 0.1 mM $CaCl_2$, 10 mM HEPES, 2 mM Na_2ATP, 0.3 mM NaGTP (adjust pH to 7.2). This solution can be made up in advance and stored at –20°C for a month (*see* **Note 1**).
2. Anti-Kv3.1b antibody (Alomone Labs).
3. Phosphate-buffered saline (PBS).
4. Bovine serum albumin (BSA).
5. Sucrose.
6. Sodium azide (NaN_3).
7. MicroFil non-metallic syringe needle (34 guage, 0.164 mm (outside diameter) × 0.1 mm (inside diameter)).

8. Plastic syringes (1 and 5 ml).
9. Borosilicate filamented glass capillaries (1.2 mm (outside diameter) × 0.94 mm (inside diameter)).
10. Micropipette puller (Sutter P97).
11. Data acquisition and analysis packages, Clampex and Clampfit (both Molecular Devices).
12. Upright microscope with differential interference contrast (DIC) optics (Olympus UK).
13. Axopatch-1D amplifier (Molecular Devices).
14. CV-4 headstage (Molecular Devices).
15. Digidata 1322 digitiser (Molecular devices).
16. Burleigh manipulator (PCS 5000).

19.3. Methods

19.3.1. Brain Slice Preparation

Note that all procedures were carried out in accordance with the UK Animals (Scientific Procedures) Act 1986 and the European Communities Council Directive (86/609/EEC) 1986.

1. Terminally anaesthetise rats (15–21 days) with sodium pentobarbitone (Sagatal, 120 mg/kg, I.P.).
2. Transcardially perfuse the animals with 50 ml of ice-cold sucrose aCSF.
3. Remove the skull, take the brain out, and place in ice-cold sucrose aCSF that receives a continuous supply of mixed gas.
4. Transect the brain at the level of the pons and remove the cerebellum allowing for isolation of the brainstem.
5. Clean the brainstem of the remaining dura mater using fine forceps and immerse in warm agar (3% solution in aCSF) and place in ice to allow for rapid setting.
6. Slice 300 µm sections of the embedded brainstem using a vibrating microtome (Campden Instruments) and transfer to a holding chamber containing normal aCSF at room temperature. This holding chamber should receive a continuous flow of mixed gas (*see* **Note 2**).

19.3.2. Preparation of Intracellular Solution Containing Antibody

1. Reconstitute the anti Kv3.1b antibody with water (buffer after reconstitution: PBS, pH 7.4, 1% BSA, 5% sucrose, 0.025% NaN_3) into a stock concentration (300 µg/ml) and freeze until day of experiment (*see* **Note 3**).
2. Thaw out an aliquot (500 µl) of intracellular solution (*see* **Note 1**).
3. Filter this intracellular solution with a 0.22 µm syringe disc.

4. Add the antibody to this filtered aliquot of intracellular solution at the required dilution (1:1,000, *see* **Note 3**).
5. Vortex this aliquot to ensure mixing of antibody and intracellular solution.
6. Fill a syringe with this new intracellular solution (including antibody) and fill patch electrodes using a non-metallic syringe. Do not filter this solution.

19.3.3. Electrophysiology

Ultimately, when determining specific roles for individual ion channel subunits, you need to examine a likely parameter in which the channel protein potentially plays a role (e.g. action potentials). Since previous studies have postulated a role for Kv3 channels in action potential repolarisation *(7, 8)*, we examined, using patch clamp studies, the effects of intracellular dialysis of single neurones on the characteristics of their action potentials evoked in the current clamp mode (**Fig. 19.1**). Similar protocols have been used for other antibodies in various neuronal populations *(9)*.

1. Visualised patch clamp recording should be obtained using an upright microscope with DIC optics (Olympus UK).
2. Initially target the region of interest, the nucleus of the solitary tract (NTS) at ×10 magnification on the dorsal side of the brainstem slice, and visualise individual neurones at ×60 magnification for the recordings (*see* **Fig. 19.1a**).
3. Use an Axopatch-1D amplifier interfaced with a Digidata 1322 digitiser in combination with the data acquisition package Clampex to acquire recordings.
4. Initially mount the pipette onto a patch electrode holder connected to a CV-4 headstage and test the electrode resistance and compensate for; following this adjust the offset to read 0 mV (*see* **Note 4**).
5. Apply positive pressure to the electrode via a syringe before placing the electrode in the recording bath (*see* **Note 5**).
6. View the electrode at ×10 magnification, then position over the region of interest, and lower to just above the surface of the slice using a Burleigh manipulator (PCS 5000).
7. In voltage clamp mode a hyperpolarising pulse is applied (25 mV, 10 ms, 5 Hz); release the positive pressure via the syringe.
8. Visualise the tip of the patch pipette at ×60 magnification and bring into contact with the somata of the neurone of choice.
9. Following the initial formation of a seal, observed as a decrease in the current response to the voltage step, apply a holding potential of −60 mV. This enables the formation of a tight, high-resistance seal (>5 GΩ).

10. After formation of a seal, change to current clamp mode on the amplifier with a 50 pA hyperpolarising pulse and apply a small amount of holding current (~−15 pA) to maintain cell stability.
11. Apply a small amount of negative pressure to the patch pipette via the syringe until noticeable changes in input resistance and capacitance are observed consistent with the whole cell configuration.
12. Low-pass filter the signal at 1 kHz and sample at 10 kHz.
13. To characterise the neurones electrophysiologically, apply rectangular hyperpolarising current pulses (1s duration, −10 to −90 pA) to the neurone at a holding potential of −60 mV and record the changes in voltage (*see* **Note 6**).
14. To examine the firing properties of the neurones, apply depolarising current pulses (+10 to +300 pA). Consequently, measurements of the action potential amplitude (from resting potential to peak) and the duration (from start of the rising phase to the onset of the afterhyperpolarisation (AHP)) as well as the peak amplitude and duration of the AHP can be made offline using the Clampfit analysis package (*see* **Fig. 19.1**).
15. Determine the functional consequences of the selective inhibition of the ion channel by the antibody (*see* **Notes 7–11**).

19.4. Notes

1. 100 ml of intracellular solution in 500 µl aliquots provides around a month's supply depending on the number of experiments undertaken.
2. Slices are best left for 1 h prior to beginning patch clamp recordings and are viable for at least 8 h after slicing.
3. We found that the anti-Kv3.1b antibody was effective at a concentration of 0.3 µg/ml in the patch pipette. This may vary according to your antibody of choice (*see* **Notes 7–11**).
4. The patch electrodes had a resistance of between 4 and 7 MΩ and a tip diameter of between 2 and 3 µm.
5. Apply around 5 ml of positive pressure via a plastic syringe; this helps to keep the tip of the electrode clean and free from blockages.
6. This allows you to produce a current vs. voltage plot for your recorded neurone.

   As with immunohistochemical procedures, the interpretation of data obtained from use of antibodies in electrophysiological

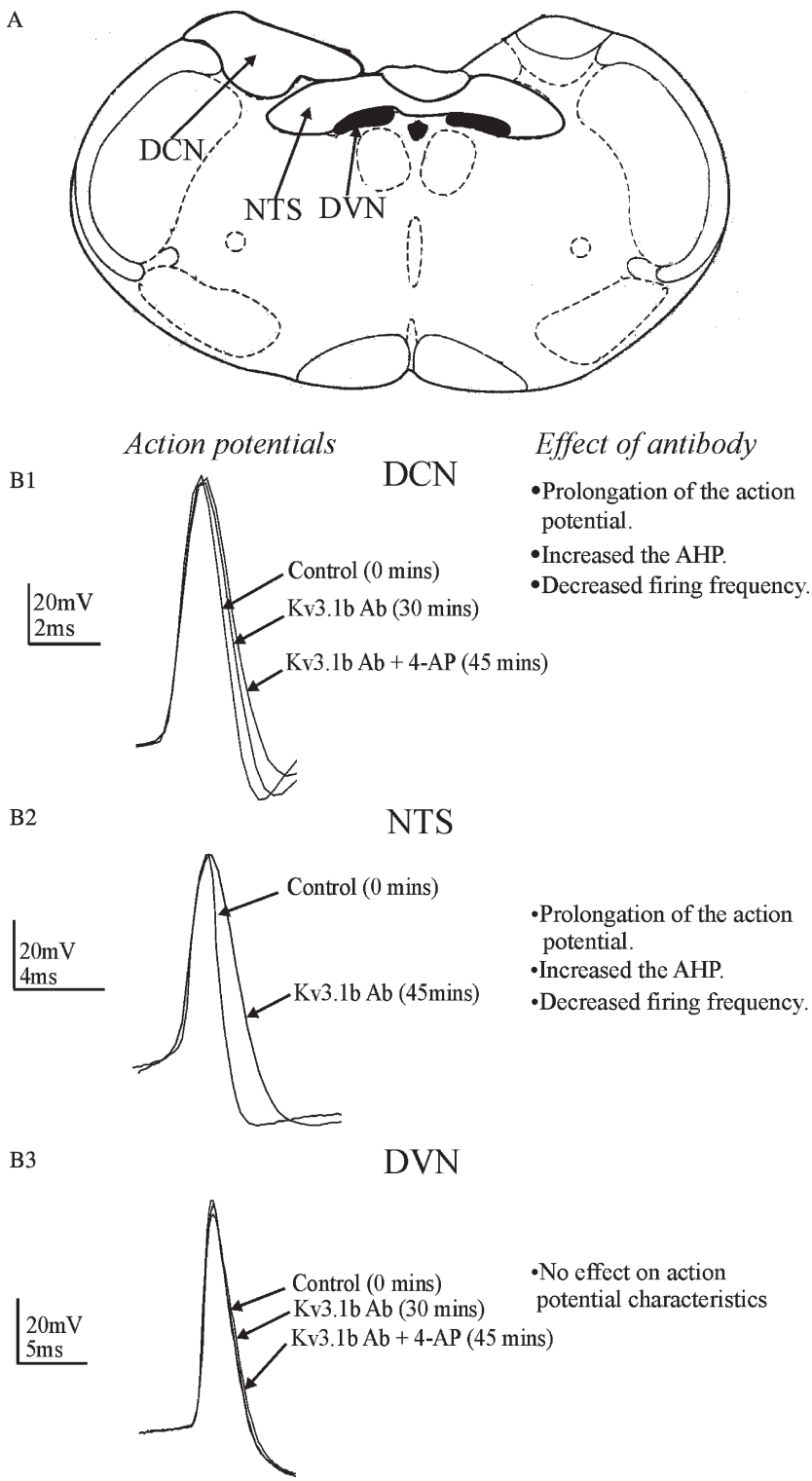

Fig. 19.1. Modulation of potassium channel subunits using specific antibodies. (**a**) A cartoon of a transverse brainstem slice highlighting the regions utilised during these studies. Note we examine the effects of the anti-Kv3.1b antibody in three regions. Two areas that were known to express Kv3.1b (NTS and DCN) and one region (*shaded*) lacking Kv3.1b expression

experiments is reliant on the specificity or selectivity of the antibody used. Here we suggest some controls experiments that could validate the functional studies utilising antibodies in an electrophysiological setup:

7. Is the antibody specific or selective for the target? This can be tested in several ways but is most commonly conducted by expressing the antigen in a cell line and staining these cell lines using the antibody; it would be expected that the cells transfected would stain positive, while a control, untransfected line would not. Alternatively, if the distribution of the target is well known, it may be sufficient to examine the antibody staining in relevant tissue. Western blotting of target tissue should result in staining of bands at only the appropriate molecular weights. The predicted molecular weights can be obtained from databases such as Swiss Prot (http://us.expasy.org/), but the protein may not match exactly due to post-translational events such as glycosylation and dimerisation. In addition, there is also the possibility that the antibody may detect another antigen that is of the same molecular weight as the target antigen *(10)*.
8. Staining tissue/electrophysiology in 'knockout' animals: perhaps the most secure approach is to immunohistochemically stain the tissue from animals in which the target antigen has been deleted. Here, there should be normal staining in wild-type animals but no staining in the knockout tissue. One cautionary note is that depending on the nature of the knockout, a portion of the target may still be produced that will provide a staining signal. In most cases, such a truncated protein will not perform normally and so there are unlikely to be effects of a specific antibody when applied to the cells from these animals.
9. Use a positive control neuronal population to functionally test your antibody of choice. It may be best to begin with

Fig. 19.1. (continued) (DVN). (**b1**) Electrophysiological recording of an action potential taken from a cell within the DCN, a region containing the Kv3.1b subunit. Intracellular dialysis led to a time-dependent blockade of the Kv3.1b channel, the effects of which are listed in the right hand panel. (**b2**) Electrophysiological recording of an action potential taken from a cell within the NTS, a region containing the Kv3.1b subunit. Again we observed a time-dependent blockade of the channel, which led to an increase in both the action potential duration and the afterhyperpolarisation (AHP). (**b3**) Electrophysiological recording of an action potential taken from a cell within the DVN, a region lacking the Kv3.1b subunit. Intracellular dialysis of the antibody did not lead to a prolongation of the action potential because of a lack of the relevant subunit to target. *NTS*, nucleus of the solitary tract; *DCN*, dorsal column nuclei; *DVN*, dorsal vagal nucleus; *4-AP*, 4-aminopyridine; *Kv3.1b Ab*, anti-Kv3.1b antibody.

a neuronal population that is known to express the target, which could have been determined from the immunohistochemical studies. In our studies we recorded action potentials form cells within the dorsal column nuclei, previously identified as containing the Kv3.1b protein (*see* **Fig. 19.1b**). However, negative results could mean that the antibody approach does not work for that particular protein, but reduces the chances of false negatives when recording from a heterogeneous population. Another approach that has been used is to express the target in a cell line and determine the effects of the antibody on the expressed protein *(11)*. One disadvantage is that the cell line may not contain all other proteins necessary to reconstruct the native protein's interactions with the possibility that a positive effect in cell lines may not be recreated in native cells because, e.g., the antigenic site is masked by interacting proteins.

10. Is the action of the antibody in these cells specific to the antibody used or is there a non-specific interaction of any antibody with cellular machinery? The use of an antibody to an antigen that is not present in the cell has been applied in several studies *(12)*. However, this control has also been approached in several other manners. In other studies, the antibody has been inactivated by heat, and this renders it non-functional *(13)*. Another method that has been effective is to incubate the antibody with the immunogenic peptide prior to application to neurones *(14, 15)*. In each case, the desired result is that the observed action is present only when the binding of the antibody is maintained.
11. Does the antibody affect cells that do not contain the antigen? Again, this test may be conducted by expressing other proteins in cell lines and testing the antibody against these *(11)*, but an advantage of neurones is that they contain a multitude of proteins in their native environment to test the antibody against. In our studies we examined the effect of the anti-Kv3.1b antibody on a region in the brainstem (the dorsal vagal nucleus) known to lack the Kv3.1b subunit (*see* **Fig. 19.1**).

References

1. Brooke, R. E., Atkinson, L., Edwards, I., Parson, S. H., and Deuchars, J. (2006) Immunohistochemical localisation of the voltage gated potassium ion channel subunit Kv3.3 in the rat medulla oblongata and thoracic spinal cord. *Brain Res.* **1070**, 101–115.
2. Chang,S.Y.,Zagha,E.,Kwon,E.S.,Ozaita,A., Bobik, M., Martone, M. E., Ellisman, M. H., Heintz, N., and Rudy, B. (2007) Distribution of Kv3.3 potassium channel subunits in distinct neuronal populations of mouse brain. *J. Comp. Neurol.* **502**, 953–972.
3. Weiser, M., Vega-Saenz de Miera E., Kentros, C., Moreno, H., Franzen, L., Hillman, D., Baker, H., and Rudy, B. (1994) Differential expression of Shaw-related K+

channels in the rat central nervous system. *J. Neurosci.* **14**, 949–972.

4. Rudy, B., Chow, A., Lau, D., Amarillo, Y., Ozaita, A., Saganich, M., Moreno, H., Nadal, M. S., Hernandez-Pineda, R., Hernandez-Cruz, A., Erisir, A., Leonard, C., and Vega-Saenz de Miera E. (1999) Contributions of Kv3 channels to neuronal excitability. *Ann. NY Acad. Sci.* **868**, 304–343.
5. Coetzee, W. A., Amarillo, Y., Chiu, J., Chow, A., Lau, D., McCormack, T., Moreno, H., Nadal, M. S., Ozaita, A., Pountney, D., Saganich, M., Vega-Saenz de Miera E., and Rudy, B. (1999) Molecular diversity of K+ channels. *Ann. NY Acad. Sci.* **868**, 233–285.
6. Dallas, M. L., Atkinson, L., Milligan, C. J., Morris, N. P., Lewis, D. I., Deuchars, S. A., and Deuchars, J. (2005) Localization and function of the Kv3.1b subunit in the rat medulla oblongata: focus on the nucleus tractus solitarii. *J. Physiol.* **562**, 655–672.
7. Deuchars, S. A., Brooke, R. E., Frater, B., and Deuchars, J. (2001) Properties of interneurones in the intermediolateral cell column of the rat spinal cord: role of the potassium channel subunit Kv3.1. *Neuroscience* **106**, 433–446.
8. Rudy, B. and McBain, C. J. (2001) Kv3 channels: voltage-gated K+ channels designed for high-frequency repetitive firing. *Trends Neurosci.* **24**, 517–526.
9. Dallas, M., Deuchars, S. A., and Deuchars, J. (2005) Immunopharmacology – antibodies for specific modulation of proteins involved in neuronal function. *J. Neurosci. Methods* **146**, 133–148.
10. Sim, J. A., Young, M. T., Sung, H. Y., North, R. A., and Surprenant, A. (2004) Reanalysis of P2X7 receptor expression in rodent brain. *J. Neurosci.* **24**, 6307–6314.
11. Murakoshi, H. and Trimmer, J. S. (1999) Identification of the Kv2.1 K+ channel as a major component of the delayed rectifier K+ current in rat hippocampal neurons. *J. Neurosci.* **19**, 1728–1735.
12. Conforti, L., Bodi, I., Nisbet, J. W., and Millhorn, D. E. (2000) O2-sensitive K+ channels: role of the Kv1.2-subunit in mediating the hypoxic response. *J. Physiol.* **524**, 783–793.
13. Liu, D. M. and Adams, D. J. (2001) Ionic selectivity of native ATP-activated (P2X) receptor channels in dissociated neurones from rat parasympathetic ganglia. *J. Physiol.* **534**, 423–435.
14. Kim, S. J., Kim, Y. S., Yuan, J. P., Petralia, R. S., Worley, P. F., and Linden, D. J. (2003) Activation of the TRPC1 cation channel by metabotropic glutamate receptor mGluR1. *Nature* **426**, 285–291.
15. Zhou, B. Y., Ma, W., and Huang, X. Y. (1998) Specific antibodies to the external vestibule of voltage-gated potassium channels block current. *J. Gen. Physiol.* **111**, 555–563.

Chapter 20

Fluorescence-Based Tl^+-Influx Assays as a Novel Approach for Characterization of Small-Conductance Ca^{2+}-Activated K^+ Channel Modulators

Susanne Jørgensen, Tina H. Johansen, and Tino Dyhring

Summary

Small-conductance Ca^{2+}-activated potassium (SK) channels constitute a family of ion channels that are regulated by the cytosolic Ca^{2+} concentration. Increases in the intracellular Ca^{2+} concentration ($[Ca^{2+}]_i$) result in opening of the channels, which in turn will lead to changes in the membrane potential. As the name implies, the channels are of small conductance, but even so, they are known to play a crucial role in several physiological processes, such as modulation of neurotransmitter and hormone secretion, as well as memory and learning (e.g., *see* Curr Med Chem 14:1437–1457, 2007). Owing to the central role of SK channels, they have attracted much attention as potential drug targets, both with respect to identification of activators and blockers of SK channel activity for indications such as, e.g., epilepsy, pain, and urinary incontinence (*see* Curr Med Chem 14:1437–1457, 2007; Curr Pharm Des 12:397–406, 2006). Thus, great efforts have been put into the development of robust high-throughput assays for detection and characterization of modulators of SK channel activity. In the present chapter, we describe two fluorescence-based Tl^+-influx assays for detection of positive and negative SK channel modulators.

Key words: Tl^+-influx, BTC fluorescence, K^+ channels, SK channel modulators.

20.1. Introduction

Previously, K^+ channels have been investigated using flux-based assays, such as $^{42}K^+$ or $^{86}Rb^+$ flux assays, which require handling of radioactive material and have a low throughput in addition to a poor temporal resolution. More recently, flux assays using cold Rb^+ have been introduced, but the throughput and the temporal resolution still remain to be increased. At present, patch clamp

Jonathan D. Lippiat (ed.), *Methods in Molecular Biology, Potassium Channels, vol. 491*

Book doi: 10.1007/978-1-59745-526-8

electrophysiology is the preferred technology when studying ion channels, but in spite of the introduction of automated patch clamp, the technology is still far from yielding a high throughput. However, an advantage to the techniques described above is that they all directly reflect channel activity. An alternative approach has been to use florescent dyes sensitive to membrane voltage (V_m). In contrast to the previously mentioned techniques, V_m-sensitive fluorescent dyes give only an indirect measure of K^+ channel activation and, in addition, the method does not discriminate between the various charge carrying channels. Fluorescent dyes that are directly affected by a given ion are well known and have been widely used, e.g., for measuring intracellular [Ca^{2+}] (e.g., *see* **ref.** *3*). A K^+-sensitive fluorescent dye, potassium-binding benzofuran isophthalate (PBFI), also exists. However, the fact that it requires UV-excitation in addition to exhibiting a relatively low selectivity towards sodium (1.5×) has made it less attractive. More recently, a thallium (Tl^+)-sensitive, fluorescence-based flux assay for detection and characterization of K^+ channel activity was introduced *(4)*. The assay technology is amenable for high-throughput characterization of K^+ channel activity and is applicable to a wide variety of K^+ channels. We have also found that fluorescence-based Tl^+-influx assays are applicable to a wide variety of K^+ channels, including SK channels. In the present chapter we will describe our protocols for characterization of positive as well as negative modulators of hSK channel activity, and the potential pitfalls one may have to consider before and when setting up this type of assay.

20.2. Materials

20.2.1. Cell Culture and Seeding

1. Dulbecco's Modified Eagle's Medium (DMEM) supplemented with 10% FCS.
2. Dulbecco's Phosphate-buffered saline (PBS).
3. Trypsin/EDTA: 500-mg/L trypsin, 200-mg/L EDTA.
4. Poly-D-lysine dissolved at 10 µg/mL in PBS.

20.2.2. Dye Loading

1. BTC-AM (benzothiazole coumarin acetoxymethyl ester, Invitrogen) dissolved in 2 mM in DMSO.
2. Cl^--free assay buffer (in mM): 140 Na^+ gluconate, 7.5 K^+ gluconate, 6 Ca^{2+} gluconate, 1 Mg^{2+} gluconate, 10 HEPES, pH 7.3 (adjusted with H_3PO_4).
3. Amaranth/tartrazine (Sigma-Aldrich) stock (10×): 100 mM amaranth, 50 mM tartrazine dissolved in Cl^--free assay buffer.

4. Loading buffer: Cl^--free assay buffer supplemented with amaranth/tartrazine (final concentration 2 mM/1 mM), 2 µM BTC-AM and 2 µM ouabain. Ouabain is added in order to prevent any contribution from the Na^+/K^+-ATPase.

20.2.3. Compound Testing

1. Test compounds are dissolved in 10 mM DMSO and diluted in Cl^--free assay buffer.
2. NS309 *(5)* was synthesized at NeuroSearch A/S (Ballerup, Denmark).
3. CyPPA *(6)* was synthesized at NeuroSearch A/S (Ballerup, Denmark).
4. NS8593 *(7)* was synthesized at NeuroSearch A/S (Ballerup, Denmark).
5. Ionomycin is dissolved in DMSO at a concentration of 1 mM and kept at –20°C in 100 µL aliquots until use.
6. ATP (adenosine 5´-triphosphate) is dissolved in H_2O (18.2 MΩ resistivity) at 30 mM and aliquoted and stored at –20°C until use.
7. Thallium stock (10×): 10 mM Tl_2SO_4 is dissolved in Cl^--free assay buffer at a concentration of 10 mM (*see* **Note 1**).
8. Cl^--free Tl^+ buffer: Cl^--free assay buffer is supplemented with amaranth/tartrazine (final concentration 2 mM/1 mM) and Tl_2SO_4 at a final concentration at 1 mM (i.e., $[Tl^+]$ = 2 mM) (*see* **Note 2**).
9. We have used a fluorimetric imaging plate reader (FLIPR, MDS Analytical Technologies, Sunny Vale, CA, USA), but any fluorescence-based bottom reader with the correct filter settings (excitation: ~488 nm, emission: ~540 nm) should work.

20.3. Methods

As mentioned in **ref.** *4*, it is well known that K^+ channels are permeable to Tl^+. In addition, the ability of Tl^+ to interact with fluorophores has also been described previously (e.g., *see* **ref.** *8*), but the use of Tl^+ in biological assays has been limited, primarily because addition of Tl^+ to a standard buffer will result in precipitation of TlCl, owing to the low solubility of the salt. However, TlCl precipitation can be overcome by using Tl_2SO_4 and replacing Cl^- in the assay buffer with gluconate, as introduced by Weaver et al. *(4)*, resulting in rapid and robust fluorescence-based assays for detection of K^+ channel activity. The fluorophore used in this assay, BTC-AM, is marketed as a low-affinity Ca^{2+}

indicator (K_d ~7 µM), but was found also to be sensitive to Tl^+ (*see* **ref. 4**; *see also* **Note 3**). One drawback of the method is that Tl^+ salts are highly toxic to mammals (primarily because of its accumulation in especially liver, brain, and skeletal muscle) (U.S. Environmental Protection Agency), and should be handled with care and disposed of properly. However, it should be mentioned that we have found it relatively easy to establish a safe working procedure for handling thallium as well as waste disposal.

20.3.1. Cell Handling and Seeding

1. 384-well plates are coated using 15 µL per well of a poly-D-lysine solution (10 µg/mL). After 30–60 min at room temperature, the solution is aspirated, and the plates are kept at 4°C until use.
2. The cells are grown in T175 culture flasks. On the day prior to the experiment, the cells are rinsed once with PBS, trypsinized, resuspended in DMEM supplemented with 10% FCS, and seeded in poly-D-lysine-coated 384-well plates at a density of ~3×10^6 cells/mL in 20 µL per well. The plates are left overnight at 37°C in a 5% CO_2 incubator. As a rule of thumb, one confluent T175 flask will contain enough cells for five plates. In case the cells have a tendency to clump, it can be helpful to pass the cells through a 23G needle to break up cell clumps.

20.3.2. Dye Loading

1. The cell plates are washed thrice in Cl^--free assay buffer (using an EMBLA plate washer (*see* **Note 4**)). After washing, 25 µL of the loading buffer is added to each well (*see* **Note 5**). The cells are incubated for a minimum of 1 h at 37°C and subsequently transferred to the plate reader.

20.3.3. Detecting Positive SK Modulators

1. The test compounds are diluted in Cl^--free assay buffer.
2. The assay is run as a two-step protocol, in which the first step is addition of test compound (*see* **Note 6**).
3. The second step is addition of Cl^--free Tl^+ buffer. For the negative control wells, the first step is addition of buffer, whereas the second step is addition of Cl^--free Tl^+ buffer. The positive control wells are also subjected to buffer in the first step; however, in the second step, 1 µM of the Ca^{2+}-ionophore ionomycin diluted in Cl^--free Tl^+ buffer is added (*see* **Notes 7** and **8**).
4. The fluorescence signal is followed over time, starting with a 15 s baseline measurement and followed by addition of compound (first step). After approximately 3 min, Cl^--free Tl^+ buffer is added (second step), and fluorescence readings are continued for another 4 min.
5. The data obtained is background-corrected by subtraction of the averaged signal obtained in the negative control wells, and the maximum value obtained in each well is normalized to that

of the averaged maximal positive control response (1 µM ionomycin) (*see* **Note 8**). An example is shown in **Fig. 20.1**, in which HEK293 cells expressing hSK1, hSK2, or hSK3, respectively,

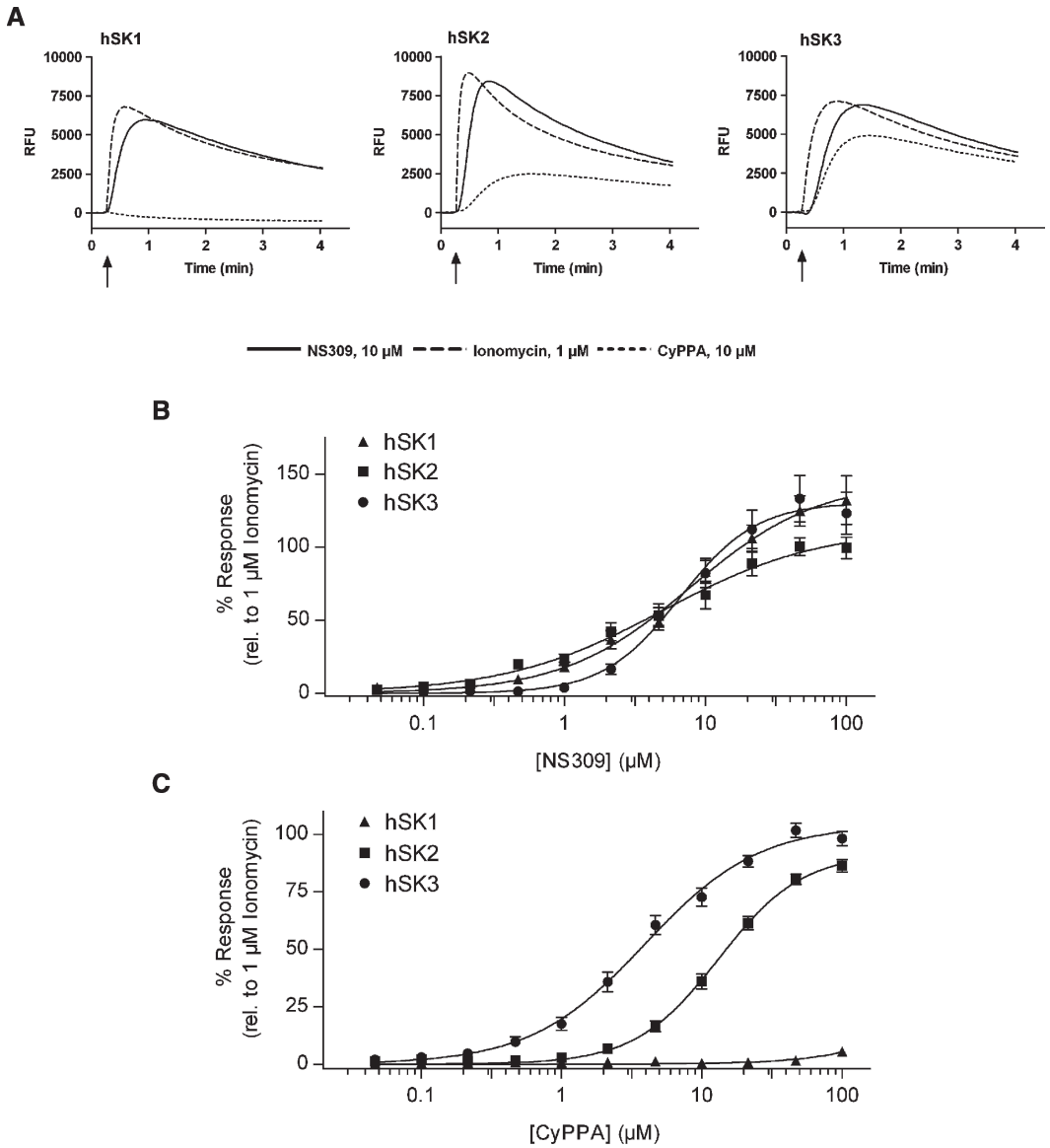

Fig. 20.1. Effect of positive modulators on hSK1, hSK2 and hSK3. In panel (**a**), the fluorescence signal from BTC-AM loaded HEK293 cells stably expressing hSK1, hSK2 or hSK3 channels, respectively, is followed over time. At the time indicated by the *arrow*, either NS309 (10 µM, *full line*), CyPPA (10 µM, *dotted line*, modified from **ref.** *6*) or Ionomycin (1 µM, *dashed line*) is added. CyPPA selectively opens hSK2 and hSK3 channels, whereas NS309 causes opening of both hSK1, hSK2 and hSK3 channels, respectively, resulting in influx of Tl^+, leading to increased BTC fluorescence. In contrast, Ionomycin activates the channels indirectly via an increase in $[Ca^{2+}]_i$, and is added as a positive control. The experiments are summarized in panels (**b**) and (**c**), which show the concentration–response curves for NS309 and CyPPA, respectively, on the three cell lines, clearly demonstrating a subtype selectivity of CyPPA for hSK2 and hSK3 over hSK1 (panel (**c**), data modified from **ref.** *6*).

are stimulated with the positive IK/SK modulator, NS309 *(5)*, or the SK2/SK3 selective positive modulator CyPPA *(6)*.

20.3.4. Detecting Negative SK Modulators

1. As for detecting positive modulators of the hSK channels, the compounds to be tested for any negative modulatory effect on hSK3 are diluted in Cl^--free assay buffer.
2. The assay is run as a two-step protocol, in which the first step is addition of test compound (*see* **Note 6**).
3. The second step is addition of Cl^--free Tl^+ buffer, in which a stimulus compound known to elevate $[Ca^{2+}]_i$ has been diluted. We have used ATP, which elevates $[Ca^{2+}]_i$ indirectly via activation of P_{2Y} receptors endogenous to the HEK293 cells. It should be noted that a Ca^{2+}-mobilizing agonist may be able to induce an increased Tl^+-influx at concentrations where no global increases in $[Ca^{2+}]_i$ can be detected. An example of this is shown in **Fig. 20.2** (*see* **Notes 8** and **9**).
4. In the first step buffer is added to the negative control wells, and in the second step Cl^--free Tl^+ buffer is added. The positive control wells are also subjected to buffer in the first addition, whereas in the second addition 100 µM ATP diluted in Cl^--free Tl^+ buffer is added.
5. As in the positive modulator assay, the fluorescence signal is followed over time, starting with a 15 s baseline, followed by addition of the compound. After approximately 3 min, Cl^--free Tl^+ buffer containing 100 µM ATP is added, and fluorescence readings are continued for another 4 min.

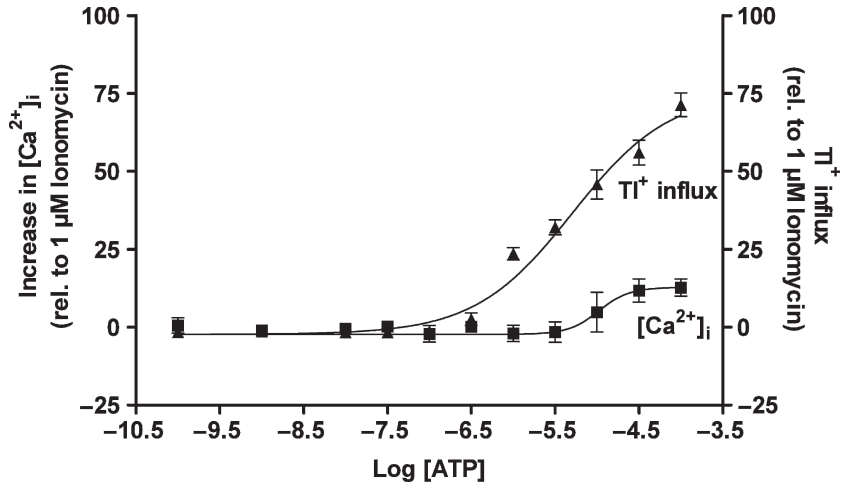

Fig. 20.2. Effect of ATP on intracellular $[Ca^{2+}]$ and Tl^+-influx. It shows concentration–response curves for the effect of ATP (100 pM–100 µM) on $[Ca^{2+}]_i$ measured using the Ca^{2+}-sensitive dye Fluo-4, as well as on Tl^+-influx in HEK293–hSK3 cells.

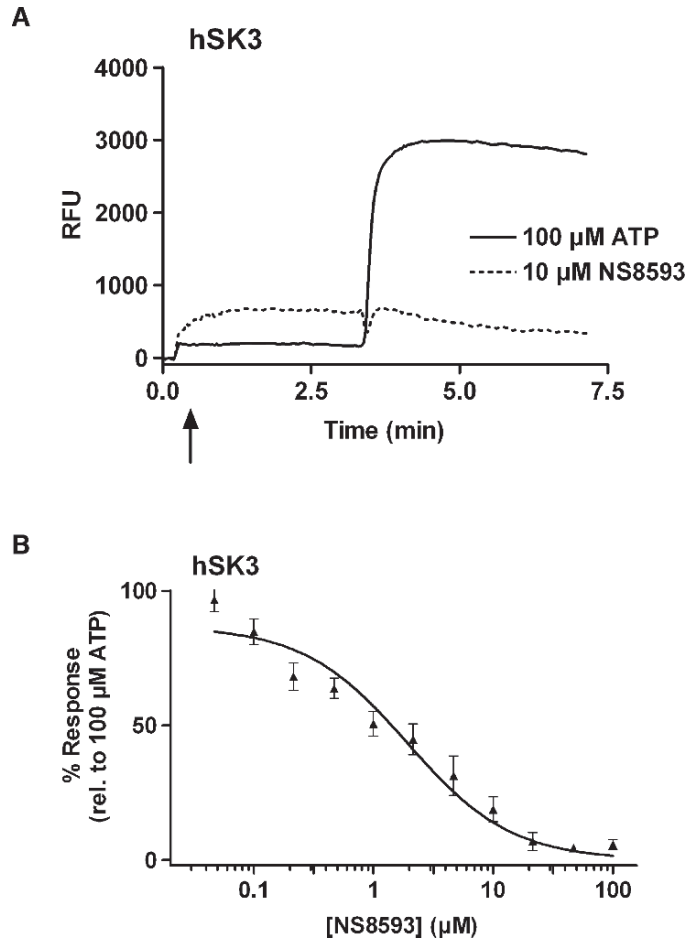

Fig. 20.3. Effect of NS 8593, a negative modulator of hSK3. In panel (**a**), the fluorescence signal from BTC-AM loaded HEK293–hSK3 cells is followed over time. At the time indicated by the *arrow*, NS8593 (10 µM, *dotted line*) is added. Approximately 2 min later, a Tl^+-containing stimulus buffer supplemented with 100-µM ATP is added, leading to an increase in Tl^+-influx if no NS8593 is present (*full line*). However, in the presence of 10-µM NS8593 (*dotted line*), the ATP-induced Tl^+-influx is greatly reduced. In panel (**b**), the concentration–response curve for NS8593 on HEK293–hSK3 cells stimulated with 100-µM ATP is shown, and the IC_{50} value was estimated at 1.9 µM.

6. The data obtained is background-corrected by subtraction of the averaged signal obtained in the negative control wells, and the maximum value obtained in each well is normalized to that of the averaged maximal positive control response (100 µM ATP in the absence of modulator). An example is shown in **Fig. 20.3** (*see* **Notes 8–10**).

20.4. Notes

1. It should be noted that the maximal solubility of Tl_2SO_4 is 4.87 g/mL at 20°C.
2. The Tl^+ concentration should be optimized and set as low as possible, because of the toxicity of Tl salts, but still high enough to yield robust signals. It should be noted that K^+ and Tl^+ are competing, which means that if the K^+:Tl^+ ratio becomes too large, it will be difficult to detect any Tl^+-influx through the K^+ channels.
3. The excitation spectrum of BTC is such that when excited at 488 nm, any increased binding of Ca^{2+} to BTC would lead to a decrease in fluorescence, which is the opposite of what is seen by increased Tl^+-influx. Owing to its relatively high K_d value for Ca^{2+} (~7 μM), even large increases in intracellular [Ca^{2+}] will only have a weak effect on BTC fluorescence at 488 nm.
4. Since the presence of residual Cl^- in the wells will cause precipitation of TlCl at a later point in the assay, it is important that the cells are washed thoroughly.
5. The cells are loaded with the fluorescent dye BTC-AM, which once inside the cell will be cleaved by intracellular esterases, thereby releasing the Tl^+-sensitive BTC. In order to minimize any contribution from residual BTC-AM on the extracellular side, the quenchers amaranth and tartrazine are present in loading- as well as in Cl^--free Tl^+ buffer.
6. Since there is no Tl^+ present to interact with the BTC fluorescence at this point, channel opening cannot be detected. However, if the compounds have any optical effects, e.g., autofluorescence, it would be obvious at this point.
7. Ideally, this maximal concentration of ionomycin should be added in the first addition; however, since ionomycin activates the hSK channels indirectly via an increase in $[Ca^{2+}]_i$, the Ca^{2+} surge will have peaked at the time of the second addition, and the degree of hSK activation induced by ionomycin will appear much smaller, and not truly reflect a close-to-maximal channel activation. By adding ionomycin along with the Tl^+, we hope to obtain a more reliable positive control response.
8. $[Ca^{2+}]_i$ is critical for the degree of activation of SK channels, but indeed very difficult to control in intact cells as used in this assay. Since the Ca^{2+}-activation curve for SK channels is very steep (Hill coefficient 3.5 for rSK3, **ref.** *9*), detection of SK modulators is complex and the choice of stimulus crucial. It should be mentioned that we have successfully applied

a variety of Ca^{2+}-mobilizing agonists, such as acetylcholine (ACh), thapsigargin (TG), ionomycin, and A23187, and chosen to use what appeared to perform best in each assay.

9. From **Fig. 20.2** it is seen that the effect of ATP on $[Ca^{2+}]_i$ is very modest (EC_{50} and maximal increase in $[Ca^{2+}]_i$ is 10.5 µM and 15% of the response induced by 1 µM ionomycin). This can be explained by the fact the $[Ca^{2+}]_i$ is measured under the same experimental conditions as when measuring Tl^+-influx, i.e., in a Cl^--free assay buffer, which we have found to affect the Ca^{2+} signaling. The effect of ATP on Tl^+ appears much more pronounced (EC_{50} and maximal increase in Tl^+-influx is 5.1 µM and 78% of the response induced by 1 µM ionomycin) and is obvious at concentrations that do not induce any detectable increase in $[Ca^{2+}]_i$. However, that does not exclude local increases in $[Ca^{2+}]_i$ at the plasma membrane, i.e., in close proximity to the channel, from taking place. Another possibility is that SK channels may be more sensitive to increases in $[Ca^{2+}]_i$ than the applied Ca^{2+}-sensitive dye. This indicates that local increases in $[Ca^{2+}]_i$, which remain undetectable in our assay, may be capable of opening the hSK3 channel, thereby making it even more difficult to control $[Ca^{2+}]_i$ in these types of assays. Since the $[Ca^{2+}]_i$ levels are crucial for the degree of activation of the hSK channels, it can be very difficult – if not impossible – to make sure that the potential negative modulators to be tested are actually exposed to the same degree of channel activation, thus making the assay less robust and therefore less useful for identifying negative modulators.

10. The effect of a negative modulator of SK in this assay strongly depends on the degree of channel activation, which in turn is determined by the intracellular $[Ca^{2+}]$. Positive modulators of SK are added to unstimulated cells presumed to have a more or less stable resting $[Ca^{2+}]_i$. However, in this type of assay, we are unable to control the intracellular $[Ca^{2+}]$ levels, which makes it complex to characterize positive SK modulators. It should be mentioned that for CyPPA we found an excellent correlation between electrophysiological data (inside-out patch clamp) and data obtained using the Tl^+-influx assay, where the EC_{50} values for the effect of CyPPA on hSK3 were estimated at 5.6 ± 1.6 and 4.3 ± 1.0 µM ***(6)***, respectively. The effect of a negative SK modulator is detected on cells stimulated with a Ca^{2+}-mobilizing agonist, and the size and temporal distribution of such an increase in $[Ca^{2+}]_i$ makes it even more complicated to detect negative modulators of SK channels. Strong negative modulators will most likely be detected, but their potencies may be underestimated compared to, e.g., electrophysiological assays. This

could very well be the case for NS8593, where Strøbæk et al. *(7)* estimated the IC_{50} value at 91 nM, using whole-cell electrophysiology on HEK293–hSK3 cells, whereas, when using the Tl^+-influx assay on the same cell line, we found an IC_{50} value of 1.92 µM (*see* **Fig. 20.3b**).

References

1. Wulff, H., Kolski-Andreaco, A., Sankaranarayanan, A., Sabatier, J.-M., and Shakkottai V (2007) Modulators of small- and intermediate-conductance calcium-activated potassium channels and their therapeutic indications. *Current Medicinal Chemistry* **14**, 1437–1457.
2. Trehene, J.M. (2006) Exploiting high-throughput ion channel screening technologies in integrated drug discovery. *Current Pharmaceutical Design* **12**, 397–406.
3. González, J.E. and Maher, M.P. (2002) Cellular fluorescent indicators and voltage/ion probe reader (VIPR™): tools for ion channel and receptor drug discovery. *Receptors & Channels* **8**, 283–295.
4. Weaver, C.D., Harden, D., Dworetzky, S.I., Robertson, B., and Knox, R.J. (2004) A thallium-sensitive, fluorescence-based assay for detecting potassium channel modulators in mammalian cells. *Journal of Biomolecular Screening* **9**, 671–677.
5. Strøbæk, D., Teuber, L., Jørgensen, T.D., Ahring, P.K., Kjær, K., Hansen, R.S., Olesen, S.P., Christophersen, P., and Skaaning-Jensen, B. (2004) Activation of human IK and SK Ca^{2+}-activated K^+ channels by NS309 (6,7-dichloro-1H-indole-2,3-dione 3-oxime). *Biochimica et Biophysica Acta* **1665**, 1–5.
6. Hougaard, C., Eriksen, B.L., Jørgensen, S., Johansen, T.H., Dyhring, T., Madsen, L.S., Strøbæk, D., and Christophersen, P. (2007) *British Journal of Pharmacology* **151**, 655–665.
7. Strøbæk, D., Hougaard, C., Johansen, T.H., Sørensen, U.S., Nielsen, E.Ø., Nielsen, K.S., Taylor, R.D.T., Pedarzani, P., and Christophersen, P. (2006) Inhibitory gating modulation of small conductance Ca^{2+}-activated K^+ channels by the synthetic compound (R)-*N*-(Benzimidazol-2-yl)-1,2,3,4-tetrahydro-1-naphtylamine (NS8593) reduces afterhyperpolarizing current in hippocampal CA1 neurons. *Molecular Pharmacology* **70**, 1771–1782.
8. Moore, H.-P.H. and Raftery, M.A. (1980) Direct spectroscopic studies of cation translocation by *Torpedo* acetylcholine receptor on a time scale of physiological relevance. *Proceedings of the National Academy of Sciences of the United States of America* **77**, 4509–4513.
9. Ishii, T.M., Silvia, C., Hirschberg, B., Bond, C.T., Adelman, J.P., and Maylie, J. (1997) A human intermediate conductance calcium-activated potassium channel. *Proceedings of the National Academy of Sciences of the United States of America* **94**, 11651–11656.

Chapter 21

Rubidium Efflux as a Tool for the Pharmacological Characterisation of Compounds with BK Channel Opening Properties

Neil G. McKay, Robert W. Kirby, and Kim Lawson

Summary

This chapter describes a method of assaying rubidium (Rb^+) efflux as a measure of potassium channel activity. In this assay, rubidium acts as a tracer for potassium movement across the cell membrane. HEK 293 cells expressing the alpha subunit of the human brain large-conductance, voltage-activated, calcium-sensitive potassium channel (BK channel) are loaded with Rb^+, washed, and then incubated under experimental conditions. The cell supernatant is removed, and the remaining cell monolayer lysed. These two samples contain Rb^+ that has moved out of the cell and Rb^+ that remains in the cell, respectively. Measurement of the Rb^+ content of these samples by flame atomic absorption spectrometry allows calculation of the percentage Rb^+ efflux and, depending on the experimental design, provides pharmacological data about the control and test compounds used. In this chapter, we describe the protocol and steps for optimisation and illustrate this with data obtained using NS1619, a well-characterised BK channel opener.

Key words: Potassium channels, BK channel; Rubidium efflux, Atomic absorption spectrometry, Channel openers, Small molecules, Drug discovery.

21.1. Introduction

In the past decade, advances in understanding the physiology and the pathophysiology of ion channel function have made them attractive therapeutic targets in numerous diseases *(1, 2)*. Electrophysiology remains the gold standard technique for measuring biophysical characteristics of ion channel function *(3–5)* but despite advances in automation remains labour intensive and highly specialised. Measurement of Rb^+ efflux offers a robust,

Jonathan D. Lippiat (ed.), *Methods in Molecular Biology, Potassium Channels, vol. 491*

Book doi: 10.1007/978-1-59745-526-8

reproducible, and informative method of assessing potassium channel activity. Traditionally, Rb^+ efflux measurement has been carried out using the radioactive isotope ^{86}Rb as a tracer of potassium ion movement. On the basis of the method of Terstappen *(6)*, and incorporating an auto-sampler coupled to atomic absorption spectrometry (AAS), we have developed a medium-throughput, non-radioactive method for qualitative and quantitative determination of Rb^+ efflux in order to assess the properties of novel compounds with potential large-conductance, voltage-activated, calcium-sensitive potassium channel (BK channel) opening properties.

AAS has long been used for the assessment of trace metals in environmental and biological samples owing to its relative simplicity, precision, and specificity in the analysis of a selected analyte *(7)*. The principle of flame-AAS is that the sample is atomised and sprayed into a flame, and the thermal energy generates free ground-state atoms that absorb light of a particular wavelength (in the case of Rb^+ this wavelength is 780.1 nm). The measured absorption of the sample is directly proportional to the concentration of the analyte in the sample and the concentration can be determined from a standard curve constructed by flame-AAS analysis of known amounts of the analyte.

The method described has proved useful for screening compounds thought to have modulating effects on BK channel activity, is low cost, and is relatively easy to perform. We have used this assay to examine the BK channel opening properties of several novel compounds and have generated pharmacological data that correlate well with that obtained by electrophysiology for the same compounds. The assay described is easily modified for most AAS systems as well as for different cell lines and tissues.

21.2. Materials

21.2.1. Cell Culture

1. Dulbecco's Minimal Essential Media (DMEM) supplemented with 10% foetal calf serum (FCS) (both Invitrogen, UK). Store at 4°C.
2. Trypsin/EDTA solution: 0.25% trypsin, 1 mM EDTA (Invitrogen, UK). Dispense into 2 mL aliquots under sterile conditions and store at –20°C.
3. Phosphate-buffered saline (PBS), calcium and magnesium free (Invitrogen, UK). Store at 4°C.

21.2.2. Rubidium Standard Solutions and Buffers

1. Rubidium buffer solution (RBS): 5.4 mM RbCl, 150 mM NaCl, 1 mM $MgCl_2$, 0.8 mM NaH_2PO_4, 2 mM $CaCl_2$, 25 mM HEPES, and 5 mM glucose, pH 7.2. Store at 4°C.

2. Potassium buffer solution (KBS): 5.4 mM KCl, 150 mM NaCl, 1 mM $MgCl_2$, 0.8 mM NaH_2PO_4, 2 mM $CaCl_2$, 25 mM HEPES, and 5 mM glucose, pH 7.2. Store at 4°C.
3. Triton X-100 lysis solution: 0.1% (v/v) Triton X-100 in potassium buffer solution (KBS). Store at 4°C.
4. Rubidium chloride (RbCl) stock solution: 1 mM RbCl in KBS. Store at 4°C.

21.2.3. Flame Atomic Absorption Spectrometry

Our instrumentation consisted of an S-series atomic absorption spectrometer (AAS) coupled to a Gilson 222XL auto-sampler (Thermo Scientific, Hemel Hempsted, UK). A DELL PC and the SOLAAR software suite of applications controlled the AAS. The protocol described can easily be adapted to other AAS systems.

21.3. Methods

The basic procedure for carrying out the efflux assay is straightforward but will require a number of optimisation steps, which are detailed in the notes section.

21.3.1. Cell Culture

Human embryonic kidney (HEK 293) cells stably expressing the alpha subunit of the human brain BK channel *(8)* were cultured in a 37°C, humidified atmosphere containing 5% CO_2. Cells were cultured in flasks with a growth surface of 75 cm^2. Upon reaching >90% confluence, cells were passaged onto 96-well plates in preparation for the Rb^+ efflux assay as follows.

1. Upon >90% confluent cell growth, pour off the spent culture media.
2. Add 10 mL of PBS to the flask and rinse the cell monolayer by rocking the flask from side to side taking care to ensure complete coverage of the cell monolayer with PBS. Pour off the PBS solution.
3. Add 2 mL of trypsin/EDTA solution, ensuring it covers the cell monolayer.
4. Return the flask to the cell culture incubator and incubate for 2 min.
5. Remove the flask from the incubator and tap the flask on a hard surface (e.g. the surface of the bench) to dislodge the cells from the growth surface of the flask. Examine the flask under a microscope to ensure complete dissociation of the cells (return the flask to the incubator for a further 2 min and repeat this step if required).

6. Add 8 mL of DMEM, supplemented with 10% FCS, to the flask to inactivate the trypsin solution and give a final volume of 10 mL cell suspension.
7. If continuing to culture the cell lines, seed a new 75 cm^2 cell culture flask at a 1:10 dilution (by growth surface) by adding 1 mL of the cell suspension to 25 mL of fresh DMEM supplemented with 10% FCS and culture as before until >90%.
8. Using a Bright-Line haemoacytometer, count the number of cells/mL in the remaining cell suspension and prepare 20 mL of a cell suspension containing 100,000 cells/mL.
9. Seed a 96-well cell culture plate with 20,000 cells per well by adding 200 µL of the 100,000 cells/mL cell suspension prepared in **step 8** to each well.
10. Culture for 48 h prior to Rb^+ efflux experiments.

21.3.2. Preparation of Solutions, Buffers, and Test Compounds

21.3.2.1. Preparation of Buffers and Rb^+ Standard Solutions

1. Prepare a fresh stock of RBS (*see* **Note 1**). Store this solution at 4°C until needed.
2. Prepare a fresh stock of KBS. Store this solution at 4°C until needed.
3. Prepare a fresh 1 mM stock solution of RbCl in KBS.
4. From this stock solution prepare standard RbCl solutions (1–100 µM) by dilution in KBS solution in 100 mL volumetric flasks.
5. Store the standard solutions at 4°C until needed. The prepared standards are used to construct the Rb^+ standard curves and for internal validation of the AAS instrument.

21.3.2.2. Preparation of Test Compounds

1. Prepare stock solutions of any control and test compounds by dissolving the compound in an appropriate solvent, e.g. NS1619, in dimethylsulfoxide (DMSO). Dilute the stock solution with KBS to obtain the required concentration of opener for efflux experiments.
2. Prepare enough of each control and test compound for the number of replicate wells. Each well requires a minimum of 200 µL of solution.
3. The preparation of control and test compounds should be carried out towards the end of the optimum loading period (*see* **Note 2**) immediately before incubation with the cells.

21.3.3. Rubidium Efflux Assay

The set-up and calibration assumes the use of an S-series AAS coupled to a Gilson 222XL auto-sampler and the SOLAAR software suite of applications, but the set-up steps will be similar for most AAS instruments.

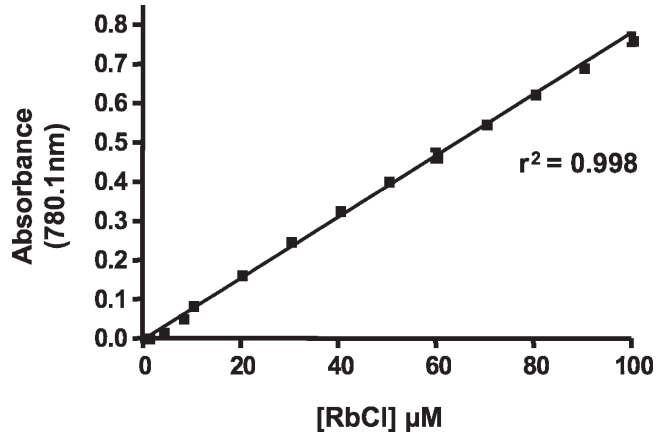

Fig. 21.1. Rubidium standard calibration curve. Rubidium standards were prepared in potassium buffer solution (KBS) and absorbance values determined by AAS at a wavelength of 780.1 nm. Data are shown as the mean absorbance value from replicate standards ± SEM, $n = 3$. Linear regression analysis of the data yields a correlation coefficient of $r^2 = 0.998$.

21.3.3.1 Flame Atomic Absorption Spectrometry: Set-Up and Calibration

1. Ensure that the instrument burner, nebuliser port, needle, and associated tubing are clean. If necessary, separate and clean them by blowing compressed air through them.
2. Clean the nebuliser port and burner slit with a metal wire.
3. Turn on the gas and air supplies to the flame-AAS and then switch on the flame-AAS instrument and the associated PC running the SOLAAR analysis software.
4. Ignite the flame and allow the AAS to warm up for 20 min with the Rb^+ hollow cathode lamp on and the instrument aspirating deionised water.
5. Optimise the optical system and warm up the photomultiplier tube and the lamp.
6. Pipette the standard solutions prepared in **Subheading 21.3.2.1** into clean tubes and place in the sampler rack in the desired orientation.
7. Pipette 300 µL of each standard solution into the wells of the first row of a clean 96-well plate.
8. Construct a calibration curve from the readings for the standard solutions (**Fig. 21.1**) in the tubes (**step 6** above) and measure the absorption of the standards in the 96-well plate (**step 7** above). Comparison of these standard curves will indicate correct calibration and internal validation if the points on the curves overlap.

21.3.3.2. Rubidium Efflux Assay of BK Channel Openers

1. Using an 8- or 12-channel multi-pipette, carefully remove the culture medium from each well of a 96-well plate seeded and cultured as above (*see* **Subheading 21.3.1**).

2. Rinse the cell monolayer by addition and removal of 200 µL PBS.
3. Add 200 µL of RBS to each well and incubate in a cell culture incubator for the determined optimal loading time (*see* **Note 2**).
4. Remove the RBS and rinse four times with PBS (*see* **Note 3**).
5. Add 200 µL of KBS containing the required concentration of test compound (prepared in **step 21.3.2.2** above) to replicate wells and incubate for the required time (*see* **Note 4**).
6. Collect paired samples of supernatant and lysate from each experimental well as follows, taking care to preserve the plate layout (*see* **Note 5**).
7. Remove the supernatant and transfer it to the corresponding well of a fresh 96-well plate (supernatant plate; extracellular Rb^+ samples).
8. Add 200 µL Triton X-100 lysis solution to the original well (containing the cells) to obtain the cell lysate (lysate plate: intracellular Rb^+ sample).

21.3.3.3. Analysis of Samples by Flame-AAS

1. Adjust the sample volume in each well to 300 µL by adding 100 µL of KBS to each well of both paired plates (supernatant samples that have been removed and transferred into the corresponding wells of a fresh 96-well plate (supernatant plate)) and the lysate samples in the wells of the original plate.
2. Place the paired sample plates (supernatant and lysate plates) on the auto-sampler in the same orientation, i.e., the order of each sample analysed from each plate will be paired.
3. Prepare fresh Rb^+ standards and construct a standard curve from the standard tubes as before.
4. Analyse the sample plates. Each sample is nebulised into the flame for 1 s prior to recording the absorption for a further 1 s, and the average absorbance value is recorded during this time (*see* **Note 6**).
5. A wash time of 10 s with distilled water between samples is required to ensure that the needle of the auto-sampler is clean and does not carryover sample between wells (*see* **Note 6**).
6. Construct a second standard curve from the standard tubes at the end of the analysis. The initial curve (**step 3** above) and this final curve should overlap, which ensures consistency during each run.
7. The Rb^+ measurements from the lysate plate are the intracellular Rb^+ concentration, and the measurements from the supernatant plate the extracellular Rb^+ measurements. Calculate the Rb^+ efflux using the following equation:

$$\%\text{Efflux} = \frac{[\text{Rb}^+]_{(\text{Extracellular})}}{[\text{Rb}^+]_{(\text{Extracellular})} + [\text{Rb}^+]_{(\text{Intracellular})}} \times 100$$

8. Depending on the experimental design (*see* **Note 7**), plotting the Rb^+ efflux under each incubation condition will generate a variety of pharmacological data. The protocol can be developed to allow concentration range effect analysis to determine comparator parameters. Such data analysis enables the construction of concentration–response curves (**Fig. 21.2**), and determination of maximal effective efflux (E_{max}), effective concentration to evoke a defined response (EC_x), and the Hill plot, an indicator of site-binding co-operativity (**Fig. 21.3**).

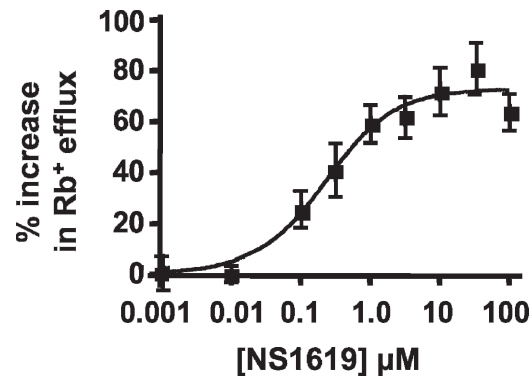

Fig. 21.2. The effect of NS1619 on Rb^+ efflux. HEK 293 cells expressing the alpha subunit of BK channels were grown on 96-well culture dishes, washed with PBS, and incubated with rubidium buffer solution (RBS). Following Rb^+ loading, the cells were washed four times and incubated with KBS containing selected concentrations of NS1619. Rb^+ efflux was determined after 10-min exposure to NS1619 and the percentage increase in Rb^+ efflux above basal levels calculated and plotted. Data are shown as mean ± SEM, $n = 24$.

BK_{Ca} Opener		E_{max} (%)	$EC_{40\%}$ (µM)
NS1619	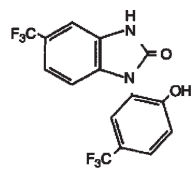	79.0±9.8	0.32±0.19

Fig. 21.3. Pharmacological parameters of NS1619 determined by Rb^+ efflux. The potency ($EC_{40\%}$) is defined as the concentration of compound required to increase Rb^+ efflux above baseline by 40%, and efficacy (E_{max}) is defined as the maximum increase in activated efflux determined from **Fig. 21.2** for NS1619. Data are shown as mean ± SEM, $n = 24$.

21.4. Notes

1. All solutions are prepared using distilled, deionised water with a resistivity of 18 MΩ/cm and prepared using good-quality, clean glassware suitable for analytical standard preparation.
2. Rb^+ enters the cells via the same routes as potassium until equilibrium is reached. It is necessary to determine the optimal loading time for each cell line used and this is easily done as follows. Using an 8- or 12-channel multi-pipette, carefully remove the culture medium from each well of a 96-well plate seeded and cultured as in **Subheading 21.3.1** and rinse the cell monolayer immediately by addition and removal of 200 µL PBS. Add 200 µL of RBS to each well and incubate in a cell culture incubator as before. To determine optimal loading of Rb^+, collect replicate lysate samples for analysis of intracellular Rb^+ at hourly intervals from 1 to 6 h by harvesting complete rows of 8 or 12 wells. Remove the RBS and rinse each row of cells to be harvested four times with 200 µL PBS to remove extracellular Rb^+ (*see* **Note 4**). Following removal of the fourth wash from the cells to be harvested, add 200 µL of Triton X-100 cell lysis solution to the each well to obtain the cell lysate (intracellular Rb^+ sample). Analyse the lysate samples by flame-AAS (*see* **Subheading 21.3.3.2** above) to determine the Rb^+ content. Plotting the intracellular Rb^+ concentration against time will indicate the optimal loading time (**Fig. 21.4**).
3. Once the cells have been loaded, it is important to remove all extracellular Rb^+ prior to the efflux experiments. Failure to do so will cause the measured efflux values to be artificially high due to elevated Rb^+ concentrations in the supernatant sample. Washing the cell monolayer with PBS repeatedly will accomplish this, and we have found that four washes are sufficient to remove extracellular Rb^+ effectively and subsequent washes do not remove significantly more Rb^+ from the surface of the cell (**Fig. 21.5**). It is important to wash the cells rapidly but gently: rapidly so that the loaded Rb^+ does not naturally efflux out (particularly if the basal Rb^+ efflux is high) and gently so as not to dislodge the cells (which will lead to artificially high Rb^+ efflux values by reducing the amount of cell lysate).
4. Potassium channel activity is regulated by several mechanisms within the cell with the result that a basal efflux level will exist in all cells. It is important to determine the basal Rb^+ efflux in each cell line used so that Rb^+ efflux measurements can be made during a period of stable basal efflux. This will

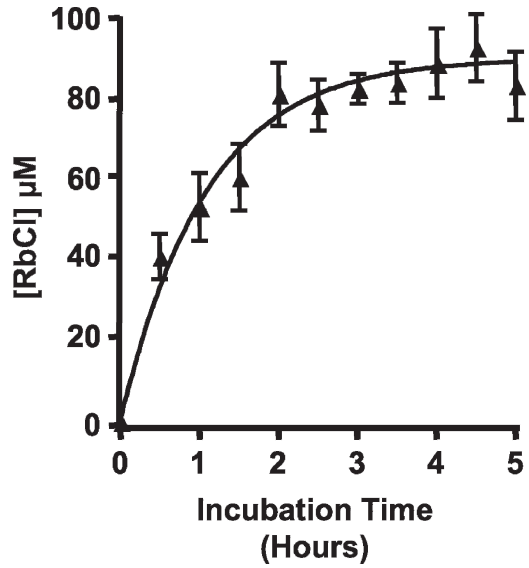

Fig. 21.4. Rubidium loading curve. HEK 293 cells expressing the alpha subunit of BK channel were grown on 96-well culture dishes, washed with PBS, and incubated with rubidium buffer solution (RBS). At selected time intervals, the RBS was removed and the cells washed four times with PBS before lysis with 0.1% (v/v) Triton-X100 in PBS. The Rb^+ concentration of cell lysates, expressed as mean ± SEM, $n = 24$, were plotted against incubation time.

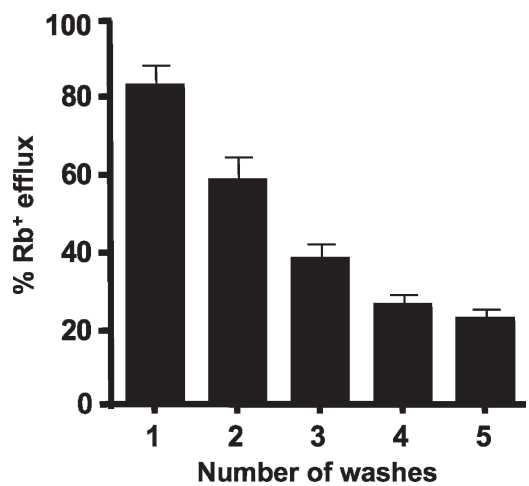

Fig. 21.5. The effect of removal of extracellular rubidium on rubidium efflux values. HEK 293 cells expressing the alpha subunit of BK channel were grown on 96-well culture dishes, washed with PBS, and incubated with rubidium buffer solution (RBS) for 4 h. The Rb^+ efflux was determined after 1–5 washes. Data are shown as mean ± SEM, $n = 24$.

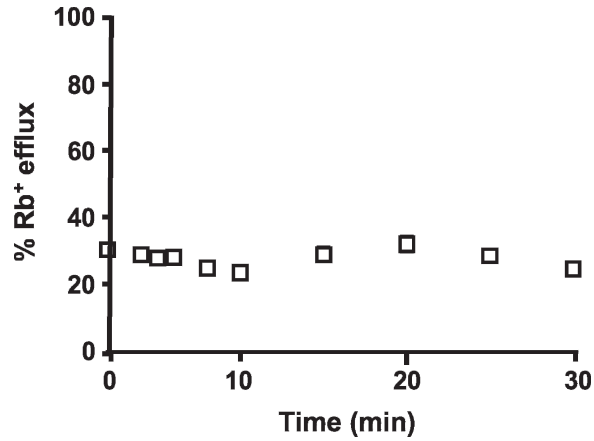

Fig. 21.6. Determination of basal rubidium efflux. HEK 293 cells expressing the alpha subunit of BK channel were grown on 96-well culture dishes, washed with PBS and incubated with rubidium buffer solution (RBS). Following Rb^+ loading the cells were washed four times and incubated with KBS. At regular time intervals the supernatant was removed from selected wells for analysis to determine the extracellular Rb^+ concentration and the corresponding cell lysate analysed to determine the intracellular Rb^+ concentration. Efflux values were calculated and the basal efflux plotted against time. Data are shown as mean ± SEM, $n = 32$.

ensure that the measurements of Rb^+ efflux are due to the compounds being studied and not a result of natural leakage from the cells. This can be done as follows. Incubate the cells with RBS for the pre-determined optimal time and then remove the RBS and rinse four times with PBS. Add 200 µL KBS to each well and incubate in a cell culture incubator. Collect replicate samples at the desired time points to construct an efflux time course, e.g. 5 min intervals. Analyse the supernatant and lysate samples by flame-AAS to determine the extracellular and intracellular Rb^+ content, respectively. Calculate the % Rb^+ efflux from the equation in **Subheading 21.3.3.3, step 7**. Plotting % Rb^+ efflux vs. time will indicate the basal efflux level and its stability over the incubation period (**Fig. 21.6**).

5. The cells are plated on 96-well culture plates (the original plate). Once the cells have grown to the required confluence and have been washed and loaded with Rb^+, control or test compounds are added to the wells of the 96-well plate and incubated under the desired conditions. Following this incubation, the supernatant (containing any extracellular Rb^+) is transferred to the corresponding wells of a fresh 96-well plate (the supernatant plate). The cells remain in the wells of the original plate and are lysed to obtain the cell lysate sample (containing any intracellular Rb^+). The cell lysates

can be assayed directly from this plate and do not need to be transferred to a fresh plate. In effect, at the completion of the experiment the original 96-well plate has become the cell lysate sample plate and a corresponding supernatant sample plate is prepared. The two 96-well plates will contain paired supernatant and cell lysate samples in the corresponding wells, thus preserving the plate layout; e.g., removing the supernatant from well A1 of the original plate into well A1 of a fresh plate will mean that once the cells in well A1 of the original plate are lysed the paired supernatant sample is in the corresponding A1 well of the supernatant plate.

6. The settings described have been optimised for the assay and instrument used. These will need to be determined empirically for each individual system used but should provide an initial reference point.
7. Experimental design can be extended to confirm the identity of channels involved in alterations to Rb^+ efflux by use of specific pharmacological tools, which allow opener/blocker interaction studies, e.g., iberiotoxin, which prevents increased Rb^+ efflux in response to NS1619.

References

1. Bennett P. B. and Guthrie H. R. (2003) Trends in ion channel drug discovery: advances in screening technologies. *Trends in Biotechnology* **21**, 563–569.
2. Ebneth A. (2002) Ion channel screening technologies: will they revolutionise drug discovery? *Drug Discovery Today* **7**, 227.
3. Birch P. J., Dekker L. V., James I. F., Southan A., and Cronk D. (2004) Strategies to identify ion channel modulators: current and novel approaches to target neuropathic pain. *Drug Discovery Today* **9**, 410–418.
4. Zheng W., Spencer R. H., and Kiss L. (2004) High throughput assay technologies for ion channel drug discovery. *Assay and Drug Development Technologies* **2**, 543–552.
5. Gill S., Gill R., Lee S. S., Hesketh J. C., Fedida D., Rezazadeh S., Stankovich L., and Liang D. (2003) Flux assays in high throughput screening of ion channels in drug discovery. *Assay and Drug Development Technologies* **1**, 709–717.
6. Terstappen G. C. (1999) Functional analysis of native and recombinant ion channels using a high-capacity non-radioactive rubidium efflux assay. *Analytical Biochemistry* **272**, 149–155.
7. Apostoli P. (2002) Elements in environmental and occupational medicine. *Journal of Chromatography B* **778**, 63–97.
8. Hartness M. E., Brazier S. P., Peers C., Bateson A. N., Ashford M. L. J., and Kemp P. J. (2003) Post-transcriptional control of human maxiK potassium channel activity and acute oxygen sensitivity by chronic hypoxia. *Journal of Biological Chemistry* **278**, 51422–51432.

Chapter 22

Recording hERG Potassium Currents and Assessing the Effects of Compounds Using the Whole-Cell Patch-Clamp Technique

Ray M. Helliwell

Summary

The complex gating of the hERG channel makes it ideally suited to its principal role in controlling phase 3 repolarization of the cardiac ventricular action potential. Any abnormal delay in repolarization can lead to the re-activation of Ca^{2+} channels, giving rise to early after-depolarizations, and coupled with increased cardiac dispersion, typically associated with these delays, provides respectively both the trigger and substrate for the potentially life threatening arrhythmia Torsardes de Pointes (TdP). Owing to the fundamental role of hERG in controlling the duration of the cardiac action potential, it is not surprising that any drugs that potently and selectively block this channel are liable to have these effects. Consequently, much effort has been expended in developing standard voltage protocols to reliably assess the effects of compounds on hERG currents in vitro. This chapter describes how to record hERG currents in a recombinant cell line using the whole-cell patch-clamp technique. It also provides typical voltage protocols used for assessing the basic electrophysiological properties of these currents and for assessing the effects of compounds on hERG tail currents.

Key words: hERG; Patch-clamp, Ion channels, Safety pharmacology, long QT.

22.1. Introduction

The role of hERG K^+ channels in ventricular cardiac repolarization and the fact that a diverse array of drugs can block this channel, leading to lengthening of the QT interval and the potentially fatal tachyarrhythmia Torsades des Pointes (TdP), are now well documented *(1, 2)*. The consequences for the pharmaceutical industry have been severe, as, in the light of this, a number of

Jonathan D. Lippiat (ed.), *Methods in Molecular Biology, Potassium Channels, vol. 491*

Book doi: 10.1007/978-1-59745-526-8

high-revenue drugs were withdrawn from the market and other promising drugs in development had to be abandoned because of their hERG liability *(3)*. A particularly troubling time for such companies was in the mid- to late 1990s when the link between hERG block and the rare cases of TdP reported in the clinic became so compelling *(4)*.

Subsequently, a variety of approaches have been adopted to understand this relationship and the nature of drug interaction with the hERG channel, from high-throughput hERG screens *(5–8)*, mutagenesis studies *(9, 10)*, in silico modelling *(11–13)*, trafficking assays *(14, 15)* to the development of sophisticated pro-arrhythmia models *(16–19)*. The use of patch-clamp electrophysiology with recombinant cell lines that over-express hERG or other cardiac ion channels has played an important role in many of these approaches and will no doubt continue to do so.

This chapter restricts itself to the practical methods used to record these currents and to the establishment of the basic biophysical and pharmacological properties. While the conventional micropipette-based patch-clamp technique is described, the experimental protocols apply equally to automated planar patch-clamp platforms. A particularly useful review that covers some additional aspects of recording hERG currents should also be consulted *(20)*.

22.2. Materials

22.2.1. Cell Culture

1. Phosphate buffered saline (Invitrogen).
2. Trypsin/EDTA solution (Invitrogen).
3. HEK293 cell line robustly expressing hERG (e.g. Millipore PrecisION hERG cell line).
4. Culture medium: D-MEM/F-12 with L-glutamine (Invitrogen), 10% foetal bovine serum (Invitrogen), 1% non-essential amino acids (Invitrogen), selection antibiotic (e.g. 400 µg/mL G418).

22.2.2. Solutions for Patch-Clamp Electrophysiology

Solutions used typically approximate to 'physiological' ionic composition and concentration.

1. External solution: 137 mM NaCl, 4 mM KCl, 4; 1 mM $MgCl_2$, 1.8 mM $CaCl_2$, 10 mM HEPES, 10 mM glucose, pH 7.3 with 10 M NaOH.
2. Internal solution: 140 mM KCl, 2 mM $MgCl_2$, 10 mM HEPES, 10 mM EGTA, 5 mM Mg_2ATP, pH 7.2 with 10 M KOH.

22.2.3. Patch-Clamp Electrophysiology

1. Patch-clamp amplifier: many are computer-controlled with proprietary software and connected to computer via an analogue–digital interface.
2. Personal Computer: typical specifications are Pentium 4 processor, 1 GB RAM, 20 GB hard disk, 19″ colour monitor, software OS Windows 2000/XP.
3. Software: Computer-controlled amplifiers are supplied with their own software although additional modules are frequently required. Additional software such as Microcal Origin is also required for further data analysis and preparation of figures for publication.
4. Vibration isolation table and Faraday cage.
5. Inverted microscope equipped with a low- (×10) and high-power objectives (×40), and piezo-drive/hydraulic manipulators.
6. Oscilloscope for the continuous monitoring of signals.
7. Gravity-feed perfusion system, recording chamber that can accommodate coverslips with cells, and a vacuum source with a bottle trap to remove solution from the bath.
8. Patch pipette puller.
9. Borosilicate capillary glass (1.5 mm o.d./0.9 mm i.d.).
10. Tubing of various diameters.
11. Ag/$AgCl_2$ pellets (Warner Instruments).
12. Ag wire.
13. Syringe (1 mL).
14. Microfil filaments.

22.3. Methods

22.3.1. Preparation of Cells for Whole-Cell Recording

Cells should be maintained in the log phase of growth and at a maximum of 70% confluence prior to use for experimentation. All reagents should be pre-warmed to 37°C before use.

1. Decant the spent media from a T 25 cm flask (30–70% confluent).
2. Add 2 mL of PBS and rock the flask gently to rinse the cell sheet. Decant PBS.
3. Add 2 mL of Trypsin/EDTA and rock the flask gently to cover the cell sheet; decant most of the excess solution.
4. Incubate for 2–3 min at 37°C and tap the flask to dislodge cells.

5. During the incubation, prepare dishes with coverslips; place approximately six 5 × 0.15 mm glass coverslips in a 35-mm Petri dish, and store in a 95-mm Petri dish.
6. Add 5 mL complete media to the flask, triturate to form a homogenous cell suspension.
7. Pipette 2.5 ml of this suspension into the coverslips in the 35-mm Petri dish.
8. Place at 37°C for 1 h to allow the cells to adhere.

22.3.2. Solution Preparation

1. Make up sufficient external solution for the day's experiment (1–2 L is usually enough).
2. Make up 100 mL of the internal solution, omitting the Mg_2ATP, and store in 1 mL aliquots in eppendorf tubes at –20°C. An aliquot can be defrosted as required on the day of experimentation.
3. Mg_2ATP is made up separately as a 100 mM stock in distilled water and stored in 50 µL aliquots at –20°C.
4. Take a 1 mL aliquot of internal solution and add it to a 50 µL aliquot of Mg_2ATP and mix thoroughly.
5. Draw the solution up into a 1 mL syringe and attach a Microfil™ filament to the end. Store on ice.

22.3.3. Whole-Cell Patch-Clamp

Prior to performing the step-by-step instructions below, ensure that all equipment described in **Subheading 22.2.3** is configured correctly, line (mains) noise minimized, and the patch-clamp amplifier calibrated according to the manufacturer's instructions. A detailed description of many of the finer points of patch-clamp set-up and implementation can be found in **refs.** *21–23*.

22.3.3.1. Standard Recording Procedure

1. Pull glass-recording electrodes according to pipette puller instructions (*see* **Note 1**).
2. Connect all tubing from gravity feed reservoirs to the manifold that leads to the bath. Fill all gravity feed reservoirs with external and drug solutions and ensure a smooth, uninterrupted flow from the external solution reservoir through into the bath and out via vacuum suction (*see* **Note 2**).
3. Switch the valves to each drug solution reservoir in turn ensuring that the flow is minimally interrupted and there are no air bubbles. Switch back to external solution.
4. Place a $Ag/AgCl_2$ pellet in the bath and connect to the headstage of the amplifier (*see* **Note 3**).
5. Place a coverslip with adherent cells on the surface into the bath. Locate a desirable cell using the ×10 objective (*see* **Note 4**).

6. Fill a glass electrode with pipette solution using the 1 mL syringe connected to the Microfil™ filament (*see* **Note 5**).
7. Attach the glass electrode to the electrode holder and connect the assembly to the amplifier headstage mounted on the manipulator, making sure the $Ag/AgCl_2$ wire in the holder is in contact with pipette solution within the electrode.
8. Ensure that the tubing is connected to the side-port of the holder (*see* **Note 6**).
9. Align the electrode over the bath and advance it into the solution using the coarse controls on the manipulator.
10. Once in the bath, use the computer-controlled amplifier controls and adjust the gain settings to observe the current in the oscilloscope window on the computer monitor (*see* **Note 7**).
11. For ensuring that the electrode and ground are at more or less the same potential, cancel the voltage offset using the amplifier software. The recorded current should now be close to zero and the offset voltage required to keep it there registered as V_{offset} (*see* **Note 8**).
12. Apply a 1–2 mV voltage step. This will cause a proportionate step change in the current level so that the resistance of the electrode can be measured according to Ohm's law. For whole-cell recording the resistance should be 3–5 MΩ (*see* **Note 9**).
13. Locate the tip of the electrode under the microscope using the ×10 objective by focusing above the plane of the cells. Once the tip is in focus, advance the electrode downwards towards the cell using the coarse controls of the manipulator, while simultaneously moving the objective to keep the tip in focus.
14. When directly over the cell, switch to the ×40 objective and use the fine controls of the manipulator to approach the surface of the cell in small steps while continuously monitoring the electrode resistance using the 1–2 mV steps.
15. When the electrode just touches the cell, a slight increase in resistance will be registered.
16. Carefully advance the tip still further until the resistance increases by 1/3–2/3. Stop moving the electrode and apply gentle suction through the side-port of the electrode holder to form a gigaohm seal (*see* **Note 10**).
17. Once a gigaseal has formed, the current step in response to the 1–2 mV voltage step, used to monitor the resistance, will be barely visible as a deflection. Increase the voltage step to 10 mV.

18. Use the C_{fast} cancellation control to remove the capacity current that is in coincidence with the voltage step. Increase the amplifier gain to around 10 mV/pA and obtain the whole-cell configuration by applying repetitive, brief, strong suction until the membrane patch has ruptured (*see* **Note 11**).
19. Make sure that V_{com} is set negative (around –80 mV) at this point to ensure that hERG channels are not open, as this will interfere with measurements of C_{slow}/R_{series}.
20. The spikes of capacity current should then be cancelled using the C_{slow} compensation control on the amplifier. If the capacity current has been completely cancelled, then the amplifier reports two important values: the cancelled C_{slow} is the capacitance of the cell and R_{series} is the access resistance (*see* **Note 12**).
21. If the access resistance is high or begins to increase over time ('seal over'), more brief suction must be applied and C_{slow} re-cancelled (*see* **Note 13**).
22. Once a stable access resistance has been achieved and sufficient time has been allowed for complete dialysis of the pipette solution with the cell interior (5–10 min or so after membrane rupture), set V_{com} to –80 mV.
23. Apply and adjust the level of series resistance compensation (50–90%) to ensure the cell is adequately voltage-clamped.

22.3.3.2. Recording hERG Currents Using Typical Voltage Protocols

There are various voltage protocols that are applied to assess the electrophysiological and pharmacological properties of hERG. The most common are described below. Running these voltage protocols prior to testing the effects of drugs and assessing some of the key parameters is advisable to ensure that the cells are adequately voltage-clamped and dialysis with intracellular solution is complete. For example, if the voltage-clamp is insufficient (i.e. there are voltage errors) then the *I/V* relationship may be negative-shifted and the kinetics slower than expected. If dialysis is incomplete, the currents may not reverse near the theoretical E_K.

Recording the Isochronal *I/V* Relationship and the Activation Curve

1. The amplifier provides the voltage stimulus (defined as a voltage protocol, see below) and records the resulting currents into a data file.
2. The data file can then be recalled at a later date to measure the isochronal *I/V* and the activation curve using the amplifier manufacturer's own software.
3. For fitting the data, figure preparation, and more specialized analysis, the relevant data can be exported to other software packages (e.g., Origin, Prism, etc.).
4. The voltage protocol used is shown in **Fig. 22.1**. The voltage is first stepped from the holding potential of –80 to –60 mV

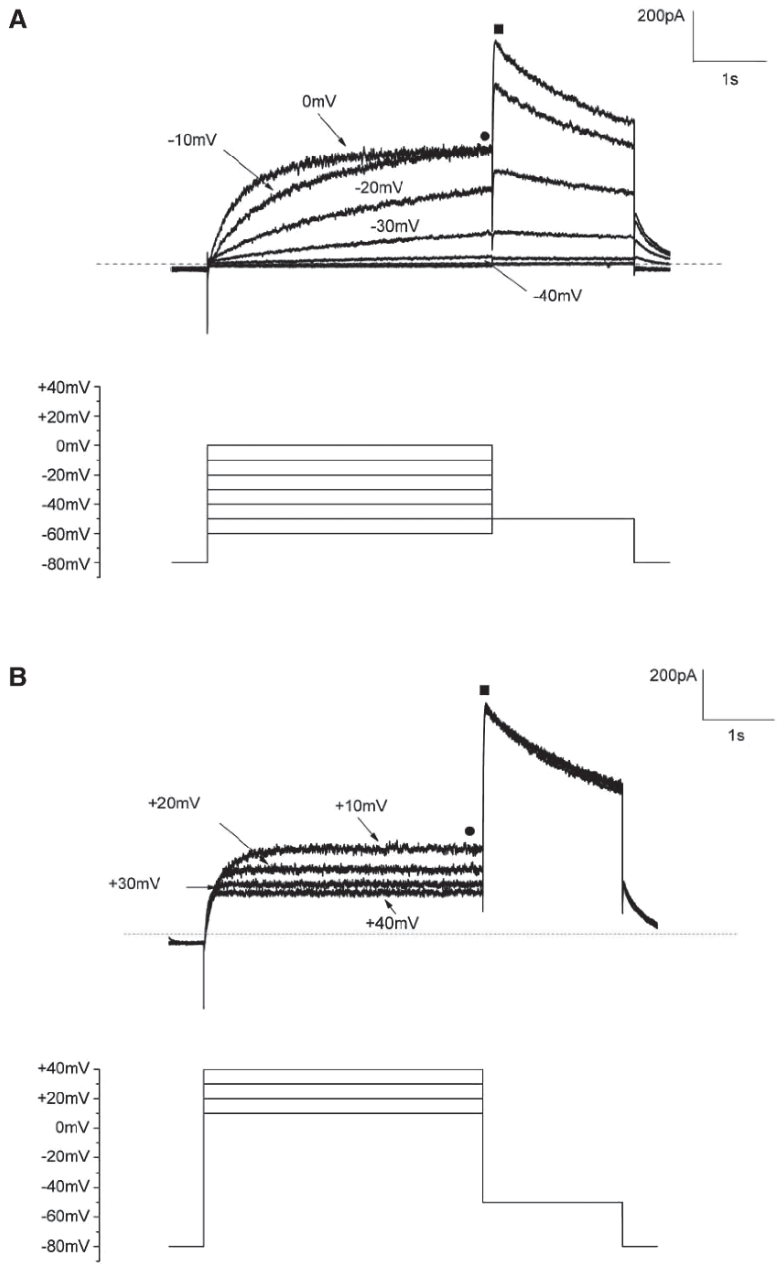

Fig. 22.1. Typical voltage protocol used to evoke hERG currents. The voltage protocol is divided into two parts for clarity ((**a**) −40 to 0mV pulses and (**b**) +10 to +40 mV pulses) and can be used to examine the *I/V* relationship and construct an activation curve.

for 4 s before stepping the membrane voltage back to −50 mV for 2 s. Finally, the voltage is returned to −80 mV. This is one voltage sequence in the protocol.

5. In **Fig. 22.1**, a family of voltage sequences is shown each following another with a 20 s delay. The only difference between

each sequence is the magnitude of the 4 s depolarizing step. In the first sequence it is –60 mV, the next it is –50 mV, then –40 mV, and so on. In other words, the step is incremented by +10 mV with each sequence. In this particular voltage protocol, there are 11 such voltage sequences where the voltage is incrementally increased in 10 mV steps from –60 to +40 mV. The voltage protocol is defined in the amplifier software.

6. For clarity, in **Fig. 22.1** the first seven voltage sequences (–60 to 0 mV), and corresponding evoked currents, are shown separately (upper panel) from the subsequent four sequences (+10 to +40 mV, lower panel).

Recording the 'Fully Activated' *I/V* Relationship

The voltage protocol used is shown in **Fig. 22.2a**. It can provide a relatively accurate measure of the reversal potential and allows for the measurement of time constants of deactivation at negative potentials (*see* **Note 14**).

Recording the Effects of Compounds on hERG Currents

1. The voltage protocol used is shown in **Fig. 22.2b**.
2. The membrane voltage is stepped from the holding potential of –80 mV to +40 mV for 4 s and then stepped back to –50 mV for 4 s to evoke a tail current. The voltage is then returned to –80 mV.
3. The sequence is evoked continuously every 20 s.
4. The lowest dose of the compound is first added, but only when stable tail currents have been obtained. Increasing concentrations of the compound can be subsequently applied provided 'steady-state' block has been achieved at the previous dose (*see* **Fig. 22.4**).

Leak Subtraction

1. Generally leak subtraction is not necessary provided; leak current is small compared to the evoked hERG current.
2. A good indicator of a high resistance seal, and therefore low leak current, is to examine the holding current at –80 mV where all hERG channels are closed. The holding current, measured from zero, should be <50 pA.
3. Depending on the experiment and the level of accuracy required, leak subtraction is necessary. This can be done with a P/4 protocol (described in (**20**)) or by adding a supra maximal concentration of a selective hERG blocker and subtracting the currents from those in the absence of blocker, prior to addition. This latter approach assumes that the level of leak has not changed after addition.

22.3.4. Analysis of Current Records

Typically, the measured values are obtained using the patch-clamp amplifier software and exported as a text file. The text file is then imported into other analysis software (e.g., Origin) to construct *I/V* relationships and for fitting the data (e.g., the Boltzmann distribution for the activation curve, logistic equation

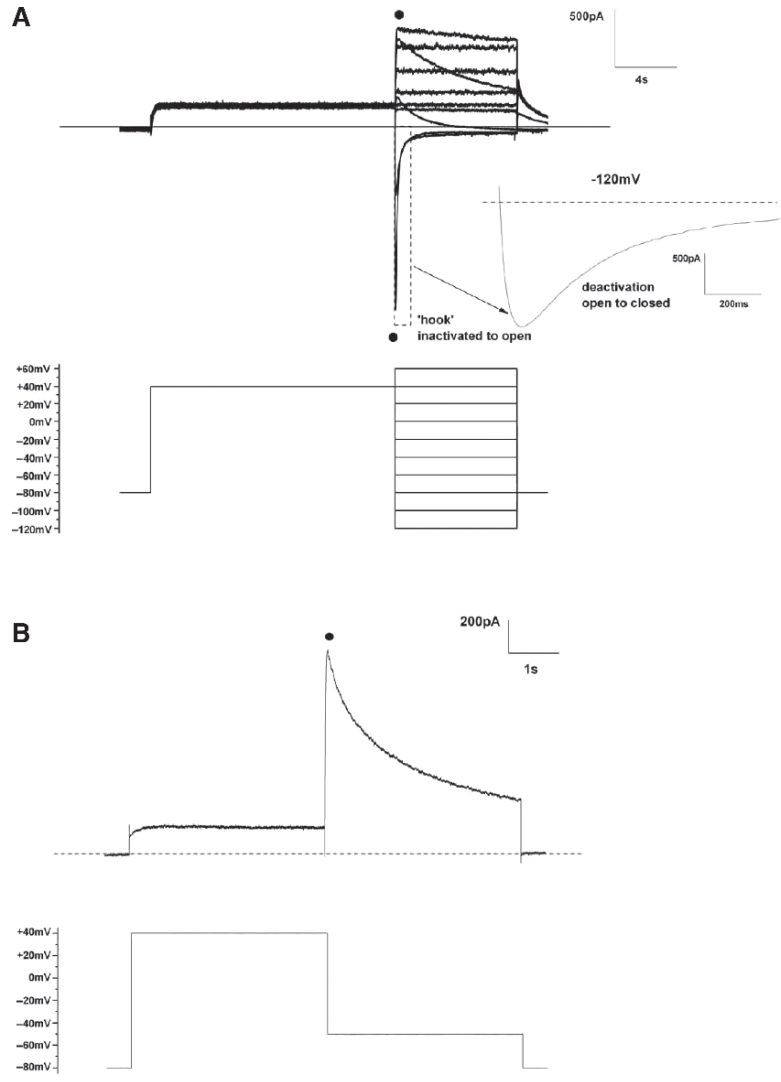

Fig. 22.2. Other voltage protocols used to evoke hERG currents. The voltage protocol in (**a**) can be used to accurately measure the reversal potential and time constants of deactivation at negative potentials. The voltage protocol in (**b**) is frequently used to assess block of compounds.

for dose–response data, etc.). Representative traces can also be exported to the software by following a similar procedure.

22.3.4.1. Constructing the Isochronal I/V Relationship and the Activation Curve

1. Applying this voltage protocol (**Fig. 22.1**) it is possible to construct the *I/V* relationship shown in **Fig. 22.3**.
2. The current measurements are taken at the same instant of time, at the end of the 4 s depolarizing step (**Fig. 22.1**, solid circle), and plotted against the magnitude of the voltage step (*see* **Note 15**).

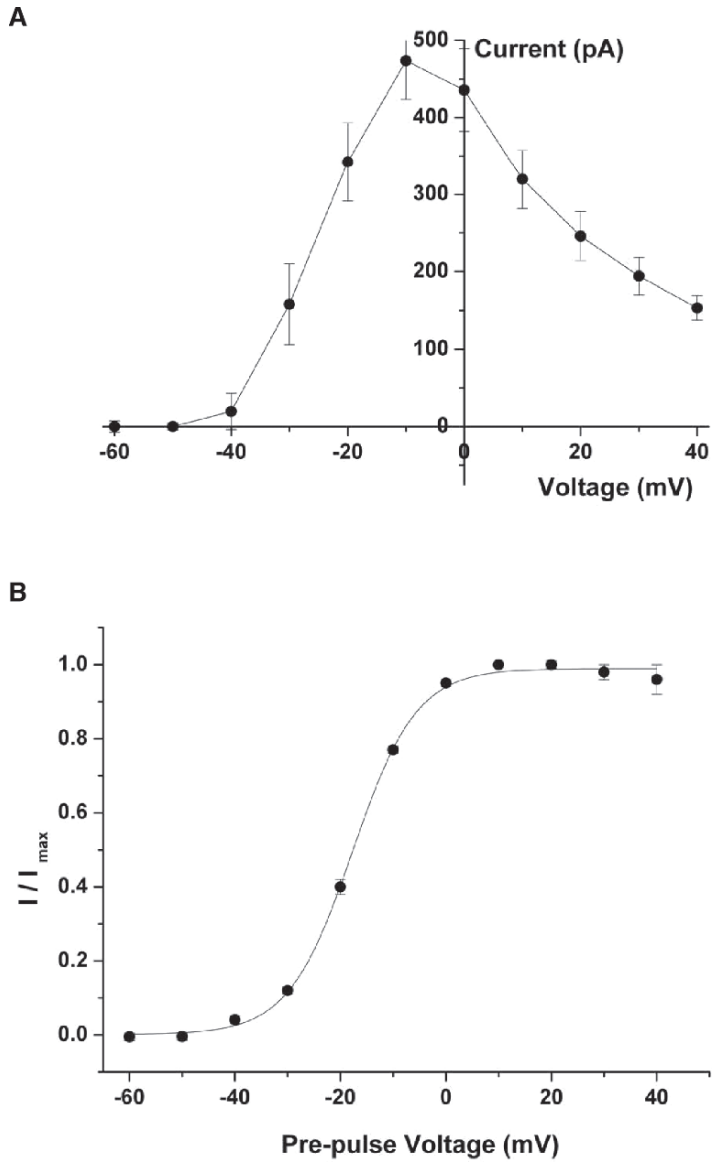

Fig. 22.3. The isochronal *I*/*V* relationship and activation curve. The isochronal *I*/*V* relationship is shown in (**a**) and is taken from the data in **Fig. 22.1** where the current amplitudes were measured at the end of the 4 s depolarizing step (*solid circle*) and plotted against the voltage. The activation curve in (**b**) was constructed by measuring the peak current amplitude on stepping to −50 mV from various potentials (*solid square* in **Fig. 22.1**). The amplitude was normalized to the peak current at +10 mV and plotted against pre-pulse potential. The Boltzmann fit of the data gave a $V_{1/2}$ activation of −18 mV and slope of 6 mV. The number of replicates is four.

3. To construct the activation curve in **Fig. 22.3b**, measurements are taken at the solid square in **Fig. 22.1** (i.e., the peak tail current is measured on stepping back to −50 mV).

4. The tail current is maximal at +10 mV (I_{max}) and so the relative amount of current (I) at the other voltages can be calculated by dividing I/I_{max} and plotted against the pre-pulse voltage (i.e., the magnitude of the voltage step immediately prior to the step to −50 mV) to give the activation curve in **Fig. 22.3**.
5. The data can be described by a Boltzmann distribution so that the $V_{1/2}$ of activation and the slope can be calculated. In the example shown, the $V_{1/2}$ and slope is −18 mV and 6 mV, respectively (*see* **Note 16**).

22.3.4.2. Constructing the 'Fully Activated' I/V Relationship

1. Applying this voltage protocol (**Fig. 22.2**) it is possible to construct the I/V relationship that is shown in **Fig. 22.4**.
2. Plotting the peak inward current on stepping back to various test potentials from +40 mV as in **Fig. 22.1b** (solid circles) against the relevant test potential gives rise to the 'fully activated' I/V curve in **Fig. 22.4** (*see* **Note 17**).

22.3.4.3. Assessing the Effects of Compounds on hERG Currents

1. Applying the protocol described in **Fig. 22.2b** (*see* **Note 18**) it is possible to measure the amplitude of the tail current on stepping back to −50 mV for each pulse (measured as net outward current at solid circle in **Fig. 22.2b**) and plot vs. pulse number (**Fig. 22.5a**).
2. **Figure 22.5a** illustrates the effect of three concentrations (3, 30 and 300 nM) of cisapride (*see* **Note 19**) cumulatively applied to the cell (added at bars). Individual current records,

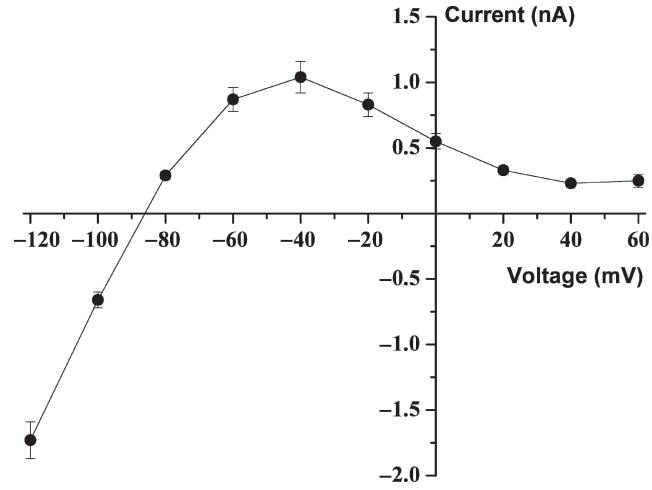

Fig. 22.4. The fully activated I/V curve. The hERG current reverses direction around −87 mV and shows a peak in the I/V at −40 mV. The number of replicates is four.

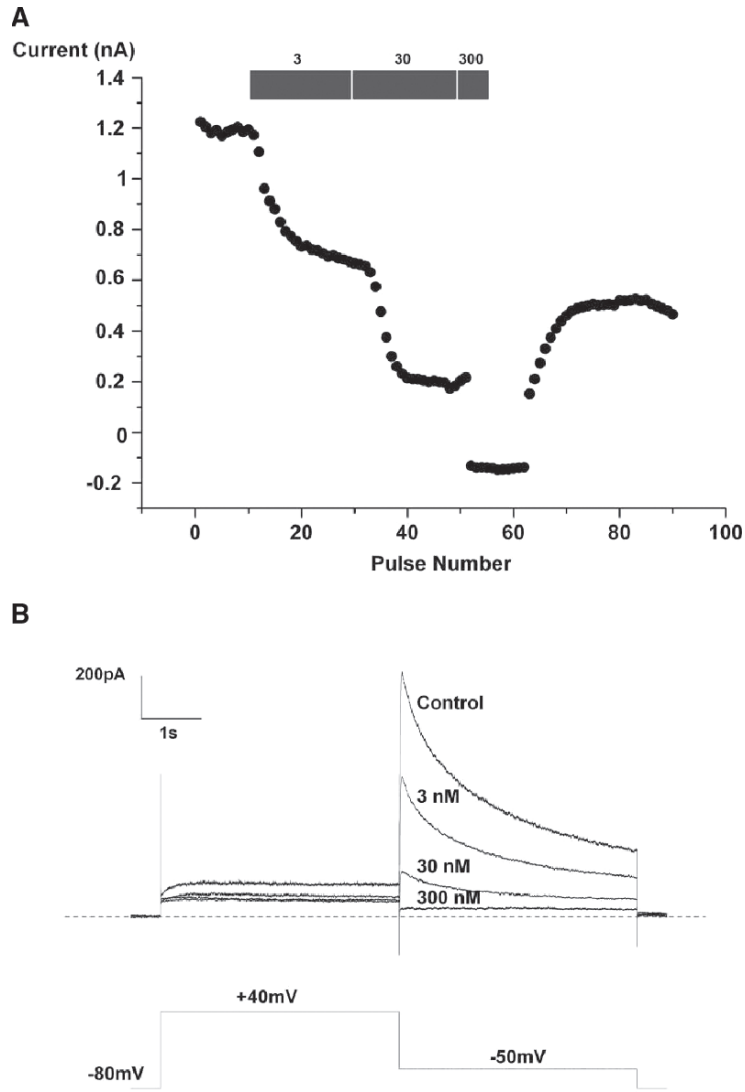

Fig. 22.5. The effect of cisapride on hERG tail currents. The tail current amplitude for each successive pulse number is plotted in (**a**) and the presence of cisapride indicated by the bars. Cisapride dose-dependently inhibited the amplitude of the tail currents that was only partially reversible. Typical current records are also shown in (**b**), before (control) and in the presence of the indicated concentrations of cisapride (3–300 nM as indicated).

recorded in the presence of the indicated concentrations of cisapride are shown in **Fig. 22.5b**.

3. The peak tail current in the presence of various concentrations of drug can be expressed relative to the peak tail current prior to addition either as a ratio or percent inhibition. If sufficient concentrations are tested (usually a minimum of 5)

a dose–response relationship can be obtained by plotting the ratio/percent inhibition vs. concentration on a log scale. If appropriate, a standard four-parameter logistic equation can be used to fit the data so that an estimate of the IC_{50} value can be obtained, e.g., $100 \times (1 + ([\text{drug}]/IC_{50})^{p})^{-1}$, where IC_{50} is the concentration required to inhibit 50% of the response and p is the slope of the curve.

22.4. Notes

1. Adjusting the resistance of the pipette once the basic geometry has been formed is usually made by fine alterations in the heat setting of the second pull. For most whole-cell applications, a simple vertical two-stage puller is all that is required and fire-polishing of the electrode tips is rarely necessary.
2. Obtaining a smooth flow may take some adjustment of the amount of suction and the angle/height of the suction capillary in the bath. Overflow of the bath usually occurs because of air bubbles blocking the flow or if the areas surrounding the bath edges are wet. In this case, the surface tension of the solution is insufficient to keep it within the bath, and the solution is 'dragged' over the sides of the bath instead of flowing out through the suction capillary. So, ensure that areas immediately adjacent to the bath are dry.
3. If one intends to change the composition of the external solutions during the experiment, particularly $[Cl^-]$, this may cause a change in the junction potential. The pellet is best placed in a side-bath containing pipette solution and connected to the main bath by means of an agar salt bridge.
4. 'Good' cells for patch-clamp typically have a well-delineated cell membrane appearing as a halo under phase-contrast and a smooth clear cytoplasm.
5. To successfully fill the electrode, insert the filament down to the neck of the electrode and slowly depress the syringe while moving the filament back up the electrode. Fill the electrode approx half way up. Air bubbles can be removed by holding the electrode firmly and flicking the wrist a couple of times.
6. The other end of the tubing, leading out of the cage, is attached to a plastic syringe and is used to provide suction when forming gigaohm seals. This tubing must be taped down firmly along much of its length (i.e., on the headstage

and vibration isolation table) to prevent vibrations being transmitted to the electrode tip.

7. This recorded current is invariably offset from zero and results from the voltage difference (offset) between the recording electrode and ground. If no current can be recorded or there is a significant amount of mains noise, ensure that there is an electrical circuit between the ground and electrode, i.e., electrodes are fully immersed in bath solution and that they are connected to the amplifier.
8. Note that during this process the command voltage must be set to zero. V_{offset} should be typically <10 mV between good $Ag/AgCl_2$ electrodes immersed in physiological salt solutions. If the offset current fluctuates wildly, drifts from zero and/or the offset voltage is large; the electrodes may need re-chloriding or replacement.
9. If the resistance is lower/higher, try increasing/reducing the heat on the second stage pull, respectively, when making the electrodes.
10. The resistance may increase rapidly and approach a gigaohm within a few seconds. If so, stop the suction; otherwise, continue applying steady suction and apply a steady negative pipette voltage of –20 mV at V_{com}, even more negative if the resistance has increased enough. Briefly halt the suction. On many occasions the resistance will then increase dramatically and approach gigaohm. If the resistance does not increase sufficiently, try applying suction again and then releasing the pressure once more. Repeat this process until a gigaseal is formed. Note that the precise method for gigaseal formation will vary with cell type, the day, and the experimenter.
11. Membrane rupture will be manifest by the appearance of large 'spikes' of capacity current coincident with the step changes in voltage. This is the whole-cell recording configuration. Sometimes one may successfully rupture the patch but lose the seal, so care must be taken to provide just the right amount of suction for break-in without losing the seal. Once a number of cells have been tried, most experimenters get a good idea of how much suction is required.
12. Access resistance should be around 2–3 times the original pipette resistance if you have ruptured the patch sufficiently. Acceptable values are therefore 6–15 MΩ although the value will depend ultimately on the amplitude of channel current to be recorded and the amount of series resistance compensation that can safely be used.
13. Particularly with cells that have a tendency to 'seal-over', applying slight positive pressure can sometimes lower the

resistance to within acceptable limits. However, care must be taken not to apply too much or one will inflate the cell and lose the seal!

14. This protocol also reveals another hallmark feature of hERG that is shown on an expanded timescale in the inset of **Fig. 22.2**, at −120 mV. On immediately stepping from +40 to −120 mV, the instantaneous current is at first relatively small since most channels have not recovered from the inactivation produced by the +40-mV step. However, the current then begins to increase (opening of channels), reflecting recovery from inactivation prior to decaying (subsequent deactivation of channels). This behaviour forms a characteristic hook in the current record.

15. Strictly speaking, this cannot be termed a 'steady-state' *I/V* since at voltages more negative than 0 mV the currents have not reached a steady level at the end of the 4 s step where the values are taken.

16. The activation curve can be described by a Boltzmann equation of the form

    $I/I_{max} = 1/(1 + \exp^{(V-V_{1/2})}/k)$,

    where I is the peak tail current for a given pre-pulse voltage, V, and I_{max} is the maximum peak tail current. The $V_{1/2}$ of activation describes the voltage at which half the channels are open (relative to an assumed maximum level beyond which the current level does not change, +10 mV in **Fig. 22.3b**) and the slope, k, indicates how voltage dependent the channels are. Evidently, the more voltage dependent they are, the steeper the slope. Typically, different channels will have different values for these parameters allowing the experimenter to use them as distinguishing features.

17. The hERG current crosses the voltage axis at around −87 mV close to the theoretical equilibrium potential for K^+ (E_K) under these ionic conditions (around −90 mV) and the peak hERG outward current occurs around −40 mV to −30 mV.

18. There are variations on this theme, either stepping to slightly less depolarized potentials (+20 mV instead of +40 mV), altering the duration of this pulse or instead of stepping back to −40/−50 mV to evoke a tail current, ramping back to −80 mV (0.5 mV/ms) to simulate the repolarization phase of the action potential. The merits of each type of protocol have been discussed elsewhere *(24)*; suffice to say that the one given here is satisfactory for detecting most hERG channel blockers.

19. Cisapride is a gastro-intestinal prokinetic (5-HT4 receptor agonist) that was withdrawn from the U.S. market in the

year 2000 due to fatalities caused by TdP, ultimately linked to potent block of the hERG channel *(25)*.

Acknowledgments

I would like to thank the Millipore Ion Channel Group (Cambridge, UK) particularly Helen Swain and Louise Webdale for help with the tissue culture and cell preparation sections.

References

1. Haverkamp, W., Breithardt, G., Camm, A.J., Janse, M.J., Rosen, M.R., Antzelevitch, C., Escande, D., Franz, M., Malik, M., Moss, A., and Shah, R. (2000) The potential for QT prolongation and pro-arrhythmia by non-anti-arrhythmic drugs: clinical and regulatory implications. Report on a Policy Conference of the European Society of Cardiology. *Cardiovasc. Res.* **47**, 219–233.
2. Gupta, A., Lawrence, A.T., Krishnan, K., Kavinsky, C.J., and Trohman, R.G. (2007) Current concepts in the mechanisms and management of drug-induced QT prolongation and torsade de pointes. *Am. Heart J.* **153**, 891–899.
3. Fermini, B. and Fossa, A.A. (2003) The impact of drug-induced QT interval prolongation on drug discovery and development. *Nat. Rev. Drug Discov.* **2**, 439–447.
4. Shah, R.R. (2002) The significance of QT interval in drug development. *Br. J. Clin. Pharmacol.* **54**, 188–202.
5. Dorn, A., Hermann, F., Ebneth, A., Bothmann, H., Trube, G., Christensen, K., and Apfel, C. (2005) Evaluation of a high-throughput fluorescence assay method for HERG potassium channel inhibition. *J. Biomol. Screen.* **10**, 339–347.
6. Guthrie, H., Livingston, F.S., Gubler, U., and Garippa, R. (2005) A place for high-throughput electrophysiology in cardiac safety: screening hERG cell lines and novel compounds with the ion works HTTM system. *J. Biomol. Screen.* **10**, 832–840.
7. Diaz, G.J., Daniell, K., Leitza, S.T., Martin, R.L., Su, Z., McDermott, J.S., Cox, B.F., and Gintant, G.A. (2004) The [3H]dofetilide binding assay is a predictive screening tool for hERG blockade and proarrhythmia: comparison of intact cell and membrane preparations and effects of altering [K+]o. *J. Pharmacol. Toxicol. Methods* **50**, 187–199.
8. Tang, W., Kang, J., Wu, X., Rampe, D., Wang, L., Shen, H., Li, Z., Dunnington, D., and Garyantes, T. (2001) Development and evaluation of high throughput functional assay methods for HERG potassium channel. *J. Biomol. Screen.* **6**, 325–331.
9. Kamiya, K., Niwa, R., Mitcheson, J.S., and Sanguinetti, M.C. (2006) Molecular determinants of HERG channel block. *Mol. Pharmacol.* **69**, 1709–1716.
10. Rodriguez-Menchaca, A., Ferrer-Villada, T., Lara, J., Fernandez, D., Navarro-Polanco, R.A. and Sanchez-Chapula, J.A. (2006) Block of HERG channels by berberine: mechanisms of voltage- and state-dependence probed with site-directed mutant channels. *J. Cardiovasc. Pharmacol.* **47**, 21–29.
11. Bottino, D., Penland, R.C., Stamps, A., Traebert, M., Dumotier, B., Georgiva, A., Helmlinger, G., and Lett, G.S. (2006) Preclinical cardiac safety assessment of pharmaceutical compounds using an integrated systems-based computer model of the heart. *Prog. Biophys. Mol. Biol.* **90**, 414–443.
12. Crumb, W.J., Jr., Ekins, S., Sarazan, R.D., Wikel, J.H., Wrighton, S.A., Carlson, C., and Beasley, C.M., Jr. (2006) Effects of antipsychotic drugs on I(to), I (Na), I (sus), I (K1), and hERG: QT prolongation, structure activity relationship, and network analysis. *Pharmacol. Res.* **23**, 1133–1143.
13. Jamieson, C., Moir, E.M., Rankovic, Z., and Wishart, G. (2006) Medicinal chemistry of hERG optimizations: highlights and hang-ups. *J. Med. Chem.* **49**, 5029–5046.
14. Wible, B.A., Hawryluk, P., Ficker, E., Kuryshev, Y.A., Kirsch, G., and Brown, A.M. (2005) HERG-Lite: a novel comprehensive high-throughput screen for drug-induced

hERG risk. *J. Pharmacol. Toxicol. Methods* **52**, 136–145.

15. van der Heyden, M.A., Smits, M.E., and Vos, M.A. (2007) Drugs and trafficking of ion channels: a new pro-arrhythmic threat on the horizon? *Br. J. Pharmacol.* **153**, 406–409.
16. Hancox, J.C. and Curtis, M.J. (2006) Methods for screening drugs for their pro-arrhythmic liability: does the rabbit ventricular wedge hold the key? *J. Pharmacol. Toxicol. Methods* **54**, 257–260.
17. Lawrence, C.L., Pollard, C.E., Hammond, T.G., and Valentin, J.P. (2005) Nonclinical proarrhythmia models: predicting Torsades de Pointes. *J. Pharmacol. Toxicol. Methods* **52**, 46–59.
18. Shah, R.R. and Hondeghem, L.M. (2005) Refining detection of drug-induced proarrhythmia: QT interval and TRIaD. *Heart Rhythm* **2**, 758–772.
19. Valentin, J.P., Hoffmann, P., De Clerck, F., Hammond, T.G., and Hondeghem, L. (2004) Review of the predictive value of the Langendorff heart model (Screenit system) in assessing the proarrhythmic potential of drugs. *J. Pharmacol. Toxicol. Methods* **49**, 171–181.
20. Witchel, H.J., Milnes, J.T., Mitcheson, J.S., and Hancox, J.C. (2002) Troubleshooting problems with in vitro screening of drugs for QT interval prolongation using HERG K+ channels expressed in mammalian cell lines and *Xenopus* oocytes. *J. Pharmacol. Toxicol. Methods* **48**, 65–80.
21. Rudy, B. and Iversen, L.E. (eds.) (1992) *Ion channels methods in enzymology* **207**. Academic, London.
22. Molleman, A. (2003) *Patch clamping: an introductory guide to patch clamp electrophysiology*. Wiley, Chichester.
23. Sakmann, B. and Neher E. (eds.) (1995) *Single-channel recording*. Plenum, New York.
24. Yao, J.A., Du, X., Lu, D., Baker, R.L., Daharsh, E., and Atterson, P. (2005) Estimation of potency of HERG channel blockers: impact of voltage protocol and temperature. *J. Pharmacol. Toxicol. Methods* **52**, 146–153.
25. Rampe, D., Roy, M.L., Dennis, A., and Brown, A.M. (1997) A mechanism for the proarrhythmic effects of cisapride (Propulsid): high affinity blockade of the human cardiac potassium channel HERG. *FEBS Lett.* **417**, 28–32.

INDEX

E

F

G

H

I

L

M

N

O

P

Q

Q

S

T

V

W

X